SPECIES PRODUCED IN FIRES BURNING IN TWO-LAYERED AND HOMOGENEOUS VITIATED ENVIRONMENTS

Thesis by

James Henry Morehart

In Partial Fulfillment of the Requirements

for the Degree of

Doctor of Philosophy

California Institute of Technology

Pasadena, California

1991

Thesis Adviser: Professor E. E. Zukoski

(Submitted August 15, 1990)

Acknowledgements

I would like to express my sincerest thanks to my adviser, Professor E. E. Zukoski, for his generous support and interest in these endeavors. The process of a graduate education is a collaborative one, and many people are owed thanks for their part in assisting me. I extend my deep appreciation to Professors T. Kubota, R. H. Sabersky, S. Serdengecti, and F. E. Marble. Their efforts on my behalf have been numerous and immeasurably valuable.

Also, thanks are due to some of my fellow students in Mechanical Engineering, particularly Mr. J. Yang and Mr. R. Chan, whose discussions have been helpful. My wife, Tammy, deserves special thanks for her continual encouragement and unselfish dedication in supporting my work.

This research work was financially supported by the Center for Fire Research, National Institute of Standards and Technology, Department of Commerce, through grant no. 60NANB9D0958. Many helpful discussions with members of the CFR staff, especially Drs. D. Evans and W. Pitts, are gratefully acknowledged.

Abstract

The chemical species produced in a buoyant, turbulent diffusion flame exposed initially to a supply of fresh air and extending into a reduced-oxygen environment containing products of combustion are investigated. The stably stratified, vitiated region is formed by placing a hood above a burner so that it accumulates the gases of the fire plume, while the direct injection of air into the upper portion of the hood allows conditions to be studied where the stoichiometry of the collected gases is different than that of the plume flow crossing the interface between these two regions.

Measurements of the composition show that the species produced in the flame depend primarily on the stoichiometry of the gases in the vitiated region, but are independent of the fuel-air ratio of the mass transported across the interface by the plume. A weak dependence of species concentrations on the temperature of the product gas layer was observed over the range 500 to 900 K. Using a detailed chemical kinetics model, the composition of the product gases is found to be stable for the temperatures measured in the experiments, but reactions do occur at temperatures above 700 K.

The effects of varying the fuel's molecular structure on the product gas composition are also considered. Experiments were conducted with natural gas, ethylene, and propylene fuels. The presence of a double bond between carbon atoms appears to assist the combustion process towards further completion. As expected, the behavior of the propylene fuel (which contains both single and double carbon-carbon bonds) fell between that of the other fuels.

Additionally, the minimum oxygen concentration necessary to support a diffusion flame in a homogeneous, vitiated environment is investigated. By submerging the entire flame into the interior volume of the hood, the oxygen content of the supporting atmosphere is controlled. As conditions approach the limit of flammability, radiation from soot in the reaction zone becomes imperceptible, leaving only a weakly-luminous blue flame. Even with significant reductions in both the flame height and luminosity, these fires near the limiting conditions completely consume the fuel and generate no measurable amounts of incomplete combustion products.

Contents

	Acknowledgements	ii
	Abstract	iii
	Table of Contents	iv
	List of Figures	vii
	List of Tables	xi
	List of Symbols	xii
1	Introduction	1
2	Experimental Technique and Apparatus	8
	2.1 A Steady Experiment which models a Transient Problem	8
	2.2 Chemistry Measurements	9
	2.3 Gas Analysis Technique	11
	2.3.1 Natural Gas	11
	2.3.2 Ethylene and Propylene	12
	2.4 Gas Burning and Sample Analysis Facilities	13
3	Validation of the Experimental Method	22
	3.1 Homogeneity of the Product Layer	22
	3.1.1 Profiles of the Product Layer without Air Addition	23
	3.1.2 Profiles of the Product Layer with Air Addition	24
	3.2 Effects of Removal of Water Vapor from the Sample	25
	3.3 Effects of the Sample Line Filter	26
	3.4 Chemical Reactions in the Sample Probe	26
4	Species Production and Heat Release Rates in Natural Gas Fires burning in Two Layers	34
	4.1 Equivalence Ratios	35
	4.2 Measurements of Product Species	37
	4.3 Rates of Entrainment	39
	4.3.1 Measurements of Air Entrainment below the Interface	41
	4.3.2 Comparison of Air Addition Measurements	43
	4.4 Heat Release Rates	44

4.5 Modeling Species Production and Heat Release Rates in Transient Fire Plumes burning in Two Layers 46
4.5.1 Correlation between a Transient Room Fire and the Experimental Model 47
4.5.2 Analytical Models 47
4.5.2.1 Species Production Rates 48
4.5.2.2 Heat Addition Rates 50

5 The Effect of Product Layer Temperture on Combustion Completeness 71
5.1 Temperature Increases due to the Insulation of the Hood 72
5.1.1 Tests with Insulation on the Exterior of the Hood 72
5.1.2 Tests with Insulation on the Interior Ceiling of the Hood 72
5.1.3 Species Measurements from Experiments with Elevated Temperature 73
5.2 Temperature Increases due to Fires using a Larger Burner 75
5.3 Chemical Stability of the Ceiling Layer Composition 77
5.3.1 Detailed Chemical Kinetics using a Plug Flow Reactor Model 78
5.3.2 Species Concentration Profiles 79

6 Species Produced in Fires burning in Two Layers using Alternate Fuels 94
6.1 Experiments with Ethylene Fuel 95
6.2 Experiments with Propylene Fuel 99
6.3 Comparison of Results between Different Fuels 102
6.3.1 Entrainment below the Interface 103
6.3.2 Chemical Species Produced 105
6.3.3 Quantitative Observations Of Soot Characteristics 106
7 Chemical Species Produced in Fires near the Limit of Flammability 129
7.1 Development of Homogeneous, Vitiated Conditions in an Enclosure Fire 129

7.2 Experimental Method 131
7.3 Results for Natural Gas and Ethylene Fuels 132
7.4 Observations from Experiments with Propylene Fuel 136

8 Conclusions 143

References 146

Appendix A – Gas Analysis Data Reduction Programs 150

Appendix B – Data Reduction Program Output Sheets 177

Appendix C – Detailed Chemical Kinetics Modeling Programs 242

Appendix D – Tabulated Data from Experiments with Alternate Fuels 252

List of Figures

1.1 Three distinct stages in the development of a fire in an enclosure 6

1.2 Room fire analogs for experimental models 7

2.1 Schematic of experimental apparatus used in previous investigations 16

2.2 Schematic of experimental apparatus with air addition network used in this study 17

2.3 Views of hood with air addition network 18

2.4 Time history of separations and component elutions 19

2.5 Schematic of gas burning and sample analysis facilities 20

2.6 Diagram of flow monitoring systems 21

3.1 Range of possible probe positions with an interface height of 10 cm 28

3.2 Temperature and concentration profiles without air addition 29

3.3 Concentration profiles without air addition 30

3.4 Temperature and concentration profiles with air addition 31

3.5 Concentration profiles with air addition 32

4.1 Comparison of equivalence ratios for forced ventilation fires with exponential growth rates 53

4.2 Hydrogen measurements for natural gas fires burning in two layers 54

4.3 Oxygen measurements for natural gas fires burning in two layers 55

4.4 Nitrogen measurements for natural gas fires burning in two layers 56

4.5 Methane measurements for natural gas fires burning in two layers 57

4.6 Carbon monoxide measurements for natural gas fires burning in two layers 58

4.7 Carbon dioxide measurements for natural gas fires burning in two layers 59
4.8 Water vapor measurements for natural gas fires burning in two layers 60
4.9 Acetylene measurements for natural gas fires burning in two layers 61
4.10 Ethane measurements for natural gas fires burning in two layers 62
4.11 Comparison of entrainment data for a 19 cm diameter burner with a natural gas fuel and small interface heights 63
4.12 Comparison of entrainment data for a 19 cm diameter burner with natural gas fuel and large interface heights 64
4.13 Comparison of air addition measurements 65
4.14 Actual heat of reaction compared to that of a stoichiometric reaction 66
4.15 Actual heat of reaction compared to a theoretical maximum based on available quantities of fuel and air 67
4.16 Plume reactor model for enclosure fire 68
4.17 Plume reactor model for experiment 69
5.1 Comparison of product layer temperature measurements for two different hood constructions 83
5.2 Upper layer temperatures for natural gas layers burning in two layers 84
5.3 Phases of hood insulation 85
5.4 Product layer compostion as a function of temperature with insulation applied to hood 86
5.5 Product layer compostion as a function of temperature for two different burner diameters (no insulation applied to hood) 87
5.6 Reactant and temperature profiles through the reaction zone of a diffusion flame 88
5.7 Oxygen concentration in a fuel-rich mixture introduced into an isothermal plug flow reactor 89
5.8 Carbon monoxide concentration in a fuel-rich mixture introduced into an isothermal plug flow reactor 90
5.9 Carbon dioxide concentration in a fuel-rich mixture introduced into an isothermal plug flow reactor 91

5.10 Methane concentration in a fuel-rich mixture introduced into an isothermal plug flow reactor 92
5.11 Water vapor concentration in a fuel-rich mixture introduced into an isothermal plug flow reactor 93
6.1 Hydrogen measurements for ethylene fires burning in two layers 108
6.2 Oxygen measurements for ethylene fires burning in two layers 109
6.3 Nitrogen measurements for ethylene fires burning in two layers 110
6.4 Methane measurements for ethylene fires burning in two layers 111
6.5 Carbon monoxide measurements for ethylene fires burning in two layers 112
6.6 Carbon dioxide measurements for ethylene fires burning in two layers 113
6.7 Water vapor measurments for ethylene fires burning in two layers 114
6.8 Temperature measurements for ethylene fires burning in two layers 115
6.9 Hydrogen measurements for propylene fires burning in two layers 116
6.10 Oxygen measurements for propylene fires burning in two layers 117
6.11 Carbon monoxide measurements for propylene fires burning in two layers 118
6.12 Carbon dioxide measurements for propylene fires burning in two layers 119
6.13 Water vapor measurements for propylene fires burning in two layers 120
6.14 Hydrocarbon measurements for propylene fires burning in two layers 121
6.15 Temperature measurements for propylene fires burning in two layers 122
6.16(a) Average entrainment rates below a 5 cm interface height for various gaseous fuels 123

6.16(b)	Average entrainment rates below a 10 cm interface height for various gaseous fuels	124
6.17	Comparison of oxygen measurements in two-layered fires stabilized on a 19 cm diameter burner	125
6.18	Comparison of carbon monoxide measurements in two-layered fires stabilized on a 19 cm diameter burner	126
6.19	Comparison of carbon dioxide measurements in two-layered fires stabilized on a 19 cm diameter burner	127
6.20	Comparison of water vapor measurements in two-layered fires stabilized on a 19 cm diameter burner	128
7.1	Schematic of experiment showing extending curtain which prevents entrainment	138
7.2	Measurements of species in natural gas fires as conditions approach the limit of flammability	139
7.3	Measurements of species in ethylene fires as the conditions approach the limit of flammability	140
7.4	Schematic of experiment showing behavior of fire when burning propylene fuel	141
C.1	Methyl radical concentration for a fuel-rich mixture introduced into an isothermal plug flow reactor	246
C.2	C_2H_2O concentration for a fuel-rich mixture introduced into an isothermal plug flow reactor	247
C.3	H_2O_2 concentration for a fuel-rich mixture introduced into an isothermal plug flow reactor	248
C.4	CH_2O concentration for a fuel-rich mixture introduced into an isothermal plug flow reactor	249
C.5	H radical concentration for a fuel-rich mixture introduced into an isothermal plug flow reactor	250
C.6	OH radical concentration for a fuel-rich mixture introduced into an isothermal plug flow reactor	251

List of Tables

3.1	Comparison of average peak areas	33
3.2	Comparison of peak areas with varying sample treatment	33
4.1	Physiological effects of carbon monoxide on humans	70
7.1	Comparison of measurements for methane fires	142
7.2	Comparison of measurements for ethylene fires	142

List of Symbols

a	fuel mole fractions
b	air mole fractions
A	coefficients from fuel components
B	coefficients from air components
D	burner diameter, cm
$\mathcal{D}_{ab}$	diffusivity of gas a into gas b
E_a	activation energy for Arrhenius reaction rate
f	chromatographic response factor, (amount/area)
f_ℓ	fuel-air ratio of layer
f_p	fuel-air ratio of plume at interface
f_s	stoichiometric fuel-air ratio
$h_{j,i}$	sensible enthalpy of i_{th} species at position j
$H_{j,i}$	total enthalpy of i_{th} species at position j
$\Delta H^\circ_{j,i}$	enthalpy of formation
ΔH°_r	heat of reaction, actual
ΔH°_s	heat of stoichiometric reaction
I	total air addition rate to the layer, moles
k	reaction rate constant, Arrhenius form
$\dot{m}_{air}$	air mass flow rate
$\dot{m}_{fuel}$	fuel mass flow rate
$\dot{m}_{add}$	air mass addition rate
$\dot{m}_{ent}$	air mass entrainment rate
$\dot{m}_p$	mass flux in fire plume at interface
$\dot{m}_u$	mass flux leaving reactor
M_ℓ	total mass of gas in layer
$\dot{Q}_{rad}$	net radiant energy from plume reactor
Re	Reynolds number, based on burner diameter
Ri	Richardson number, buoyant forces to initial momentum ratio
S_i	mass fraction of i_{th} species from plume equivalent source
T^*	effective activation temperature for bulk reactions
W	molecular weight
x_i	moles of product species i

$\chi_{j,i}$	mass fraction of i_{th} species at j_{th} position
Y	coefficients from product components
z	elevation coordinate
α	ratio of response factors for oxygen and argon
β	multiple of peak area normalized by N_2 peak
ε	fraction of heat release due to radiation
λ	effective flamesheet thickness
φ_ℓ	equivalence ratio of layer gases
φ_p	equivalence ratio of plume flow at interface height
μ	dynamic viscosity

Chapter 1

Introduction

Annually, fires in the U.S. cause nearly 6000 deaths, 120,000 serious injuries, and $8 billion in direct costs (Karter, 1989). The total costs of fires are hard to estimate, but appear to be increasing in real terms, and burden the economy at $50 to $100 billion per year. The magnitude of these losses demonstrates that we have not yet developed a cohesive understanding of the processes occurring in a building fire. The development and spreading of fires in buildings involves the contributions and interactions of many component processes, including topics related to fluid mechanics, heat transfer, and detailed reaction chemistry. Improvements in our understanding are hampered by the difficulties presented in solving such multi-disciplinary problems.

Recent enhancements in our predictive capabilities can be credited to developments in two fundamental areas—a better understanding of the mathematical modeling of fires in buildings, and an increase in the use of computers in fire research. An important simplification in the analysis of enclosure fires is the concept of the two-layer model (Kawagoe, 1958). Essentially, the volume of the room is divided into two distinct zones, each of homogenous composition and temperature (outside of the plume flow). The upper ceiling layer is assumed to be composed of hot, buoyant products of combustion mixed with entrained air. This warm gas layer is stably stratified above the cool, uncontaminated room air below. This two-layer fire model is the basis for much of the recent work aimed at improving our understanding of fires in enclosures (e.g., Cetegen, 1982; Beyler, 1983; Lim, 1984; Toner, 1986). Presently, the use of computers in fire research is widespread. Topics ranging from turbulent combustion modeling to detailed chemical kinetics modeling to fire hazard assessment are now being addressed.

The development of a fire in an enclosure with restricted ventilation can proceed through three distinct phases, described in Figure 1.1. During the initial growth period, the flames are exposed only to the air in the room. Products of the combustion rise to the higher elevations in a plume which entrains and mixes with the room air. These warm gases impinge on the ceiling and are turned to spread radially outward in a ceiling jet. Eventually this flow reaches the walls of the enclosure where the momentum is again redirected downward until the buoyant forces fold the gases back beneath the ceiling jet.

Until this time, the finite dimensions of the enclosure have had no effect on the processes occurring in the fire. Since the flames are exposed to air, an excess amount of oxygen is available and the combustion processes are essentially complete. The product species are primarily carbon dioxide and water vapor (assuming a simple hydrocarbon fuel), with excess entrained air acting as a diluent. The entrainment behavior of a buoyant plume flow in a uniform environment has been considered by many investigators, starting with works by Schmidt (1941), Rouse et al. (1952), Morton et al. (1956), and Yokoi (1961). Some more recent studies have concentrated on regions in the near-field of a fire plume (see McCaffrey, 1979; Zukoski et al., 1980; Cetegen, 1982; and Toner, 1986). The action of the counterflowing gases beneath the ceiling jet creates a well-stirred, nearly homogeneous layer of combustion products and entrained air. The primary effect of confinement then is the production of a stably stratified warm gas layer in the upper portion of the compartment.

With continued burning, the depth of the ceiling layer can extend to occupy a significant portion of the room's volume. During this intermediate phase, it is possible for the interface between the ceiling layer gases and the room air to position itself so that some of the combustion processes occur in the ceiling layer. When the fire burns in this two-layered configuration, the oxygen concentration in the upper layer may be reduced to a small value. This vitiated gas is then reentrained into the part of the plume which extends into the upper layer. Hence, the effects of confinement can now reach back to the fire and influence flame geometry, chemical species production, and heat release rates. If the composition of the ceiling layer is fuel-rich, i.e., when not enough air is present to completely burn the fuel supplied, experimental measurements of the combustion products deviate from their corresponding equilibrium values (Beyler, 1983; Toner, 1986; Zukoski et al., 1990).

When the ventilation is severly restricted, the layer of combustion products can grow to fill the entire volume of the enclosure. Despite the complete immersion of the fire in a vitiated atmosphere, burning can continue provided these gases contain the necessary concentration of oxygen to support the combustion processes. If the oxygen content of the environment falls below this critical value, burning will cease. The borderline composition, described here as the limit of flammability, is strongly dependent on the fuel type and the diluents present.

Previous studies interested in measuring entrainment and global upper layer chemistry due to a fire plume burning in a two-layered configuration have used

a direct measurement technique adopted from the approach of Ricou and Spalding (1961), who measured entrainment into turbulent jets. Because the only source of material being delivered to the upper layer is through the fire plume, the fuel-air ratio of the layer composition quickly approaches that of the plume flow. Once the product layer species reach a steady value, an analysis of the gases allows the evaluation of the entrainment rate (Cetegen, 1982; Beyler, 1983; and Lim, 1984 used a series of gas analyzers, while Toner, 1986 employed a chromatographic technique similar to the method used in this study). These experiments were performed with fixed fuel flow rates, while the fuel-air ratio of the plume flow entering the upper layer was varied by adjusting the height between the burner and the interface position, the distance over which fresh air could be entrained.

In terms of a corresponding room fire analog, this approach is limited in applicability. Figure 1.2(a) shows one possible interpretation. When a fire of fixed strength burns into a layer of constant depth, where excess products are expelled from the room through an open window or doorway, the composition of the ceiling layer will approximately match that of the plume flow crossing the interface. The experiments of Cetegen, Beyler, Lim, and Toner model this steady flow configuration. The development of the ceiling layer during an enclosure fire, however, is a transient process. In general, the layer depth and fire strength are not fixed, but may be time-dependent. Under these circumstances, the fuel-air ratio of the plume material entering the upper layer may be quite different from that of the layer (globally), since its composition reflects the complete time-history of the material carried through the interface. The most interesting and useful experiment then is one which models the conditions in this developing, time-dependent ceiling layer, idealized in Figure 1.2(b).

Without the facilities to perform full-scale tests in a "burn room", obtaining meaningful data from such experiments is difficult. However, it is possible to devise an experiment which models the desired features of transient development while preserving the scale of the original problem, but with the advantage of being conducted in a steady manner. Consider the steady flow configuration again, now with a vent or air conditioning outlet delivering air directly into the ceiling layer, as shown in Figure 1.2(c). In the spirit of our two-layer model, we will assume that the air is introduced in a uniformly distributed manner with instantaneous mixing so that the ceiling layer remains homogeneous in composition. Now despite a fixed interface position and fire strength, the fuel-air ratio of the product layer gases can be altered independent of the flow in the fire plume. With this experimental

arrangement, it is possible to investigate the chemical species produced when a fuel-rich fire plume (transporting excess fuel across the interface) burns in a fuel-lean ceiling layer (possessing an excess amount of oxygen). These conditions are possible during the growth phase of a rapidly developing enclosure fire, since an increasing fire strength and layer depth both contribute to an imbalance in these fuel-air ratios. Hence, nonsteady flow conditions such as those described in Figure 1.2(b) can be simulated with this steady experiment.

The purpose of this investigation is to examine the chemical species produced in a turbulent, buoyant diffusion flame originating from a lower air layer and burning into a stably stratified upper layer of reduced oxygen content. The experiments are conducted with equipment which allows a uniformly distributed air supply to be added directly into the upper layer to alter its global fuel-air ratio from that of the fire-driven plume flow. Results from tests with gas fires using natural gas, ethylene, and propylene fuels are presented.

A simple modification to the experiment allows us to position the interface between the room air and the product gas layer below the surface of the burner where the flames are stabilized, thereby preventing the entrainment of fresh air into the fire plume. Under these circumstances, the only source of air to support the combustion is via the air addition equipment within the upper layer. Gradual reductions in this air addition rate (with a fixed fire strength) create conditions which approach the limit of flammability. Our motive here is to examine the chemical species produced in these diffusion flames burning in a uniform, reduced-oxygen environment very near the limiting conditions.

The experiments in this study where flames burned in a two-layered configuration used fire strengths ranging from 12 to 135 kW, based on the heating value of the fuel. Three different burners were used to stabilize these fires, with diameters of 8.9, 19.0, and 50.0 cm. With interface heights ranging from 1 to 23 cm, the upper layer gases reached temperatures between 488 and 675 K. The results of these experiments and comparisons with the measurements of others and with theoretical values will be presented here. Also, the data from an investigation into the temperature-dependence of these results, and a sensitivity analysis of the stability of the product layer composition will be reported.

An overview of the experimental equipment and procedures is given in Chapter 2. A unique "burn room" hood, which is designed with an air addition network, will be described. The analysis of the product layer gases is accomplished using a gas chromatograph system with multiple columns. A schematic of the other

components of the gas burning and sample analysis facilities is included. As an extention to this description, Chapter 3 shows the results of some initial 'check out' experiments which provided validation for the model and technique. Profiles of composition and temperature in the hood show that indeed the upper layer is well-stirred and nearly homogeneous. Other possible concerns about the handling of the sample gases are also addressed.

Chapter 4 presents the measurements taken in natural gas fires burning in two layers. For fires which are quite fuel-lean, the measurements appear to follow their corresponding equilibrium values, but with fuel-rich conditions there are significant deviations. Data from over 60 experiments are presented here, and encompass a wide range of conditions. Chapter 5 further considers experiments with natural gas fuel, however, conditions are held fixed while upper layer temperatures are elevated by using varing amounts of insulation applied to the hood. Also, the results of a numerical simulation are presented in an effort to investigate the stability of the product layer composition at various temperatures using a detailed chemical kinetics model.

The results from experiments with ethylene and propylene fuels are given in Chapter 6. The ethylene data are also compared to equilibrium values computed for three different temperatures. A comparison of the measurements between each of the fuels shows some interesting trends which can be attributed to differences in the fuels' molecular structure.

Chapter 7 reports the results of our investigation into the species formed by fires burning in oxygen-reduced environments near the limit of flammability. Measurements in experiments with natural gas and ethylene show that the product layer composition follows the equilibrium values closely, despite dramatic changes to the character of these flames. Finally, Chapter 8 summarizes the conclusions of this study.

Appendix A lists the data reduction scheme programs for the experiments with natural gas fuel. Formatted report sheets for each experiment are provided in Appendix B. Information about the reaction mechanism and related input files for the numerical simulation in Chapter 5 are presented in Appendix C. Tabulated data from the experiments reported in Chapter 6 are given in Appendix D.

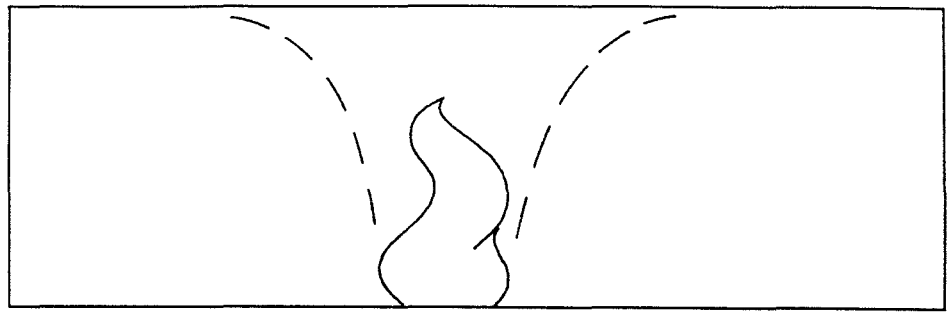

(a) Initial growth phase

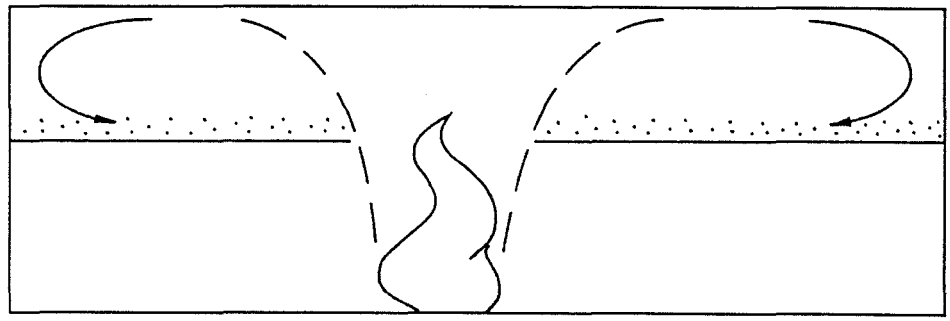

(b) Two–layered configuration

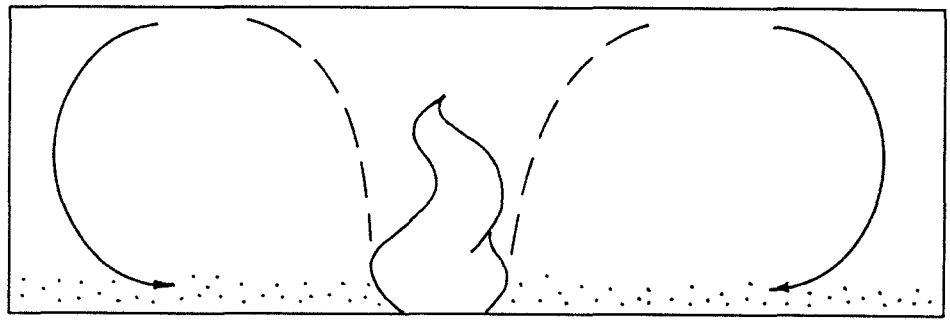

(c) Completely vitiated environment

Figure 1.1: Three distinct stages in the development of a fire in an enclosure

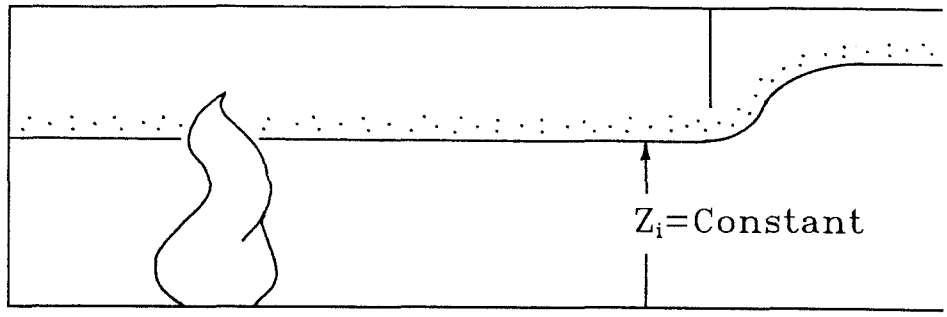

(a) Steady room fire analog

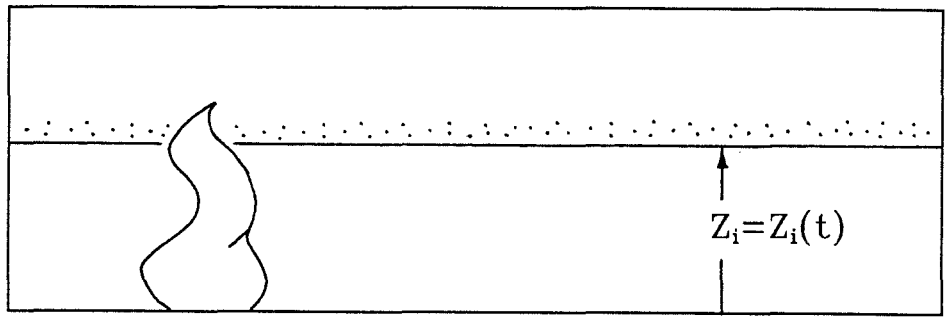

(b) Transient development of the ceiling layer

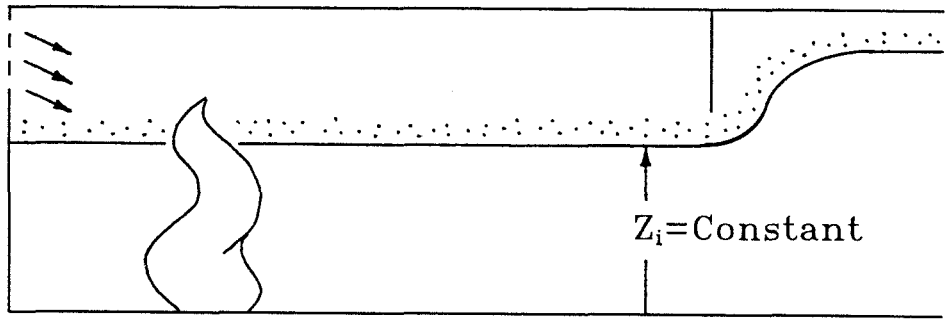

(c) Steady flow analog which mimics features of transient development

Figure 1.2: Room fire analogs for experimental models

Chapter 2

Experimental Technique and Apparatus

The two-layer model is the basis for the experimental investigations of Cetegen (1982), Beyler (1983), Lim (1984), and Toner (1986). In these studies, a buoyant diffusion flame is stabilized below a "catch hood" which accumulates the gases from the fire plume. Cetegen and Lim were primarily interested in measuring the entrainment rate into the fire plume below the interface, while Toner also considered its impact on the species produced. By allowing excess products to spill out beneath the edges of the hood, as shown in Figure 2.1, the conditions within the hood could reach a steady state with a sharply defined interface between the product gases and the fresh air below. With this arrangement, the fire plume entrains fresh air only over the region below the interface. Once steady conditions are established, an analysis of the product layer gases allows the evaluation of the entrainment rate. Beyler was concerned with the production and ignition of combustibles residing in the product layer. In his experiment, excess products are withdrawn from near the top of the hood, balancing the elevation of the interface inside. This technique does not produce a sharp stratification of the layers, thus it is not clear over what height entrainment occurs.

The experimental technique of these studies relies on recirculation through the plume flow to provide a well-stirred upper layer composition. Due to the stable stratification, the only significant source of air into the upper layer is by entrainment into the plume. Hence, the eventual composition matches that of the plume material crossing the interface. In an actual enclosure fire, these conditions can occur only for a limited number of geometries, such as those suggested in Figure 1.2(a). In this investigation, we are interested in the more general problem where these compositions are not equal. Of concern are the species produced in flows when the fuel-air ratio of the upper layer gas is significantly lower than that of the plume flow at the interface height, conditions which occur in enclosure fires when the depth of the ceiling layer and/or the fire strength are rapidly increasing.

2.1 A Steady Experiment which Models a Transient Problem

The approach of this study closely follows that described in Figure 2.1, but with the addition of an air injection system located in the upper portion of the

hood. Shown schematically in Figure 2.2, this system allows the direct addition of air into the upper layer independent of the plume flow. In this manner, the fuel-air ratio of the gas composition within the hood is maintained at a different value than that of the plume flow crossing the interface. As mentioned above, these are the circumstances which arise during the transient development of the ceiling layer.

The experiments were conducted using the hood diagrammed in Figure 2.3, which measures 1.8 meters square by 1.2 meters tall and is constructed of 0.61 mm thick sheet metal. The top of the hood is reinforced with angle braces to provide the necessary structural integrity for its suspension using cables bolted to the ceiling's four corners and center. By adjusting the tension of the individual support cables, the bottom edges of the hood can be aligned to within 1 cm. Installed on the front side are three pyrex glass windows measuring 59.1 cm × 30.5 cm × 0.635 cm each, giving a view of the central lower 75% of the hood's interior.

The air addition network installed in the upper central portion of the hood consists of a 5 cm diameter copper feed line supplying three tiers of 2.54 cm diameter copper distribution lines. An array of 365 injection ports distributes the air through 1.6 mm diameter holes spaced 2.54 cm between centers. These small holes promote the rapid mixing between the injected air and the gases present in the hood. The air is injected in a radial direction roughly parallel to the mean stream lines of the flow as the gases in the plume impinge on the ceiling and are turned to recirculate within the hood. Flame heights are maintained below the injection plane to prevent air from being added directly into the reacting regions of the flame.

2.2 Chemistry Measurements

The arrangement of the chemistry equations in this analysis and the chromatographic technique employed here closely follow the methods outlined by Toner (1986). We will briefly discuss some relevant portions here, but for a detailed description of the technique, this reference should be consulted.

The reaction equation for the combustion of natural gas in air can be written:

$$\begin{aligned} &a_1 CH_4 + a_2 C_2H_6 + a_3 C_3H_8 + a_4 N_2 + a_5 CO_2 \\ &\qquad + I(b_1 O_2 + b_2 N_2 + b_3 H_2O + b_4 CO_2 + b_5 Ar) \longrightarrow \\ &x_1 H_2 + x_2 O_2 + x_3 N_2 + x_4 CH_4 + x_5 CO + x_6 CO_2 + x_7 H_2O \\ &\qquad + x_8 C_8 H(s) + x_9 C_2H_2 + x_{10} C_2H_4 + x_{11} C_2H_6 + x_{12} Ar \end{aligned} \tag{2.1}$$

where the a_i's represent the mole fractions of the constituent species of the natural gas, the b_i's represent those of air, I represents the moles of air added to the hood per mole of fuel, and the x_i's correspond to the number of moles of each product species formed by the combustion of one mole of fuel. This equation is applicable for both fuel-lean and fuel-rich mixtures. The residual soot (not consumed in the flame) is modeled with the empirical formula $C_8H(s)$, suggested by Palmer and Cullis (1965). Similar equations can be written for the other fuels considered here. Ethylene and propylene provide, respectively:

$$C_2H_4 + I(b_1O_2 + \ldots + b_5Ar) \longrightarrow x_1H_2 + \ldots + x_{12}Ar \tag{2.2}$$

and

$$C_3H_6 + I(b_1O_2 + \ldots + b_5Ar) \longrightarrow x_1H_2 + \ldots + x_{12}Ar + x_{13}C_3H_6. \tag{2.3}$$

In each case, we must determine for the values of I, the total air addition rate, and of the x_i's to characterize the combustion process. Using the conservation of atoms equations, solutions can be found by combining information known about the fuel and air composition, and from measurements taken in the gas analysis. Our chromatographic technique provides the amounts of hydrogen, oxygen, methane, carbon monoxide, carbon dioxide, acetylene, ethylene, ethane, and argon relative to the amount of nitrogen in the products. For the natural gas fuel, we find the solution:

$$I = \frac{A_N(16Y_H - Y_C - 16Y_O) - (16A_H - A_C - 16A_O)}{(16B_H - B_C - 16B_O) - B_N(16Y_H - Y_C - 16Y_O)} \tag{2.4}$$

$$x_3 = A_N + B_N I \tag{2.5}$$

$$x_7 = A_O + B_O I - Y_O x_3 \tag{2.6}$$

$$x_8 = \frac{1}{8}(A_C + B_C I - Y_C x_3) \tag{2.7}$$

where

$$A_C = a_1 + 2a_2 + 3a_3 + a_5 \quad , \quad B_C = b_4$$

$$A_H = 2a_1 + 3a_2 + 4a_3 \quad , \quad B_H = b_3$$

$$A_O = 2a_5 \quad , \quad B_O = 2(b_1 + \alpha b_5) + b_3 + 2b_4$$

$$A_N = a_4 \quad , \quad B_N = b_2$$

and

$$Y_C = y_4 + y_5 + y_6 + 2y_9 + 2y_{10} + 2y_{11}$$

$$Y_H = y_1 + 2y_4 + y_9 + 2y_{10} + 3y_{11}$$

$$Y_O = 2(y_2 + \alpha y_{12}) + y_5 + 2y_6$$

where $y_i \equiv x_i/x_3$ and $\alpha \equiv f_2/f_{12}$, the ratio of the response factors for oxygen and argon. A value of $\alpha = 1.05$ was used here (taken from Dietz, 1967). We also determine solution values for the amounts of nitrogen (x_3), water vapor (x_7), and soot (x_8), since we use the nitrogen measurement as the normalizing factor in the gas analysis, and the other components are not measured directly by the gas chromatograph.

Once the value of I has been determined, the total air mass addition rate into the hood can be found:

$$\dot{m}_{air} = \dot{m}_{fuel} \times I \times \frac{W_{air}}{W_{fuel}} \tag{2.8}$$

where W is the molecular weight, and $\dot{m}_{fuel}$ is monitored via a laminar flow element, described later. In order to determine the air addition rate into the upper layer using the chemistry analysis, the entrainment rate for the test configuration must first be evaluated. Therefore, the first experiment in each series is performed without air addition to the hood. For these cases, the measurement of the total air addition rate determined from the chemical analysis corresponds to the entrainment below the interface. Further experiments are performed with air addition to the upper layer, the rate of which is evaluated by differencing:

$$\dot{m}_{add} = \dot{m}_{air} - \dot{m}_{ent} \tag{2.9}$$

where the entrainment value is assumed to remain unchanged by the air addition. Appendix A, which lists the programs and subroutines used here, can provide more information about the data reduction scheme.

2.3 Gas Analysis Technique

The gas analysis system consists of a Hewlett-Packard 5890A gas chromatograph, a 3392A numerical integrator, and a 19405A sampler/event controller. This system is used to determine the relative amounts of the species in the sample gas, y_i for $i = 1, 4-6, 9-11, 13$, plus the combination $y_2 + \alpha y_{12}$. The basic system and component selection are discussed by Toner (1986) in detail, thus we will describe the minor alterations to the technique.

2.3.1 Natural Gas

For analyses of samples from experiments with natural gas fuel, some minor changes were made to the setup used by Toner. The length of the upstream column

(porapak T) was increased from 6′ to 8′, and this was compensated with an increase in the carrier flow rate of helium from 20 to 25 mL/minute. This provided additional time between the elutions of the light gases (H_2, O_2, N_2, CH_4, and CO) and the first heavy gas from the first column, CO_2. This allowed the opportunity to switch the order of the columns sending effluent to the detector. The previous design stored the light gases ($O_2 + Ar$, N_2, CH_4, and CO) in the molecular sieve 5A column after hydrogen was eluted, and allowed the heavy gases (CO_2, C_2H_4, C_2H_6, and C_2H_2) to be sent to the detector first. Rather than storing the light gases, these are allowed to exit directly while the heavy gases are stored in the porapak T column. This is done to minimize diffusion of the light gas peaks which may cause peak broadening and reduce peak heights. Such problems with the heavy gases are less of a concern since their diffusion rates are much smaller.

The cost of this switch is an increase in the magnitude of the baseline disturbance when the porapak is reinserted into the circuit. As mentioned above, additional time was available due to the increased column length. The increased separation between the last light gas (CH_4) and the first heavy gas (CO_2) is sufficient to allow this disruption to settle. The decision was made at the outset not to attempt the measurement of water vapor, hence the water was removed from the sample and the time-temperature programming was avoided. The progression of the eluting peaks from each column is otherwise comparable to the description of Toner.

2.3.2 Ethylene and Propylene

The selection of the porapak T porous polymer column packing to separate the heavy gases was based on a concern regarding the elution of water vapor. Since this packing is a very polar material, retention times for water are minimized, and the resulting peak does not exhibit trailing (a problem common to most of the other porous polymers). A limitation of this column material is that elution times for the C_2 hydrocarbons are close together and very near that of CO_2. An overlap in the tails of the peaks is tolerable when the peak areas are small, but when the areas are significant, interference between the peaks can cause large estimation errors or the integrator may treat the eluting components as a single peak. The case of natural gas fuel presents minimal problems since small amounts of these C_2 components are found in the product gases. For the more complex fuels, however,

this is not the case, and thus modifications to the column selection are required.

After some experimentation, a suitable arrangement of columns and parameters was found that could satisfy the requirements imposed by the presence of larger quantities of the C_2 hydrocarbons. The system description includes the following:

- $6' \times .125''$ OD (.085″ ID) washed porapak N, mesh size 80/100 in stainless steel
- $8' \times .125''$ OD (.085″ ID) washed molecular sieve 5A, mesh size 80/100 in stainless steel
- Carrier flowrate of helium = 25 mL/minute
- Oven temperature = 80°C, held constant

with all other parameters regarding the chromatographic technique remaining unaltered. The time history of the separations and the eluting components are shown schematically in Figure 2.4 for the case of a sample containing all of the species measured. As before, the light gases are eluted directly without storage, while the heavy gases are held in the porapak to protect the molecular sieve. The difference in the elution times between the CH_4 and CO_2 is again sufficient to allow baseline stabilization after the disturbance caused by the valve switching when the porapak N is replaced into the circuit.

Occasionally the performance of the molecular sieve column suffered some degradation marked by reductions in the elution times of the light gases, and by a decrease in the separation of the oxygen and nitrogen peaks. This behavior is the result of column contamination by water, which deactivates the molecular sieve. Once these effects are recognized, the column is reactivated by baking it in a furnace at 600 °C with a normal carrier flow of helium for about eight hours (to drive out the moisture). After this, the column is reinstalled in the chromatograph oven and the system is recalibrated to determine proper switching times and response factors.

2.4 Gas Burning and Sample Analysis Facilities

A schematic of the gas burning facility is shown in Figure 2.5 which details the treatment of the sample gas. The sample flow is withdrawn from within the hood through a 9.5 mm diameter stainless steel probe submerged into the upper layer. No cooling of the probe is attempted, thus the possibility of continued chemical reactions of the withdrawn gas is a concern here. This topic is addressed

experimentally in Chapter 3, and additional information is pursued in Chapter 5 using a chemical kinetics model to investigate the propensity of further reactions. Due to the low temperatures of these experiments, further reactions were not a problen in this setup.

To remove the moisture (water) from the sample, the flow is directed through two sets of copper coils submerged in water-ice baths. The condensed water is held in the bottom coil of each trap, causing most of the soot in the sample to be withdrawn also. To remove the remaining solid soot, the sample gas is passed through a 0.1 μm filter assembly. The effects of both the water-ice baths and the filter on the species in the sample are also considered in Chapter 3. After exiting the filter assembly, the sample flow is directed through the 0.1 cc sample loop of the gas chromatograph which is maintained at 120°C. The flow rate of the sample stream is monitored with a Matheson glass/stainless steel spherical float rotometer (tube number 604). The sample flow is initiated using a Thomas vacuum pump model 107CA18 3, located at the downstream end of the sample path. This pump provides flowrates on the order of 10 cc/sec, which translates to an estimated delay time (from probe inlet to sample loop) of 0.8 minutes. During the experiments, the pump is activated for a minimum of 5 minutes before the sample is taken.

The temperatures of the gas sample and of the hood above the plume impingement point are monitored. The probe arm is equipped with an aspirated, type K (chromel-alumel) thermocouple placed at the inlet, shielded from external radiation. This allows the temperature of the sample gas to be measured before it is changed significantly by its intake into the probe tubing. The position of the other thermocouple is on the ceiling of the hood's exterior. A bare type K thermocouple is mounted on the metal surface near the center of the ceiling area. Both of these thermocouples are connected to a reference junction which is electronically compensated to provide accurate measurements at room temperature.

The exhaust hood and attached pulley hoist for the fire hood are the same as those described by Cetegen and Toner. This larger fire hood possesses only a 30 cm clearance all around its perimeter until the exhaust hood is reached. Hence, this setup relies on the screens surrounding it to minimize flow disturbances and prevent exhaust fumes from spilling into the laboratory. The 19 cm and 50 cm diameter axisymmetric burners are also the same as those previously described. Fires are stabilized on a bed of spherical glass beads through which the fuel percolates, thereby eliminating any swirl in the exiting gas flow. A similar burner was constructed with a diameter of 8.9 cm for use in the study reported in Chapter 7.

The flow rates of fuel to the burner and air through the addition network are monitored using the parallel systems diagrammed in Figure 2.6. The components of the arrangement include:

- Meriam Laminar Flow Element model 50MC2-2P (LFE1)
- Meriam Laminar Flow Element model 50MC2-4 (LFE2)
- Datametrics Barocel Pressure Sensor type 581D, range 100 Torr (PT1)
- Datametrics Barocel Pressure Sensor type 590D, range $10''H_2O$ (PT2)
- Wallace and Tiernan Pressure Gauge model FA145161 (PT3)
- Datametrics Electronic Manometer type 1014A, analog readout (AM1)
- Datametrics Electronic Manometer type 1400, digital readout (DM2)

These are arranged in two independent monitoring systems capable of determining the flowrate of fuel or air individually, and are selected using two-way valves which connect the pressure taps. The additional pressure transducer (PT3) is used to measure the pressure difference between the upstream pressure tap and the laboratory environment. This gauge pressure is then added to the absolute pressure, measured with a mercury column barometer, to find the upstream absolute pressure of the flow. Because the flowrates of ethylene and propylene are smaller than for the natural gas, due to restrictions of the bottle regulators, the above fuel measuring element (LFE1) is replaced for these tests. Instead, a Meriam Laminar Flow Element model 50MW20 monitored the flow of these fuels. A comparison of the flowrate measurements for these systems and also using the chemistry technique, is presented in Chapter 4.

The procedure for a typical series of experiments begins with allowing the conditions to reach steady state, once the fire is started, without air addition to the upper layer. Thermal steady state is usually reached after about 20 minutes. The first sample of the gas composition is taken after an additional 10 minutes. Subsequent changes to the conditions, i.e., air addition rate increases, are made directly after the sample is taken, allowing the new conditions to take effect while the chromatograph processes the sample from the previous experiment. This typically provides for 25 to 30 minutes between sample times. Experimental conditions are not altered in any systematic manner, thereby allowing the opportunity to identify the effects of possible systematic procedural errors.

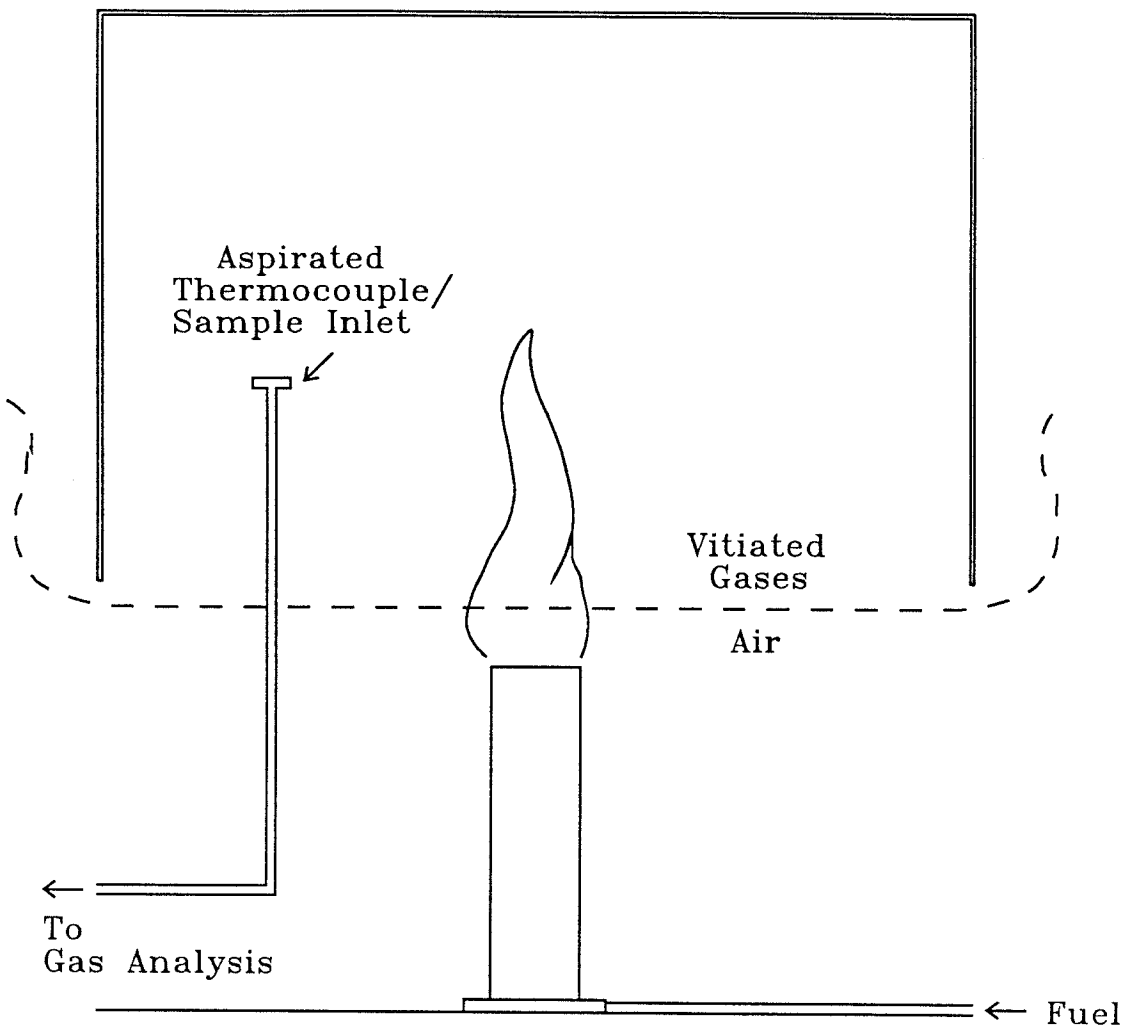

Figure 2.1: Schematic of experimental apparatus used in previous investigations

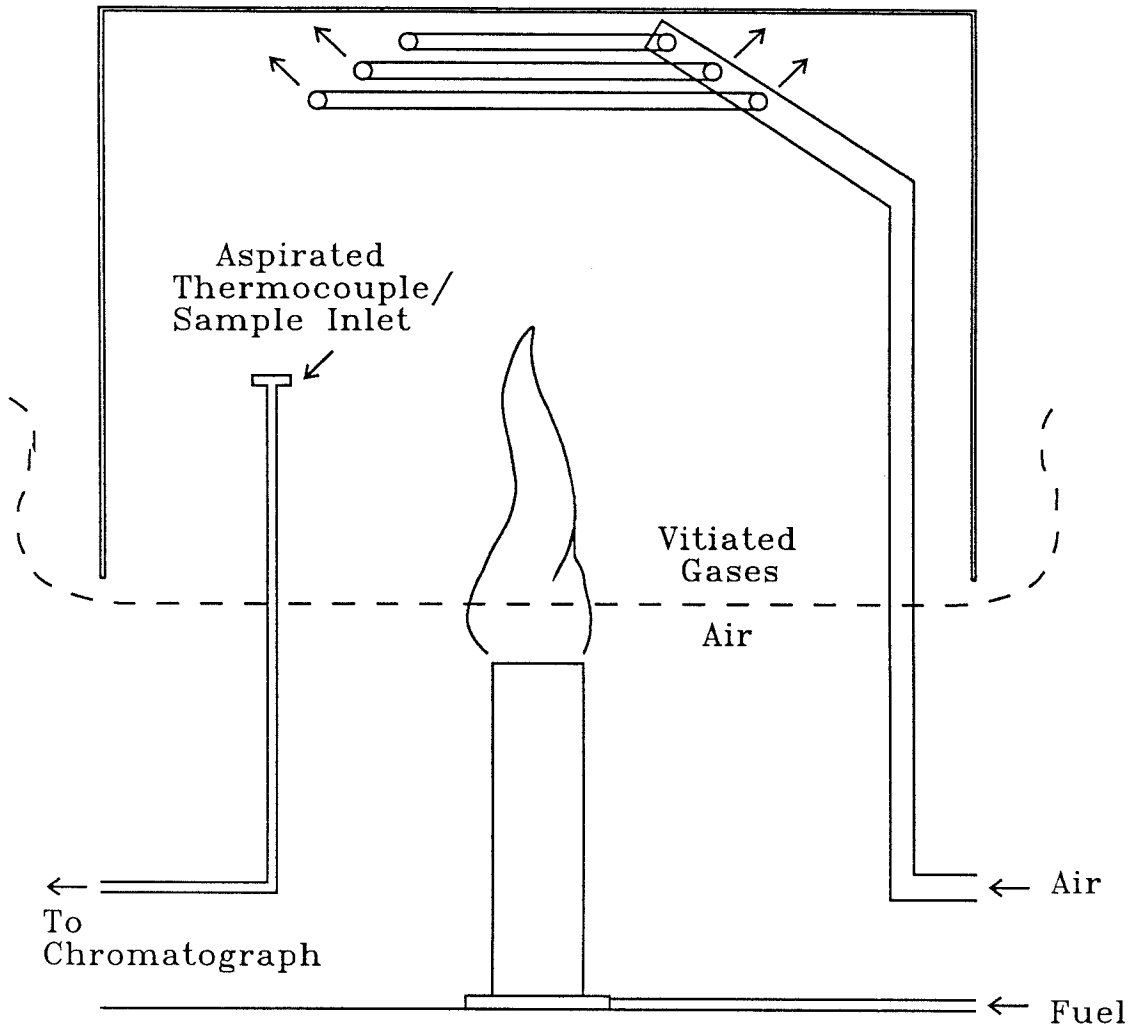

Figure 2.2: Schematic of experimental apparatus with air addition network used in this study

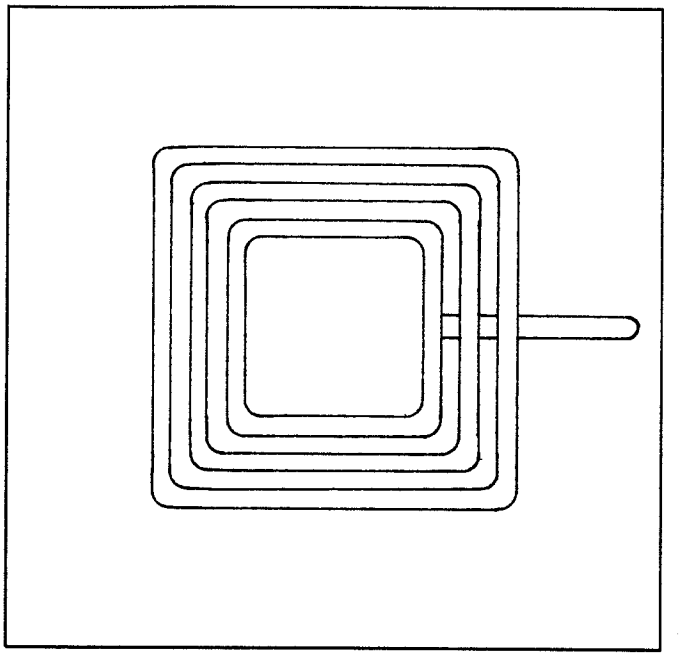

(a) Top view (through ceiling)

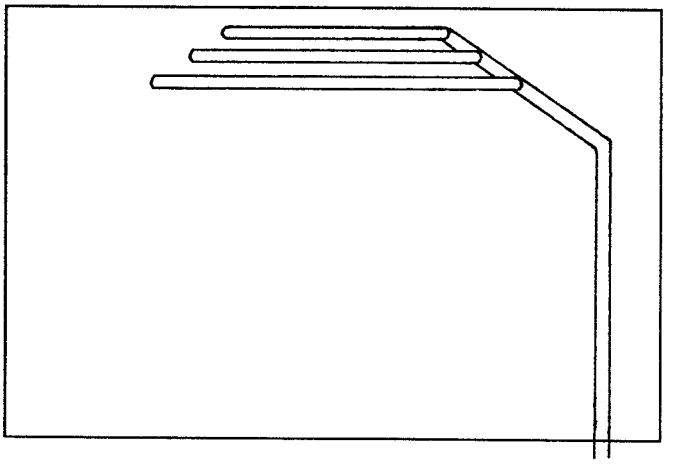

(b) Side view (showing injection orientation)

Figure 2.3: Views of hood with air addition network

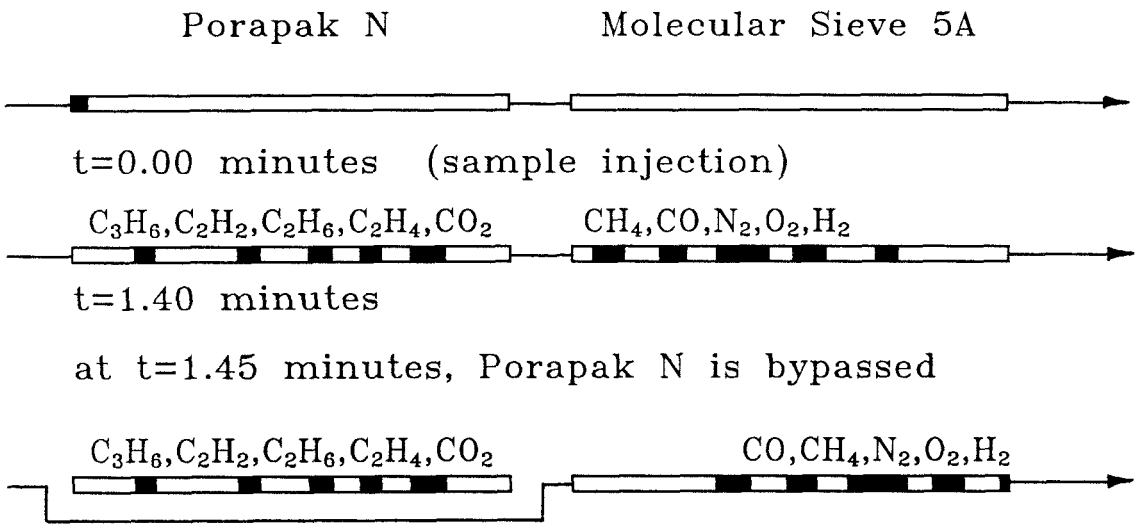

t= 1.86 minutes - hydrogen peak elutes
2.82 " - oxygen peak elutes
4.20 " - nitrogen peak elutes
6.03 " - methane peak elutes
10.81 " - carbon monoxide peak elutes

at t=13.50 minutes, Molecular Sieve 5A is bypassed
Porapak N is reinserted

t=14.51 minutes - carbon dioxide peak elutes
15.13 " - ethylene peak elutes
15.61 " - ethane peak elutes
16.68 " - acetylene peak elutes
24.36 " - propylene peak elutes

Figure 2.4: Time history of separations and component elutions

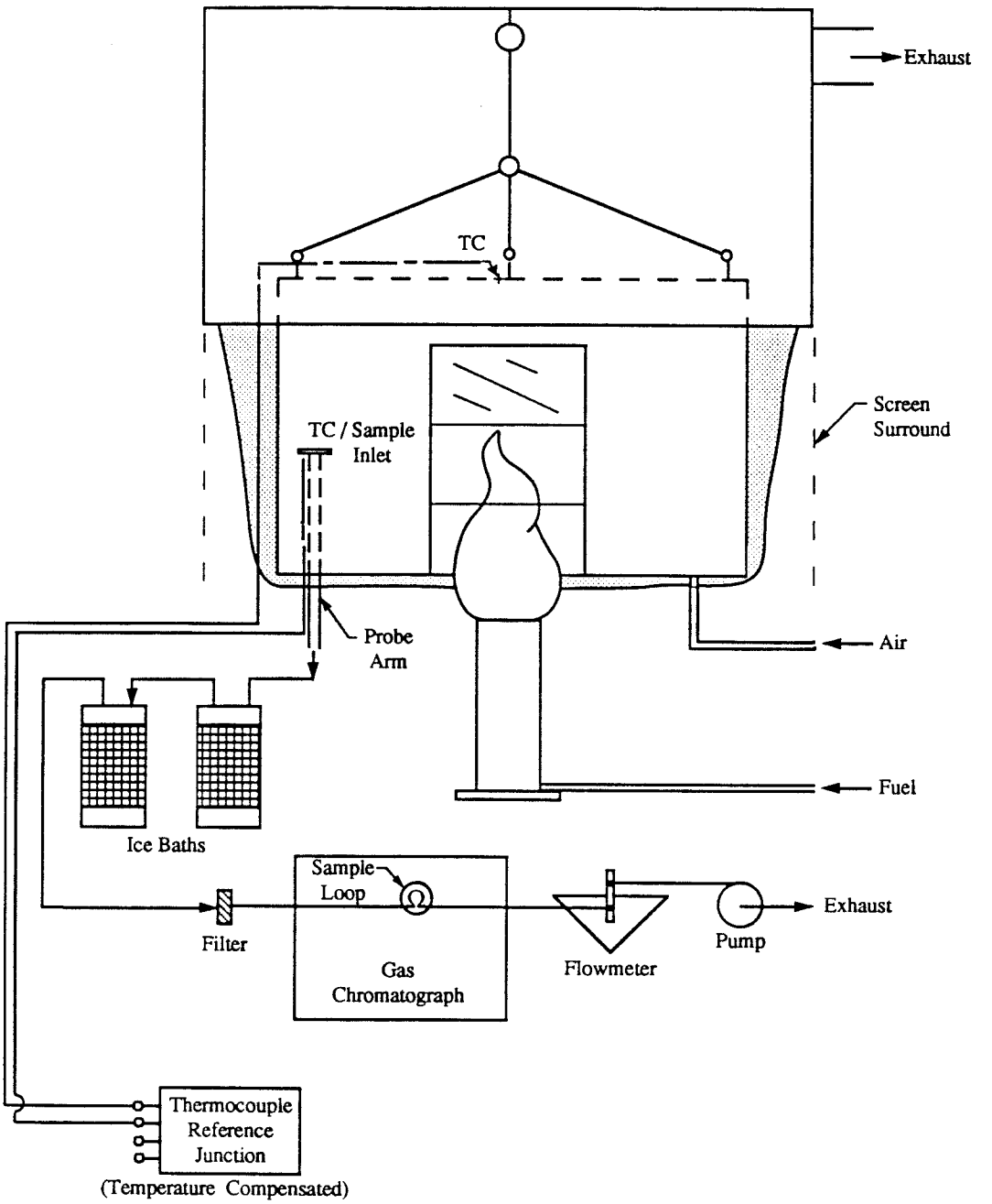

Figure 2.5: Schematic of gas burning and sample analysis facilities

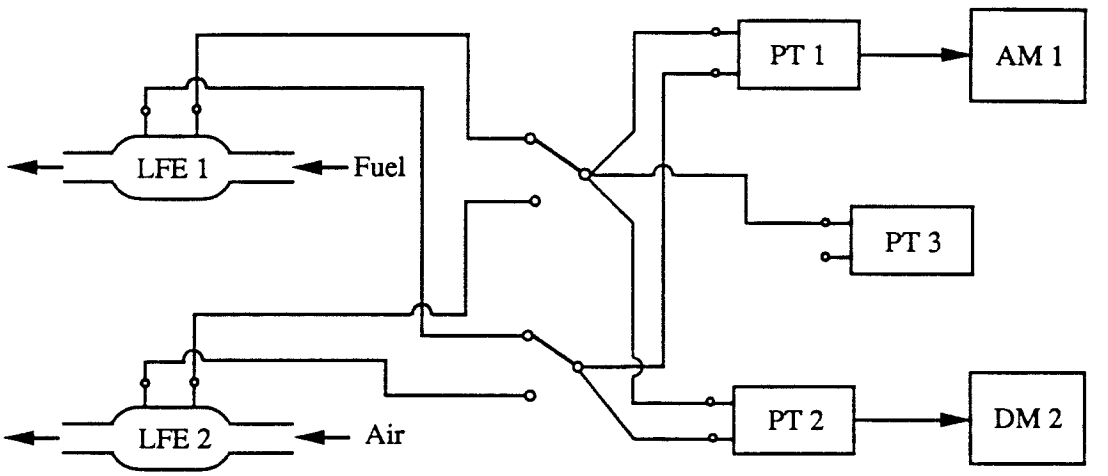

Figure 2.6: Diagram of flow monitoring systems

Chapter 3

Validation of the Experimental Method

Before any confidence can be placed in the experimental measurements, the issue of how well they represent the composition of the product layer must be addressed. For this experimental model and technique to prove satisfactory, several criteria must be considered:

- The product layer composition must be homogeneous and well stirred
- Air addition in the hood must mix rapidly (no stratification or pockets of higher O_2 concentration)
- The interface between the product layer and the laboratory air must be stable and not allow mixing
- The occurence of further chemical reactions in the sample probe cannot be permitted
- The condensed water vapor in the ice baths must not absorb measurably significant amounts of the other gas species
- The 0.1 μm filter must not remove measurably significant amounts of the gas species (even after a soot deposit is collected)

Once these issues have been resolved, it is then possible to present experimental measurements as an accurate representation of the product layer composition.

3.1 Homogeneity of the Product Layer

The two-layer room fire model describes the environment of an enclosure during a fire as consisting of a warm, stably stratified, homogeneous layer of combustion products mixed with entrained air above a cooler layer of unvitiated air. In the experiments performed with this apparatus, a continuous sample is withdrawn from the product layer with a variable-position probe. Of concern is the issue of how well stirred the product layer was in these experiments, i.e., did the chemistry or temperature measurements depend on the position of the probe within the hood? Also, the effects of air addition on the uniformity of the product layer must be considered.

A side view of the hood, shown in Figure 3.1, details the positions of the burner and the air addition network within the hood. The dashed line indicates

the perimeter of the range of possible probing positions when the bottom of the hood is 10 cm above the burner's surface. The highest elevation the probe can reach is 122 cm above the burner, thus for this interface height

$$(Z_{max} - Z_i) = 112 \text{ cm}$$

where Z_i is the height from the burner's surface to the position of the interface between the product layer gases and the laboratory air. The actual positions probed, labeled (A) through (G), are in a plane parallel to the front side and bisecting the hood's volume. Temperature measurements were slightly elevated (by about 40 K) due to the presence of a 5 cm thick layer of high temperature fiberglass insulation on the exterior ceiling of the hood.

3.1.1 Profiles of the Product Layer without Air Addition

The first set of experiments was performed without air addition to the upper layer. A 75 kW fire using natural gas fuel was stabilized on the 19 cm diameter burner. The gases accumulating within the hood were allowed to reach chemical and thermal equilibrium (temperatures were monitored using an aspirated thermocouple attached to the probe and a thermocouple mounted on the exterior ceiling of the hood) before beginning the measurements. The probe was moved to the positions indicated, in alphabetical order, where the temperatures were recorded and a gas sample was withdrawn and analyzed.

These experimental conditions provided an average upper layer equivalence ratio of 1.87, thus the 10 cm interface height did not allow for sufficient air entrainment to completely burn the natural gas fuel. Figures 3.2 and 3.3 show the data points of temperature and species mole fractions for the components measured by the chromatographic technique. Also shown are best fit curves for each data set. A maximum temperature of 615 K was measured in these tests, while the ambient temperature of the laboratory was 295 K. The data show that the product layer possesses uniform species concentration profiles throughout the hood for nitrogen, oxygen, carbon monoxide, carbon dioxide, methane and acetylene. Also, values for the mole fraction of water vapor determined by differencing are included. These observations are in keeping with those of Toner (1986) who found that species profiles in a similar apparatus varied by less than 5% over the range of positions probed. Figure 3.2 shows that a vertical temperature gradient existed within the hood. Although the temperatures at each elevation were nearly uniform, temperatures at the lowest positions probed were 80 K lower than those at the highest

elevations probed. Cetegen (1982) measured gas temperatures (in the same hood used by Toner) for an interface height of 30 cm and the same 19 cm diameter burner using natural gas fuel. For upper layer equivalence ratios of 0.75 and 1.0, temperature differences of 115 and 135 K, respectively, were measured over the same elevation change as in the present apparatus. Cetegen attributed this gradient in temperature to heat losses through the uninsulated side walls of the hood. Toner's measurements were performed with the same hood after insulation had been applied to the side walls, however, no profile of temperature measurements was reported.

3.1.2 Profiles of the Product Layer with Air Addition

A second set of experiments was performed with conditions identical to the first set, with the exception of air addition to the upper layer using the air injection network. Approximately 15.0 g/sec of air was added to the product layer, determined by subtracting the average entrainment rate of the first set of experiments from the total air addition rate of these experiments, computed from the chemistry measurements. This provided an average upper layer equivalence ratio of 0.880 which indicates that enough air was now being delivered to the product layer to burn all of the fuel. Since the gases were recirculated through the plume several times before exiting the hood, a significant reduction in the measurements of residual methane was expected. There was concern that samples withdrawn from positions nearest the air addition network might show artificially exaggerated entrainment rates due to the possibility of incomplete mixing. The probe position nearest the 1.6 mm diameter injection ports, position (G), was located 144 diameters from the closest injection port. It was expected that this distance would be sufficient to allow complete mixing and that the chemistry measurements would verify a homogeneous product layer. Indeed, Figures 3.4 and 3.5, which show the temperature and mole fraction data for these experiments, do confirm nearly uniform concentrations for the measured species at all elevations. Because the composition of the upper layer was slightly fuel-lean, more of the fuel was consumed and the product layer gases were about 60 K higher than the temperature at the same elevation in the experiments without air addition. The maximum temperature for this set of experiments was 665 K, and notably the gas temperatures at the highest elevations were 15 K higher than those of the insulated ceiling. Again a vertical temperature gradient was found, with measurements at

the lowest elevations being 62 K lower than those at the highest positions, thus the magnitude of the temperature gradient was slightly smaller for these experiments with air addition.

3.2 Effects of Removal of Water Vapor from the Sample

Gases from the ceiling layer are transported from the 9.5 mm diameter stainless steel tubing through two water-ice baths and a 0.1 μm filter to the sample loop of the gas chromatograph via 6.4 mm diameter flexible copper tubing. Multiple coils of this flexible tubing are submerged in each water-ice bath where the lowest coil acts as a reservoir for the condensed liquid.

For each experiment, a sample is continuously withdrawn for a period of 5 minutes (the time delay due to the volume of the sample line upstream of the chromatograph's sample loop is approximately 50 seconds, considering the pump's delivery rate). During this sample time enough water is condensed in the submerged coils to remove some of the soot in the sample gases. An obvious concern is that the condensed water may also absorb some of the other gas phase components of the sample which are measured by the chromatograph.

To investigate the possibility of gas sample components being absorbed in measurably significant amounts, calibrated gases were analyzed both directly and after being slowly bubbled through a 15 cm column of water. The calibrated gases contain roughly the same proportions of the species found in a dry sample of ceiling layer gases. If any substantial reductions in the peak areas occur for the calibrated gases passed through the water, then these changes can be attributed to absorption into the water.

A series of eight chromatographic analyses was performed with the direct injection of the calibrated gases into the sample loop. This provided a usable statistical base against which other tests could be compared. The sample probe was then positioned to withdraw from a "sample bag" which was partially inflated with the calibrated gases which had been bubbled through the column of water. Eight additional chromatographic analyses were performed to measure these gases and compare the peak areas with the earlier measurements.

Table 3.1 lists the average peak areas for the major species from both sets of tests. The standard deviation of the values for the first set are also included (and agree quite well with those for the second set of tests). These measurements show that no significant effect is caused by transporting the gases through the

condensed liquid. Except for the nitrogen peak areas, all of the average peak areas increased slightly (due to the dominance in the size of the nitrogen peak). Note that the measurements for each test were scaled to provide the same total area for all peaks. This procedure allowed the direct comparison of measurements since the pressure in the sample loop varied for each test, thus a different amount of total gas was introduced into the columns for each test. There was no effect, however, on the comparisons or the relative uncertainty of the measurements.

3.3 Effects of the Sample Line Filter

As mentioned at the beginning of this chapter, the 0.1 μm filter must not remove measurably significant amounts of the product gas components, even after a soot deposit is collected on the filter. To determine if this is the case, an additional series of chromatographic tests are performed with the calibrated sample gas. For these analyses, a soot-laden filter (resulting from a series of fuel-rich, two-layer experiments with natural gas fuel) is left in the sample path.

The results of these tests are given in Table 3.2 (second set of 5 tests), and are compared to the results of similar tests without the filter (first set of 5 tests). These normalized peak areas show that there was no measurable effect on the sample gas composition due to the presence of the filter. The peak areas reported here have been normalized by the nitrogen's peak area to identify changes in the relative amounts of the species. Because the filter assembly is maintained at ambient temperatures, its effect on the presence of any residual water vapor in the sample is unclear (note that the filter is placed after the ice baths). These effects are unimportant, however, since no effort is made to measure the water content during the experiments.

3.4 Chemical Reactions in the Sample Probe

The probe arm through which the upper layer gases were withdrawn was not cooled or shielded in any manner. Hence, the possibility of reactions between the gas-phase species present (or between the gaseous species and the probe material) was a concern. Since the probe tubing was submerged more than 60 cm into the upper layer, and was exposed to radiant heating from the flames, it is possible that the material attained temperatures sufficient to promote such reactions. Here we will describe the results of a series of chromatographic analyses of a calibrated sample gas aimed at determining the extent of these reactions occurring in the

probe arm.

The technique is simple – transport a known gas (the composition of which matches that produced in the experiments) through the same tubing material, subjecting it to the same elevated temperatures found in the experiments. The composition of the gas included 1.124% H_2, 1.963% O_2, 88.459% N_2, 2.029% CH_4, 0.965% CO, and 5.46% CO_2. A 100 cm length of the T-304 stainless steel tubing was exposed to the upper layer conditions, where the position of this inverted U-shaped section was approximately the same as for the probe during the experiments. The results of these chromatographic runs are given in Table 3.2 (third set of 5 tests), along with results from tests with the same sample treatment without the temperature elevation (first set of 5 tests). As indicated by the values of the relative standard deviations, σ_{rel}, the consistent agreement between these normalized peak areas shows that no significant changes occurred due to exposing the sample gas to the heated tube section. The larger uncertainty for the hydrogen peak areas is due to the amplification of the output signal necessary for detecting this small quantity of hydrogen with the small sample loop volume.

The larger concerns here involved the possibility of oxidation reactions occurring between the carbon monoxide and the oxygen available in the sample. Although they did not occur to a significant degree for the above tests, additional analyses were performed with copper tubing in place of the stainless steel, which gave a different result. When the sample gas was transported through an equal length of heated 6.4 mm diameter flexible copper refrigeration tubing, nearly 80% of the CO had combined with oxygen to form CO_2. When the tubing was heated further (up to 750 K), nearly all of the CO disappeared. Repeating the tests when the tubing was at ambient temperatures provided results which agreed well with those shown in Table 3.2. It appears that the heated copper line promotes this oxidation reaction, most likely due to catalytic effects of the copper itself, and not due to surface features or contaminants.

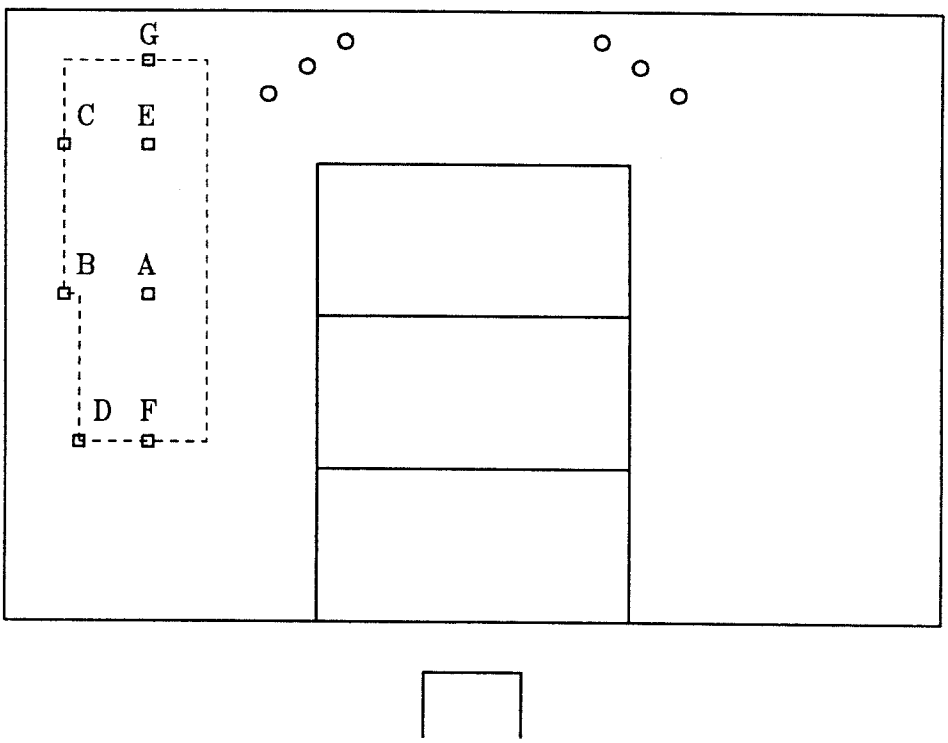

Figure 3.1: Range of possible probe positions with an interface height of 10 cm

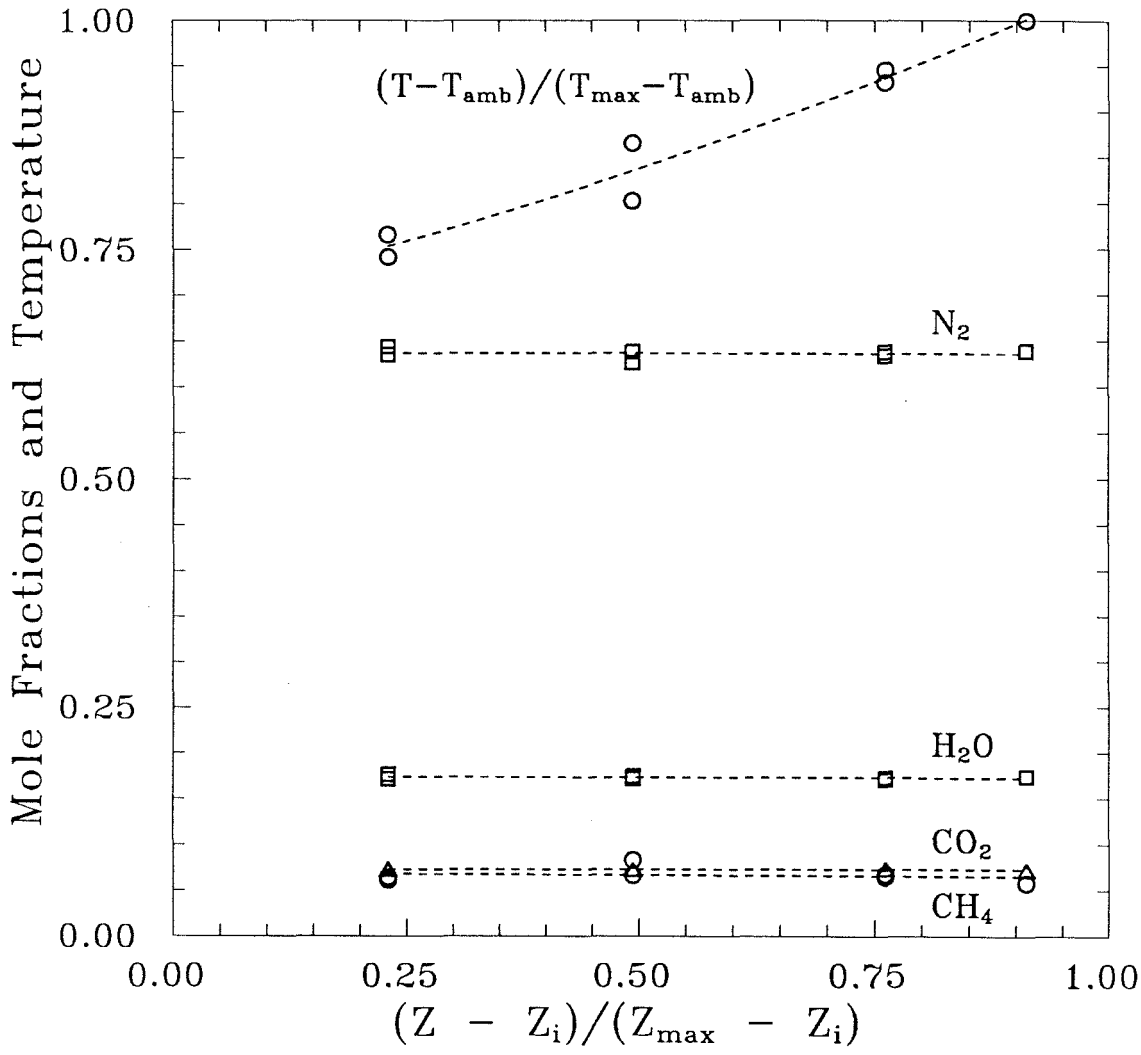

Figure 3.2: Temperature and concentration profiles without air addition

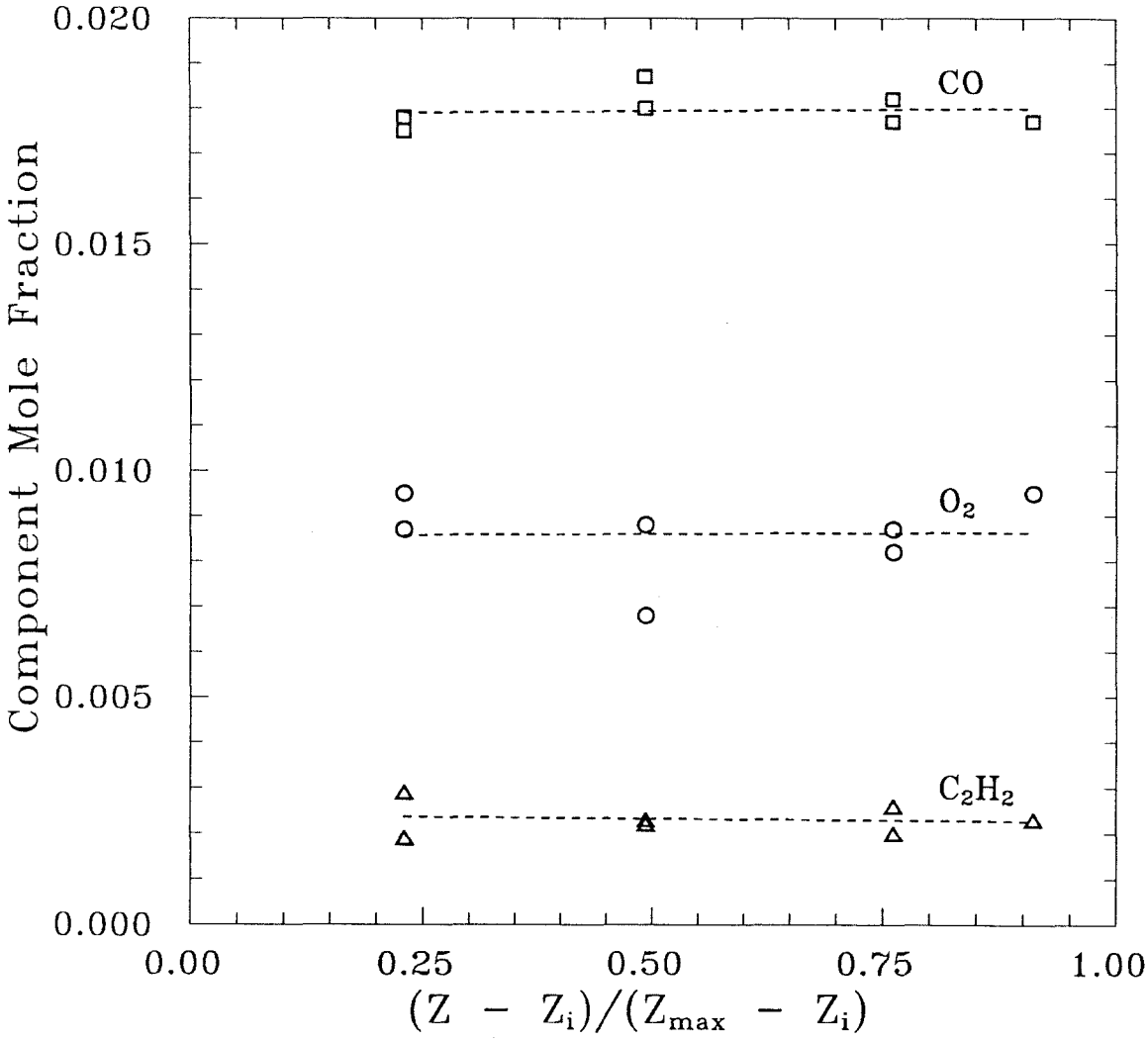

Figure 3.3: Concentration profiles without air addition

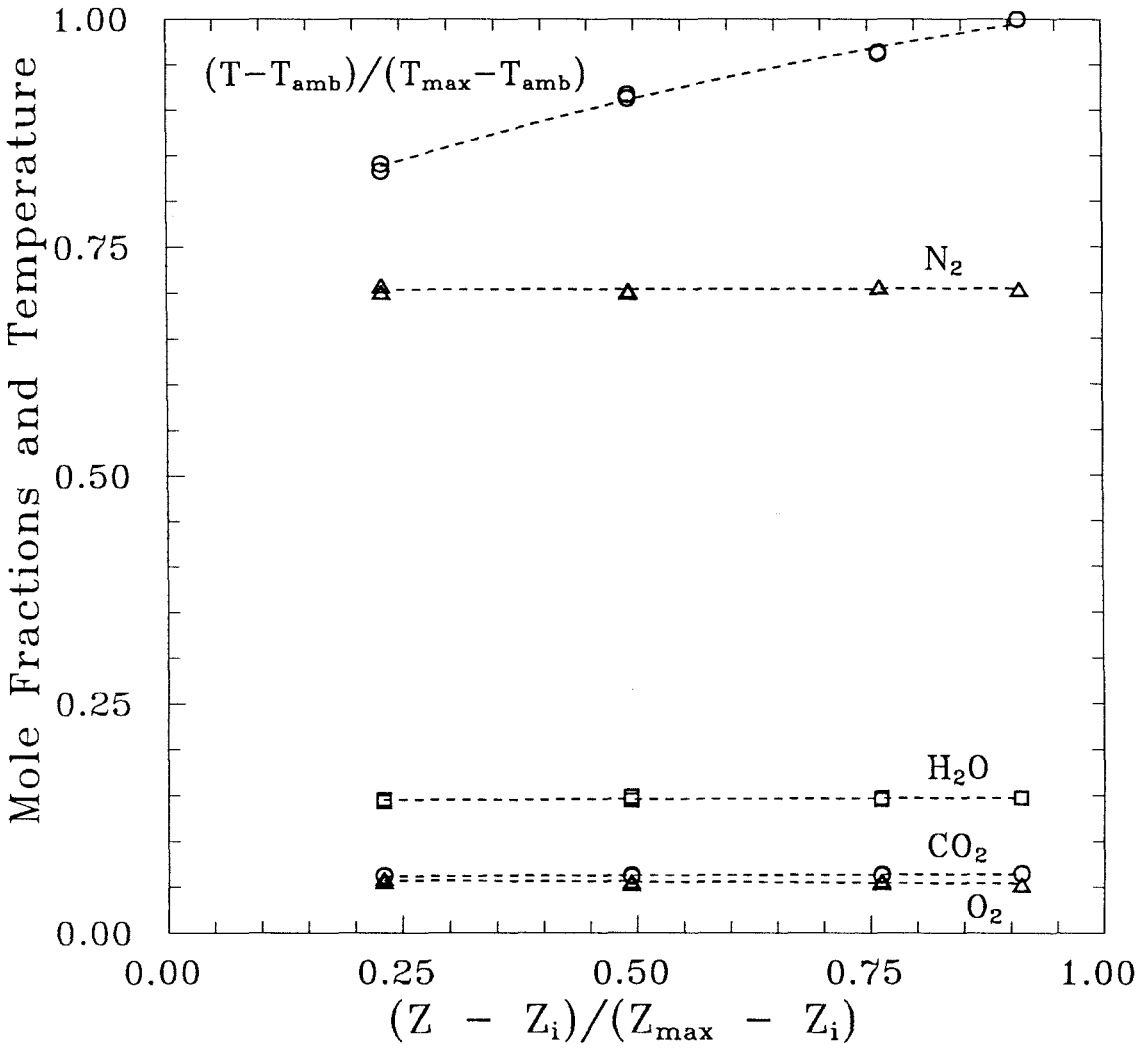

Figure 3.4: Temperature and concentration profiles with air addition

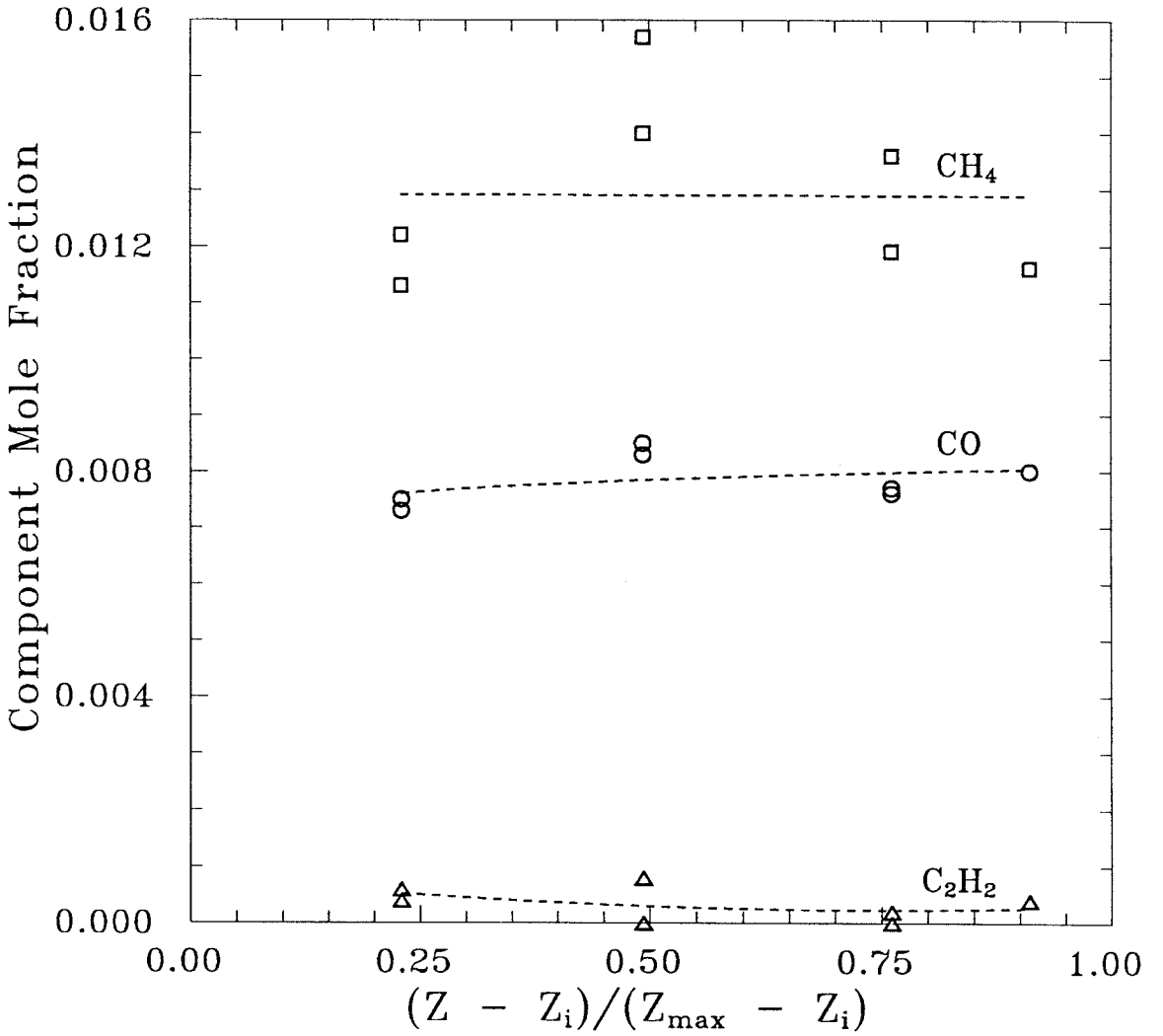

Figure 3.5: Concentration profiles with air addition

TABLE 3.1

Comparison of Average Peak Areas

Component	Mole Fraction	⟨ Peak Area ⟩ Direct	⟨ Peak Area ⟩ with H_2O	Δ %
O_2	.0196	51800 ± 4897	51921	0.2336
N_2	.8846	2324359 ± 4828	2321414	–.1267
CH_4	.0203	46968 ± 1383	48929	4.1752
CO	.0096	26186 ± 2170	27891	3.3689
CO_2	.0546	175495 ± 1471	179986	0.2798

TABLE 3.2

Comparison of Peak Areas with Varying Sample Treatment

1	2	3	β_{H_2}	β_{O_2}	β_{CH_4}	β_{CO}	β_{CO_2}	T (K)
x			6.517	7598	1913	1115	6356	amb
x			5.796	7532	1908	1106	6383	amb
x			7.086	7547	1922	1122	6393	amb
x			10.178	7537	1916	1125	6397	amb
x			7.419	7529	1915	1114	6396	amb
x	x		6.153	7559	1922	1146	6400	amb
x	x		6.629	7513	1916	1127	6418	amb
x	x		7.220	7506	1926	1136	6403	amb
x	x		8.489	7464	1929	1133	6416	amb
x	x		5.991	7530	1917	1117	6410	amb
x		x	5.356	7426	1917	1137	6413	580
x		x	6.567	7557	1911	1111	6423	601
x		x	8.626	7517	1908	1130	6412	601
x		x	8.733	7564	1908	1113	6413	602
x		x	9.051	7541	1909	1100	6416	602
Mole %			1.0	7.0	2.0	0.99	3.97	
σ_{rel} $(\sigma/\bar{\beta})$			19.1%	0.55%	0.37%	1.14%	0.27%	

1. Sample passed through ice baths
2. Sample passed through soot-laden filter
3. Sample passed through high temperature tubing

$\beta_i \equiv (peak\ area)_i/(peak\ area)_{N_2} \times 10^5$

Chapter 4

Species Production and Heat Release Rates in Natural Gas Fires burning in Two Layers

During the development of a fire within an enclosure, the flames will initially be exposed to an environment of air. Since an excess amount of oxygen is available to the flames at this stage, nearly all of the fuel is reacted to form stoichiometric products. Measurements of residual fuel and products of incomplete combustion in the plume gases are quite small for experiments conducted with unrestricted ventilation (McCaffrey and Harkleroad, 1988). The warm plume of combustion products mixed with entrained air rises to the ceiling of the enclosure where the gases are turned to spread radially outward in a ceiling jet. Once these gases reach the walls of the enclosure, the momentum of the jet gases is redirected downward. Buoyant forces cause the gases to fold back under the ceiling jet and begin creating a well-stirred layer of product gases mixed with entrained air. Eventually, the depth of this ceiling layer can extend to occupy a significant portion of the volume of the enclosure. The interface between the vitiated gases and the uncontaminated environment below can position itself so that some of the combustion processes occur in the ceiling layer. When flames burn in this two-layered configuration, the concentration of oxygen in the ceiling layer may be reduced to a small value and this vitiated gas will be entrained into that part of the fire plume which extends into the upper layer.

An investigation of combustion in two-layered fires by Cetegen (1982) used natural gas fuel and an experimental technique for creating the product layer similar to the method used in this study. A major portion of this work involved the description of entrainment into the fire plume in both the near and far fields. A study which was more concerned with the chemical species produced in two-layered fires was performed by Beyler (1983), who burned a variety of fuels and demonstrated that the composition of the product layer was sensitive to the molecular structure of the fuel. An extension of the work of Cetegen was described by Lim (1984) who took rough measurements of ceiling layer species for both fuel-lean and fuel-rich mixtures. Toner (1986) employed a chromatographic technique to measure the chemical species of the ceiling layer with more detail. The work of Cetegen, Lim, and Toner used natural gas fuel and the same experimental appa-

ratus to create the vitiated environment.

4.1 Equivalence Ratios

Two equivalence ratios are used to characterize the stoichiometry of the gases which enter the ceiling layer via the fire plume and the gases present in the ceiling layer. Neither of these parameters depend on the degree of completion of the combustion process.

If the case of steady supply rates of fuel and air is considered, as in this experimental approach, then the equivalence ratios can be defined in a straightforward manner. The fuel-air ratio of the gas entering the upper layer as a result of the flow in the fire plume, f_p, is defined by:

$$f_p = \frac{\dot{m}_{fuel}}{\dot{m}_{air,\ entrained}} \tag{4.1}$$

which is simply the ratio of the rates of mass addition to the upper layer of fuel and entrained air from the fire plume. The corresponding equivalence ratio, φ_p, is defined as:

$$\varphi_p = \frac{f_p}{f_s} = \frac{1}{f_s}\left(\frac{\dot{m}_{fuel}}{\dot{m}_{air,\ entrained}}\right) \tag{4.2}$$

where f_s is the fuel-air mass ratio for the stoichiometric reaction of the given fuel. Similarly, the fuel-air ratio for the upper layer, f_ℓ, is the ratio of the rate of mass flow of fuel supplied to the burner plus any fuel added directly to the upper layer to the rate of mass flow of the air entrained into the fire plume from the lower layer plus any additional air supplied to the upper layer. As before, the equivalence ratio for the layer, φ_ℓ, is given by:

$$\varphi_\ell = \frac{f_\ell}{f_s} = \frac{1}{f_s}\left(\frac{\dot{m}_{fuel,\ burner} + \dot{m}_{fuel,\ layer}}{\dot{m}_{air,\ entrained} + \dot{m}_{air,\ layer}}\right) \tag{4.3}$$

which describes the stoichiometry of the layer independent of that for the fire plume at the interface height.

For experiments where the rate of fuel mass flow supplied to the fire and the thickness of the ceiling layer are constant, and if no additional fuel or air is supplied to the upper layer, then the mass fractions of the elements within the upper layer quickly approach those of the gas supplied to the layer by the fire plume. In this case (which includes the experiments of Cetegen, Lim, and Toner), φ_ℓ will be equal to φ_p. In contrast, a rapid growth or decline in the rate at which

fuel is supplied to the flame or a growing ceiling layer can produce a situation in which the fuel-air ratio of the layer is much less or much greater than that of the plume, and φ_ℓ will be less than or greater than φ_p, respectively.

Now consider the more general case of a fire burning in an enclosure. If the enclosure is not ventilated, then the ceiling layer will develop quickly and its composition will reflect the history of the gases transported through the interface by the fire plume. In this case, both the fire's strength and the depth of the ceiling layer will be time dependent. Since the plume equivalence ratio is defined at the elevation of the interface between the ceiling layer and the room air below, the previous definition can be simply modified to accomodate the time varying quantities:

$$\varphi_p(t) = \frac{1}{f_s}\left(\frac{\dot{m}_{fuel}(t)}{\dot{m}_{air,\ entrained}(t)}\right)_{at\ interface\ height} \tag{4.4}$$

where the mass flow rates being delivered to the upper layer now reflect the unsteady nature of the problem. If the lower layer is not composed of air, but experiences contamination by combustion products or unburned fuel, then the effects on the plume equivalence ratio can be accounted for by adjusting the value of f_s.

The description of the equivalence ratio of the ceiling layer for this scenario must now reflect the complete time history of the material transported through the nonstationary interface. The assumption of upper layer homogeneity becomes important since the value of φ_ℓ is used to describe the entire ceiling layer (except for regions of active combustion which extend beyond the interface). For the case where none of the products of combustion are escaping from the enclosure, the upper layer equivalence ratio can be written:

$$\varphi_\ell(t) = \frac{1}{f_s}\left(\frac{\int_0^t \dot{m}_{fuel,\ plume}(\tau)\ d\tau + \int_0^t \dot{m}_{fuel,\ layer}(\tau)\ d\tau}{\int_0^t \dot{m}_{air,\ entrained}(\tau)\ d\tau + \int_0^t \dot{m}_{air,\ layer}(\tau)\ d\tau}\right) \tag{4.5}$$

which also accounts for sources of fuel and air in the ceiling layer.

In the case of a fire within an enclosure, the unsteady development of the ceiling layer can lead to significant differences in the values of the equivalence ratios. For example, consider the results of a computer model study of forced ventilation fires using exponential growth rates for fire sizes†. Figure 4.1 shows a comparison of the equivalence ratios for these fires with varying growth rate

† Performed by Professors T. Kubota and E. E. Zukoski, unpublished (1988).

coefficients. In each case, the growth continued until the fire size reached 200 kW, at which point the fire's strength was held constant. As the rate of growth was increased, the maximum deviation between the values of φ_ℓ and φ_p also increased. This behavior was due to the faster growth of the ceiling layer and a larger fire size at each point in the layer's development. It was possible to develop conditions where the plume equivalence ratio was almost 1.5 times the stoichiometric value while that for the upper layer was still about 0.5. The dotted line along the main diagonal of the plot, where $\varphi_\ell = \varphi_p$, indicates the conditions where the measurements of Cetegen, Lim, and Toner were taken.

4.2 Measurements of Product Species

Experiments were performed with natural gas fuel using the apparatus described in Chapter 2. Eight sets of experiments were conducted, each with matched test conditions (fuel flow rate, interface height, and burner diameter) and varying amounts of air added to the upper layer. The results from measurements of the gases in the upper layer are given in Figures 4.2 through 4.10 for the species determined by the chromatographic technique.

For each set of experiments, the first test was performed without air addition to the upper layer. Chemistry measurements allowed the computation of the entrainment rate of air from the lower layer into the fire plume. It was assumed that the entrainment rate for each test configuration was independent of the rate of air addition in the hood. The air addition rate determined from the chemistry measurements was then checked against direct flow rate measurements using a laminar flow element. These results can be found in section 4.3. The open symbol for each series represents data for the test without air addition; the corresponding filled symbols represent data taken with air addition to the upper layer using the same fuel flow rate and interface height. From the definitions of section 4.1, the effect of air addition to the upper layer is to reduce the equivalence ratio of the layer, while the value of φ_p remains unchanged. Each figure also contains information about the plume equivalence ratio and the height of the interface above the burner surface for each series of tests.

The most interesting feature of these results is that the mass fractions of the species are well correlated by the equivalence ratio of the upper layer. These measurements are from tests conducted with widely varying plume equivalence ratios, interface heights, and gas residence times (based on fluid-mechanical considera-

tions). For example, consider the data for a fire plume with an equivalence ratio of 2.17 which burns in a layer with equivalence ratios ranging from 2.17 down to 0.55. This data agrees well with the other experimental results which have plume equivalence ratios between 0.81 and 2.83, and shows the dominant influence of φ_ℓ on the species produced.

The measurements from tests with layer equivalence ratios below 0.5 follow those values predicted by equilibrium computations† for products formed at the temperatures observed in the experiments. No carbon monoxide, methane, hydrogen, or other hydrocarbons were detected at these conditions. Although the presence of these species begin to appear when φ_ℓ =0.5, the oxygen measurements do not begin to deviate from equilibrium values until φ_ℓ =0.7. For stoichiometric conditions (φ_ℓ =1), the point where products of incomplete combustion begin to be predicted by the equilibrium computations at these temperatures, significant levels of carbon monoxide and unburned fuels are measured (CO levels approach 0.9% and CH_4 levels are above 1.0% mass fraction). Hydrogen is not observed in the product gases until fuel-rich conditions are reached, and then it appears in levels slightly lower than those predicted at equilibrium. When the experimental conditions are fuel-rich (φ_ℓ >1), acetylene, ethane, and methane components are present in levels higher than those predicted by the equilibrium computations.

The measurements of Toner (1986) for natural gas fires burning in two-layered environments are also included in Figures 4.2 through 4.10, represented by crosses. Although all of the present data fall mostly on the same curve, this is slightly different behavior than the curve fitting the data of Toner for the range $\varphi_\ell > 0.75$. Since the hood used by Toner was insulated and smaller than the bare metal hood used here, the product layer temperatures in Toner's experiments were consistently higher for otherwise identical test conditions. The differences between the product layer chemistry measurements in these studies suggests that the temperature of the upper layer had an effect on the completion of the combustion process. This issue is discussed in detail in Chapter 5.

Toner measured small amounts of ethylene in the products of natural gas fires when conditions were fuel-rich ($\varphi_\ell > 1$), while none was detected in these experiments. Differences in the chromatographic techniques do not account for any loss in the ability to measure this component, thus it is possible that this

† CHEMKIN (Kee et al., 1980) was used for these computations, reported in Toner (1986).

difference in the presence of ethylene (not a component of the natural gas) may be real, not instrumental. Figures 4.9 and 4.10 show that there is generally good agreement between Toner's results and the present measurements for acetylene and ethane. Note that ethane is a component of the natural gas fuel (approximately 2.5% mole fraction), while acetylene is a by-product of the fuel-rich combustion process. This suggests that the upper layer species are not in equilibrium, despite the considerable residence times of the gases within the hood. It is interesting that unburned methane fuel (which possesses only single $H-C$ bonds) recombines into acetylene (which has a triple $C \equiv C$ bond), or as noted by Toner, into ethylene (which possesses a double $C = C$ bond). These observations were consistent for all fuel-rich tests where $\varphi_\ell > 1.25$. An examination of the stability of these upper layer species is found in section 5.3.

For this simple fuel, the toxicity of the product gases is primarily due to the presence of carbon monoxide. Unburned methane presents a breathing hazard only to the extent that it is an asphyxiant gas, and thus can displace oxygen during breathing‡. Figure 4.6 shows that when conditions are fuel-rich in the upper layer, levels of carbon monoxide rise to above 2.0%—concentrations high enough to be almost instantly lethal! Table 4.1 outlines the physiological effects of carbon monoxide on humans. For fuel-lean conditions in the upper layer ($\varphi_\ell < 0.5$), no measurable amounts of carbon monoxide were detected here. This observation agrees well with the experimental measurements of Cetegen (1982), Lim (1984), and Toner (1986), for natural gas fires, and also with the results of Faeth (1989), who probed laminar methane/air diffusion flames. Other studies with methane fuel have measured small amounts of carbon monoxide for this range of conditions (Tsuji and Yamaoka, 1967; Orloff et al., 1985), albeit with time-averaged samples taken from within the combusting regions.

4.3 Rates of Entrainment

‡ The hazards being addressed here are those due to chemical effects of product species on humans, besides the obvious fire and explosion risks. Methane gas is life-threatening only when present in concentrations which sufficiently impare or block oxygen intake. In contrast, carbon monoxide bonds to hemoglobin to form carboxyhemoglobin, and has a binding affinity of 220 to 280 times that of oxygen. Carbon monoxide remains the primary toxicant responsible for death in enclosure fires, despite the widespread use of plastics in building construction during the last thirty years (Babrauskas, 1989).

The rate of air entrainment into the fire plume from below the interface was determined for these experiments through the chemical species measurements, as described in Chapter 2. For each test configuration, the first experiment was performed without air addition after the upper layer gases and hood reached thermal equilibrium (about 30 minutes for most configurations). Flow visualization techniques demonstrated that the interface between the cool ambient air and the product layer gases was stable, except for the region disturbed by the penetration of the plume into the upper layer. The mass of air transported into the upper layer was then assumed to be that due to entrainment.

A major portion of the work by Cetegen (1982) dealt with describing and measuring rates of entrainment into fire plumes. He proposed models for entrainment over three separate regions of the flame—an initial (laminar) region, an intermediate (turbulent) transition region, and a far-field. His model predicted that the entrained mass flux would increase as $z^{3/4}$ over the initial region of the flame, and measurements from fuel-lean fires followed this behavior. From entrainment data, he found a transition height for the intermediate region of 60 to 70 cm (with the 10 and 19 cm diameter burners), thus the entrainment data of the present study fall within the initial region. Lim (1984) measured entrainment rates below interface heights of 1 to 23 cm using a product species analysis technique similar to Cetegen's. Although he did not propose a model to describe entrainment behavior, he reported that the data correlated well with the values presented by Cetegen. Lim also found that the entrainment rate was a weak function of the equivalence ratio of the layer and the heat release rate of the fire for these small interface heights.

Toner also measured entrainment rates of air below interface heights of 1 to 23 cm using a 19 cm diameter burner and natural gas fuel. His measurements show that the entrainment rate is nearly linear with height for the first 10 cm of the flame, and again linear for the rest of the plume above the first 10 cm, but with a different slope. When comparing his data to Cetegen's measurements, Toner used a 3/4–power fit to Cetegen's data. Toner noticed that an extention of the linear fit to his data also represented Cetegen's data for interface heights up to 80 cm, and indeed the linear fit does appear to represent the data even better than the 3/4–power fit for interface heights above 60 cm. However, since these data points were in the intermediate transition region, the initial region's model was no longer applicable. For the intermediate region, Cetegen's model predicted entrainment to behave as $z^{5/2}$, with some dependence on the heat release rate. For interface heights above 80 cm, neither the 3/4–power fit nor Toner's linear fit match the

data taken by Cetegen.

4.3.1 Measurements of Air Entrainment below the Interface

Entrainment into the fire plume was measured for interface heights of 5, 10, and 23 cm with heat release rates ranging from 40 to 67 kW. This data is presented in Figures 4.11 and 4.12 with the results of the other investigations where natural gas fuel was used. The fuel inlet Reynolds numbers (based on burner diameter) for these tests ranged from 500 to 830, while the inlet Richardson numbers (ratio of buoyant forces to momentum flux) ranged from 0.94 down to 0.34 (based on burner diameter and an approximate burner surface temperature of 675 K). For these tests without air addition, upper layer temperatures ranged from 500 to 610 K at the probed positions, while the hood temperatures (monitored above the plume impingement point) were 440 to 540 K. The upper layer temperature data and its effects are considered in Chapter 5 .

For interface heights less than 25 cm, the entrainment data of Cetegen, Lim, Toner, and the present study are shown in Figure 4.11. Although the scatter in the data increases for the larger interface heights, this trend does not follow any consistent correlation with the heat release rate. For instance, the large uncertainty in Lim's measurements with an interface height of 23 cm does not reflect the variation in fire size, but may be due to limited resolution in his measurements. With the 19 cm diameter burner, Cetegen took only a few measurements for this range of interface heights, leaving the verification of his initial region model questionable in the very near field.

In general, there appears to be agreement between the results of these studies, the trends showing larger entrainment rates with increasing interface heights, as expected. The models proposed by Cetegen and Toner are also plotted in these figures, represented as solid and dashed lines, respectively. Cetegen's initial region model consisted of a cylindrical reaction sheet extending upward from the burner until transition to turbulence occurs. He anticipated that actual entrainment rates would be somewhat larger due to increased consumption of fuel and air in a wrinkled flame sheet and the periodic production of vortical structures. Over this range of interface heights, however, this expected underestimation is not the case. Without developing a physical model, Toner offered a simple linear fit to his data, with a "kink" after the first 10 cm. For interface heights greater than 10 cm, the linear fit does pass through the origin, but this is not the case for the

near-field measurements, which are discussed below. This linear model also fits the measurements of Lim and the results of this study quite well.

Toner noted that his kinked linear fit predicted a nonzero amount of entrainment even when the interface height is zero. He attributed this to distortions of the interface due to the penetration of the fire plume and uncertainty in precisely locating the position of the interface (although he acknowledges that the magnitude of the uncertainty does not account for the offset). In the experiments of the present study, the position of the interface was marked by the presence of smoke in the product gases. The stably stratified interface positioned itself approximately even with the lower edges of the hood, except for around the perimeter where the exiting gases bulged downward as they escaped from beneath the walls of the hood. This was probably due to the redirection of the horizontal momentum (driven radially outward from the plume) of the upper layer gases after reaching the walls of the hood. Maximum horizontal exit velocities observed at the midpoint of each side ranged from 5 to 20 cm/sec, depending on the heat release rate and interface height.

The interface region adjacent to the plume experienced distortions due to the momentum of the penetrating plume gases. This disturbance region extended into the upper layer by as much as a full burner diameter, with an unsteady, plunging behavior. This is similar to the interface distortions mentioned by Toner, and may be the cause of the offset noted in Figure 4.11. As long as the plume flow was able to entrain air from below the interface (which occurred for zero interface heights), the disturbance region was present. When the burner's surface was submerged into the upper layer sufficiently so that only vitiated gases were re-entrained into the plume, there was no visible disturbance to the interface.

The entrainment measurements of Cetegen, Lim, Toner, and the present study are shown in Figure 4.12 for interface heights up to 1 meter. The models of Cetegen and Toner are again represented by the solid and dashed lines, respectively. As before, the scatter in the measurements increases with the larger interface heights. It is important to note that the entrainment behavior changes substantially for interface heights above 60–70 cm, as predicted by the turbulent transition region model of Cetegen, but for interface heights below 60–70 cm, Toner's fit appears to represent the data better.

Toner made comparisons of entrainment rates with the measurements of Beyler (1983), who worked with a variety of gas and liquid fuels (correlations of entrainment were based on the results of his experiments with propane). Since

these fuels are of higher molecular weight than the natural gas, and also radiate heat back to the fuel bed at different rates, the initial buoyancy of the fuels are quite different, which has an impact on the initial entrainment behavior and the production of the vortical structures in the plume. Since these vortical structures affect entrainment over the entire plume, it is not reasonable to compare the entrainment behavior of the different fuels.

4.3.2 Comparison of Air Addition Measurements

The air delivered into the upper portion of the hood through the air addition network was taken from within the laboratory, about 2 meters away from the enclosed region. The pressure differential across the laminar flow element in the air supply line was measured by two different pressure transducers, one monitored with an analog electronic manometer, the other with a digital electronic manometer (see Chapter 2). If we also consider the air addition measurement through the chemistry analysis, then we have three methods of determining the air addition rate into the hood. As a direct check on the accuracy of the chromatographic technique, we can compare these air addition measurements for a range of flow rates.

Figure 4.13 shows a comparison of the air addition measurements from each method, correlated as a function of the differential pressure across the laminar flow element as sensed by the transducer monitored with the digital manometer. Since none of the measurement techniques were exact, the choice of a standard was an arbitrary one, the only important values being the relative deviations between the measurements. Although the resolution of the pressure differential measurements was better on the analog manometer, reversing the standard did not have an impact on the comparisons.

The air flow rates measured by the differential pressure techniques agreed well over most of the conditions examined, but with some differences at the largest flow rates. The measurements from the chemical analyses were slightly less than the other values at the lower air flow rates, while at the highest flow rates this method provided values larger than the other measurement techniques. These differences may be the result of small uncertainties in the chromatographic technique being amplified in the data reduction scheme. It appears that the worst cases occurred when the air addition rate was set to its maximum value. A sensitivity analysis with the data reduction scheme showed that for large air addition rates, a 1%

change in the nitrogen peak measurement caused a 15.9% change in the air addition value. The carbon dioxide measurements were almost as sensitive, since a 1% change here caused a 13.9% change in I. The data of Figure 4.13 were taken from experiments which used the full range of possible air flow rates—limits were established by the supply fan's capabilities. Since the air supply network could provide enough air to widely vary the conditions of the experiments, the range of air supply rates was sufficient for our purposes.

4.4 Heat Release Rates

The heat release per mole of natural gas was approximated by considering the heat of combustion for the reaction, computed as though the reaction occurred at standard conditions (1 atm, 298 K). The enthalpy required to balance the equation, ΔH_r°, was calculated using the species concentration measurements of the gas within the upper layer. The results from these experiments, along with the results of Toner (1986), are shown in Figure 4.14. These values are normalized by the heat release expected for a stoichiometric reaction, also at standard conditions, of one mole of natural gas burning in air, ΔH_s°.

In the experiments of this study and in those of Toner, values of the ratio $\Delta H_r^\circ / \Delta H_s^\circ$ approached unity when the upper layer equivalence ratio was less than one. This is plausible since there was more than enough oxygen available to the flames, and nearly all of the fuel was consumed. For conditions near $\varphi_\ell = 1$, the measurements of this study follow a smooth decline, whereas the results of Toner show slightly higher heat release rates, but with larger scatter to the data. When φ_ℓ exceeded one, not all of the fuel was burned, due to a reduced availability of oxygen, thus the heat release in the fire plume decreased.

When conditions in the upper layer are fuel-rich, it is more useful to consider the consumption of the oxygen rather than of the fuel. Huggett (1980) noticed that the heat release from a fire involving conventional organic fuels is nearly constant for a fixed amount of oxygen consumed. Incomplete combustion has only a minor impact on this result. Following this idea, a limiting value for $\Delta H_r^\circ / \Delta H_s^\circ$ is shown as a solid line in Figure 4.14, and corresponds to the heat which would be released if the fuel and oxygen present react in stoichiometric proportions to form water and carbon dioxide, with excess species remaining in an unreacted state. For fuel-lean conditions, this limit reflects the complete consumption of the fuel with only stoichiometric products formed. When conditions are fuel-rich, this

limit reflects the complete consumption of the oxygen in the upper layer, again with only stoichiometric products formed (no incomplete combustion products), and the remaining fuel left unburned.

If we consider this limiting value as the maximum amount of heat release which could be expected, then it is possible to describe a combustion efficiency based on a comparison of our estimated heat release to this limit. Recasting the experimental data into this form, Figure 4.15 shows the ratio of the actual to the maximum amount of heat release in the two-layered natural gas fires. Also, best-fit curves are shown for the measurements from each study.

For fuel-lean conditions in the upper layer ($\varphi_\ell < 0.7$), our experimental measurements maintained values for $\Delta H_r^\circ / \Delta H_{max}^\circ$ greater than 0.95. In this range of stoichiometries ($\varphi_\ell < 1$), $\Delta H_{max}^\circ = \Delta H_s^\circ$ since it is the amount of fuel available which limits the heat release in the fire plume, i.e., all of the fuel is expected to be consumed when burning in the presence of excess oxygen. When the upper layer is fuel-rich ($\varphi_\ell > 1$), it is the amount of oxygen which limits the heat release, allowing only part of the fuel to be burned, thus $\Delta H_{max}^\circ = (1/\varphi_\ell)\Delta H_s^\circ$, which accounts for the reduction in the heat release due to the incomplete consumption of the fuel. In our experiments where the upper layer conditions were $0.7 < \varphi_\ell < 2.35$, larger amounts of unreacted fuel and air remained, with the lowest combustion efficiency near stoichiometric conditions. For this range, our measurements followed the behavior $\Delta H_r^\circ / \Delta H_{max}^\circ = 0.95 \times (0.7/\varphi_\ell)^{3/4}\varphi_\ell$, which reflects the reduction in the performance of the "plume reactor" due to the large amounts of incomplete combustion products. It is possible that further reactions were suppressed due to the relatively low upper layer temperatures (see Chapter 5 for the temperature measurements and the effects of layer temperature on combustion completeness). Although a limited amount of data is presented for more fuel-rich conditions ($\varphi_\ell > 2.35$), it appears that the measurements from this study match those of Toner, with a value for $\Delta H_r^\circ / \Delta H_{max}^\circ$ of 0.90. Toner proposed an approximate fit for his experiments over all conditions, $\Delta H_r^\circ / \Delta H_{max}^\circ = 0.90$. Figure 4.15 shows that his measurements are linearly approaching this value in the fuel-rich regime, while there is large scatter to the data under fuel-lean conditions. Toner attributes this to larger uncertainty in the species measurements for fuel-lean fires. The deviation between the estimates of combustion efficiency for these two studies is consistent with the idea that the reactions were not as complete in the fires burning in the larger, bare-metal hood of the present study.

4.5 Modeling Species Production and Heat Release Rates in Transient Fire Plumes burning in Two Layers

During the transient development of an enclosure fire and the corresponding ceiling layer, the rates of chemical species production and heat release by the fire are important parameters in modeling the progress of the fire and in evaluating its potential hazards. A method will be described here by which the steady state measurements of the upper layer species in our experiments (cf. section 4.2) can be used to predict the net production rate of chemical species and the net heat release rate in a large diffusion flame which penetrates far into a vitiated gas layer that has developed beneath the ceiling of the room (Figure 4.16 shows the configuration being modeled). This approach will provide a description applicable to the transient growth phase of the fire and ceiling layer, and when the interface between the vitiated gas layer and the room air nears the base of the fire.

In a room fire, the ceiling layer is a mixture of the products of combustion and air entrained into the fire plume from the lower air layer. Buoyancy effects produce a sharply defined interface between the ceiling layer and the room air. With restricted ventilation, the depth of this ceiling layer can become large enough to approach the base of the flame, causing the region of flaming combustion to penetrate far into the upper layer. The combustion processes will continue in the upper layer even when the oxygen content is virtually depleted there, since the fire can be supported by the air entrained into the plume from below the interface. For these conditions, the heat release rate is limited by the oxygen entrainment rate rather than the fuel flow rate. Most of the gas entrained into the fire plume, however, is entrained from the upper layer, thus the composition of the upper layer gas influences the characteristics of the combustion processes including the chemical species formed and the heat release rate.

When the fire burns in a steady condition (constant interface height and fire strength), the stoichiometry of the plume gases at the interface height will be equal to that of the upper layer gases, that is $\varphi_p = \varphi_\ell$. Measurement of the composition in the ceiling layer can then be used directly to develop a model for the calculation of net species production rates in the fire plume. During rapidly developing conditions, however, where the fire's strength and the depth of the ceiling layer grow quickly, there are significant differences between φ_p and φ_ℓ. For this transient case, the experimental measurement of φ_ℓ does not directly provide the information needed to predict the net production rates of chemical species in

the fire plume. Here we will describe a model which makes use of our steady state measurements to predict the rate of change of the species present and the rate of heat release in the ceiling layer of a room fire burning with restricted ventilation.

4.5.1 Correlation between a Transient Room Fire and the Experimental Model

In an accidental fire, gases from the fire plume impinge on the ceiling, spread radially in a thin ceiling jet, and mix rapidly with the gases present in the upper layer. Thus after the development of a ceiling layer, the fire plume extends into an upper layer which is well stirred and of nearly homogeneous composition (see Figure 4.16). The difference between φ_p and φ_ℓ reflects the time history of the composition of gases transported into the upper layer by the fire plume.

In our experimental model, where a hood is used to simulate the room (see Figure 4.17), the differences between φ_p and φ_ℓ are produced by adding gases to the upper portion of the hood above the top of the flame. Assuming that chemical reactions are absent outside of the fire plume, and that the added gases are well mixed before being re-entrained into the fire plume, then the experiment will model the conditions found in an actual fire in which the ceiling layer gas composition and fire characteristics are similar to those produced in the experimental hood.

4.5.2 Analytical Models

To determine the composition of the ceiling layer during transient fire conditions, we must calculate the rate at which the mass fractions of species present in the layer change with time due to reactions which occur in the fire plume. Consequently, it is necessary to be able to predict the net production rates of species in the fire plume. We can begin by treating the fire plume as a reactor, separate from the ceiling layer (see dashed lines in Figures 4.16 and 4.17). All chemical reactions are assumed to occur within this reactor, while in the mixing region (where gas addition to the upper layer occurs) and in the rest of the ceiling layer it is assumed that no reactions take place.

For the purpose of modeling the transient problem during the growth phase of the fire and ceiling layer, air is added to the upper layer in the experiment. This provides a more fuel-rich plume burning into an upper layer containing additional oxygen, which is the situation occurring in the developing room fire. The alternate circumstance where the fire strength is waning, or the ceiling layer is

receiving unburned fuel (possibly from an adjacent room experiencing earlier fire involvement), is modeled by the addition of fuel into the upper layer of the experiment. Due to safety reasons, only the growth phase of the fire was modeled through air addition to the upper layer, but these experimental measurements do provide some insight into the conditions in the declining fires.

4.5.2.1 Species Production Rates

Gases are entrained into the plume reactor from the ceiling layer along the vertical sides of the reactor at a rate $\dot{m}_\ell$ with species mass fractions $\chi_{\ell,i}$. These gases are returned to the ceiling layer by the flow from the top of the reactor. Species mass fractions in the flux of gases from the top of the reactor are $\chi_{u,i}$ and their corresponding mass flux, $\dot{m}_u$, is the sum of the mass flow rates of fuel from the fire, $\dot{m}_f$, the entrained air from the lower layer, $\dot{m}_e$, and gases entrained from the upper layer, $\dot{m}_\ell$. After mixing with the injected air, the mass fractions of the species are assumed to be identical to those found in the hood outside of the reactor and mixing regions.

The mass flux in the fire plume at interface height, $\dot{m}_p$, is the sum of the rates of entrainment from the lower layer, $\dot{m}_e$, and the fuel flow, $\dot{m}_f$:

$$\dot{m}_p = \dot{m}_e + \dot{m}_f. \tag{4.6}$$

In the fires of most interest here, $\dot{m}_\ell \gg \dot{m}_p$. In the experimental model, air is added in the mixing region at a rate $\dot{m}_a$, with species mass fractions $\chi_{a,i}$. In the experiments, the relationship between $\chi_{u,i}$ and $\chi_{\ell,i}$ is given by the conservation equation for the i^{th} species in the mixing process due to the addition of air. Since there are no reactions in this region,

$$\dot{m}_u\chi_{u,i} + \dot{m}_a\chi_{a,i} = (\dot{m}_u + \dot{m}_a)\chi_{\ell,i}.$$

A mass balance on the plume reactor provides:

$$\dot{m}_u = \dot{m}_p + \dot{m}_\ell$$

and now the mass balance for the i^{th} species in the mixing region can be expressed as:

$$\dot{m}_u\chi_{u,i} + \dot{m}_a\chi_{a,i} = (\dot{m}_p + \dot{m}_\ell + \dot{m}_a)\chi_{\ell,i}.$$

This relation can be solved for the flux of the i^{th} species present in the gas leaving the top of the plume reactor:

$$\dot{m}_u \chi_{u,i} = (\dot{m}_p + \dot{m}_\ell + \dot{m}_a)\chi_{\ell,i} - \dot{m}_a \chi_{a,i}. \tag{4.7}$$

The net generation rate of the i^{th} species in the fire plume is the difference between the mass flux of that species from the top of the fire plume and its rate of entrainment into the plume. It is convenient to write this difference in terms of the net mass flux into the ceiling layer from the fire plume, $\dot{m}_p$, and an effective mass fraction for the production rate of the i^{th} species, S_i, defined by the identity:

$$\dot{m}_p S_i = \dot{m}_u \chi_{u,i} - \dot{m}_\ell \chi_{\ell,i}. \tag{4.8}$$

Using equation (4.7) to eliminate the first term on the right-hand side of equation (4.8), this relationship can be rewritten in terms of the variables determined in the experiment. When $\dot{m}_\ell$ terms are eliminated, we obtain:

$$\dot{m}_p S_i = \dot{m}_p \chi_{\ell,i} + \dot{m}_a(\chi_{\ell,i} - \chi_{a,i}) \tag{4.9}$$

The value of $\dot{m}_a$, however, can be written in terms of the variables $\dot{m}_p$, φ_p, and φ_ℓ. In the experiments,

$$\varphi_p = \frac{1}{f_s}\frac{\dot{m}_f}{\dot{m}_e} \qquad \text{and} \qquad \varphi_\ell = \frac{1}{f_s}\frac{\dot{m}_f}{\dot{m}_e + \dot{m}_a}$$

so that

$$\frac{\dot{m}_a}{\dot{m}_f} = \frac{1}{f_s}\left(\frac{1}{\varphi_l} - \frac{1}{\varphi_p}\right) \qquad \text{and} \qquad \frac{\dot{m}_p}{\dot{m}_f} = 1 + \frac{1}{f_s}\left(\frac{1}{\varphi_p}\right).$$

The ratio of these results provides:

$$\frac{\dot{m}_a}{\dot{m}_p} = \frac{\varphi_p - \varphi_\ell}{\varphi_\ell(1 + f_s\varphi_p)} \tag{4.10}$$

and the substitution of this relation into equation (4.9) leads to:

$$S_i = \chi_{\ell,i} + \left\{\frac{\varphi_p - \varphi_\ell}{\varphi_\ell(1 + f_s\varphi_p)}\right\}(\chi_{\ell,i} - \chi_{a,i}). \tag{4.11}$$

Thus given the values for φ_p and φ_ℓ, the experimental measurements of $\chi_{\ell,i}$ (which are known as a function of φ_ℓ), and the stoichiometric fuel-air ratio, f_s, equation (4.11) can be used to determine the mass fractions of the effective source,

S_i. Additionally, when the values of the entrainment rate, $\dot{m}_e$, and the fuel flow rate, $\dot{m}_f$, can be estimated, $\dot{m}_p$ can also be determined from equation (4.6). Note that although the values of $\chi_{\ell,i}$ measured in the experiment depend primarily on φ_ℓ, values of S_i depend on both φ_p and φ_ℓ.

4.5.2.2 Heat Addition Rates

Heat addition to the upper layer due to the combustion processes can be found from an energy balance on the plume reactor. Let $H_{j,i}$ represent the enthalpy including the heat of formation, $\Delta H^\circ_{j,i}$, of the i^{th} species at the j^{th} position, and let $h_{j,i}$ indicate the corresponding sensible enthalpy. The enthalpy per unit mass due to the flux of the i^{th} species leaving the top of the reactor can then be expressed as:

$$H_{u,i} = \Delta H^\circ_{u,i} + h_{u,i} = \Delta H^\circ_{u,i} + \int_{T_\circ}^{T} c_{p,i}(T')dT'$$

with similar terms representing the enthalpy of the fuel, the air entrained from the lower layer, and the vitiated gases re-entrained into the plume.

Since we assume that chemical reactions within the ceiling layer are negligible, the energy balance for the layer can be expressed in terms of sensible enthalpies, as the heat of formation terms can be eliminated from the equation. The net flux of sensible enthalpy from the reactor to the ceiling layer due to the fire plume is:

$$\sum_i (\dot{m}_u \chi_{u,i} h_{u,i} - \dot{m}_\ell \chi_{\ell,i} h_{\ell,i}) = \sum_i (\dot{m}_p S_i h_{p,i}) \equiv \dot{m}_p h_p \qquad (4.12)$$

where $\dot{m}_p$ is the net mass flux from the reactor to the ceiling layer, and h_p is defined by this equation as the effective sensible enthalpy carried by the flux $\dot{m}_p$ from the plume reactor to the ceiling layer.

The energy balance for the plume reactor, where all of the chemical reactions are assumed to occur, must be written in terms of $H_{j,i}$:

$$\sum_i (\dot{m}_u \chi_{u,i} H_{u,i}) = \sum_i (\dot{m}_\ell \chi_{\ell,i} H_{\ell,i} + \dot{m}_e \chi_{e,i} H_{e,i} + \dot{m}_f \chi_{f,i} H_{f,i}) - \dot{Q}_{rad} \qquad (4.13)$$

where $\dot{Q}_{rad}$ is the net radiant energy from the reactor lost to the upper layer gases and surroundings. Equation (4.13) can be rearranged to solve for the terms which appear on the left-hand side of equation (4.12), once the heat of formation and

sensible enthalpy terms are separated. The use of equation (4.8) allows this result to be written:

$$\dot{m}_p h_p = \sum_i (\dot{m}_e \chi_{e,i} H_{e,i} + \dot{m}_f \chi_{f,i} H_{f,i} - \dot{m}_p S_i \Delta H^\circ_{p,i}) - \dot{Q}_{rad} \tag{4.14}$$

or

$$h_p = \sum_i \left\{ \frac{\dot{m}_e}{\dot{m}_p} \chi_{e,i} H_{e,i} + \frac{\dot{m}_f}{\dot{m}_p} \chi_{f,i} H_{f,i} - S_i \Delta H^\circ_{p,i} \right\} - \frac{\dot{Q}_{rad}}{\dot{m}_p}. \tag{4.15}$$

Modeling the radiant losses from the plume is a difficult problem for practically any flame configuration, and is further complicated by the additional complexities of our two-layered arrangement. As a simple approximation to this term, we will assume that the energy lost by radiation is some fraction, ε, of the approximate heat release in the reaction, ΔH°_r. This provides:

$$\dot{Q}_{rad} = \varepsilon \Delta H^\circ_r = \varepsilon \sum_i (\dot{m}_u \chi_{u,i} \Delta H^\circ_{u,i} - \dot{m}_f \chi_{f,i} \Delta H^\circ_{f,i} - \dot{m}_e \chi_{e,i} \Delta H^\circ_{e,i} - \dot{m}_\ell \chi_{\ell,i} \Delta H^\circ_{\ell,i})$$

or, with the use of equation (4.8),

$$\frac{\dot{Q}_{rad}}{\dot{m}_p} = \varepsilon \sum_i \left\{ S_i \Delta H^\circ_{p,i} - \frac{\dot{m}_f}{\dot{m}_p} \chi_{f,i} \Delta H^\circ_{f,i} - \frac{\dot{m}_e}{\dot{m}_p} \chi_{e,i} \Delta H^\circ_{e,i} \right\}.$$

Using this approximation in equation (4.15) gives the following result:

$$h_p = \sum_i \left\{ \frac{\dot{m}_e}{\dot{m}_p} \chi_{e,i} (H_{e,i} - \varepsilon \Delta H^\circ_{e,i}) + \frac{\dot{m}_f}{\dot{m}_p} \chi_{f,i} (H_{f,i} - \varepsilon \Delta H^\circ_{f,i}) - (1-\varepsilon) S_i \Delta H^\circ_{p,i} \right\}. \tag{4.16}$$

The fraction of heat released from the fire plume by radiation ($0 < \varepsilon < 1$) is dependent on several factors. Radiant losses in free-burning fire plumes range from 15 to 40%, depending on the fuel type. The configuration of the fire plume in the room, as well as the aspect ratio of the combusting regions to the enclosure walls, will affect these losses. Additionally, smoke obscuration and the other contents of the ceiling layer gas will impact on the radiation exchange with this participating media. Since no approximate value for ε is applicable to all possible situations, we recommend that any computation attempting to model this problem be carried out with an understanding of the net radiant exchange taking place, allowing for a reasonable approximation to be determined for the circumstances.

The ratios $\dot{m}_e/\dot{m}_p$ and $\dot{m}_f/\dot{m}_p$ can be obtained from equation (4.6) and from experimentally measured quantities. When the gaseous form of the pyrolysis products from a solid or liquid fuel are known, $H_{j,i}$ and $\Delta H^\circ_{j,i}$ can be found from tabulated values. Given this information, equation (4.16) can be used to estimate the

enthalpy flux into the upper layer required to model the heat input to the layer from the fire.

In summary, the equivalent mass source term for the i^{th} species due to the fire plume can be expressed in the form $\dot{m}_p S_i$ and determined from equations (4.6) and (4.11), and the enthalpy flux term (heat addition term) can be put in the form $\dot{m}_p h_p$, and is given by equation (4.16).

The rate of change of the mass of gases and the mass of the i^{th} species in the ceiling layer due to flow and chemical reactions occurring in the fire plume are given by:

$$\frac{dM_\ell}{dt} = \dot{m}_p \qquad \text{and} \qquad \frac{d(M_\ell \chi_{\ell,i})}{dt} = \dot{m}_p S_i \tag{4.17}$$

where M_ℓ is the total mass of the gases in the ceiling layer. The rate of change of internal energy of the ceiling layer, e_ℓ, due to the fire plume will be of the form:

$$\frac{d(M_\ell e_\ell)}{dt} = \dot{m}_p h_p. \tag{4.18}$$

The relationships given in equations (4.17) and (4.18) are the results necessary in two-layered fire models to describe species production and heat release rates in unsteady fires.

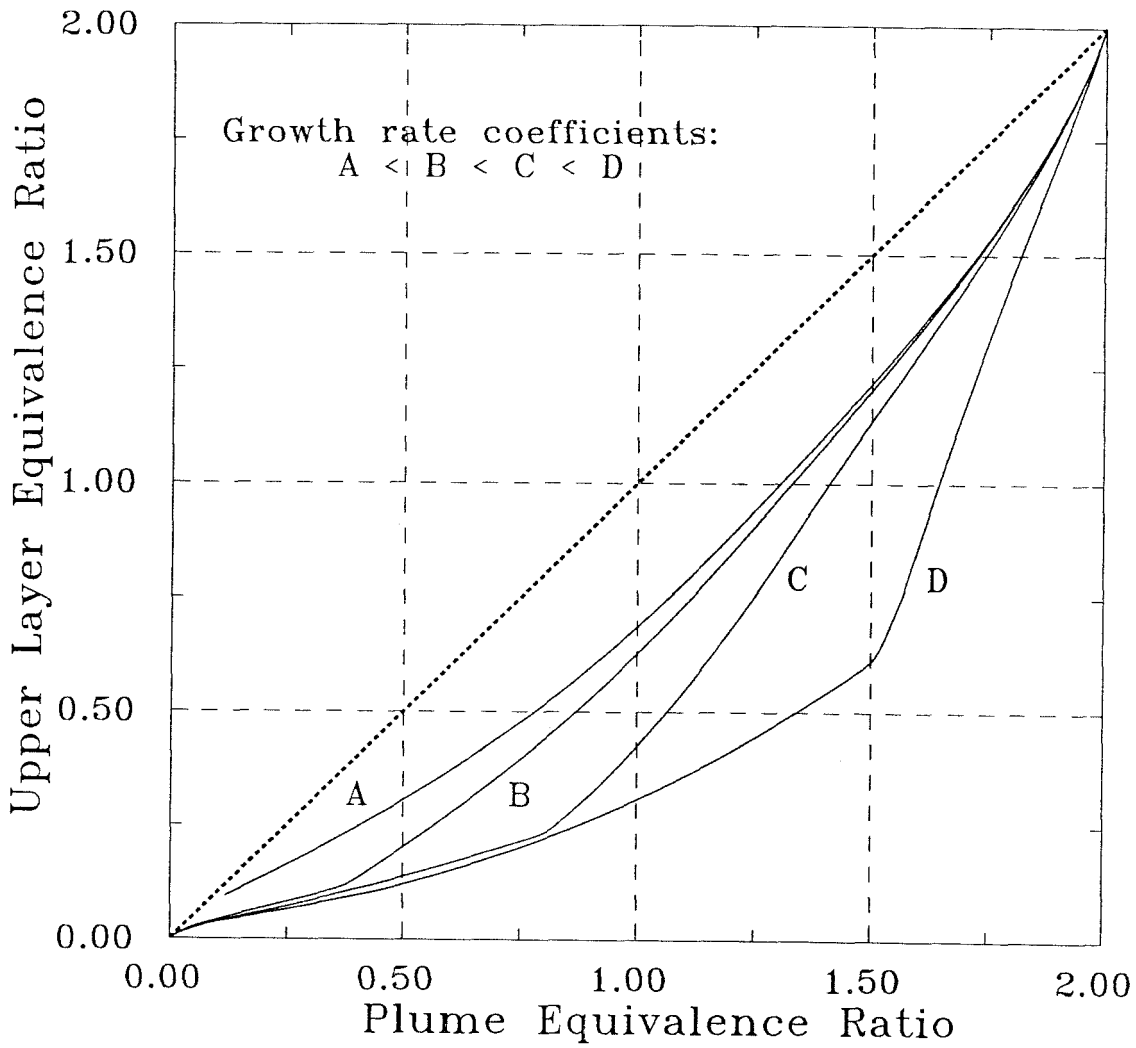

Figure 4.1: Comparison of equivalence ratios for forced ventilation fires with exponential growth rates

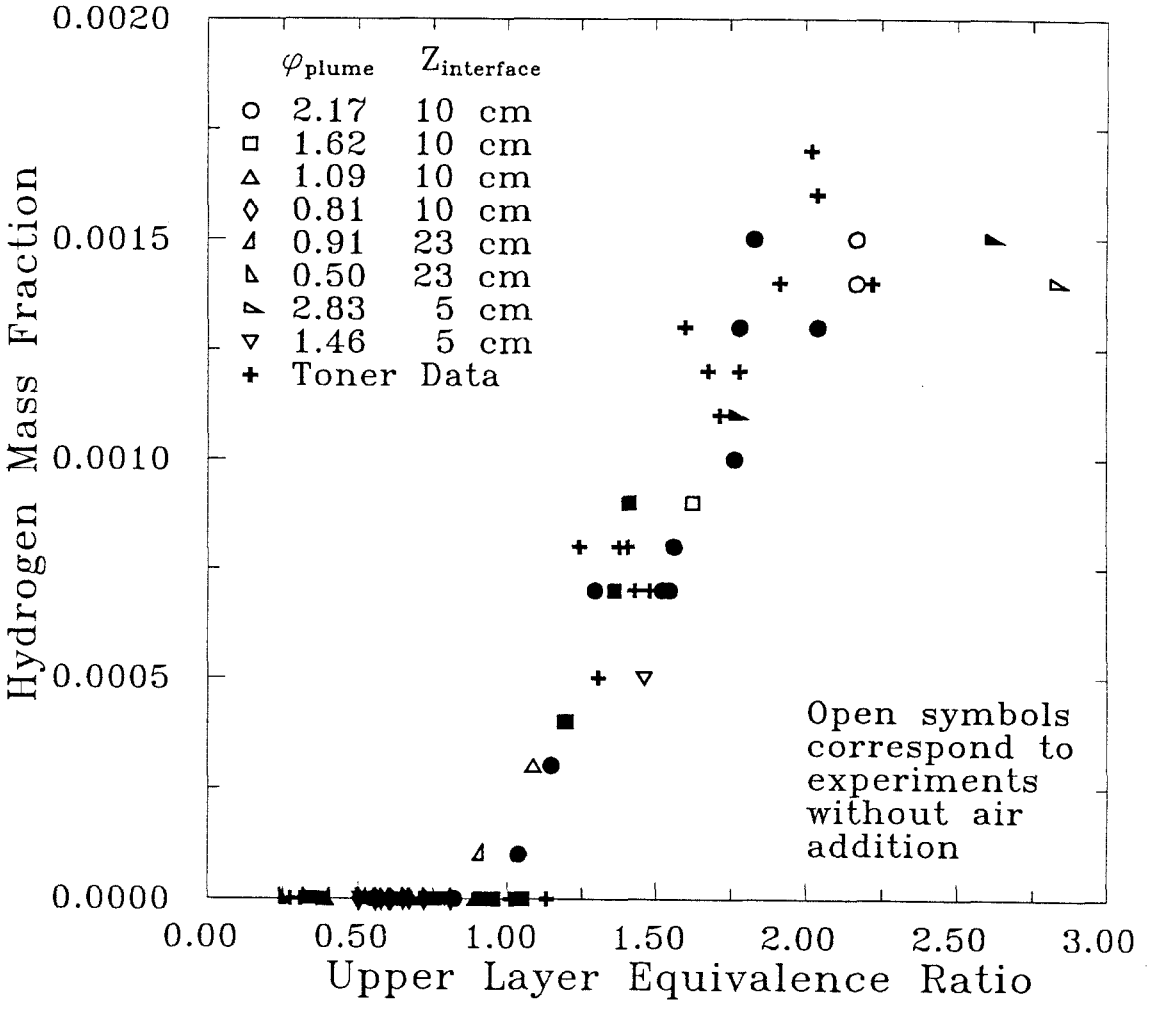

Figure 4.2: Hydrogen measurements for natural gas fires burning in two layers

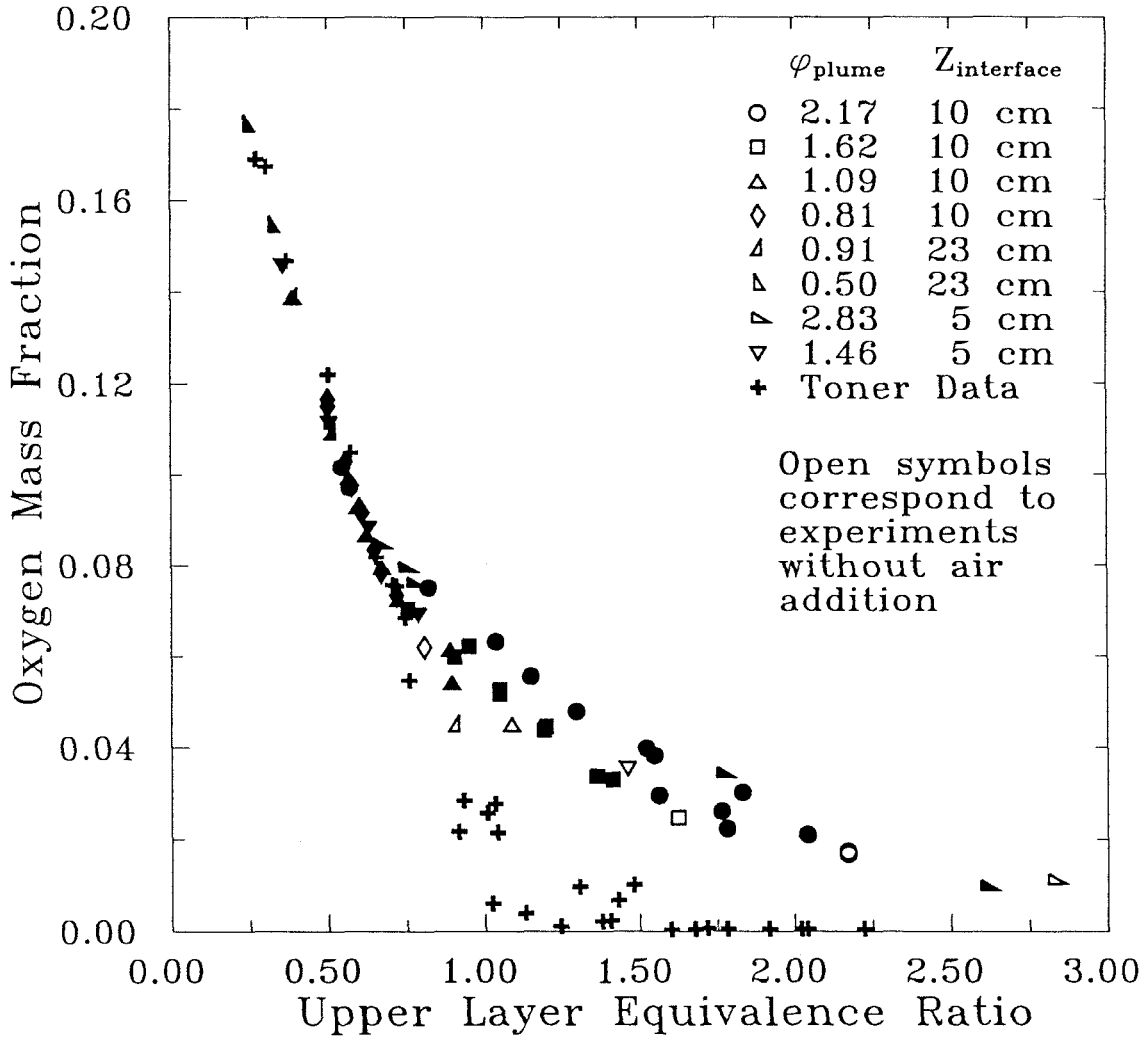

Figure 4.3: Oxygen measurements for natural gas fires burning in two layers

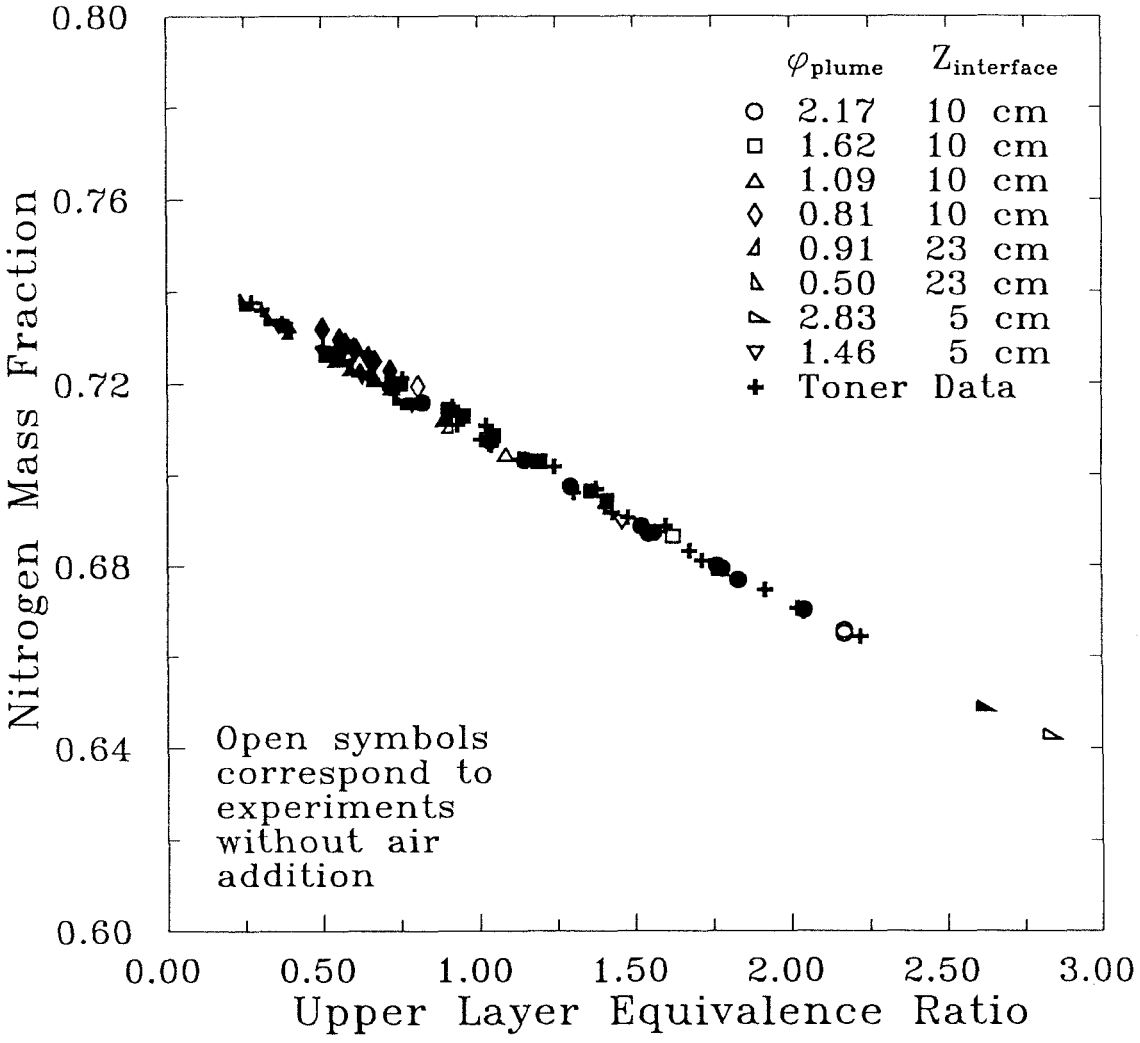

Figure 4.4: Nitrogen measurements for natural gas fires burning in two layers

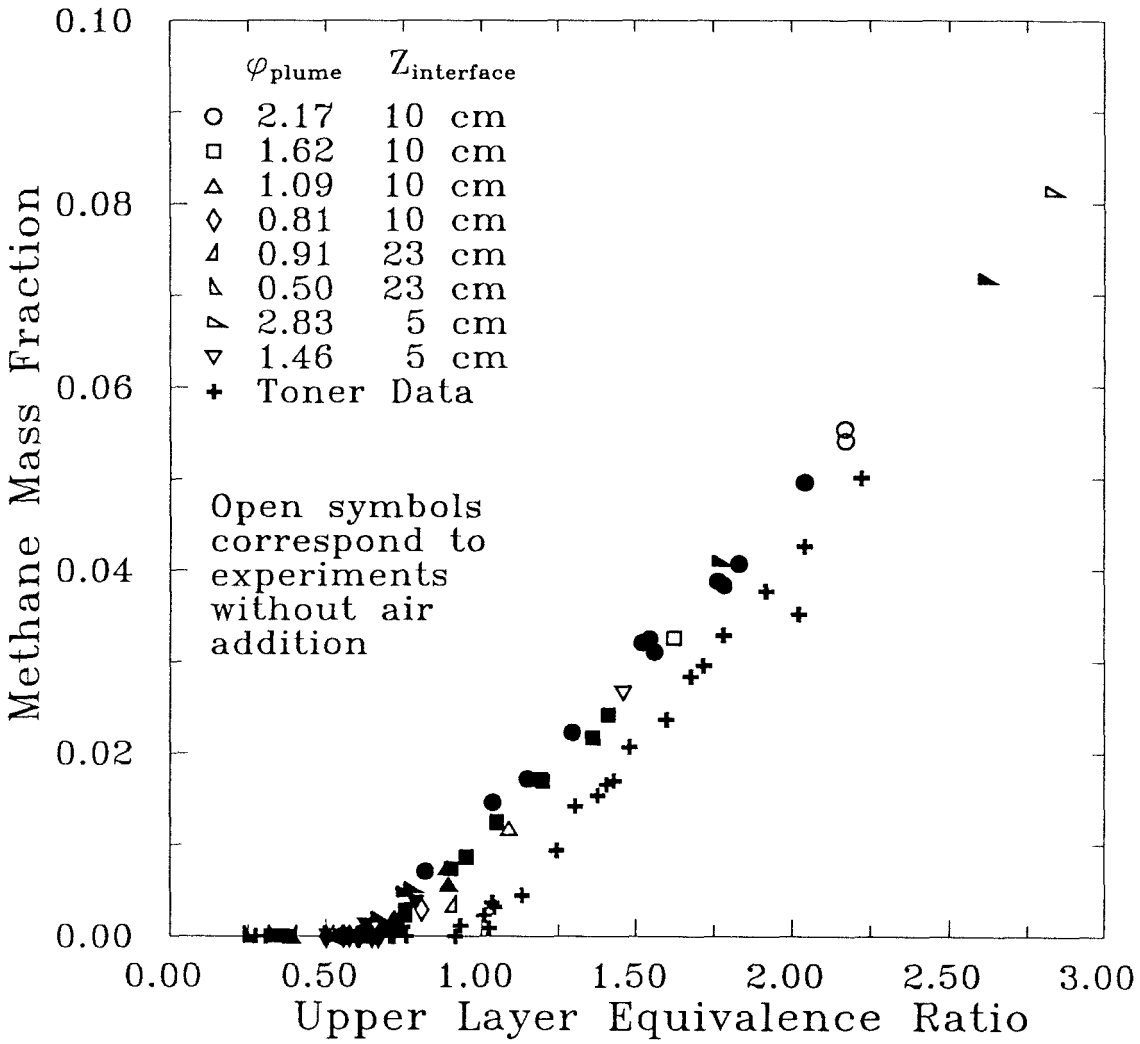

Figure 4.5: Methane measurements for natural gas fires burning in two layers

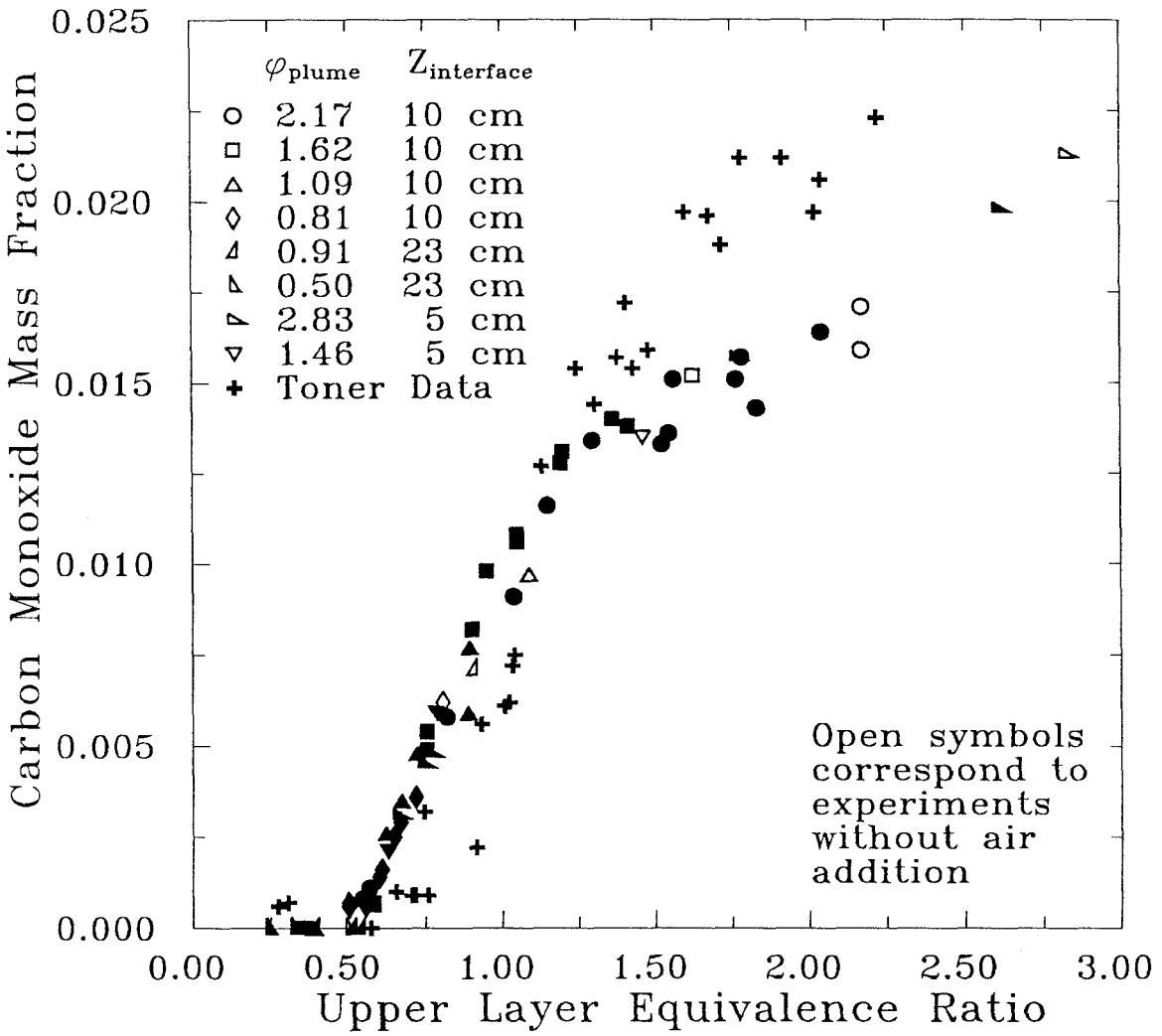

Figure 4.6: Carbon monoxide measurements for natural gas fires burning in two layers

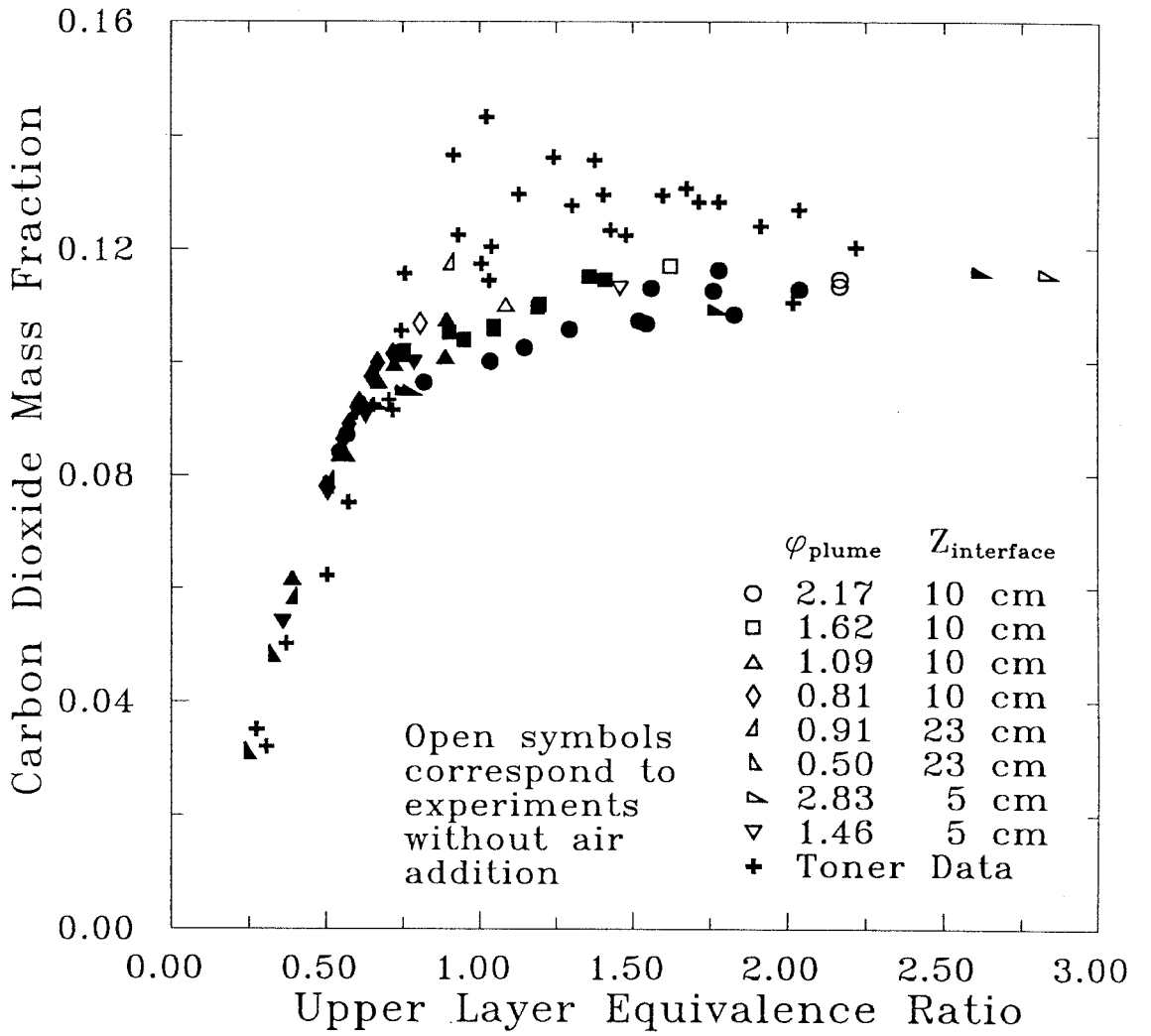

Figure 4.7: Carbon dioxide measurements for natural gas fires burning in two layers

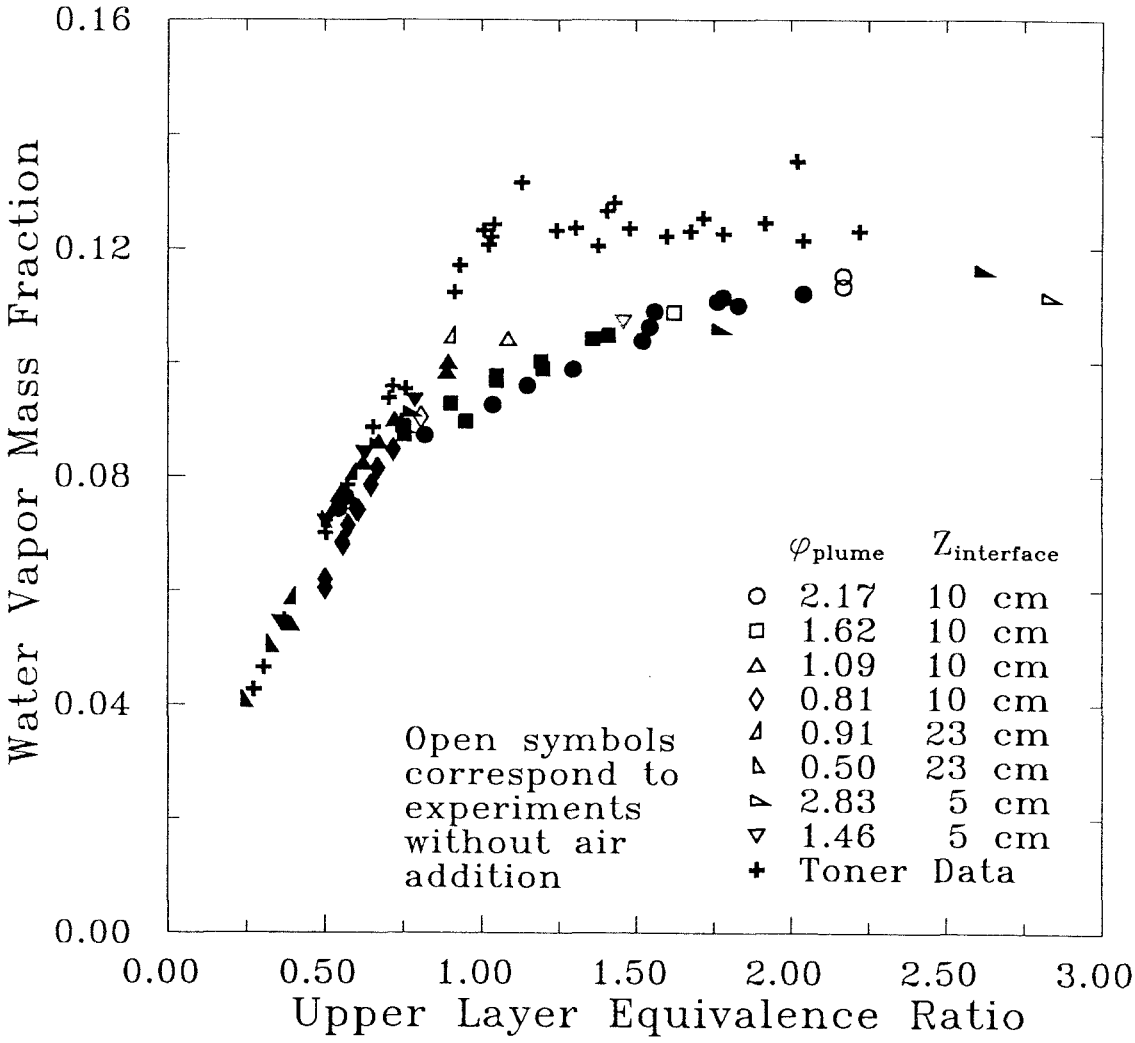

Figure 4.8: Water vapor measurements for natural gas fires burning in two layers

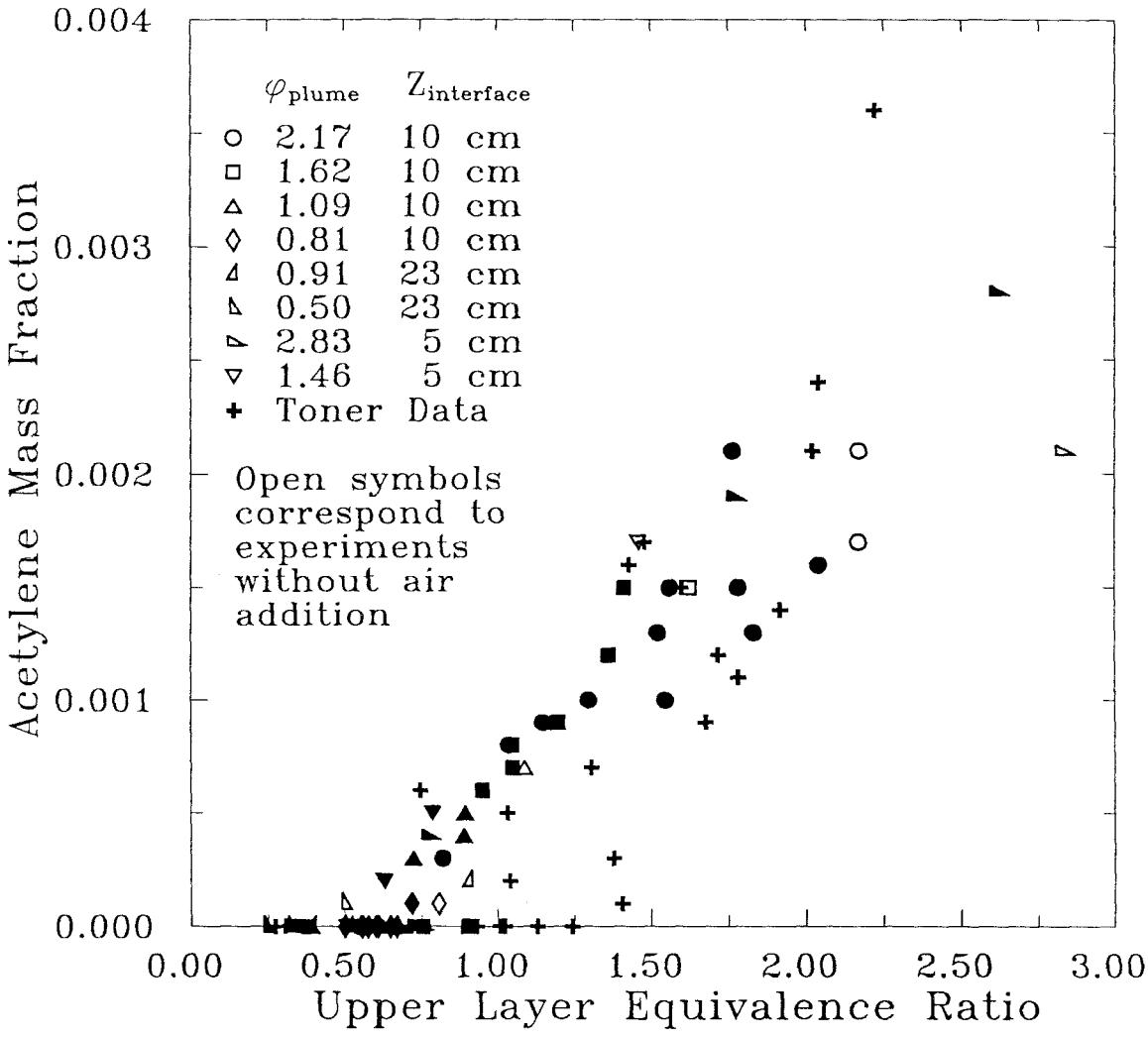

Figure 4.9: Acetylene measurements for natural gas fires burning in two layers

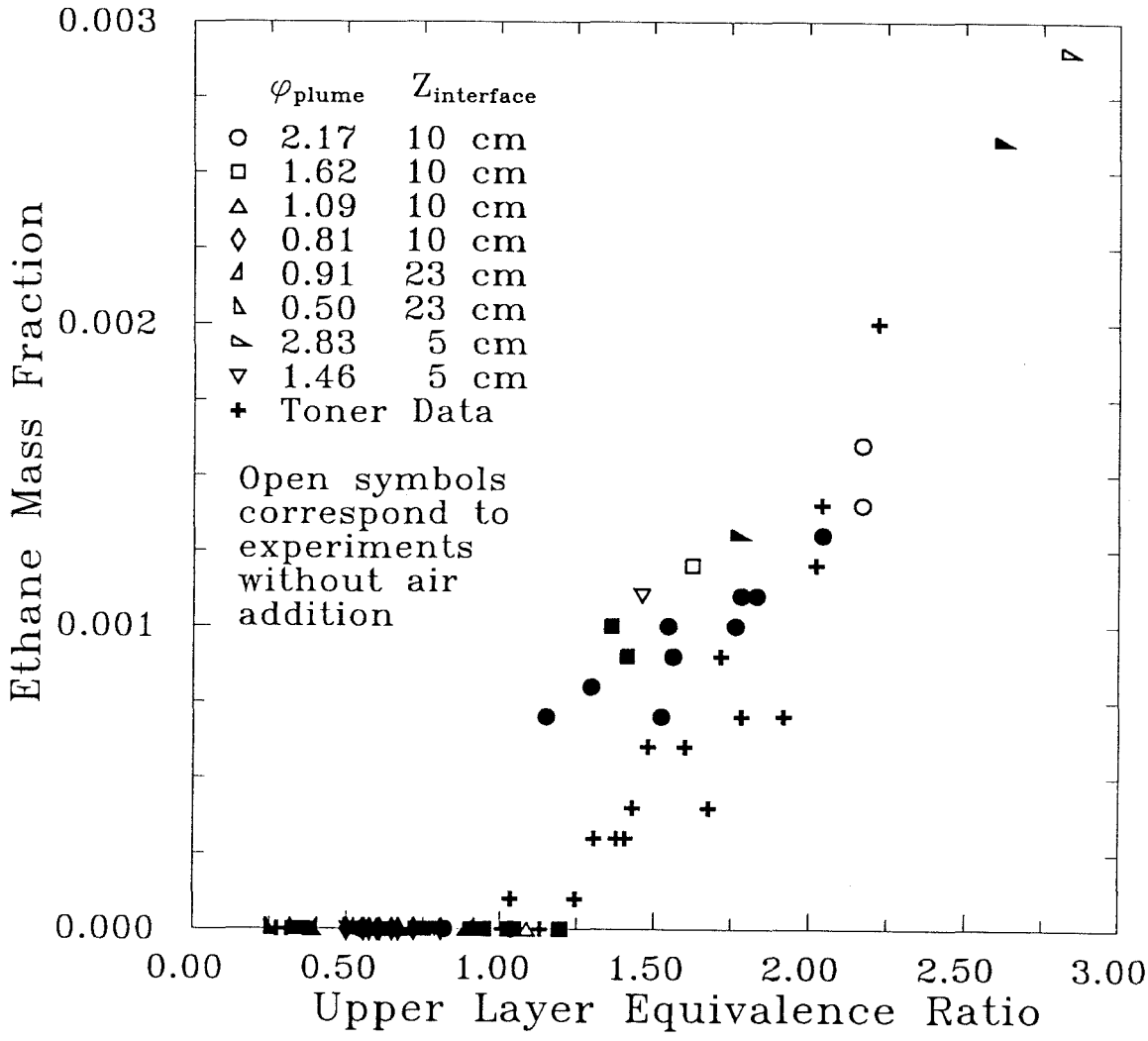

Figure 4.10: Ethane measurements for natural gas fires burning in two layers

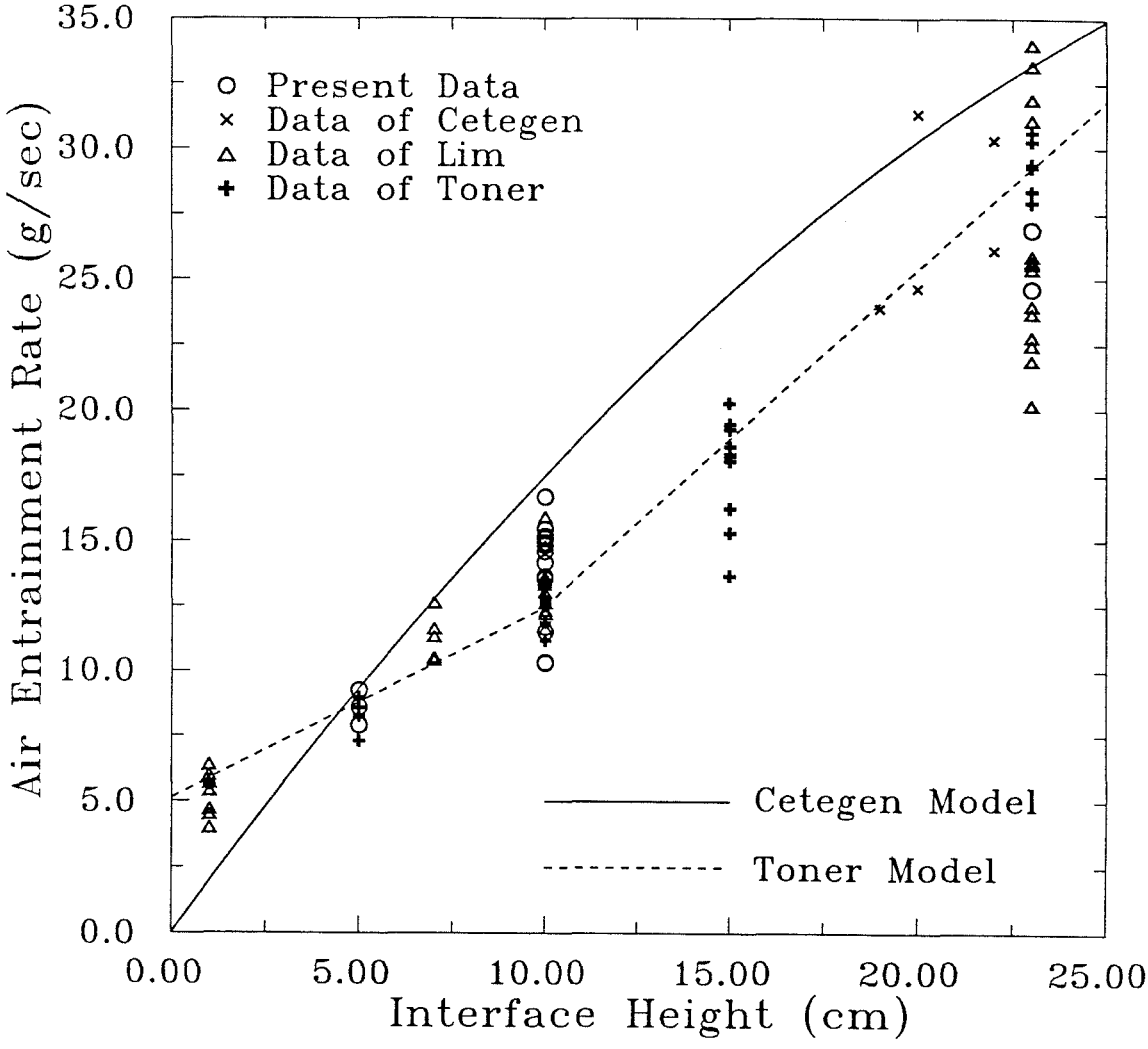

Figure 4.11: Comparison of entrainment data for a 19 cm diameter burner with natural gas fuel and small interface heights

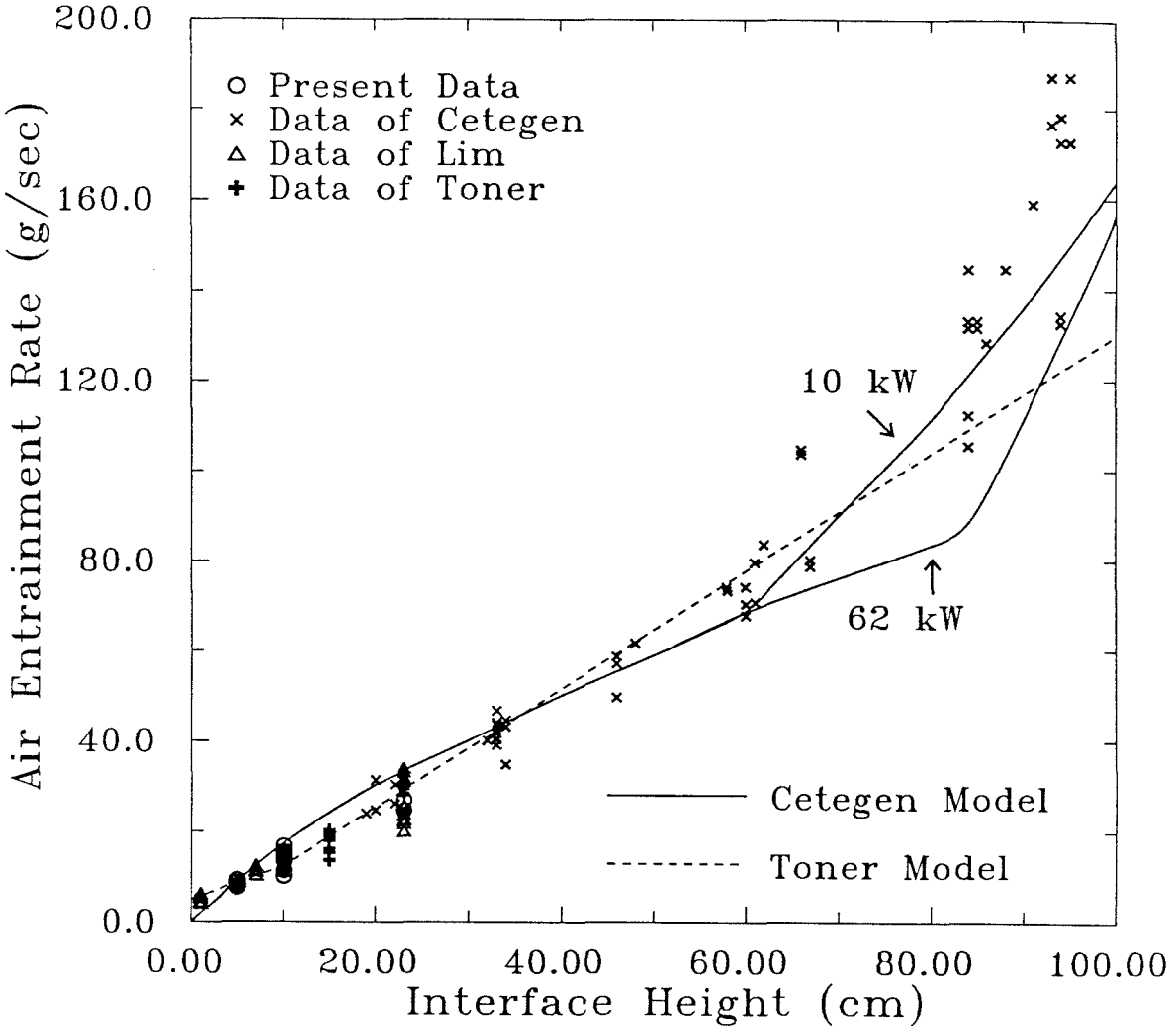

Figure 4.12: Comparison of entrainment data for a 19 cm diameter burner with natural gas fuel and large interface heights

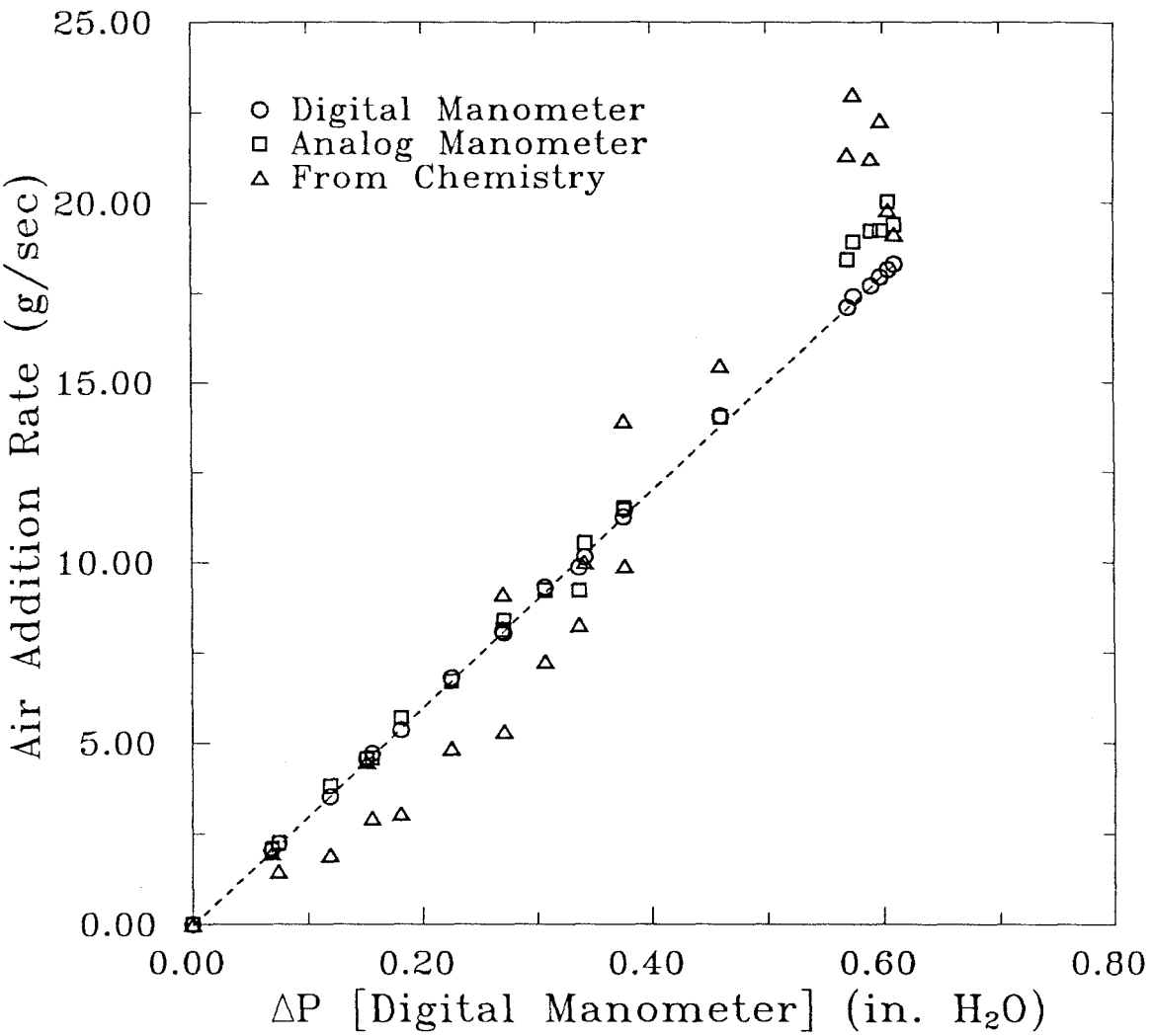

Figure 4.13: Comparison of air addition measurements

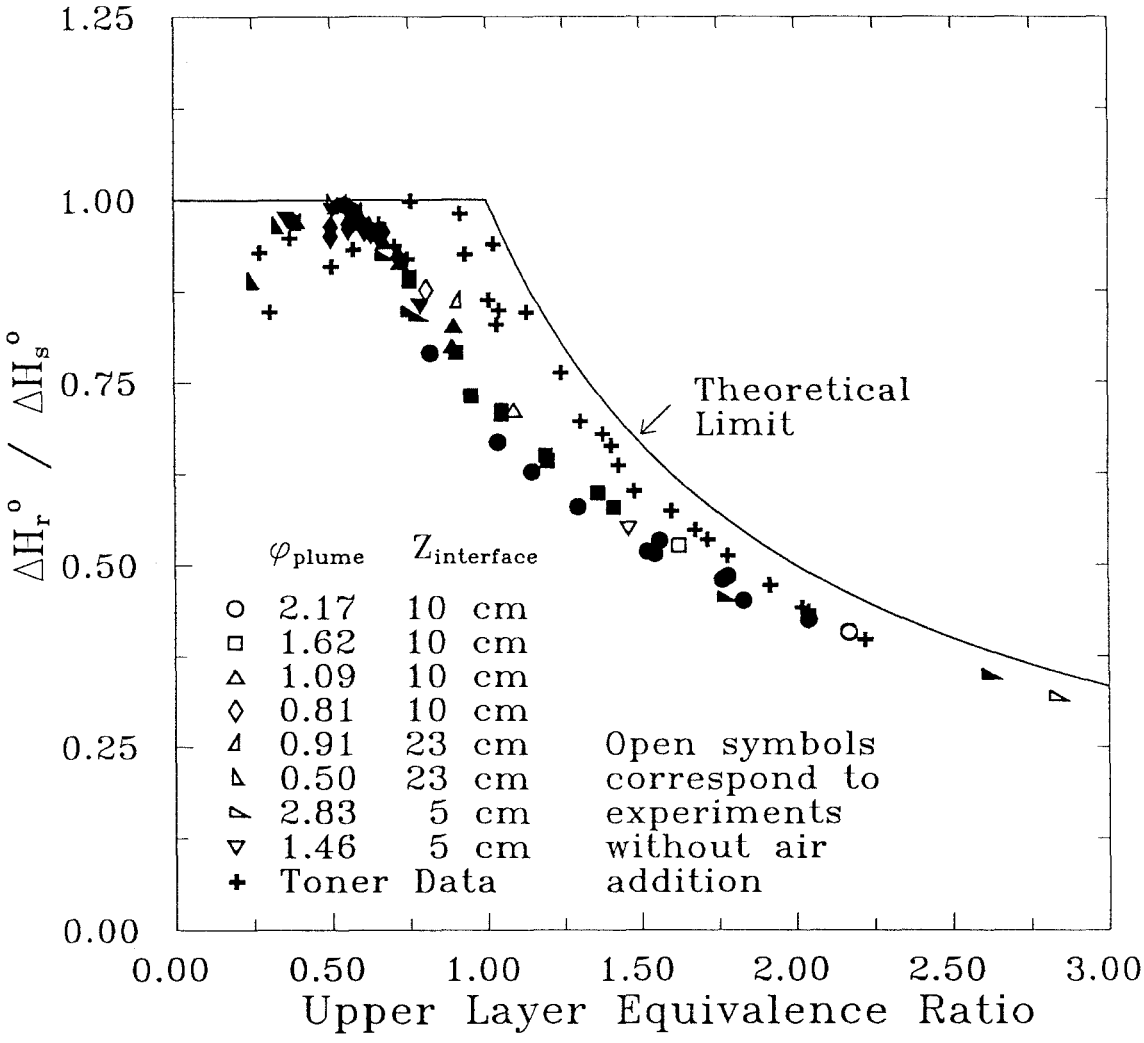

Figure 4.14: Actual heat of reaction compared to that of a stoichiometric reaction

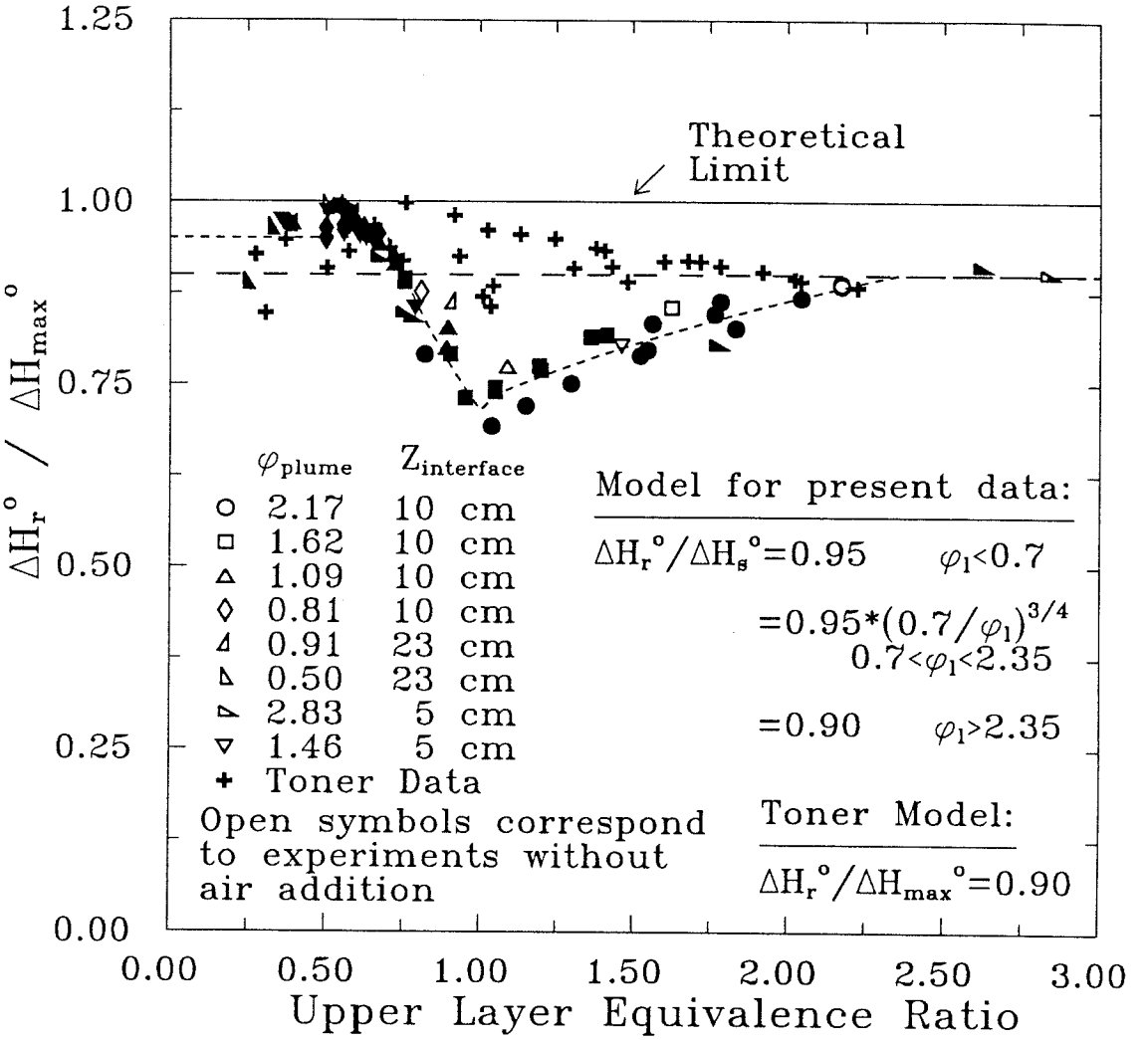

Figure 4.15: Actual heat of reaction compared to a theoretical maximum based on available quantities of fuel and air

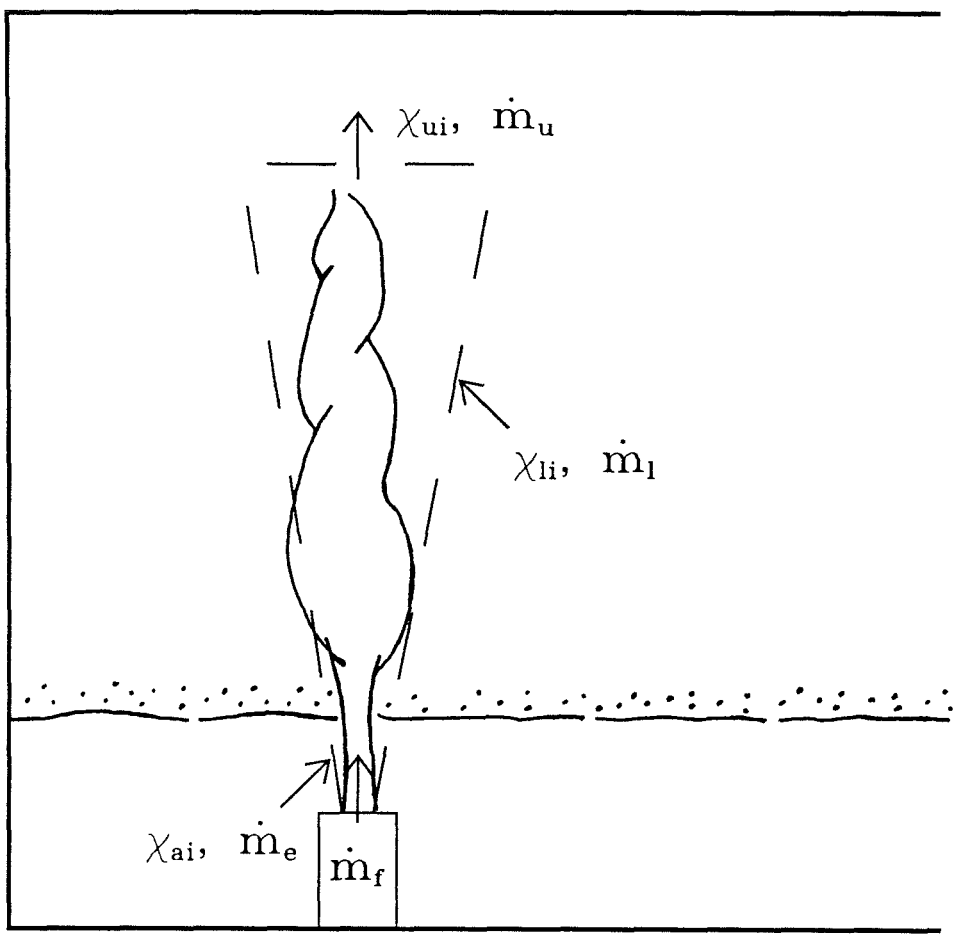

Figure 4.16: Plume reactor model for enclosure fire

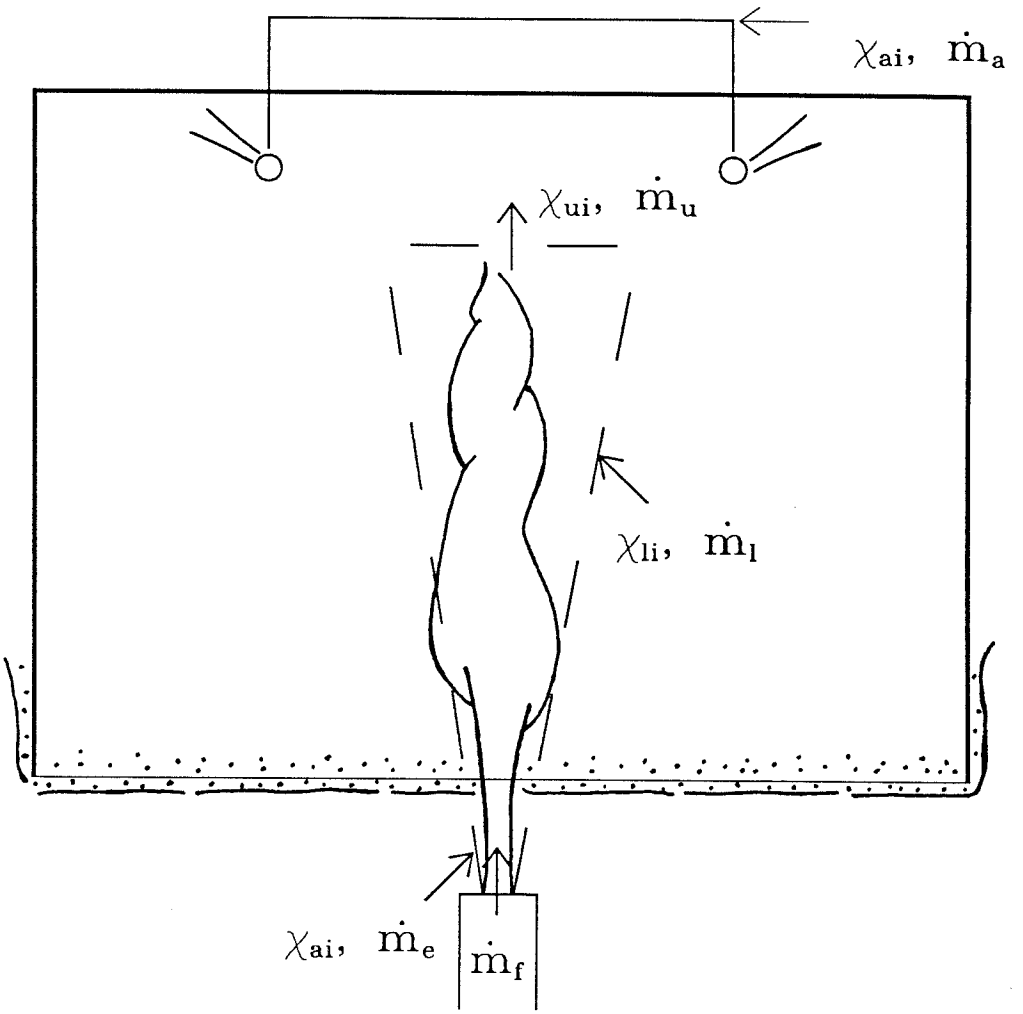

Figure 4.17: Plume reactor model for experiment

TABLE 4.1

Physiological Effects of Carbon Monoxide on Humans (Pitts, 1989)

Concentration	Effect
35 ppm	U.S. standard for maximum safe exposure
50 ppm	Maximum tolerance for industrial workrooms
200 ppm	First stage episode—unhealthful air quality
2,000-2,500 ppm	Produces unconsciousness in 30 minutes
4,000 ppm	Fatal exposure in less than 1 hour
13,000 ppm	Unconsciousness and danger of death in 1 to 3 minutes
50,000 ppm	Can result in fatal cardiac arrhythmia and death before carboxyhemoglobin saturation is significantly elevated

Chapter 5

The Effect of Product Layer Temperature on Combustion Completeness

Although some differences were noted in Chapter 4 between the chemical species measurements of this study and those of Toner (1986) for natural gas fires burning in two layers (when $\varphi_\ell > 0.75$, cf. Figures 4.2 through 4.10), it appeared that these deviations were due to real variations in the experiments, not instrumental offset. The only significant changes to the experimental apparatus were those which involved the construction of the hoods. The hood used by Toner was smaller (measuring 1.2 m square by 1.2 m tall), and the interior was insulated with a fibrous ceramic insulating material. These changes resulted in a consistently higher product layer temperature than in our larger (1.8 m square by 1.2 m tall), uninsulated hood for otherwise identical test conditions.

With matched fuel flow rates, interface heights, and burner diameters, Toner reported temperature measurements from 120 to 200 K higher than in our case, as shown in Figure 5.1. In each study, higher product layer temperatures were observed for experiments with larger interface heights, allowing increased air entrainment rates. As expected, temperatures were nearly constant in each case once fuel-rich conditions existed. This follows the idea of a relatively uniform amount of heat release due to the consumption of a fixed amount of oxygen, as mentioned in Chapter 4.

The temperature data for all of the experiments in this study using natural gas fuel are presented in Figure 5.2, which shows the effect of air addition to the upper layer on the layer temperature when the experimental configuration was otherwise fixed. If the plume gases are fuel-rich, air addition to the layer provides the oxygen necessary for the combustion of more fuel, since unburned fuel is readily available. The heat release is then increased when more fuel is consumed, causing product layer temperatures to increase. When the plume gases are fuel-lean, however, the additional air does not assist to further consume the fuel (except for conditions very near $\varphi_\ell = 1$), since oxygen supplies are plentiful. Thus the additional air acts as a diluent to the combustion products in the layer, and causes a decrease in the product layer temperature.

Since the nominal species measurements from both of these studies followed a consistent behavior, the differences in the trends of the data suggested that the

temperature of the upper layer had an effect on the completion of the combustion process.

5.1 Temperature Increases due to the Insulation of the Hood

To investigate the effects of temperature on the product layer composition, a series of experiments was performed with varying amounts of insulation applied to our bare-metal hood. All other test conditions (fuel flow rate, interface height, burner diameter, and no air addition to the upper layer) were held constant. The fixed conditions were selected to provide a layer equivalence ratio of about 1.45, where the deviation between the measurements of these two studies was largest. The tests were conducted with various phases of insulating material applied to the exterior of the hood, and additional tests included the application of the same ceramic insulation as used by Toner on the hood's interior ceiling.

5.1.1 Tests with Insulation on the Exterior of the Hood

The insulation placed on the outside of the hood was a 5 cm thick blanket of high temperature fiberglass, manufactured in sheets of 244 cm by 61 cm. The various phases of the insulating process provided the opportunity to incrementally increase the upper layer temperature without changing the stoichiometry of the plume gases delivered to the layer. Sketches of the surface area covered during each phase are given in Figure 5.3, with the corresponding effect on the temperature measurement. As expected, with increases in the surface area covered by insulation, the product layer temperatures increased. The largest gains in insulating effect were made with the first two phases, with further temperature increases of smaller magnitude thereafter. Although the net increase in the layer temperature due to the exterior insulation was 130 K, these experiments did not reach temperatures comparable to the hottest conditions investigated by Toner. There was a significant overlap in temperatures, however, for data taken in both studies, and it was expected that any effects due to elevated temperature would be observed in both sets of data (at least for the range of temperatures in this study).

5.1.2 Tests with Insulation on the Interior Ceiling of the Hood

Another possible explanation for the differences in the species measurements previously noted may have been the presence of the insulating material on the interior of Toner's hood. With a layer of soot deposited on the fibers and the

energy provided by the plume flow, it is possible that some of the available carbon (from the soot) was being oxidized by the gases in the upper layer, since even fuel-rich conditions possessed a small amount of oxygen. The fibrous structure of the insulation provided not only an ideal surface to assist with such reactions (exposed to radiant heating by the flame and exhibiting low thermal conductivity), but also increased the amount of surface area in contact with the upper layer gases.

While the exterior of our hood was fully insulated, including the windows, a layer of the same insulation material used in Toner's hood (Fiberfrax Duraboard LD, 12.7 mm thickness) was installed on the interior ceiling of our larger hood. The insulation was held in place by the air addition network and was secured with 18 AWG tinned copper wire. Experiments were performed after a significant layer of soot had been deposited on this interior insulation. As noted in Figure 5.3, this caused a temperature increase of an additional 20 K for these otherwise fixed experimental conditions.

If the insulating material was responsible for supporting these surface reactions, then it should be anticipated that the oxygen measurements would decrease for these tests, beyond any changes expected due to the temperature elevation. Also, a corresponding increase in the levels of carbon monoxide and carbon dioxide would accompany the oxygen reduction. Since the oxidation reaction of

$$CO + \frac{1}{2}O_2 \longrightarrow CO_2$$

is relatively slow in comparison to the carbon oxidation reaction, and the amounts of available oxygen are small, most of the oxygen reductions should appear as contributions to the carbon monoxide levels.

5.1.3 Species Measurements from Experiments with Elevated Temperature

The multiple insulation phases had the cumulative effect of increasing the upper layer temperature by about 150 K. With larger amounts of insulation installed, the amount of time necessary for reaching thermal equilibrium increased from about 25 minutes to more than 3 hours. At each phase, 3 to 4 chromatographic samples were withdrawn and analyzed. With increases in the surface area of the hood covered by insulation, product layer temperatures increased and the amounts of oxygen and methane measured in the upper layer decreased, as shown in Figure 5.4. This plot also includes all of the data taken in experiments at this

stoichiometry before insulation was applied to the hood. The reductions in the oxygen and methane concentrations with increasing temperature were balanced by increases in the amounts of carbon dioxide and water vapor. Despite these variations, the levels of carbon monoxide (also shown) remained nearly constant.

These measurements clearly show that the upper layer temperature had an impact on the completeness of the combustion process over this temperature range of 500 to 675 K. For example, the levels of residual oxygen before the insulation was applied showed measurements as high as 0.04 mass fraction, while oxygen levels in the fully insulated experiments fell to below 0.01 mass fraction. The data taken at the highest temperatures in this study are from the experiments with insulation on the interior ceiling of our hood. The behavior of these measurements does not verify that significant changes occurred due to the presence of the interior insulating material. The oxygen measurements were consistent with the behavior of the previous exterior-only insulation phases, and no increases in the carbon monoxide levels were observed. The agreement of these measurements suggests that the significance of any reactions occurring on the interior surface of the hood was not accelerated in this temperature range (500 to 700 K). The balanced reductions in the oxygen and methane measurements and the accompanying increases in the carbon dioxide and water vapor indicate that the combustion process was driven further to completion as the product layer temperatures increased.

Also included in Figure 5.4 are the measurements of Toner from experiments with matching upper layer equivalence ratios. These data were taken with varying fire strengths and interface heights. The trends of these experimental measurements are consistent with the behavior of the present data, showing decreases in the oxygen and methane concentrations with increasing temperature, while carbon monoxide levels remained nearly constant (these data points are presented on an exaggerated scale). Although the curves fitting each set of data are slightly different, this does suggest that the differences observed in the species measurements noted in Figures 4.2 through 4.10 are largely due to temperature effects associated with variations in the construction of the hoods.

This temperature dependence of the product layer composition is in contrast with the interpretation of the data by Toner, who assumed that the temperature had no effect on species measurements over the range of conditions in his experiments. This was probably due to the smaller gradients for his data, even where there is an overlap in the temperatures of these two studies. Despite this weak dependence on temperature for the data over the range 500 to 875 K, the ob-

servation that the species concentrations did not match equilibrium values when $\varphi_\ell > 0.75$ suggests that some of the chemical reactions in natural gas flames are quenched at temperatures below 900 K due to the entrainment of vitiated gas.

5.2 Temperature Increases due to Fires Using a Larger Burner

A survey of species measurements as a function of the upper layer temperature similar to the data presented in Figure 5.4 was also compiled for data from experiments with φ_ℓ of about 1.0. These measurements are shown in Figure 5.5, and again represent all of the data taken at this stoichiometry for various interface heights, fuel flow rates, and air addition rates. The experiments performed at these conditions were conducted without insulation, and hence the temperature of the ceiling layer ranged from 530 to 600 K.

To extend the temperature range of the data taken in our larger hood at this stoichiometry, additional experiments were performed with a 50 cm diameter burner (this burner is described in Cetegen et al., 1982, and in Part 2 of Toner, 1986). The larger diameter burner allowed the use of higher heat release rates, thus producing higher ceiling layer temperatures, while maintaining the flame heights below the air injection region. Upper layer temperatures in these tests were elevated up to 700 K, while Toner's experiments at this stoichiometry had product layer temperatures ranging from 600 to 875 K, all of which were performed with the same 19 cm diameter burner used here.

The trends of the data from our experiments are consistent with the previous observations of decreasing oxygen and methane concentrations with increasing temperature. Data taken in experiments with the 50 cm diameter burner also agreed well with the measurements from tests with the 19 cm diameter burner. Figure 5.5 also includes Toner's measurements for this range of values for φ_ℓ. The temperature dependence of his data is more pronounced at this stoichiometry, except for the negligible variations in the levels of carbon monoxide. Although the curves fitting each set of data remain slightly different, there appears to be even better agreement at these conditions, especially with respect to the oxygen measurements.

The data of Figures 5.4 and 5.5 show that a major part of the differences in the species measurements between the experiments in this study and those of Toner can be attributed to variations in the temperature of the ceiling layer gas when the stoichiometry of the upper layer was fixed. These temperature offsets

were due to differences in the size and insulation of the hoods used in these two studies. Despite a careful check of our experimental technique and the procedures used in each investigation, we cannot explain the residual differences between the measurements of these two studies.

In an effort to explain why the combustion process is driven to further completion when the upper layer temperature is elevated, consider the effect of the temperature of the reactants on the adiabatic flame temperature of a diffusion flame. For example, a fuel-rich mixture of natural gas and air ($\varphi = 1.56$) supplied at a temperature of 550 K will form equilibrium products at 2025 K when allowed to react in an adiabatic manner. If the temperature of the reactants is increased to 700 K, then the same mixture ratio will produce an equilibrium composition with an adiabatic flame temperature of 2145 K. It is possible to extend this idea to consider the effect of an increase in the temperature of the upper layer on the temperature profile of the reaction zone of a diffusion flame burning in this layer.

Figure 5.6(a) represents a view of the fuel, oxidant, and temperature profiles of a diffusion flame in a frame of reference attached to the flamesheet (i.e., the diffusion front where reactions are occurring between the fuel and oxidant supply streams). Since conduction and radiation heat transfer act to remove some of the energy released by the combustion reactions, the maximum temperature found in the flame will actually be lower than the adiabatic flame temperature. For the purpose of this arguement, we assume that there is an activation temperature, T^*, which is the minimum temperature required to support the reactions in the combustion process (treating the process as a set of bulk reactions). Thus an effective reaction zone thickness, λ_1, can be defined for a prescribed temperature profile, T_1, through the diffusion front ($T_1 = T_1(x)$, a function of position).

Now consider the changes to the temperature profile and to the effective reaction zone thickness accompanying an increase in the temperature of the reactants, as shown in Figure 5.6(b). Note that both fuel and oxidant temperatures would increase in this flamesheet model due to the diffusion of higher temperature products away from the flame, opposing the supply streams. When the temperature profile is increased from T_1 to $T_2(x)$, there is a corresponding increase to the maximum and adiabatic flame temperatures, however, the activation temperature T^* is absolute and does not depend on the temperature of the reactants. The increased temperature profile provides further extention of the flamesheet above the activation temperature, causing an increase in the thickness of the effective reaction zone, $\lambda_2 > \lambda_1$. Now if the thickness of the effective reaction zone is increased, the

fuel and oxidizer streams will have an extended opportunity to react, and thus consumption of the reactants should continue to further completion.

5.3 Chemical Stability of the Ceiling Layer Composition

As mentioned in Chapter 4, species measurements of the upper layer gases followed values predicted by equilibrium computations when $\varphi_\ell < 0.5$. For more fuel-rich conditions, the measurements begin to deviate from equilibrium levels and, in some cases, significant amounts of unconsumed fuel and oxygen were present in the upper layer. Within the confinement of our experimental hood, the product gases and added air are recirculated through the fire plume many times before escaping through the exiting gas stream. Residence times for the gases within the hood, but outside of the fire plume, may be small when compared with the time required for these gases to react (without the additional energy provided by the plume flow).

In an actual room fire, however, the situation can be quite different. The aspect ratio between the room's volume and the plume region can be much larger than in our experiment. This would allow for the possibility of the ceiling layer gases to be driven further from the plume, providing the opportunity for these species to react without additional energy supplied by the fire plume. Our aim here is to consider the possibility of further reactions occurring in the ceiling layer when fuel and an oxidizer are present, but in the absence of additional energy input from the plume flow. This sensitivity analysis of the stability of the ceiling layer composition considers the propensity for reactions when a homogeneous mixture is introduced into an ideal isothermal plug flow reactor at various temperatures.

As a test case, we have used the composition measured in an experiment with fuel-rich conditions in the upper layer (see Appendix B, Experiment 08, Chromatographic Run 312). While the probe was located at position A (cf. Figure 3.1), the temperature measured at the sample inlet was 546 K. This experiment had a plume equivalence ratio of 2.17, but with air addition to the hood, the value of φ_ℓ was reduced to 1.56 (still within the fuel-rich regime). The composition of the upper layer gases included 2.5% oxygen and more than 5% methane, with other fuel species in smaller concentrations, in a diluent composed of nitrogen (mostly), carbon dioxide, and water vapor.

To determine an upper limit for the ceiling layer temperature, an adiabatic flame temperature calculation was performed on the product composition, allow-

ing for a wide range of species to exist after equilibrium conditions were reached. These computations were performed using the STANJAN Chemical Equilibrium Code, version 3.31 (Reynolds, 1989), and showed that for an adiabatic process, an equilibrium composition is attained at 1034 K after the complete consumption of the oxygen and hydrocarbon fuels (except for methane, which was available in excess amounts). Significant quantities of carbon monoxide and carbon dioxide were produced, with a modest increase in the hydrogen concentration. Since the maximum temperature that the ceiling layer could be expected to reach corresponds to these conditions, we can consider the detailed chemical kinetics in a plug flow reactor using an isothermal temperature profile, with conditions varying from the upper layer temperature of 546 K to the adiabatic limit of 1034 K.

5.3.1 Detailed Chemical Kinetics Using a Plug Flow Reactor Model

A group of computer programs designed to investigate detailed chemical kinetic processes (Senkan, 1989) was employed here to investigate the stability of the ceiling layer composition. The objective of these programs is to predict the species concentration and reaction rate profiles in an ideal plug flow reactor based on fundamental chemical parameters and a mathematical model of the process. The parameters of interest involved the thermochemistry of the reaction species (enthalpies of formation, ΔH_f°; absolute entropies, S°; and temperature-dependent specific heats, $c_p(T)$), and the reaction rate constants A, n, and E_a for the Arrhenius rate expression

$$k = AT^n exp(-E_a/RT)$$

for each elementary reaction in the mechanism.

A reaction mechanism describing the detailed chemical kinetics of the process was built for a methane/air system using information available (Glassman, 1987) for the elementary reaction steps (see Appendix C for species and reactions in this mechanism). Our mechanism included 24 individual species and radicals, and utilized 90 reaction steps. Reactions involving argon and nitrogen were not considered due to low reactivity and poorly understood reaction mechanisms for these species†. A separate keyword input file was also built to specify the pressure and temperature of the reactor, the mole fractions of the reactants, the time

† The Zeldovich mechanism for NO production was included in some of the initial test cases. At the temperatures measured in the experiments, however, the amounts of NO produced were not significant.

duration of the computations, and other parameters controlling the tolerances on the numerical integrations and the size of the output files. The model allows for either isothermal or adiabatic conditions in the reactor, where the temperature specification is maintained or used as an initial condition, whichever is appropriate. These calculations were performed using isothermal conditions for the plug flow reactor, since adiabatic conditions would lead to the development of an unrealistic temperature history for modeling the ceiling layer behavior. In the experiments, the species measurements were taken after the upper layer gases reached chemical and thermal steady state, thus isothermal conditions are a reasonable approach for considering the stability of the upper layer gases in our experiment. The composition of reactants used for these computations were taken directly from the species measurements of the test case.

5.3.2 Species Concentration Profiles

The upper layer composition from the experiment was used as the initial mixture of gases flowing through the isothermal plug flow reactor. With temperatures ranging from 546 K to 1034 K (and several intermediate values), the gases were allowed to react for 20 seconds. This time period represented an approximate nominal residence time for the gas in the hood of our experiment. Also, it was expected that any important trends in the behavior of these reactants would become apparent in the first 20 seconds. The concentration profiles for the major stable species of interest are shown in Figures 5.7 through 5.11 as a function of time for the different reactor temperatures (minor species and radical concentration profiles are included in Appendix C). Tolerances were set to provide 5 significant digits for each of the species at each timestep for those components with maximum values greater than 10^{-10}. Species with peak concentrations of less than 10^{-10} are not reported here due to the resolution of these computations.

An interesting result of these computations, which is supported by each of the figures, is the prediction that no reactions would occur between these species at or below 700 K. When the temperature was 546 K, the conditions of the upper layer in our experiment, none of the radical species concentrations reached above the (tolerance-set) threshhold of 10^{-10}. From this result, we can make two important observations. First, when the ceiling layer of a room fire is composed of gases which are below 700 K, the species in the layer should not be expected to react, unless additional energy is provided by the fire plume, even when the gas species reflect

fuel-rich conditions with some available oxygen. Thus, these computations suggest that a chemically stable upper layer composition existed in the hood during our experiments. (Our assumption in section 4.5 of no chemical reactions outside of the plume reactor appears to be justified in this case.) Secondly, a plug flow reactor is a reasonable approximation to the conditions imposed on the gas sample by the stainless steel probe. As discussed in section 3.2, no significant changes occurred to a calibrated gas sample after passing it through a heated loop of material identical to the probe. Since the probe arm is relatively isothermal throughout the section submerged in the upper layer, we can expect that no reactions would occur in the sample line at these conditions (temperatures below 700 K), in the absence of catalytic effects from the probe material.

The oxygen levels in the gas mixture are shown in Figure 5.7, and display a trend of faster consumption rates with increased temperature. Although the consumption of oxygen is nearly complete after 20 seconds when the reactor was at 900 K, some level of oxygen availability was present throughout the first 15 seconds. In contrast, at 1034 K a rapid consumption rate reduced the oxygen levels to very low concentrations within the first 4 seconds, and then availability was nearly eliminated for longer times. This distinction is important in that the continued presence of oxygen was necessary to support some of the slower progressing reactions which required oxygen. Hence, the rate at which the oxygen was consumed had an impact on the remaining species after the 20 second duration.

Carbon monoxide concentrations, shown in Figure 5.8, increased with time when reactor temperatures were at or above 800 K. As expected from the behavior of the oxygen consumption, the carbon monoxide levels approached a nearly steady value after about 15 seconds when the temperature was 900 K. When the reactor was 1034 K, the carbon monoxide levels grew faster and reached a nearly steady value after about 4 seconds. Note that although the CO levels were nearly constant after 20 seconds at these temperatures, there was an offset in the CO concentrations due to the remaining presence of oxygen at 900 K to support the $CO \rightarrow CO_2$ oxidation reaction. Since some of the carbon monoxide being produced was then consumed at 900 K, levels reached only 2.85%, in comparison to the 3.31% attained at 1034 K after 20 seconds. These ideas are further supported by the carbon dioxide concentration profiles in Figure 5.9. Notice that the initial growth rate for CO_2 is higher at 1034 K, but after 20 seconds the level of CO_2 is higher for the 900 K case, since oxygen continued to be available for a longer time. At 1034 K, CO_2 production tapered off significantly after the first 4 seconds due

to the reductions in the oxygen concentration.

Since methane was the most abundant fuel in the input gas mixture, it was primarily the reactions involving methane and oxygen that were responsible for the production of CO, CO_2, and H_2O. Profiles of the methane concentrations, found in Figure 5.10, show that more fuel was consumed after 20 seconds at 1034 K than when the reactor was at 900 K. This result is consistent with the profiles of the other species, reinforcing the idea that at 900 K, the methane combustion reactions were competing for the available oxygen with the $CO \rightarrow CO_2$ oxidation reaction. Another interesting observation about the methane concentration profiles is that the total amount of CH_4 consumed after 20 seconds at 800 K does not appear to be proportional to the observed differences in the other species at this temperature. This may be largely due to the presence of acetylene in the input mixture, which appeared to be more readily consumed than the methane. Indeed, at 1034 K the acetylene level was reduced from 0.16% to a concentration lower than 0.01% within the first 1.5 seconds. The other stable hydrocarbon species (ethylene and ethane) displayed initial increases in concentrations followed by more gradual consumption rates after reaching peak values during the first 2 seconds.

At first inspection, the profiles of water vapor appear to behave in a manner inconsistent with what would be expected based on the consumption rates of methane (see Figure 5.11). Although more of the methane is consumed at the higher temperature, the amount of water vapor produced after 20 seconds at 900 K exceeds the steady state value reached when the reactor was at 1034 K. The reason for this behavior is explained when considering the production of hydrogen in each case. At 900 K, the H_2 concentration increased from 1.02% to 1.66% during the elapsed time, while the H_2 level increased to 2.71% over the same duration at 1034 K. This difference in the hydrogen concentrations accounts for the offset in the number of hydrogen atoms released due to the consumption of different amounts of methane. One possible explanation for this is that there may be a stronger affinity towards producing H_2 at the higher temperature, as opposed to the production of H_2O. This idea is justified since peak populations of OH radicals were an order of magnitude lower than for H radicals at 1034 K, thus free H radicals were more likely to combine with other H atoms than with the less abundant OH free radicals. More oxygen was available throughout the 20 second duration at 900 K, thus a larger amount of OH was available which allowed the continued production of H_2O. Notice that the water vapor level reached a steady state value about the time that most of the readily available oxygen was depleted

at 1034 K, within the first 5 seconds.

In summary, the potential for further reactions between the product layer species was considered. Using a detailed chemical kinetics model, it was found that when the temperature was below 700 K the species concentrations did not change during a 20 second interval, while reactions between the fuels and oxygen components were significant at temperatures above 700 K.

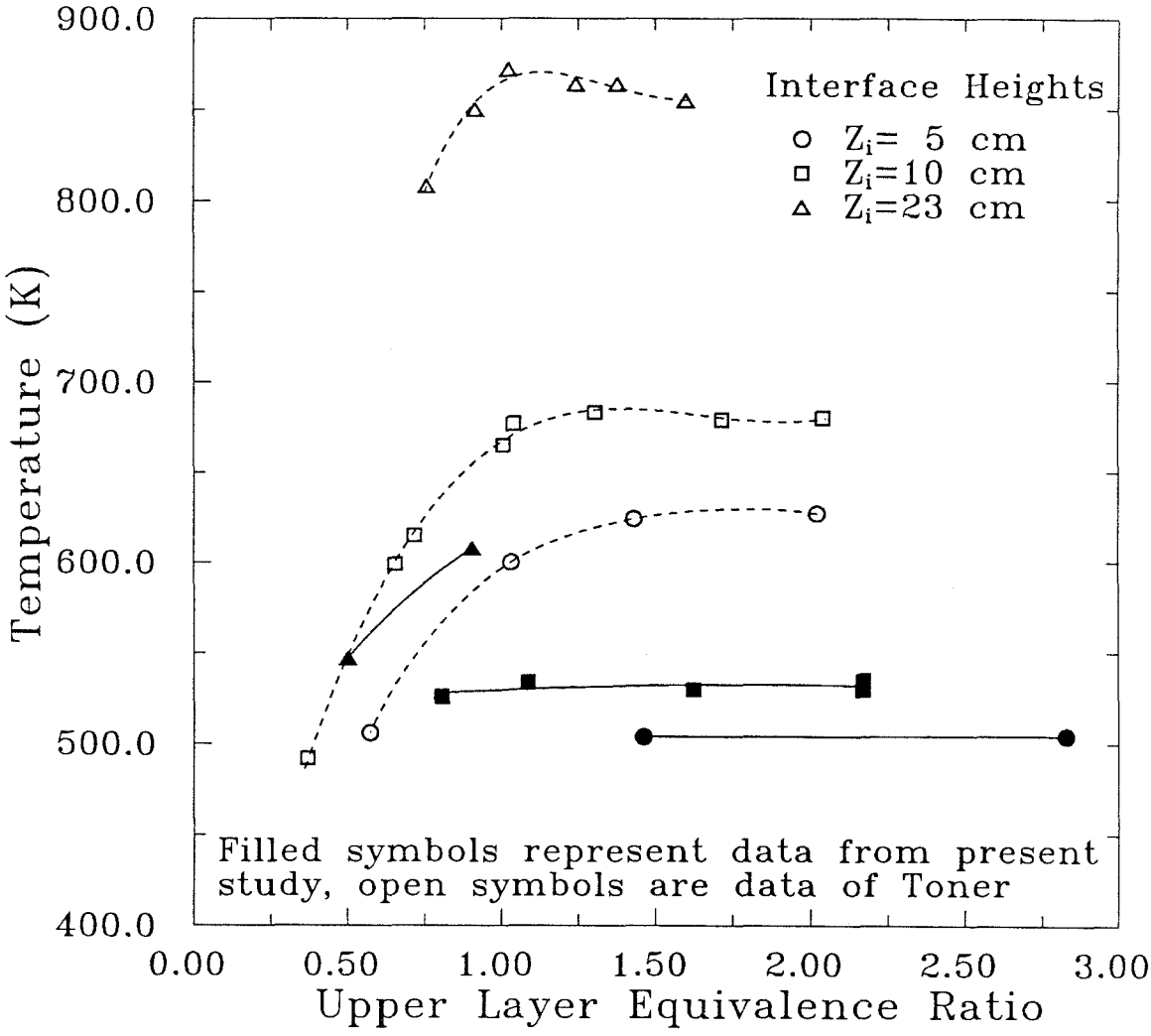

Figure 5.1: Comparison of product layer temperature measurements for two different hood constructions

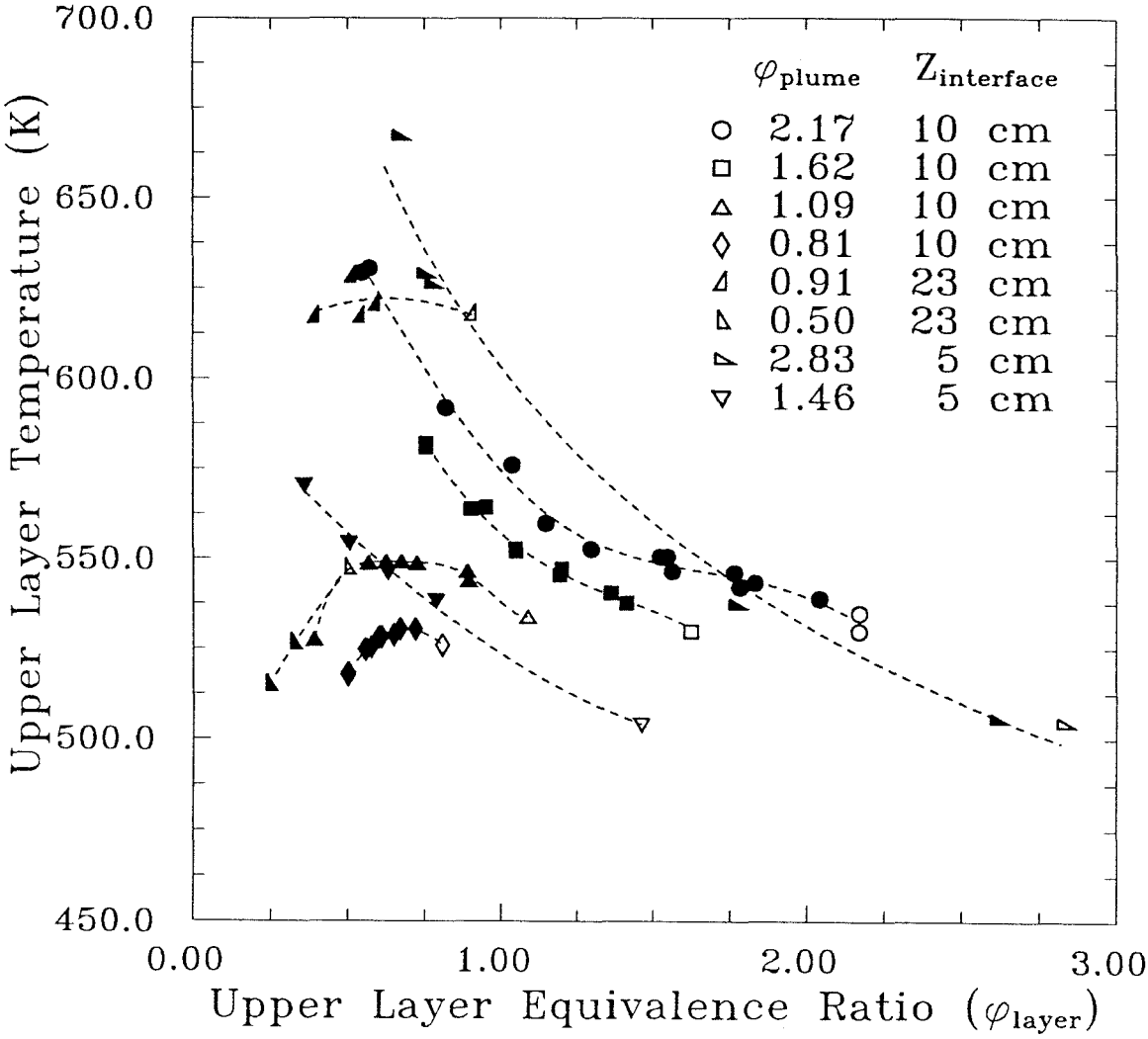

Figure 5.2: Upper layer temperatures for natural gas fires burning in two layers

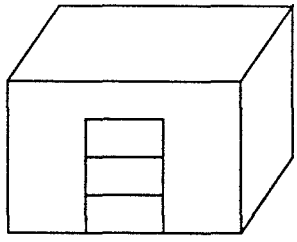

Test Conditions:

$\dot{m}_f$ = 1.35 g/sec (67 kW)
Z_i = 10 cm, D = 19 cm

No insulation:
T_{layer}=525 K

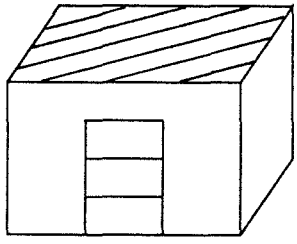

Insulation phase 1:
Single layer on exterior ceiling, T_{layer}=575 K

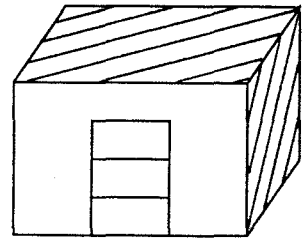

Insulation phase 2:
Exterior ceiling and two sides, T_{layer}=640 K

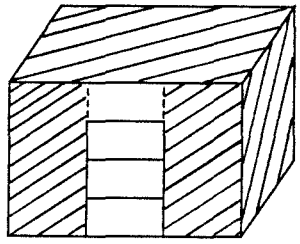

Insulation phase 3:
Exterior ceiling, sides, back, and partial front coverage, T_{layer}=655 K

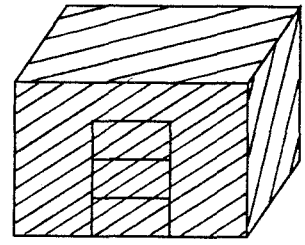

Insulation phase 4:
Exterior completely covered plus interior ceiling, T_{layer}=675 K

Figure 5.3: Phases of hood insulation

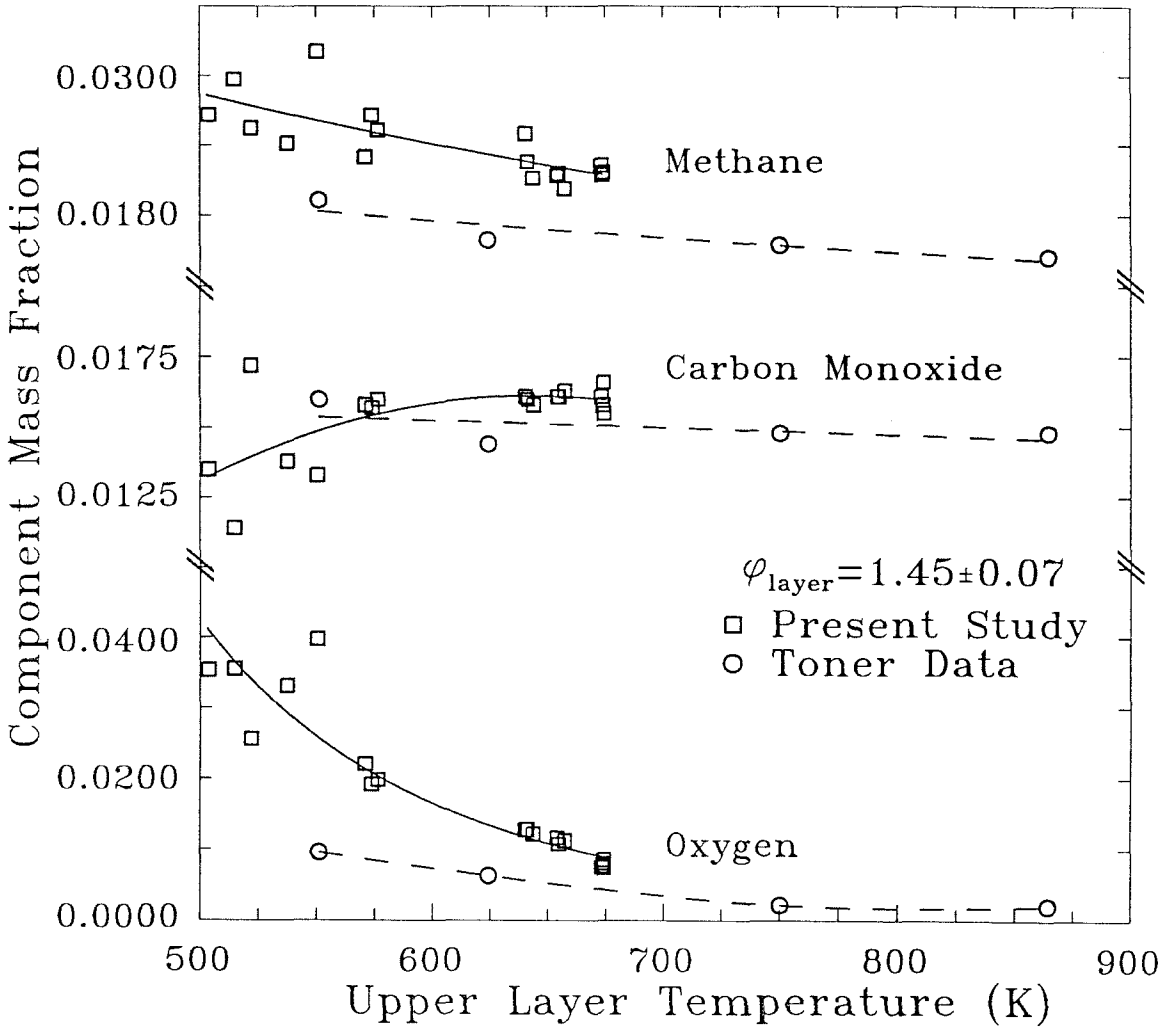

Figure 5.4: Product layer composition as a function of temperature with insulation applied to hood

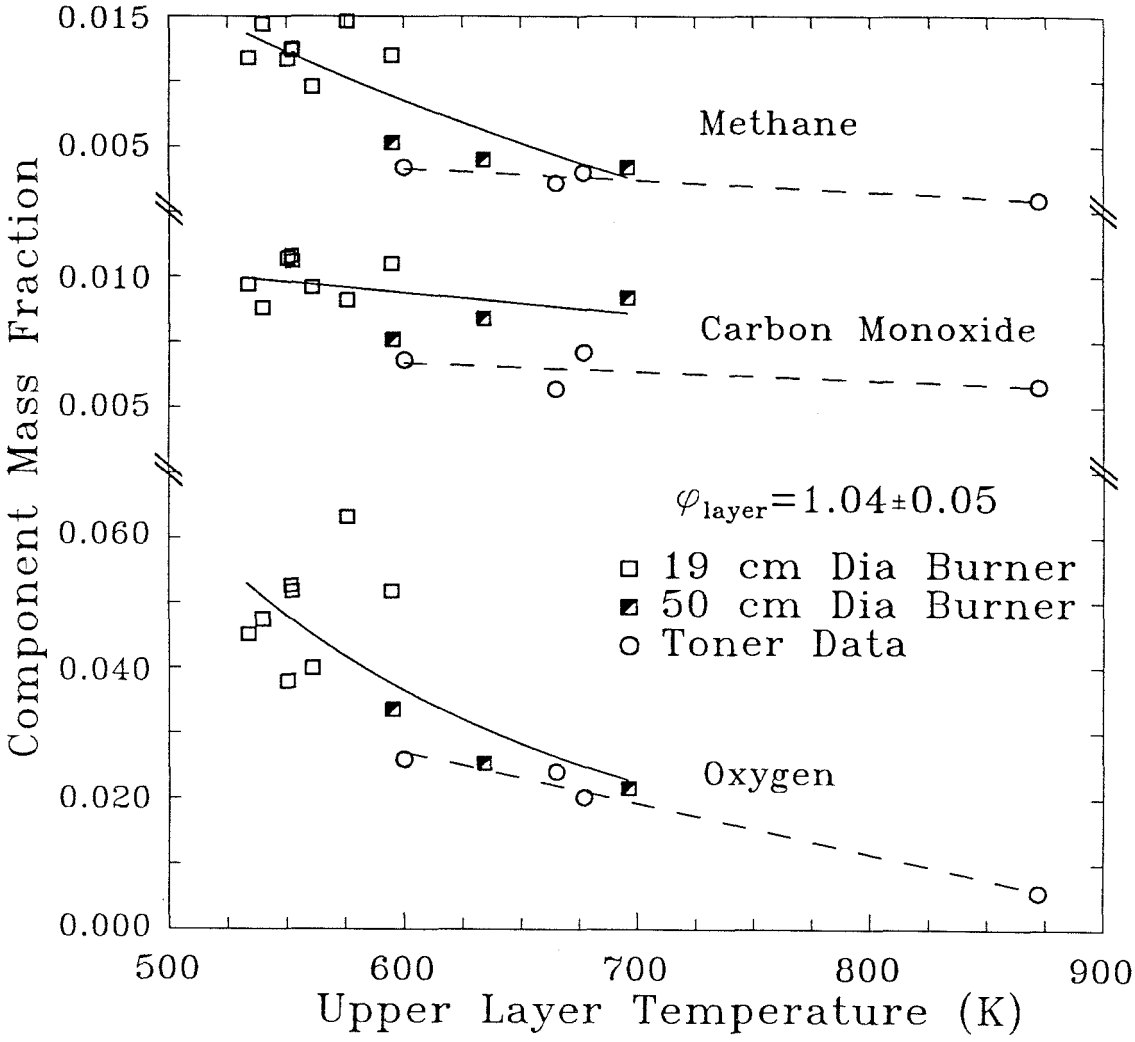

Figure 5.5: Product layer composition as a function of temperature for two different burner diameters (no insulation applied)

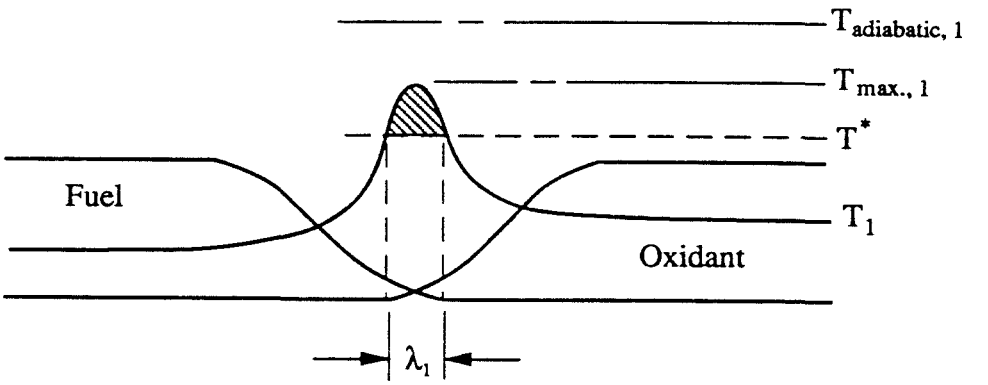

(a) Flamesheet profile for diffusion flame model

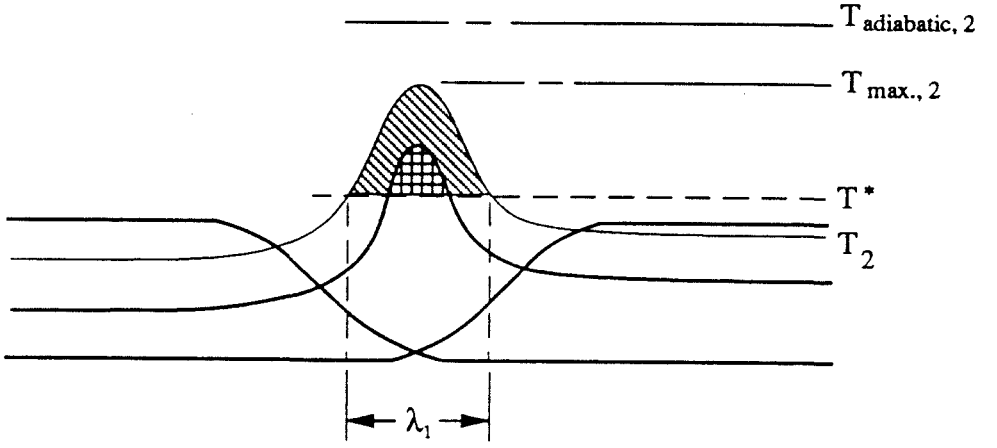

(b) Flamesheet profile for elevated layer temperature

Figure 5.6: Reactant and temperature profiles through the reaction zone of a diffusion flame

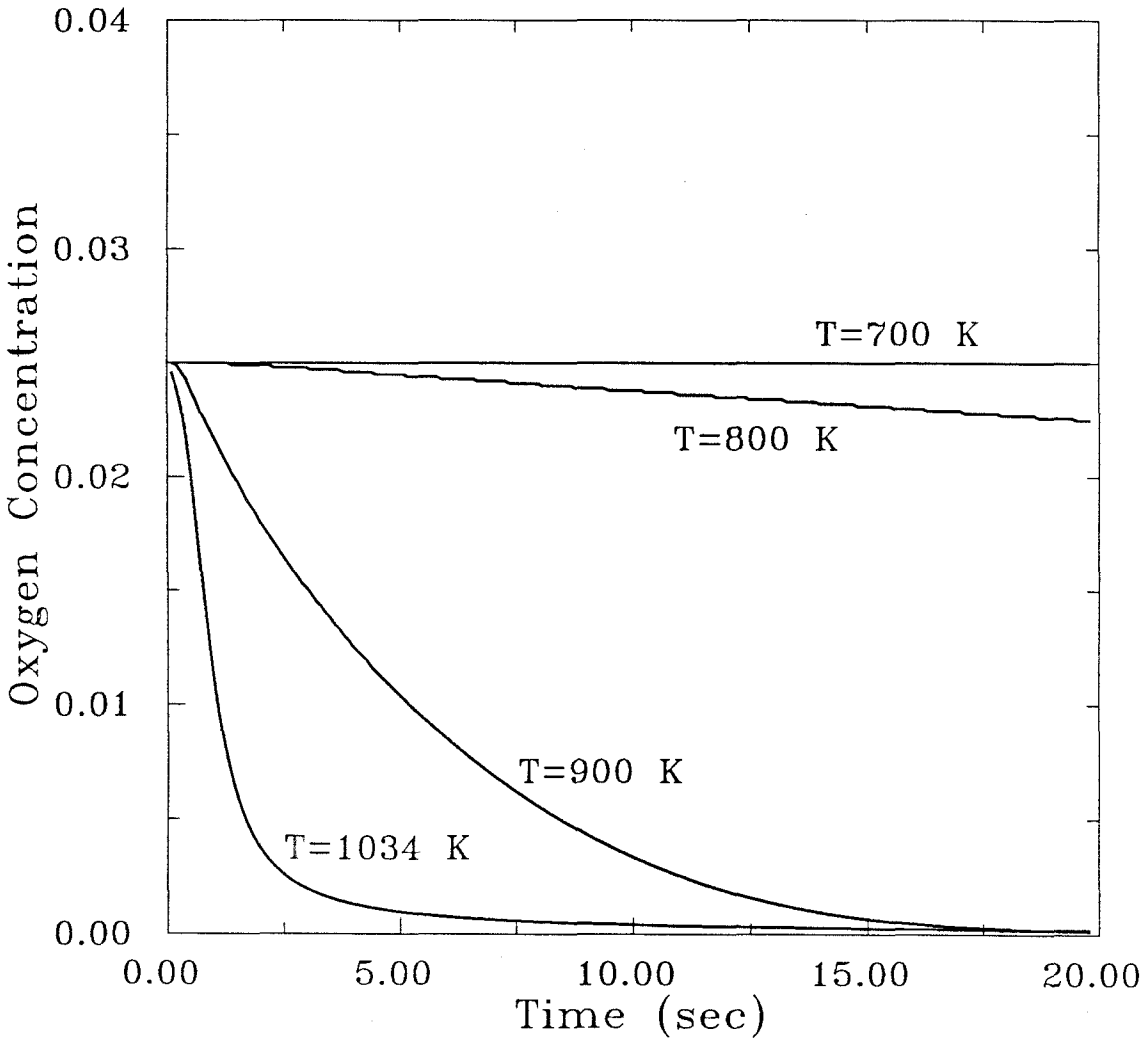

Figure 5.7: Oxygen concentration in a fuel-rich mixture introduced into an isothermal plug flow reactor

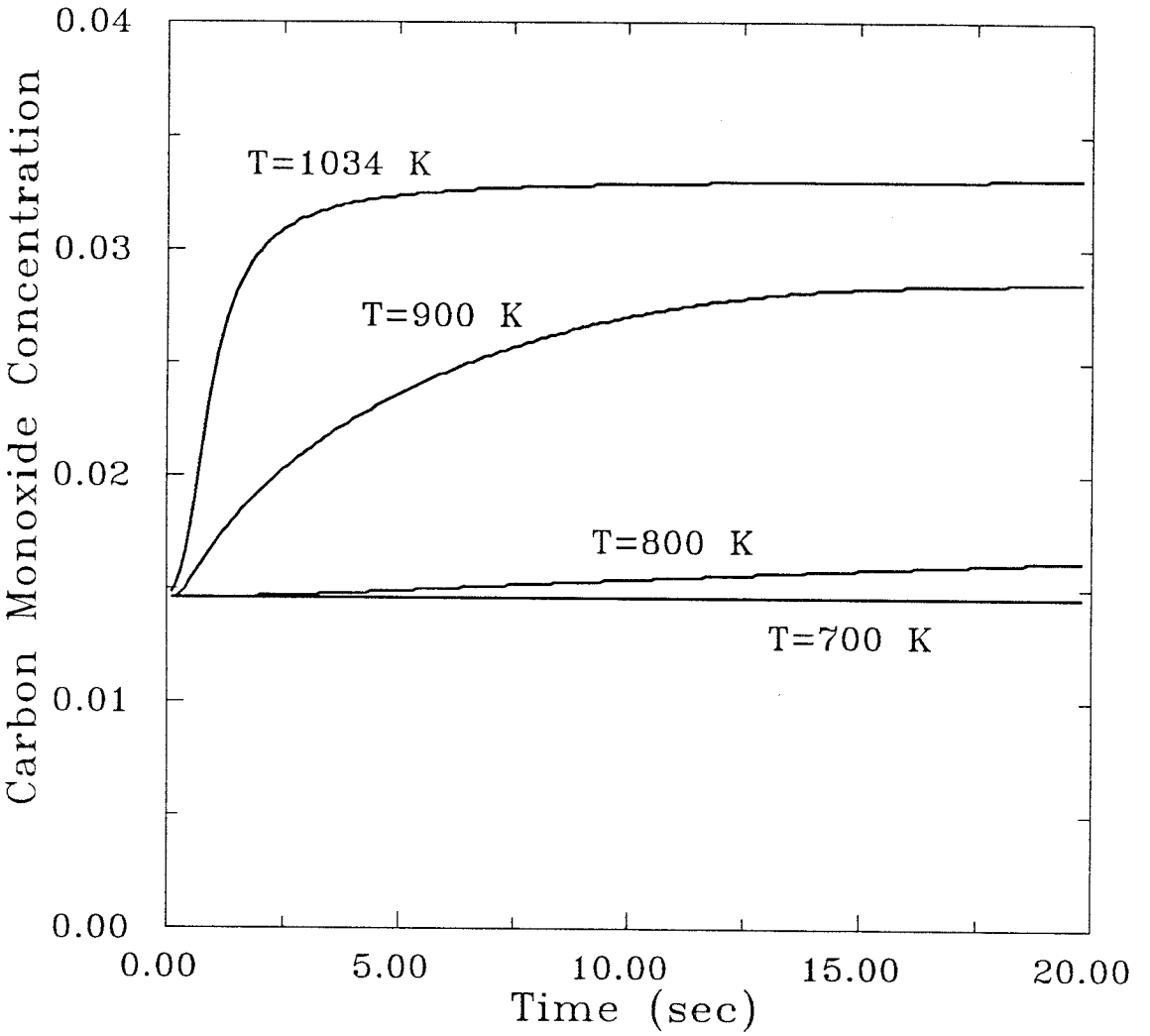

Figure 5.8: Carbon monoxide concentration in a fuel-rich mixture introduced into an isothermal plug flow reactor

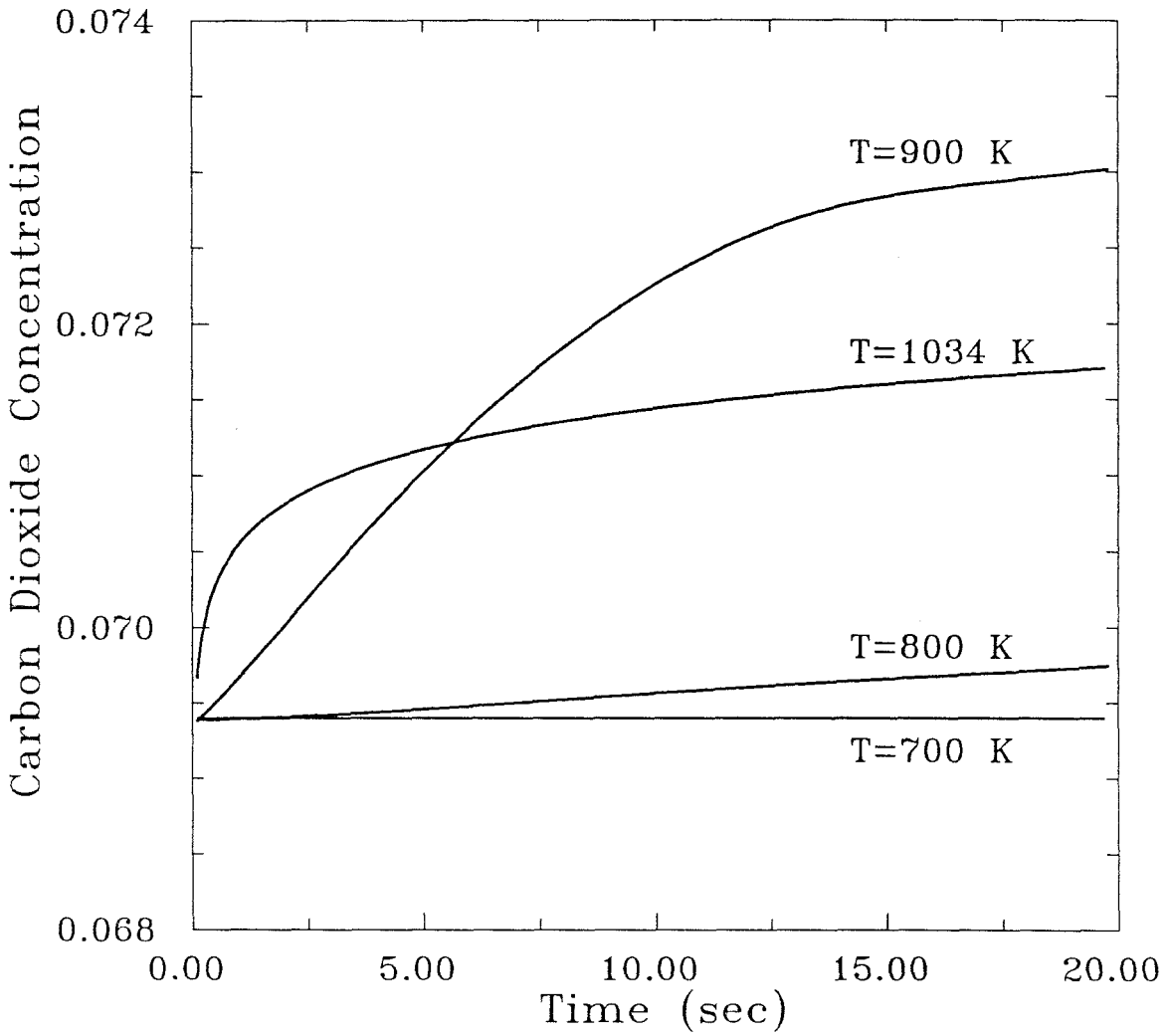

Figure 5.9: Carbon dioxide concentration in a fuel-rich mixture introduced into an isothermal plug flow reactor

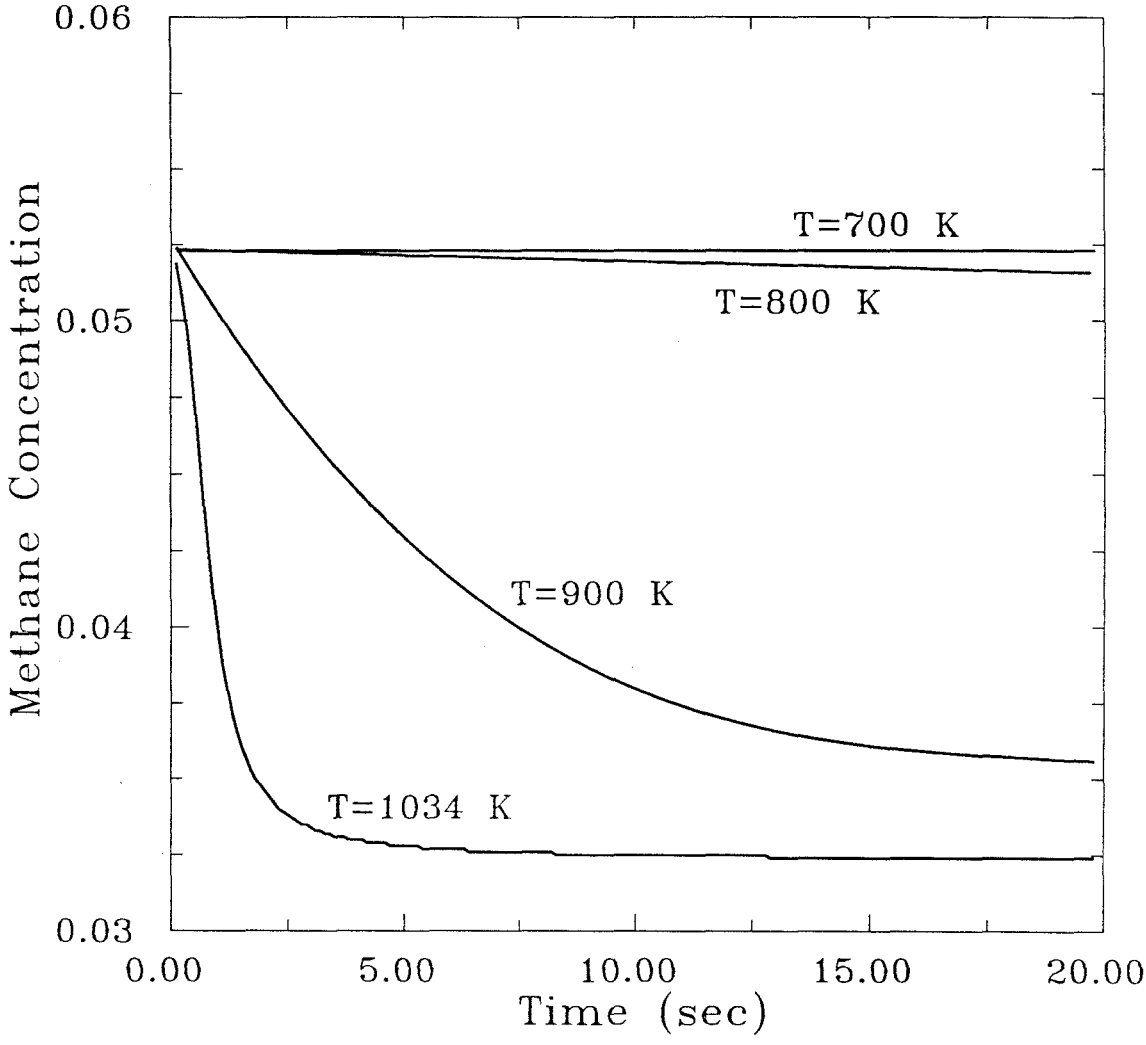

Figure 5.10: Methane concentration in a fuel-rich mixture introduced into an isothermal plug flow reactor

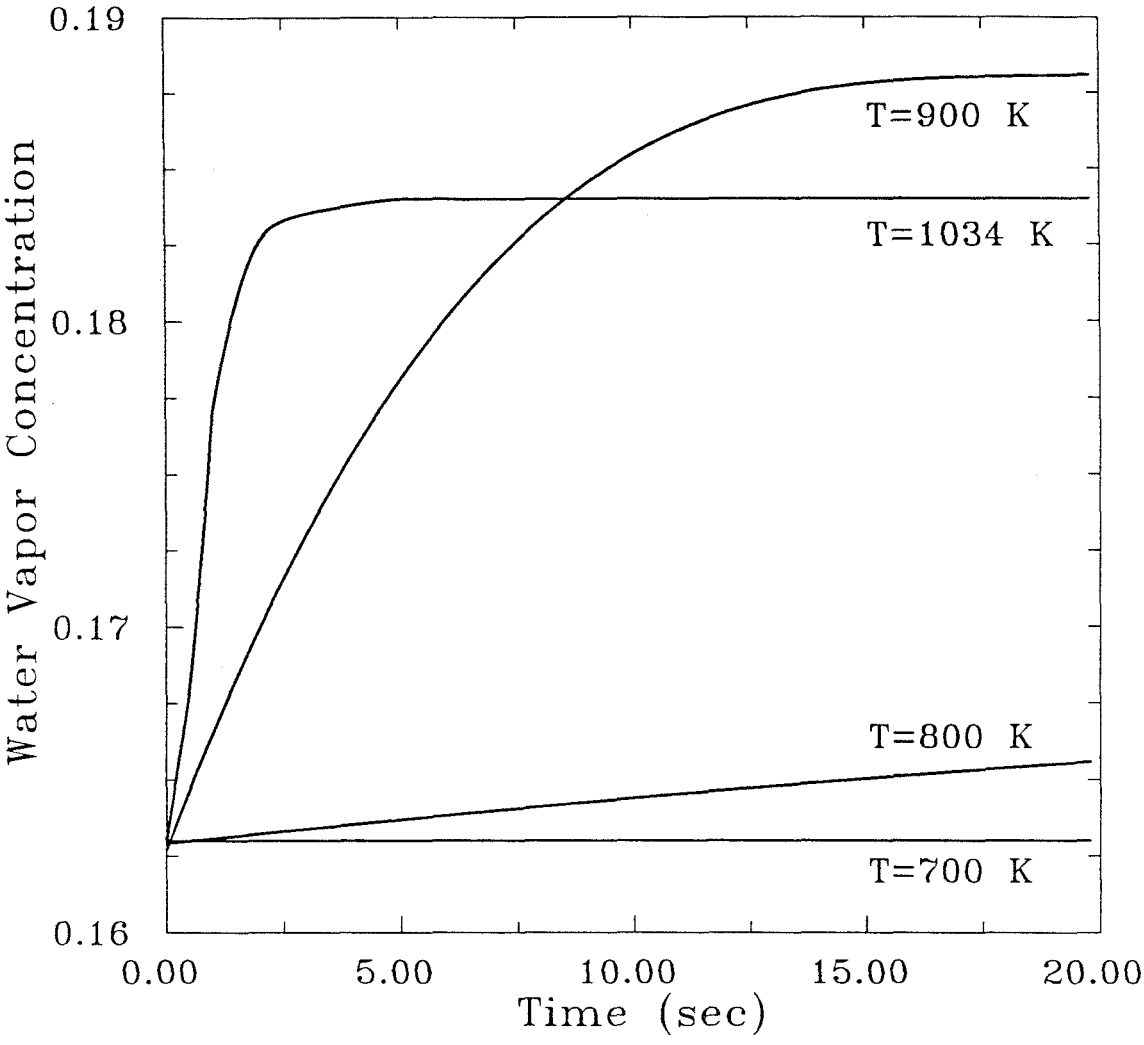

Figure 5.11: Water vapor concentration in a fuel-rich mixture introduced into an isothermal plug flow reactor

Chapter 6

Species Produced in Fires burning in Two Layers using Alternate Fuels

The experimental results presented in Chapters 4 and 5 have shown measurements taken in fires using natural gas fuel (methane is the primary component). Although the use of a gas burner is a reasonable approximation for some types of fuel materials, the actual pyrolysis process for most common combustibles involves the production of a wide variety of liquid and gaseous fuels. Often fuels with complex molecular structures can be identified during the intermediate steps of the pyrolysis, e.g., alcohols produced during the combustion of wood. The simple structure and peculiar behavior of methane (in comparison to other organic hydrocarbons) limit the applicability of these previous results.

To extend the range of applicability of the results in this study, the same procedure (as outlined in Chapter 2) was used for two other gaseous fuels: ethylene and propylene. With the additional data from these two fuels, it is possible to consider the effects of two independent parameters on our experimental measurements. The first is the effect of large differences in the initial buoyancy of the fuels. Since this will impact the flame's character over the initial region and the production rate of vortical structures (the flame's "puffing" rate), it was expected that these changes would result in differences in the entrainment behavior. Because the interface heights used in these tests were limited to small values (not larger than 10 cm), variations in the fuel type for otherwise fixed experimental conditions should amount to subtle differences in the fuel-air ratio of the plume mass flux. The second parameter being varied by the different fuels is the molecular structure. The effects of the varied carbon-to-hydrogen ratios and the multiple carbon bonding arrangements were the more important motivations for selecting these fuels. The major concern here was the possibility of particularly significant differences in the product species formed (especially the toxic components) due to a specific type of molecular structure. Since we were interested in the species produced primarily during fuel-rich upper layer conditions, smaller interface heights were used for most of these experiments, as mentioned above. This provided higher plume equivalence ratios with smaller fuel flow rates to minimize problems with freezing of the fuel tank regulator.

For each fuel, appropriate adjustments were made to the selections of chromatographic columns, calibration gas mixtures, and data reduction schemes. When ethylene was used, no additional product species were expected or found (compared to the case with natural gas fuel), thus the only alterations necessary were to accomodate the possibility of larger amounts of residual ethylene in the product gas sample. This required an increased separation between the the elution times of the carbon dioxide, ethylene, and ethane peaks. Previously, the porapak T column was selected to maximize the separation time between the methane and carbon dioxide peaks to allow sufficient time for valve switching and baseline stabilization. This was accomplished at the expense of minimal separations between the elution times of carbon dioxide, ethylene, and ethane (some overlap of peak areas was tolerable since the latter two components were present only in trace quantities when natural gas fuel was used). Replacing this column with a porapak N provided complete separations between these components while maintaining sufficient time for valve switching between the methane and carbon dioxide, since the methane peak was significantly reduced for this fuel. For the propylene fuel, an additional peak was expected (and found) which corresponded to residual propylene in the product gas. The elution time for this component was much longer than for the other species, thus it presented no difficulty for the same arrangement of columns used with ethylene. One limitation for this setup was that the porapak N did not give sufficient separation time between the propylene and propane peaks. To determine if this limitation was important, sample tests were run using a porapak Q which gave ample separation time to resolve these components, but at the expense of poor separations between the ethylene, ethane, and acetylene. After analyzing samples taken from experiments with upper layer conditions near $\varphi_\ell = 1$ and from fuel-rich upper layers (φ_ℓ of about 1.7), no measurable amounts of propane were found when propylene fuel was used. The only changes required here then were those involving the selection of the mixture for the calibration gas.

6.1 Experiments with Ethylene Fuel

Ethylene is an aliphatic hydrocarbon compound in the alkene family (olefins) which possesses the following chemical structure:

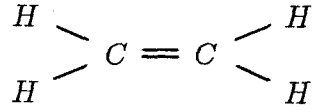

It has a boiling point of 169 K and a molecular weight of 28.05, which indicates

that this fuel is slightly buoyant in air. In contrast, natural gas fuel has a formula weight of about 17.15, and thus is positively buoyant in air (methane has a boiling point of 112 K).

In this section, we will present the measurements from experiments where ethylene fuel was used (again, as a function of the upper layer equivalence ratio), and comparisons of this data will be made to values predicted by equilibrium computations. These computations were performed using STANJAN, version 3.31 (Reynolds, 1989) for three different product temperatures. With fuel and air components supplied at 1 atm and 298 K, the product species were determined for equilibrium conditions at 1 atm and temperatures of 500 K, 800 K, and at the adiabatic flame temperature for the mixture. A temperature of 500 K represents a lower limit to the experimentally measured temperatures of the upper layer gases, while 800 K corresponds to conditions well above the upper limit of the experiment (outside of the plume). A limiting case for the equilibrium calculations occurs when the products are formed without energy losses (radiative or conductive), i.e., a perfectly adiabatic process.

Species concentration measurements and the corresponding equilibrium values are shown in Figures 6.1 through 6.7 for the major stable species, with temperature measurements and the adiabatic flame temperatures given in Figure 6.8. These experiments with ethylene fuel were conducted with fire strengths ranging from 30.7 to 55.3 kW which provided plume equivalence ratios from 0.85 to 1.46. For the overall combustion reaction, soot was again modeled as $C_8H(s)$, however, there were some interesting differences observed, which will be discussed later. Since our experimental measurements suggested that soot was only a trace component in the products for these two-layered fires, and due to a lack of accurate thermodynamic data for this empirical formula, the formation of soot was not included in the equilibrium computations. Note that these results are given in terms of species concentrations (mole fractions), whereas the previous measurements for natural gas fires were presented as mass fractions.

For fuel-lean conditions ($\varphi_\ell < 1$), hydrogen measurements and equilibrium values at 500 to 800 K, shown in Figure 6.1, were insignificant. Only the equilibrium composition at the adiabatic temperature contained a noticable level of hydrogen for this range of stoichiometries. During fuel-rich conditions, the experimental measurements fell between the equilibrium values predicted at 500 and 800 K, but for the range of these tests ($\varphi_\ell < 1.5$), the levels at the adiabatic temperatures also fell between these two curves. This behavior is due to the formation

of larger amounts of other product species at the higher temperature, and thus it is not until more fuel is supplied ($\varphi_\ell > 1.8$) that the largest amounts of hydrogen are produced at the adiabatic flame temperature. Some of the differences in the data may be due to the extremely high minimum detectable quantity (MDQ) for hydrogen, which was about 1200 ppm in these tests (despite one data point at a lower level).

Oxygen concentrations at equilibrium conditions, found in Figure 6.2, were insensitive to the temperature for the range 500 to 800 K over all stoichiometries. Even at the adiabatic flame temperature, there is only a slight increase to the presence of oxygen in the equilibrium products, when the proportions of reactants were near stoichiometric conditions. The trend of the experimental data agrees with these equilibrium values at the lower equivalence ratios, but we found significantly more oxygen remaining in the experiments than predicted at equilibrium when $\varphi_\ell > 0.75$. This is a clear indication that the processes occurring within the hood do not continue until equilibrium conditions are reached, even though the measurements attain steady state values. Most likely, the reactions occurring at the diffusion front between the fuel and oxidant in the upper layer proceeded at a temperature much lower than that of the reaction zone in the lower layer (unvitiated air) due to the reduced oxygen content of the upper layer gas. This causes some of the combustion reactions to be quenched before the complete consumption of the fuel and oxygen. Since measurable amounts of oxygen were present in all of these experiments, a value for the MDQ of oxygen was not determined here.

As with the hydrogen data, the nitrogen measurements fell between the equilibrium values at temperatures of 500 and 800 K, as shown in Figure 6.3. During fuel-lean conditions, there is good agreement between the equilibrium values and the experimental data. Reductions in the equilibrium concentration of nitrogen for fuel-rich conditions at the higher temperatures are due to the formation of larger amounts of other product species, with notable increases in the hydrogen, carbon monoxide, and water vapor. A reversal of this trend is seen for the methane concentrations in the products, given in Figure 6.4, where the largest equilibrium values are found at the lowest temperature. Now the experimental measurements are much lower than the equilibrium values at 500 and 800 K (despite appearances due to the scale of Figure 6.4, there are nonzero data from some experiments). Although the data fall close to the equilibrium value at the adiabatic conditions, this does not suggest that reactions involving methane were frozen out near this higher temperature. Rather, these measurements seem to further support the idea

that even though steady state conditions are reached, the upper layer gases are not in equilibrium. Other fuel species in the products, ethylene and acetylene, display behavior opposite to that of the methane measurements. Ethylene concentrations as high as 0.0198 were found in the experiments, while the largest computational values were predicted at 800 K and did not exceed 2.0×10^{-8}. Measurements of acetylene in fuel-rich experiments reached up to 0.0058, whereas maximum computational values were about 1.6×10^{-12}, also found at 800 K.

Carbon monoxide measurements from experiments with ethylene fuel burning in two layers are presented in Figure 6.5 using a logarithmic scale (a linear plot of this data is also included in section 6.3, comparing the data from all of the fuels). This permits a comparison of the experimental and computational values which vary over several orders of magnitude, with particularly low equilibrium concentrations predicted at 500 K. Measurements of carbon monoxide in fuel-lean experiments were significantly higher than at equilibrium conditions almost up to the stoichiometric ratio. During fuel-rich conditions, the experimental measurements did not maintain the rapid growth found for equilibrium values at 800 K and above with increasing equivalence ratios. CO levels were above the MDQ of 500 ppm in all of the experiments (except one, where φ_ℓ =0.62).

Further evidence that the upper layer gas composition was not in equilibrium is provided in Figures 6.6 and 6.7, showing the carbon dioxide and water vapor concentrations, respectively. Carbon dioxide levels are well below the equilibrium values at 500 and 800 K, but the slope of the measurements during fuel-rich conditions appears to fall between these two curves. The water vapor measurements exceed the equilibrium levels for these conditions, and despite the continued reductions for each set of equilibrium values with increasing stoichiometries, the experimental measurements appear to be constant after reaching a steady value. For both of these components, as with the other measurements (excluding the CO), agreement is best between the computations and experiments during the more fuel-lean conditions.

Upper layer temperatures ranged from 495 to 573 K in these experiments, with a trend to the data similar to the profiles for the natural gas experiments (cf. Figure 5.2). The measurements were taken at a fixed position above the burner, corresponding to position (B) described in Figure 3.1 when the interface height was 10 cm. In general, temperatures increased when more air was added to the upper layer in each series of tests until combustion efficiency reached a maximum. Further increases in the air addition rate acted to dilute the product

layer with excess air, thus reducing the temperature (see the case where $\varphi_\ell = 1.46$ in Figure 6.8). Given the importance of the effects of the upper layer temperature on the product species formed, as described in Chapter 5, caution should be used when comparing this data to measurements from different studies. Values of the adiabatic flame temperature are superimposed on this plot, but with a different scale. Maximum values exceeded 2400 K at an equivalence ratio of 1.1, with asymmetrically decreasing behavior for more fuel-lean or fuel-rich conditions. Even though this is a limiting case for the product layer composition, it demonstrates that constant upper layer temperatures are a poor approximation for use with these equilibrium calculations.

6.2 Experiments with Propylene Fuel

Propylene is also an aliphatic hydrocarbon compound in the alkene family, but it possesses a more complex chemical structure:

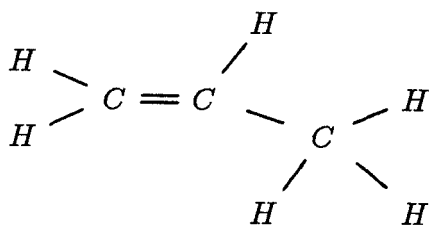

where now both a single $C-C$ bond and the double $C=C$ bond are present. The presence of the double bond confers considerably more chemical reactivity on the alkenes than is found in the alkanes (Brown and Lemay, 1977). Since propylene possesses each bonding arrangement, it is reasonable to expect its chemical behavior to fall somewhere between that of ethylene and methane. The boiling point of propylene is 225 K and its molecular weight is 42.08, thus signifying that this fuel is negatively buoyant in air. Because the results being reported here are from experiments with fires burning in two layers, the relative buoyancy of the fuel did not have an impact on the position or shape of the flames. Radiant heat feedback to the burner surface maintained an outlet temperature high enough so that the heated gas was positively buoyant in the cool room air. When the radiant flux was significantly reduced, as in the case of burning in a fully vitiated environment (see Chapter 7), the behavior of the flames was quite different.

Measurements of the upper layer composition are presented here from experiments with two-layered propylene fires ranging in size from 36.6 to 58.9 kW. With interface heights of 1 to 5 cm and the 19 cm diameter burner, these conditions provided plume equivalence ratios ranging from 1.57 to 2.06. Upper layer air addition

reduced the values of φ_ℓ to as low as 0.45. The overall combustion reaction for propylene included the same empirical model for soot, $C_8H(s)$, plus an additional term (x_{13}) corresponding to the number of moles of propylene in the products due to the combustion of one mole of fuel.

Concentrations of the major stable species of interest are presented in Figures 6.9 through 6.14 as a function of the upper layer equivalence ratio. Also included in these figures are the data of Beyler (1983) from experiments with propylene fuel burning in two layers using a similar approach. His tests were performed with fire strengths of 7.5 to 31.4 kW stabilized on 13 and 19 cm diameter burners, and a series of analyzers was used to measure O_2, CO, CO_2, H_2O, and the total hydrocarbon (THC) levels in the product gases. A simple chromatographic technique was employed to quantify the hydrogen content in the sample. Since the THC analyzer is responsive only to the carbon atoms, Beyler selected a model for the hydrocarbon structure corresponding to CH_2 (although this is the correct carbon/hydrogen ratio for this fuel, it is not an accurate representation for all of the hydrocarbon species present in the product layer gas).

As before, in each series of tests the initial experiment was performed without air addition to the upper layer, thus allowing the determination of the air entrainment rate below the interface. Subsequent tests were performed with varying amounts of air addition to the layer, thereby reducing the value of φ_ℓ. For two sets of experiments, when φ_p was 2.06 and 1.97, the fuel flow rate was adjusted to provide the largest localized fire possible for the burner size and interface height. This condition was marked by the presence of a stabilized ring of burning around the plume penetration region and the unsteady production of detached laminar flamelets (approximately corresponding to the second mode of layer burning, using the descriptions of Beyler). These detached flamelets ("fingers") travelled radially outward from the central plume for 2 to 2.5 burner diameters, starting at the stabilized ring of burning, always extending vertically upward from the interface, before the flamelets were extinguished. It is interesting that this behavior appears to be independent of the interface height, but occurs at the same value of φ_ℓ which suggests that the mechanism responsible is tied to a fundamental property of the fuel (perhaps the premixed lower flammability limit of the fuel).

Figure 6.9 shows the hydrogen measurements from the experiments using propylene fuel burning in two layers. The trend of this data is similar to the results reported here for the other fuels investigated. No measurable levels of hydrogen were detected during fuel-lean upper layer conditions, while nearly linear grow-

ing concentrations were found with increasing φ_ℓ during fuel-rich experiments. A comparison of the measurements for each fuel type will be presented in the next section. The data of Beyler also appears to agree well with our present results, except when the upper layer conditions were near the stoichiometric ratio. He reports low levels of hydrogen (below our MDQ of about 1200 ppm) for experiments with φ_ℓ values just below 1, while our measurements do not show detectable levels until φ_ℓ reaches 1.38. The trend of our fuel-rich data suggests that the hydrogen concentration would vanish at about stoichiometric conditions, which is in contrast with the behavior of Beyler's measurements in this range. Values for the species measurements of Beyler were determined by digitizing the information reported in his figures.

Measurements of the oxygen concentration are given in Figure 6.10 for these experiments using propylene fuel. As with the other fuels, when conditions are very fuel-lean ($\varphi_\ell < 0.75$), the data follow values predicted at equilibrium. During more fuel-rich conditions, significant amounts of oxygen are found in the upper layer composition. For example, a concentration of about 7.5% was measured at $\varphi_\ell = 1$, and levels were still above 1.0% even when $\varphi_\ell = 2$. The behavior of Beyler's data is different, showing much lower oxygen levels in the range $0.75 < \varphi_\ell < 1.5$. Based on our investigation of the effect of product layer temperature on combustion completeness (cf. Chapter 5), this difference is understandable. The ceiling of Beyler's apparatus was constructed of 1.27 cm thick Fiberfrax Duraboard ceramic insulation, and the apparatus was insulated all around by a 5 cm thick Fiberfrax Durablanket. As a result, he reports product layer temperatures of 680 to 780 K for experiments with a 19 cm diameter burner using propylene fuel (when $\varphi_\ell > 0.5$). In contrast, our upper layer temperatures ranged from 486 to 588 K, as shown in Figure 6.15. Hence, it is likely that the offset in the experimental results is due to these differences in the product gas temperatures. The carbon monoxide measurements, presented in Figure 6.11, also follow the trends of the results from experiments with natural gas and ethylene. Detectable amounts of CO were found in all of the tests using propylene fuel. Our data from each series of experiments and the measurements of Beyler appear to be well correlated with φ_ℓ for this fuel. Reasonable agreement was anticipated since the CO concentrations were not affected by differences in the product layer temperature when considering the results with natural gas.

When the combustion process is driven to further completion at higher product layer temperatures, reductions in the oxygen and fuel concentrations are ac-

companied by increases in the levels of carbon dioxide and water vapor. In the experiments using natural gas fuel, Toner reported measurements of these components with values higher than for the data in this study (cf. Figures 4.7 and 4.8). In a similar manner, Beyler's data from propylene fires were higher than the values determined in our experiments for these species, as shown in Figures 6.12 and 6.13. An important distinction arises when making this comparison, however, which is that the values in the tests with natural gas fuel appeared to approach steady levels with increasingly fuel-rich upper layer conditions, while this was not the case in the experiments with propylene fuel.

Figure 6.14 shows the measurements of the hydrocarbon fuels present in the product layer gases. As expected, when fuel-rich conditions are approached ($\varphi_\ell > 0.75$), significant amounts of unconsumed propylene fuel are found in linearly increasing amounts for increasing values of φ_ℓ. Other fuel components (methane, acetylene, and ethylene) are also present in linearly increasing concentrations. It was anticipated that the collective level of these fuel components would exceed the *THC* measurements of Beyler (which it does, until φ_ℓ reaches about 1.2), due to the indications of more complete combustion found in the O_2, CO_2, and H_2O concentrations. His *THC* measurements, modeled as CH_2, appear to asymptotically approach a limiting value for the layer equivalence ratio. That is, his data suggest that large increases in the residual fuel levels would result from a minor increase in φ_ℓ. This behavior is clearly inconsistent with the results of this study. Our observations indicate proportional elevations of the residual fuel levels with increases in φ_ℓ. A possible explanation for the trend of Beyler's data is his choice of a model for the *THC* measurements. Although CH_2 represents the proper carbon/hydrogen ratio for propylene and ethylene, it is not correct for the other fuel species found here.

6.3 Comparison of Results between Different Fuels

Although the trends of the species measurements are similar for each of the fuels used in this study, some interesting contrasts are seen which can be attributed to the differences in the fuels' molecular structures. In this section, comparisons of the entrainment rates and concentration profiles of the major stable species of interest will be presented for the experiments reported in Chapter 4 and sections 6.1 and 6.2. The natural gas data presented here are from the experiments performed without insulation applied to the hood. Uncertainties for the measure-

ments in ethylene and propylene fires are comparable with those reported from the experiments with natural gas fuel.

6.3.1 Entrainment Below the Interface

Entrainment rates of air below the interface were computed from measurements in experiments without air addition to the upper layer. Since only the initial test in each series provided entrainment information, the database from our experiments is limited. Additional data is included from the other investigations previously cited, with clear distinctions between the measurements for each fuel type. All of the data presented from this study were taken in experiments using the 19 cm diameter burner to stabilize the flames. The interface height was the distance measured vertically between the top (level) surface of the burner and the bottom edges of the hood (which were approximately even, within 1 cm). As previously mentioned in Chapter 4, the position of the interface was marked by smoke obscuration in the upper layer and was approximately even with the bottom of the hood.

Toner (1986) sketched approximate streamlines for the entrained flow into an unbounded source flow in a two-layer environment which suggested that the presence of the interface had an impact on the entrainment behavior. Many parameters influence the entrainment rate into the fire plume below the interface, including

$$\dot{m}_e = \dot{m}_e(Re_f, Ri_f, Z_i, D, \mathcal{D}_{af}, \mu_{air}, \ldots).$$

Changes in the fuel flow rate, $\dot{m}_f$, will have an impact on the first two of these, while the other parameters depend on the experimental geometry and the properties of the fuel and air. Since it is not possible to isolate the effects of changes in the fuel exit velocity (variations in the radiant feedback to the burner surface affect the exiting gas temperature), we can consider the impact of changes in $\dot{m}_f$ on the entrainment rate. Measurements of the entrainment rates of air are presented in Figure 6.16(a) for an interface height of 5 cm. Dashed lines show the average entrainment value from experiments with each fuel type.

The largest entrainment rates were found in tests with the ethylene fuel, despite it possessing the median value for molecular weight. This result was not anticipated, using the buoyancy relative to air as a basis for characterizing the fuels' ability to entrain. The differences in the average entrainment values between the different fuels extend beyond the estimated uncertainties for the data

presented here. The measurements of Toner agree well with our natural gas data, with an expected reduction at a lower fuel flow rate. This agreement is reasonable since the experimental technique employed here was similar to his, and the entrainment measurements were insensitive to the effects of an elevated upper layer temperature. Beyler's data at this interface height (using his "Fire Code" criterion) shows a much lower entrainment rate than our measurements in propylene fires. Toner reasoned that he and Cetegen found larger entrainment rates due to the differences in the initial buoyancy of the fuels. Beyler reported matching results, however, with both propane and methane fuels, and he found no differences in the entrainment when the surface of his burner was not water cooled. The cause for these differences in the entrainment measurements remains unresolved, but it may be related to variations in the design of the apparatus. In our experiments, the interface was well defined with an abrupt change in gas temperatures occurring over a few centimeters. Beyler reports a more gradual change in temperatures between the product layer and the room air, with interface thicknesses as large as 10 cm. With a more quiescent interface region, Beyler's experiments may have experienced a reduced amount of air captured in the disturbance region caused by the plume flow. Such a reduction would certainly appear in the measurements as a smaller entrainment rate over the same interface height.

Figure 6.16(b) presents the entrainment data from experiments with an interface height of 10 cm. These measurements show a reversal of the trends found in the previous figure, with higher average entrainment values for natural gas fires than for ethylene. No experiments were performed in this study at this interface height using propylene fuel. With the reversal of the trends seen in Figures 6.16(a) and (b), these experimental results are inconclusive.

Toner and Lim (1984) also report entrainment measurements from experiments with a 10 cm interface height using natural gas fuel. All of their data fall below our results (except two of Lim's points), with no specific trends to the data. Indeed, Toner argued that for most fire sizes, the entrainment rate was independent of the fuel flow rate. Despite some scatter to the present data, this is also the case for our results. Lim's measurements also show a relatively uniform entrainment rate in all of his experiments with a 10 cm interface height, albeit with a large amount of scatter. As before, Beyler's data from an experiment with propylene fuel is one of the lowest entrainment rates from all of the experiments with this interface height.

6.3.2 Chemical Species Produced

Differences in the entrainment rates for the different fuels have an impact on the fuel-air ratio of the plume flow entering the upper layer. Because the measurements of chemical species produced in these two-layered fires are well correlated with the parameter φ_ℓ, and are independent of the plume equivalence ratio, the effects of variations in the entrainment rate are accounted for when presenting the experimental data in this manner. Of particular interest when comparing the product species are the effects of the various carbon bonding arrangements on the fire's propensity to produce toxic species and the relative amounts of other product components. The measurements taken with each fuel are shown in Figures 6.17 through 6.20 with a dashed line tracing a best-fit interpolating polynomial for the data.

As expected, Figure 6.17 shows that the oxygen concentrations during fuel-lean conditions ($\varphi_\ell < 0.75$) behaved relatively the same for each fuel, comparing well with equilibrium values. Near stoichiometric conditions, the "hump" in the measurements from experiments with propylene provides the largest departure from equilibrium values for all of the fuels, possibly due to temperature effects. For very fuel-rich conditions ($\varphi_\ell > 1.75$), it appears that the curves agree well, with oxygen concentrations falling below 1%. The most oxygen-depleted upper layer compositions were found in experiments with ethylene fuel, once the excess oxygen had been consumed. This behavior may have contributed to some of the results found for other species in the tests with ethylene, particularly the carbon monoxide.

Significant levels of carbon monoxide were detected in the experiments starting at values for φ_ℓ of 0.5, as shown in Figure 6.18, which is a clear indication that the upper layer gases were not in equilibrium for the temperatures measured. These results correlate well with φ_ℓ for all of the fuels considered here, which is reasonable since our investigations with natural gas (see Chapter 5) showed that the CO levels were invarient with changes to the upper layer temperature. As predicted with the equilibrium computations for ethylene fuel (section 6.1), the levels of CO do not appear to reach steady values for any of the fuels as φ_ℓ continues to increase. The measurements of CO in propylene fires fall between the results with natural gas and ethylene. This observation suggests that because the propylene possesses both the single and double carbon bonds, the behavior of the fuel acquires characteristics of both the alkanes and of ethylene (the simplest

alkene). The highest concentrations of CO in these experiments were found in tests with ethylene fuel, where levels of 25,000 ppm were measured. This is in agreement with the results of the oxygen measurements in ethylene fires, where reduced levels of available O_2 inhibited the oxidation of the CO to CO_2. Carbon dioxide levels for ethylene fires are also higher than for the other fuels, reflecting more complete consumption of the ethylene fuel.

Methane is the simplest member of the alkane family, which indicates that it is a saturated hydrocarbon (in the homologous series C_nH_{2n+2}). It possesses the maximum number of hydrogen atoms to populate the available bonding sites. In contrast, ethylene and propylene are unsaturated, as they contain fewer hydrogen atoms than their alkane counterparts (these are in the homologous series C_nH_{2n}). Consequently, during the combustion of natural gas, more hydrogen is available due to this higher H/C ratio for methane. Because the reactions forming the water vapor proceed faster than those involved with creating the CO and CO_2, and since these three stable species are competing for the available oxygen, we expect the measurements for natural gas fires to show larger relative amounts of H_2O, and correspondingly lower amounts of CO and CO_2. The relative comparisons of carbon dioxide and water vapor measurements are presented in Figures 6.19 and 6.20, respectively. These figures show that more of the consumed oxygen has gone towards the production of H_2O when natural gas fuel was used, and indeed the CO and CO_2 levels are lowest in these tests. During very fuel-lean conditions ($\varphi_\ell < 0.5$), agreement with the CO_2 measurements is good, following expected equilibrium values as before. As could be anticipated from the oxygen measurements in propylene fires, the characteristic hump near stoichiometric conditions is also seen in the CO_2 and H_2O curves, showing that less of the fuel and oxygen were consumed.

6.3.3 Qualitative Observations of Soot Characteristics

The empirical formula for soot was modeled in this study as $C_8H(s)$, originally suggested by Palmer and Cullis (1965). Since the amounts of soot determined in these experiments was small, not exceeding 1% mole fraction, the analysis of the product composition was relatively insensitive to the particular model selected. Toner (1986) conducted his analysis using alternate models of $C_{16}H(s)$ and $C_4H(s)$ for soot, and found that changes in his entrainment measurements were less than 1%. Here we will describe some of the observed differences between

the characteristics of the soot deposits for the different fuels.

When fuel-rich natural gas fires were allowed to burn for extended periods of time, the viewing windows, the interior of the hood, and the sample line filter accumulated a deposit of soot. The material was dark grey/black in color and extremely low in density. The mechanical properties were such that the material possessed cohesiveness and a sponge-like resiliency. As a result, large sheets of soot could be separated from the hood's interior surface, on the order of 100 cm^2, and these sheets maintained the characteristics of flexibility and cohesiveness. Since all such material in the sample stream was collected by the 0.1 μm filter, the minimum particulate size was somewhat larger than this.

In contrast, the fuel-rich fires using ethylene and propylene fuel not only deposited soot on the hood's interior surface, there was also a significant amount of particulate precipitation (in clumps) on the floor below the hood. The color and density of the material were similar to those for the case of natural gas, but significant differences were observed in the mechanical properties. The soot deposits here were not cohesive or flexible. Hence, deposits separated from the hood's interior readily fractured into smaller pieces, none larger that 5 to 8 cm^2. When compressed, this material was crushed and did not show the resilient properties mentioned above. No important differences were observed between the soot character for the ethylene and propylene cases, but it appeared that the volume of soot produced was slightly larger for the propylene fuel.

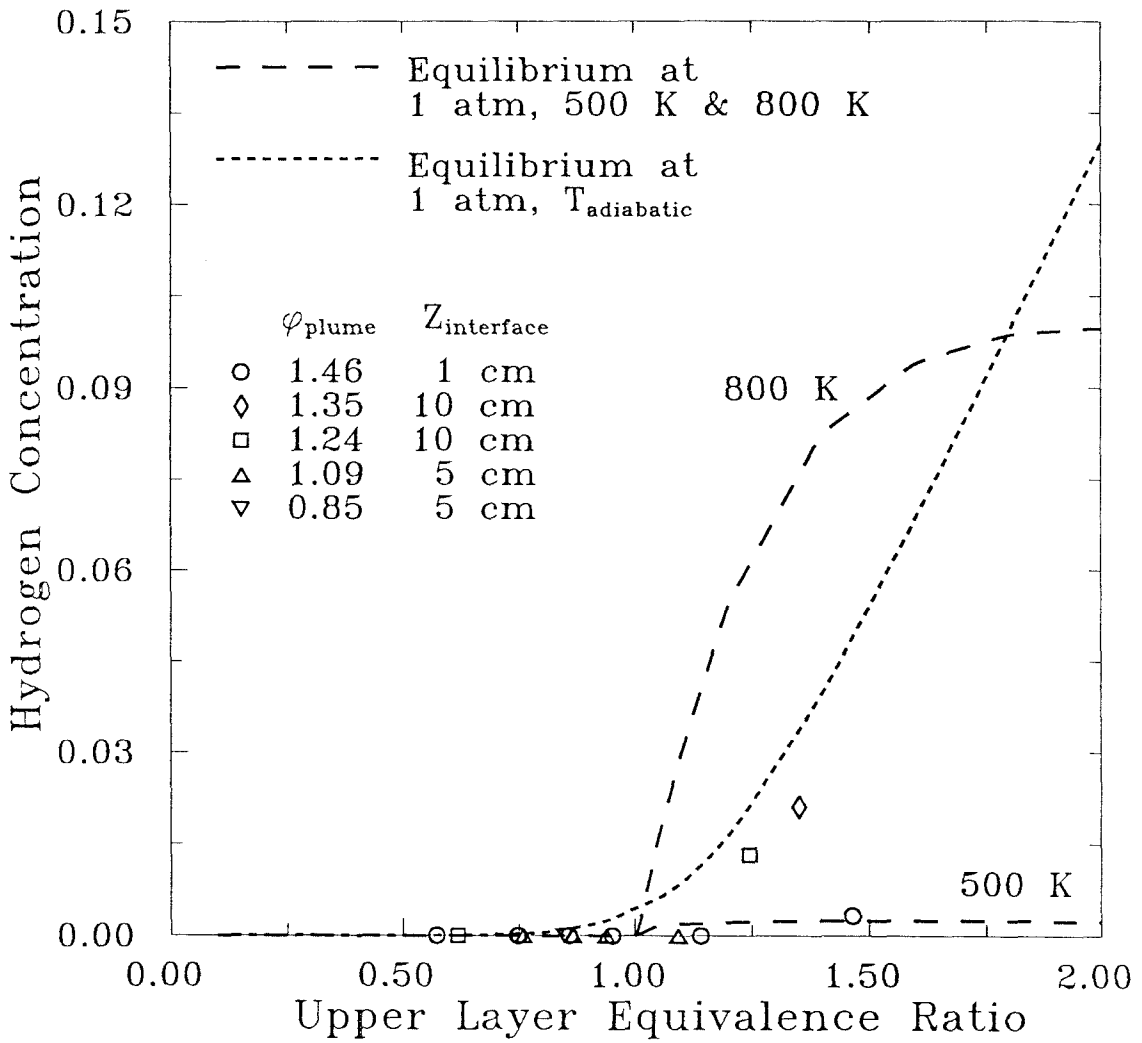

Figure 6.1: Hydrogen measurements for ethylene fires burning in two layers

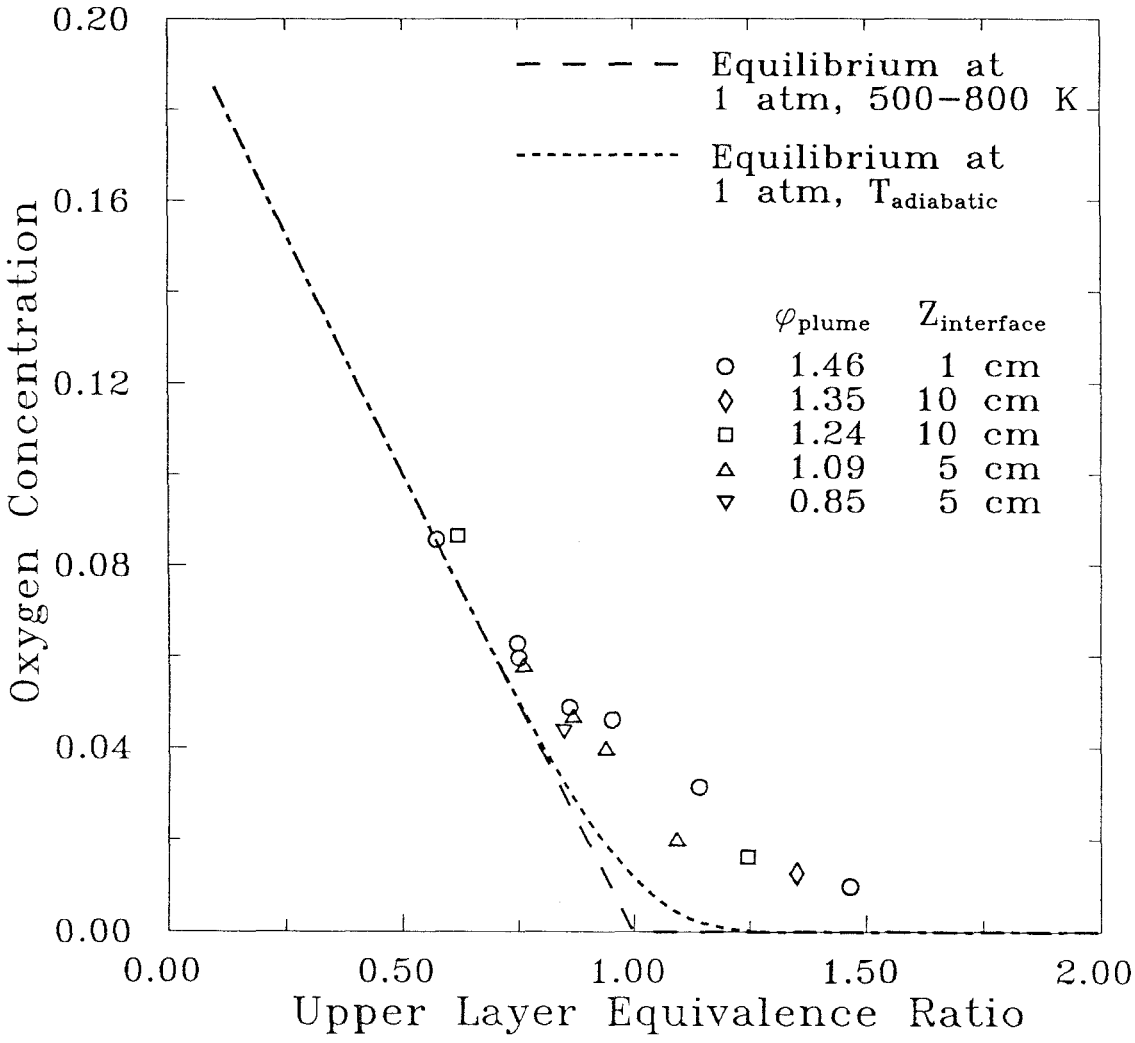

Figure 6.2: Oxygen measurements for ethylene fires burning in two layers

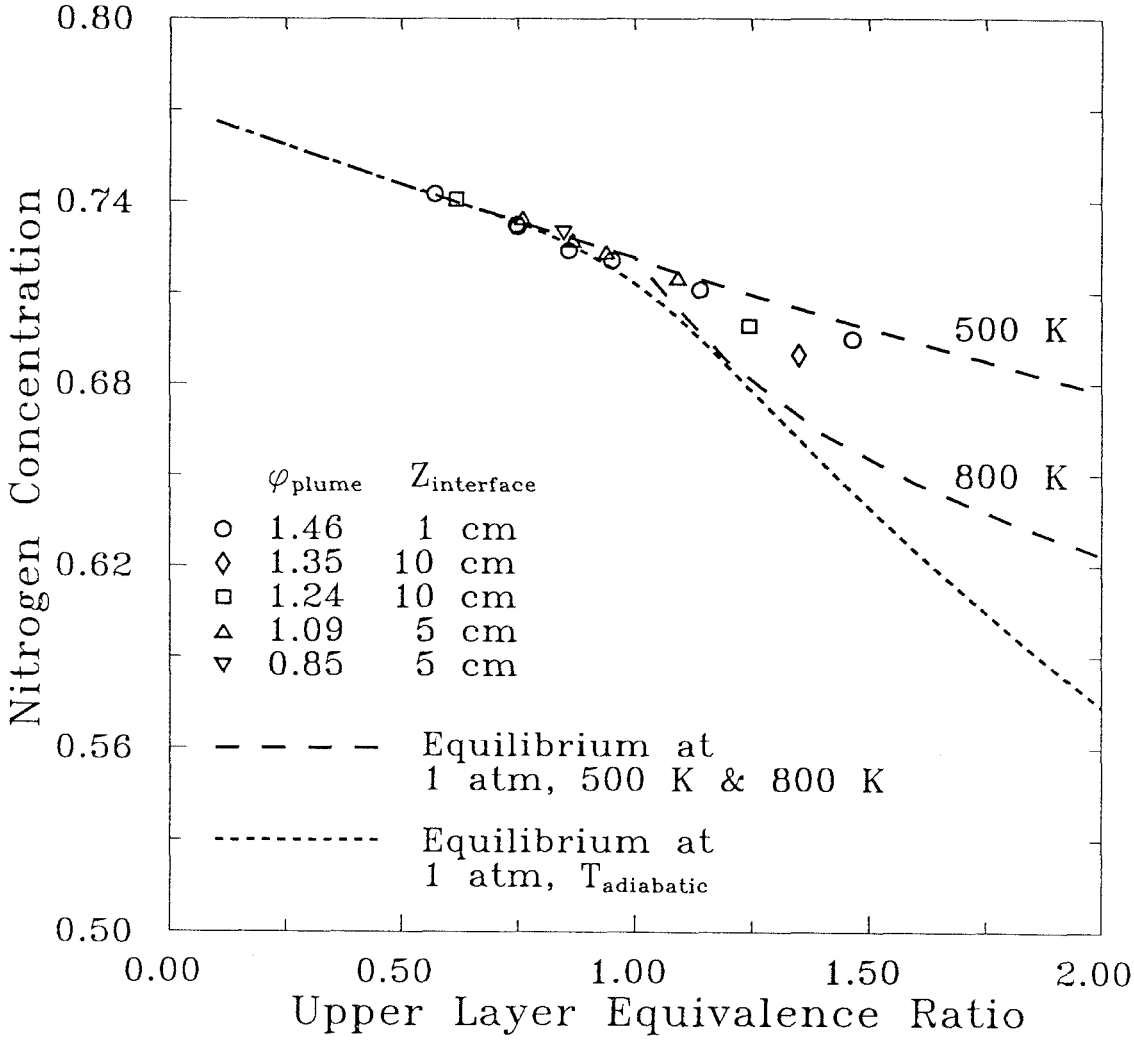

Figure 6.3: Nitrogen measurements for ethylene fires burning in two layers

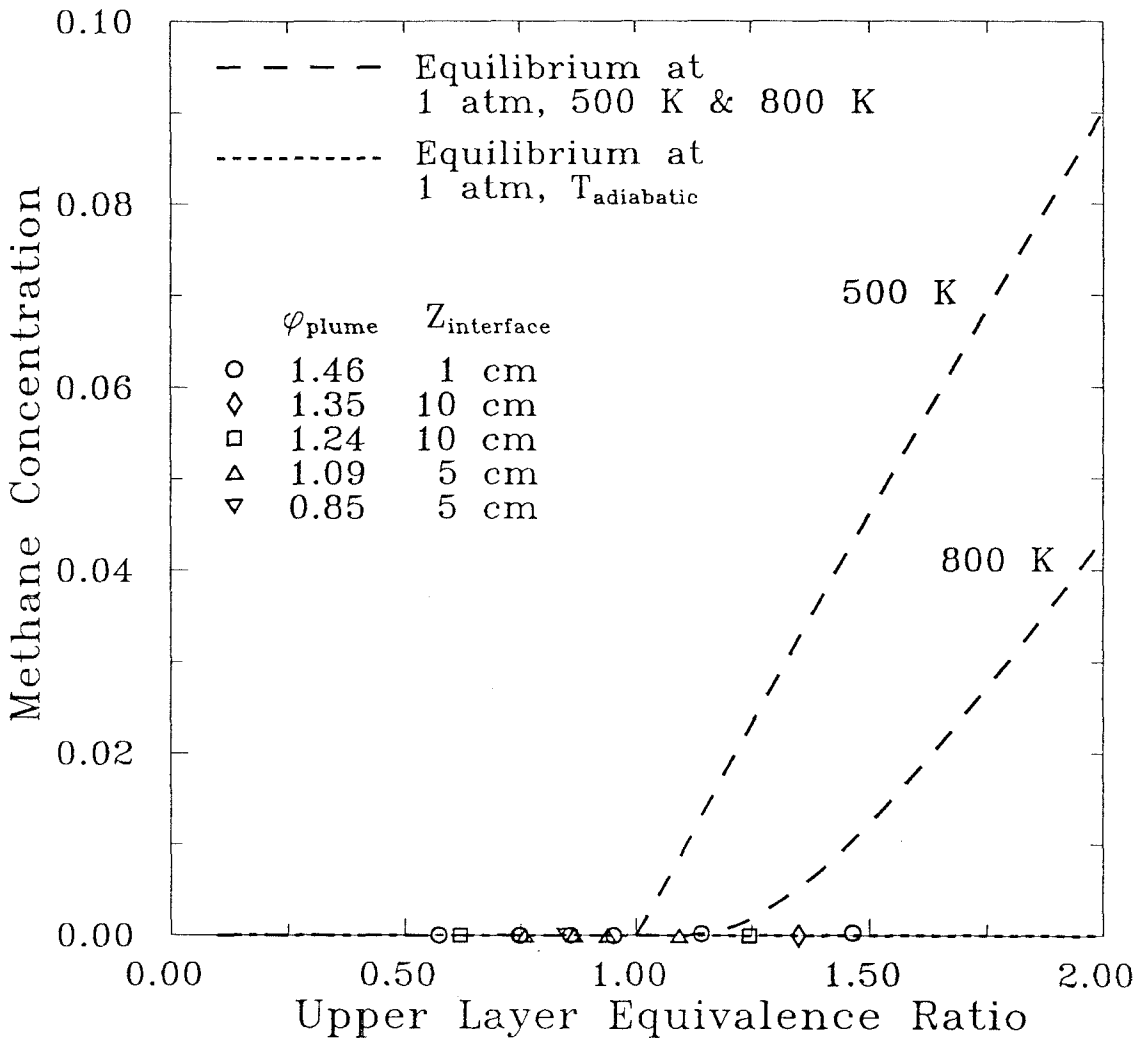

Figure 6.4: Methane measurements for ethylene fires burning in two layers

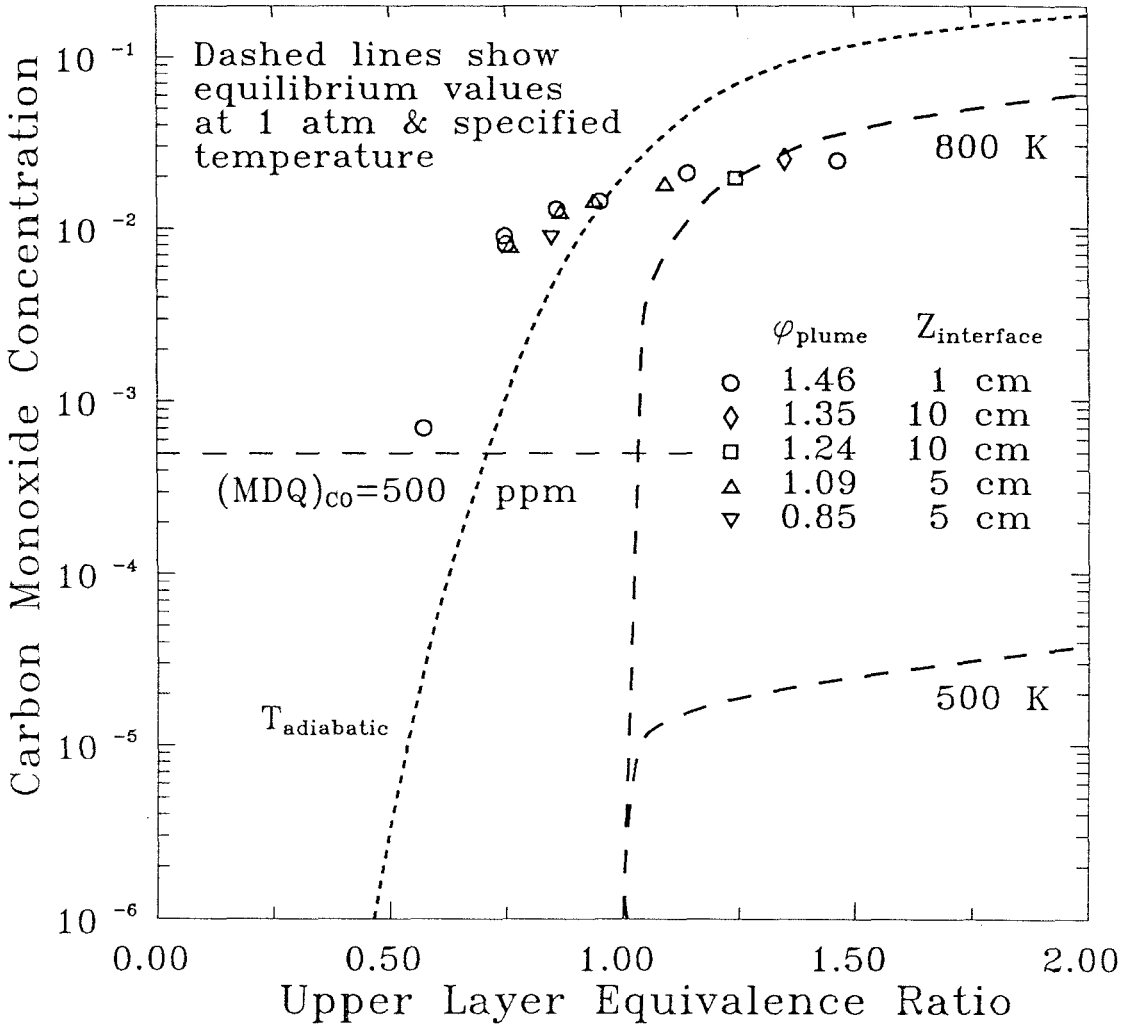

Figure 6.5: Carbon monoxide measurements for ethylene fires burning in two layers

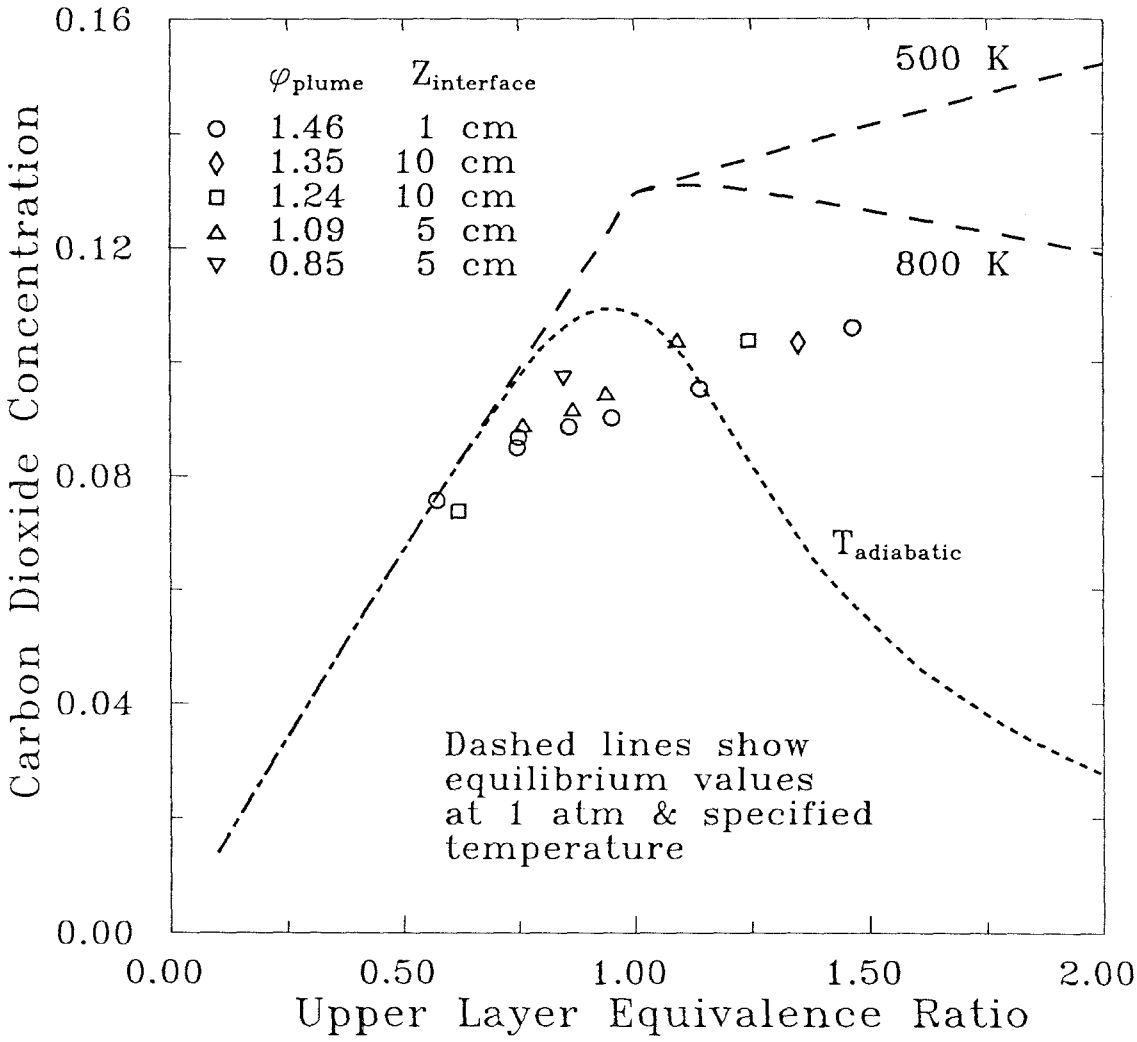

Figure 6.6: Carbon dioxide measurements for ethylene fires buring in two layers

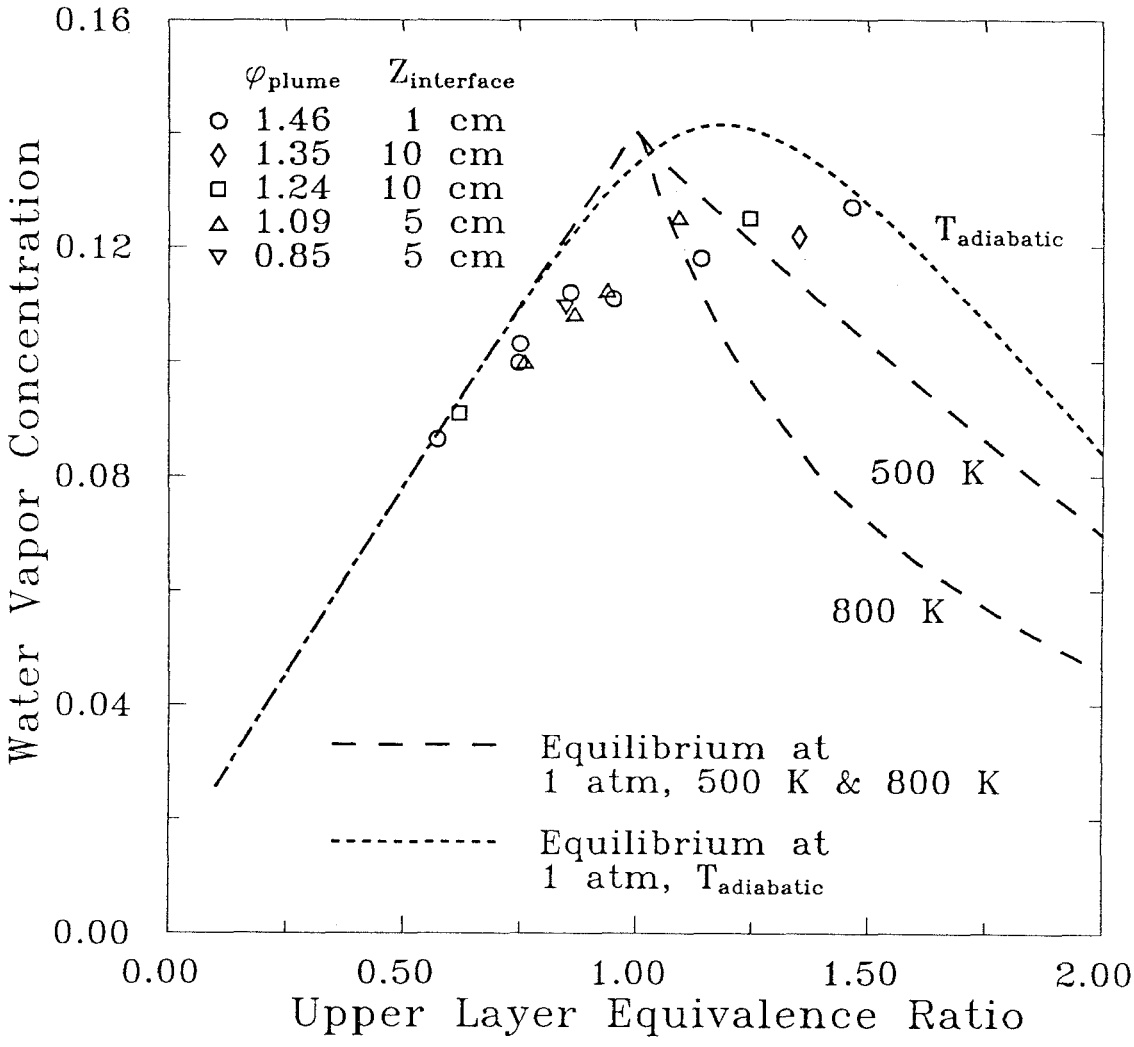

Figure 6.7: Water vapor measurements for ethylene fires burning in two layers

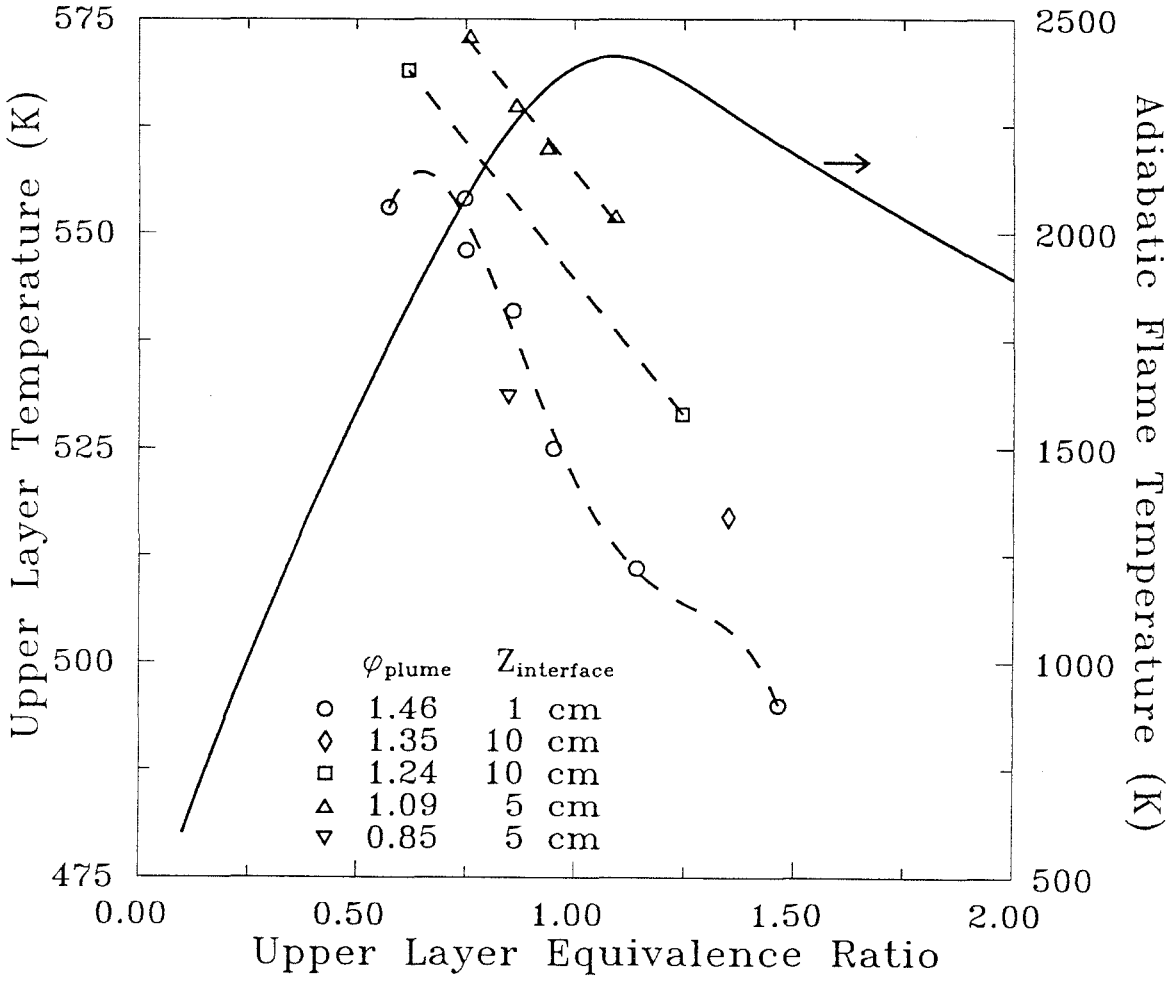

Figure 6.8: Temperature measurements for ethylene fires burning in two layers

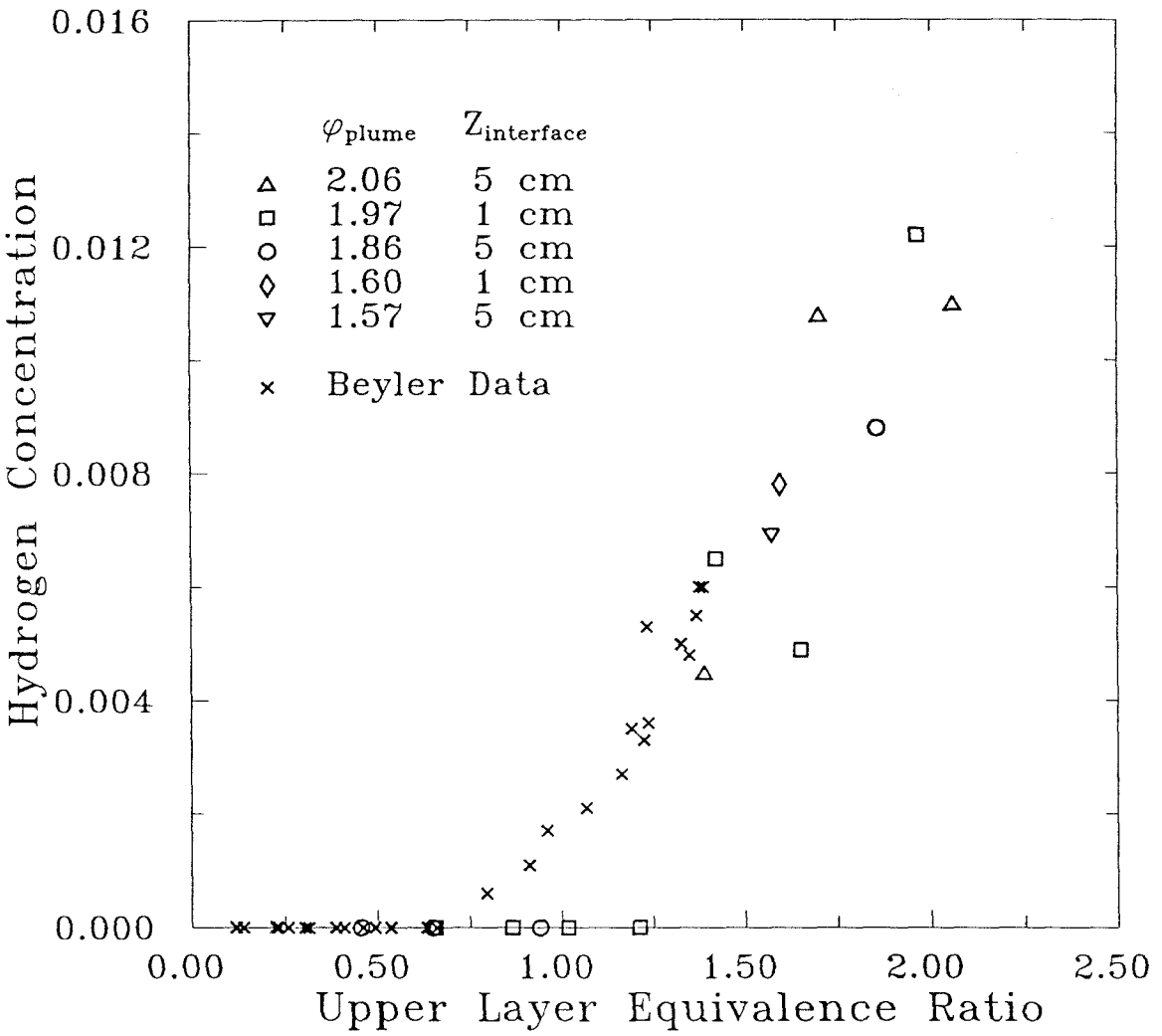

Figure 6.9: Hydrogen measurements for propylene fires burning in two layers

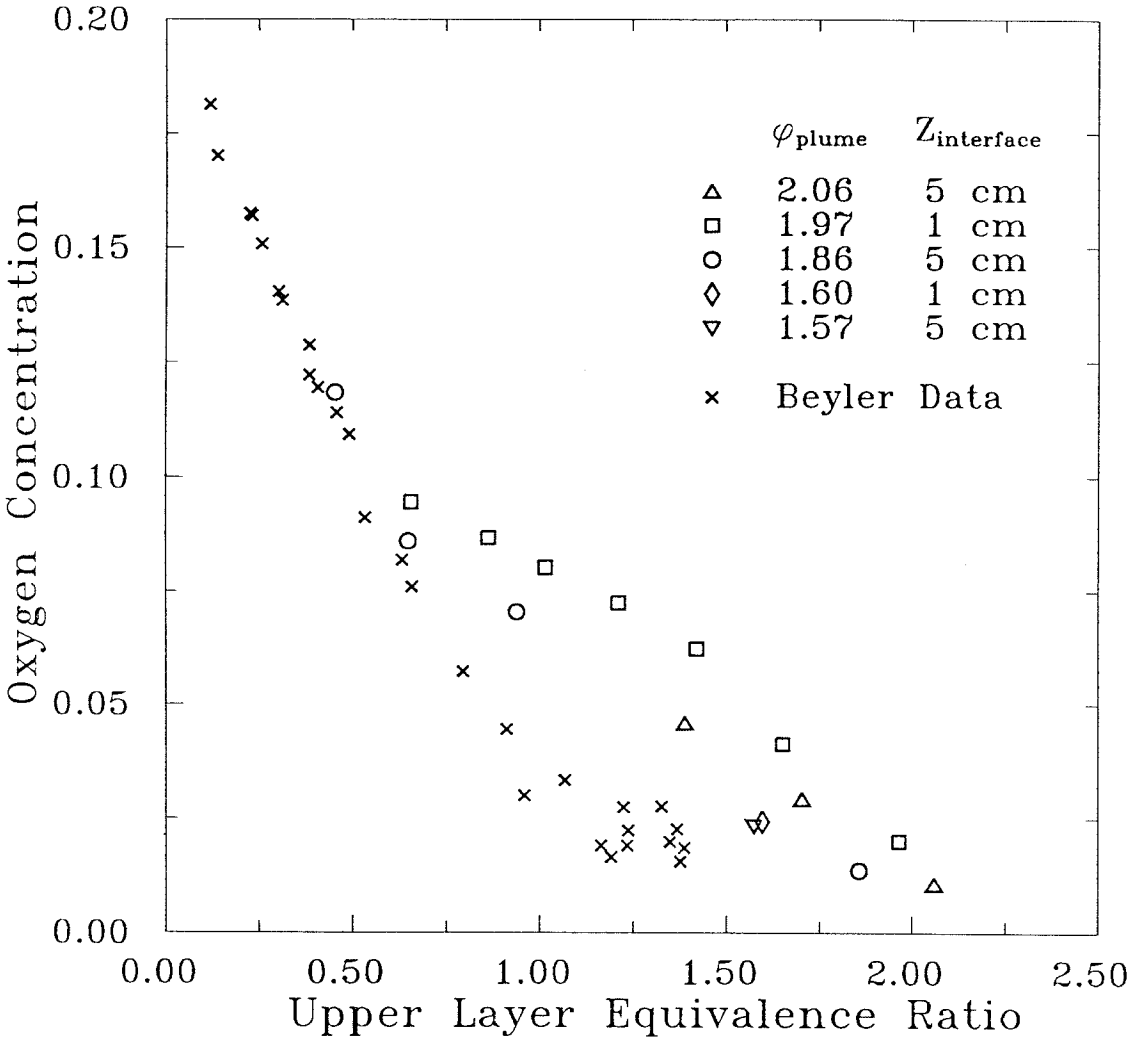

Figure 6.10: Oxygen measurements for propylene fires burning in two layers

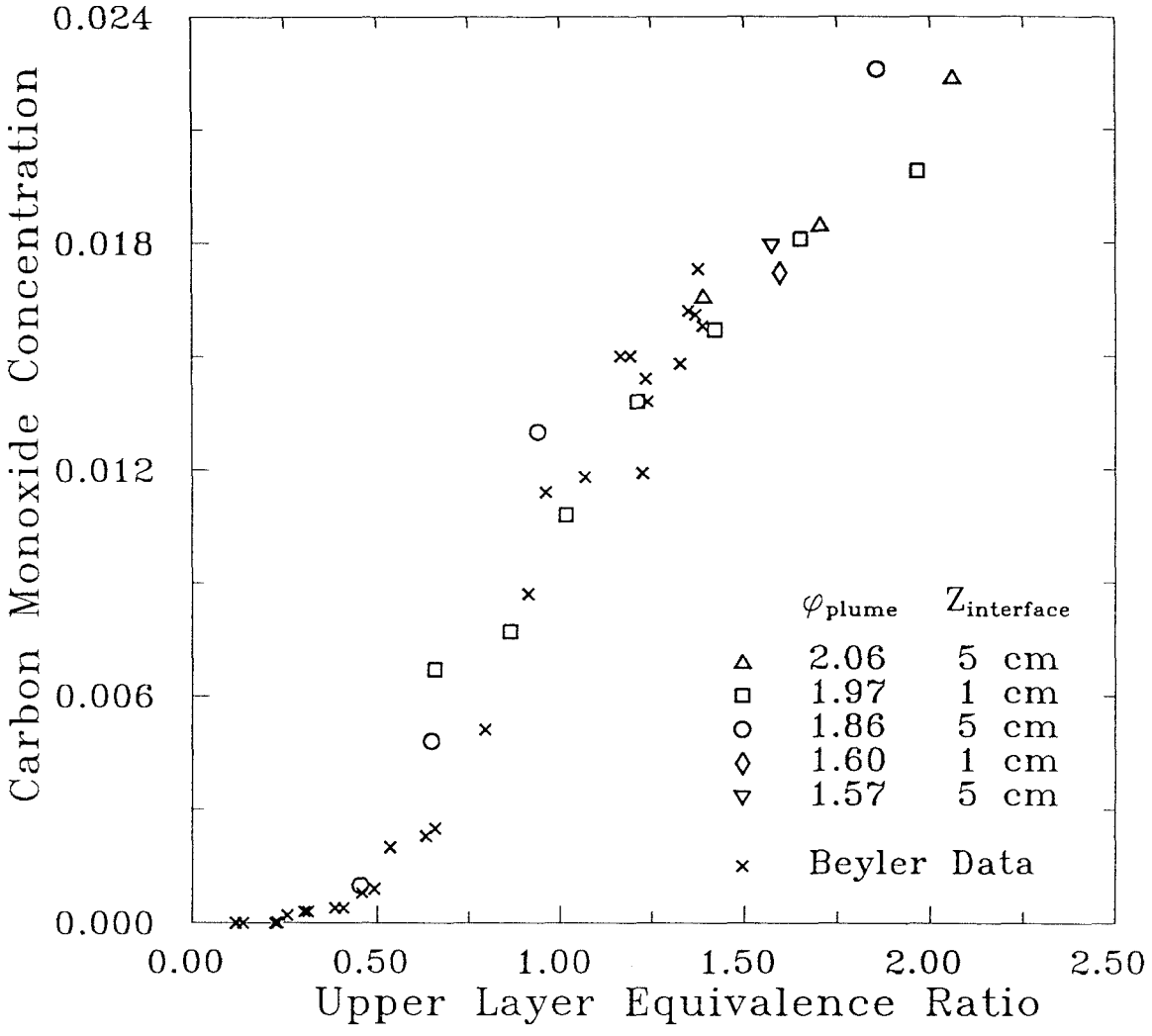

Figure 6.11: Carbon monoxide measurements for propylene fires burning in two layers

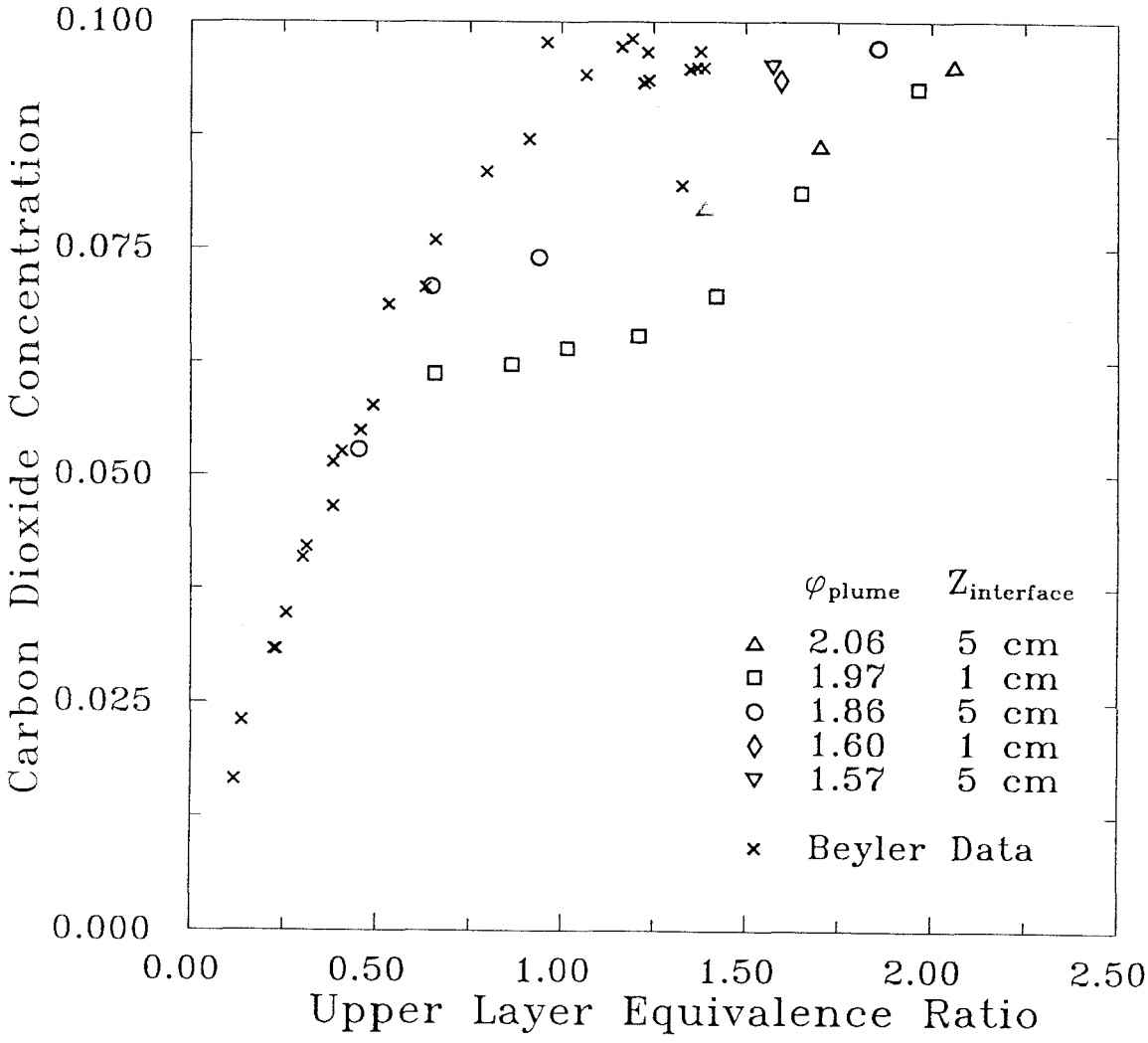

Figure 6.12: Carbon dioxide measurements for propylene fires burning in two layers

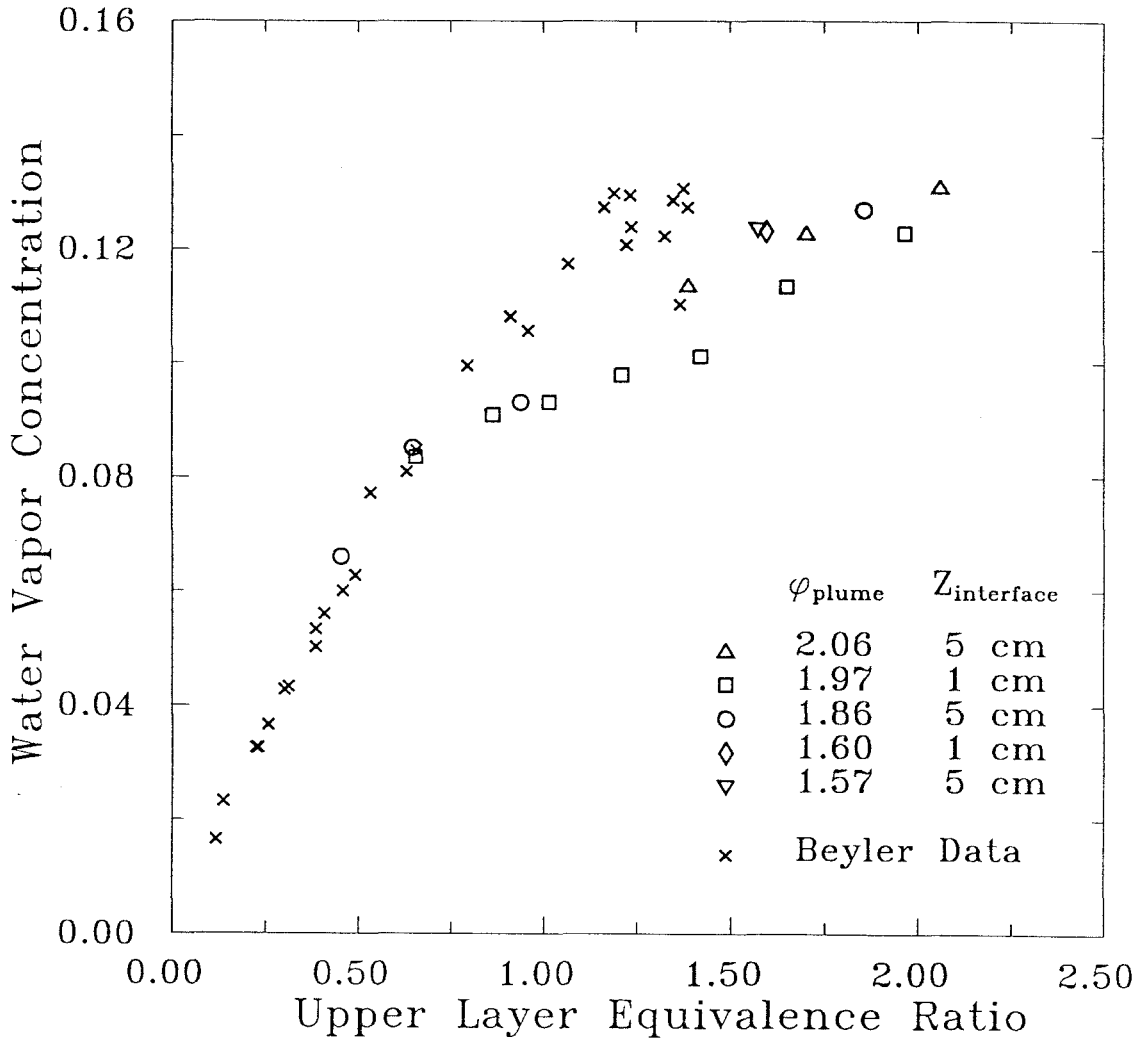

Figure 6.13: Water vapor measurements for propylene fires burning in two layers

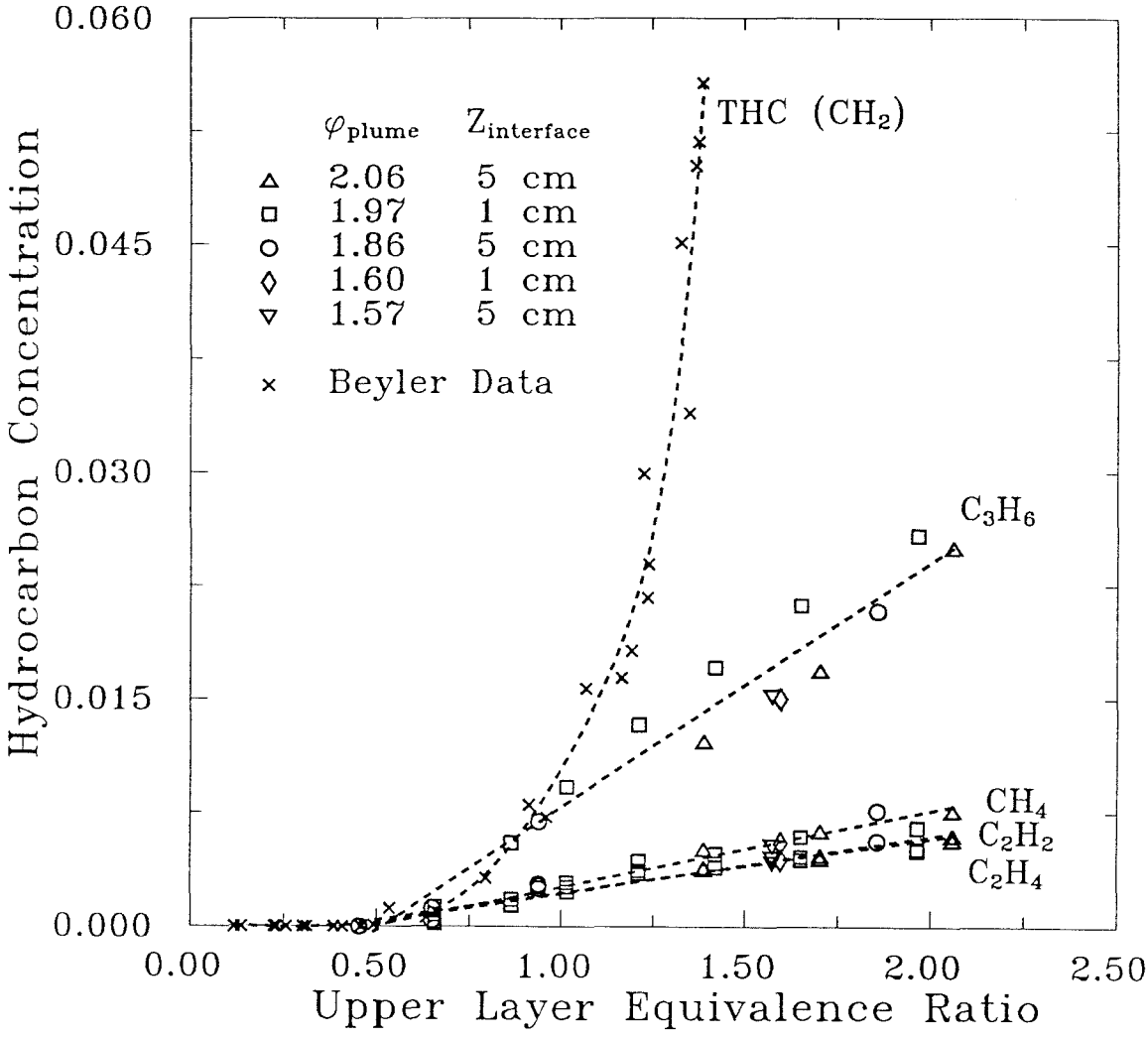

Figure 6.14: Hydrocarbon measurements for propylene fires burning in two layers

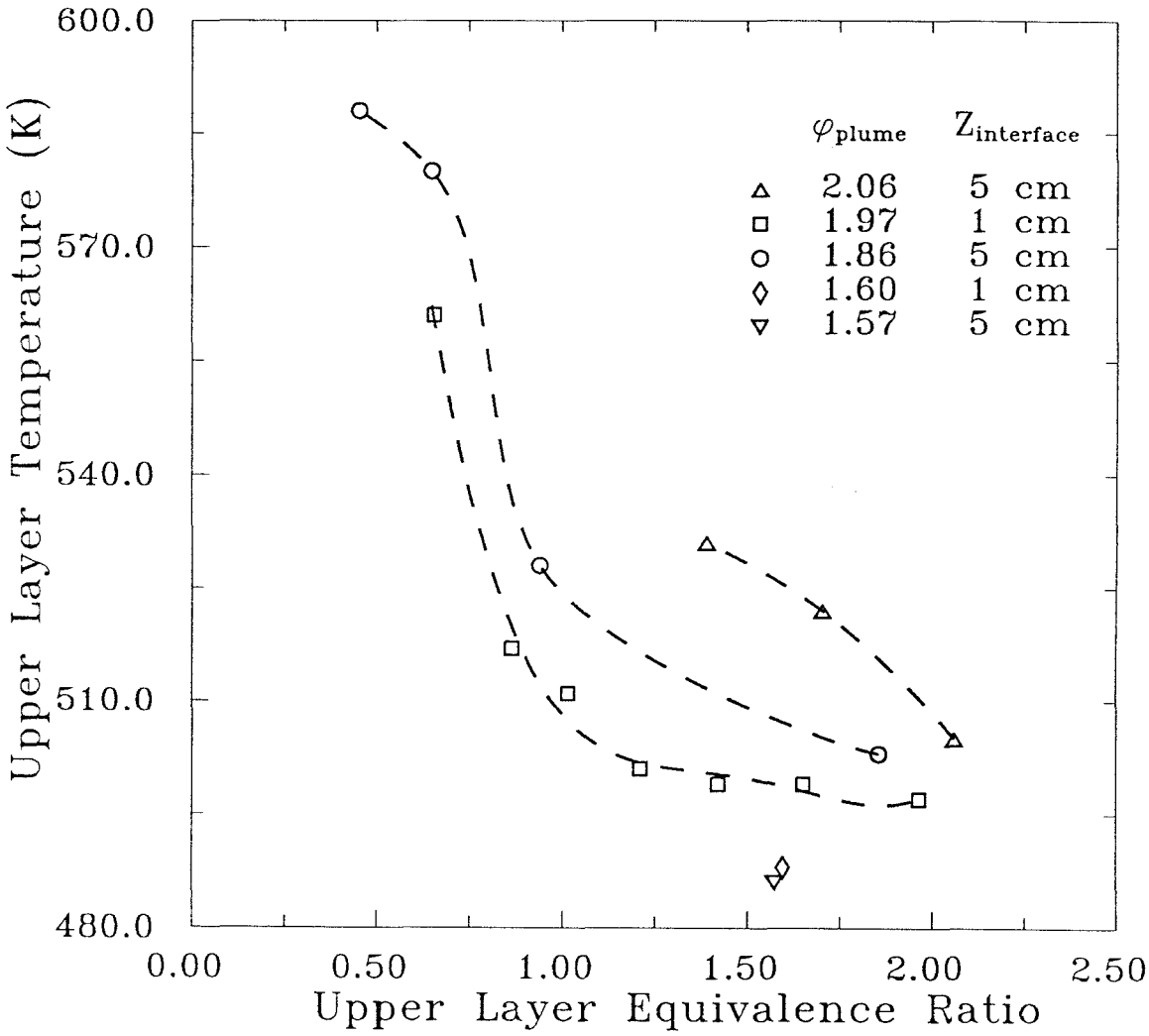

Figure 6.15: Temperature measurements for propylene fires burning in two layers

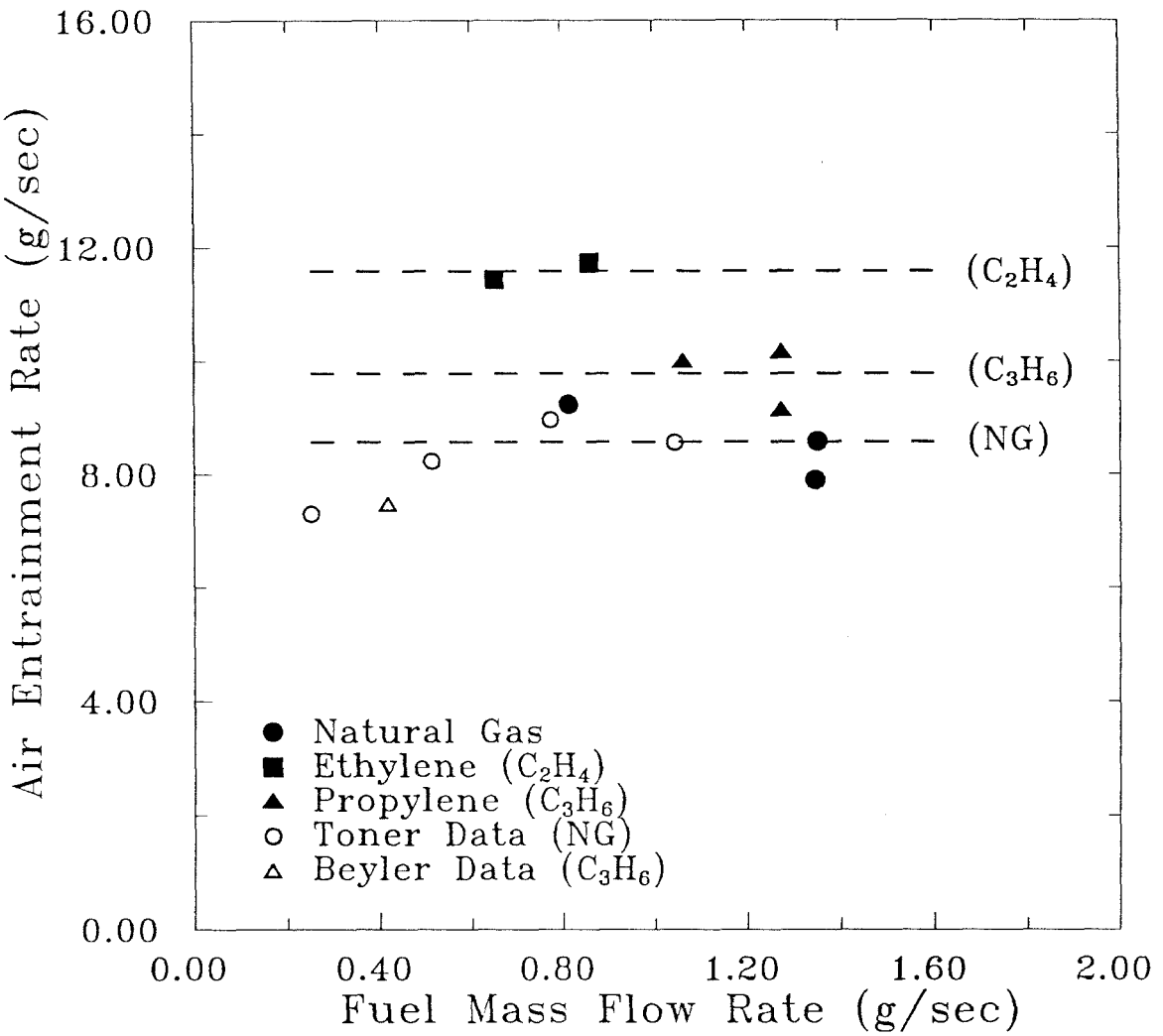

Figure 6.16(a): Average entrainment rates below a 5 cm interface height for various gaseous fuels

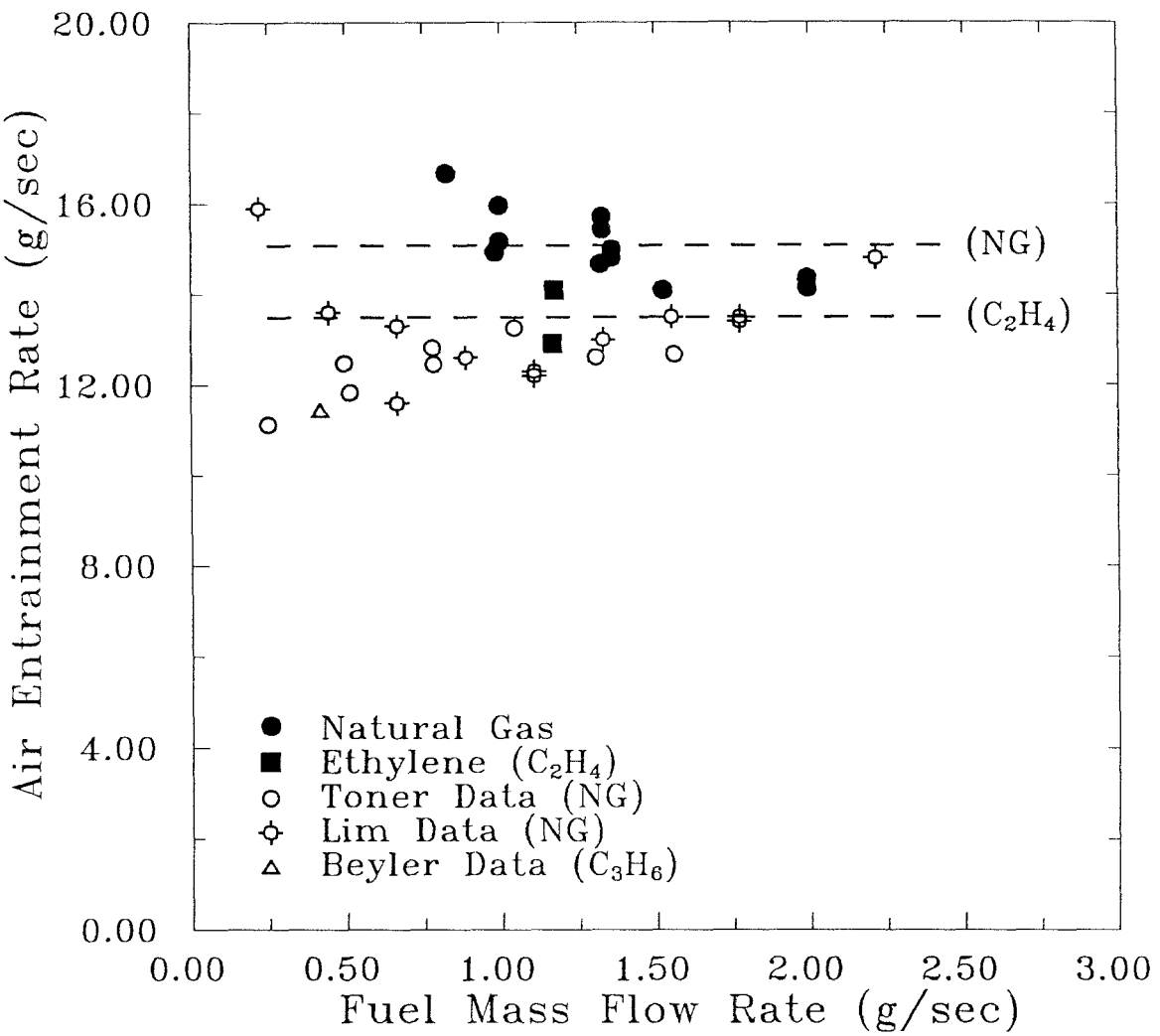

Figure 6.16(b): Average entrainment rates below a 10 cm interface height for various gaseous fuels

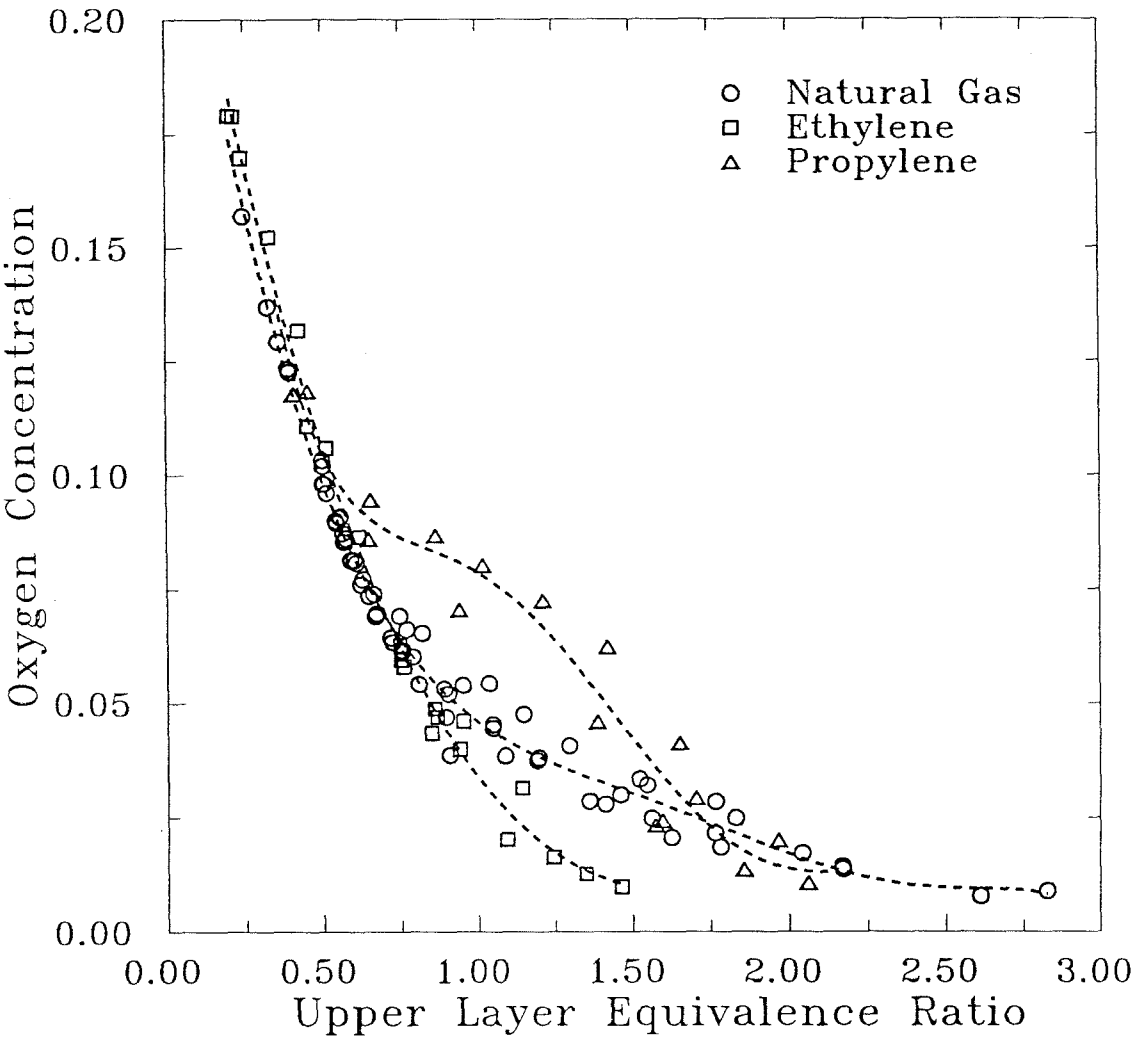

Figure 6.17: Comparison of oxygen measurements in two-layered fires stabilized on a 19 cm diameter burner

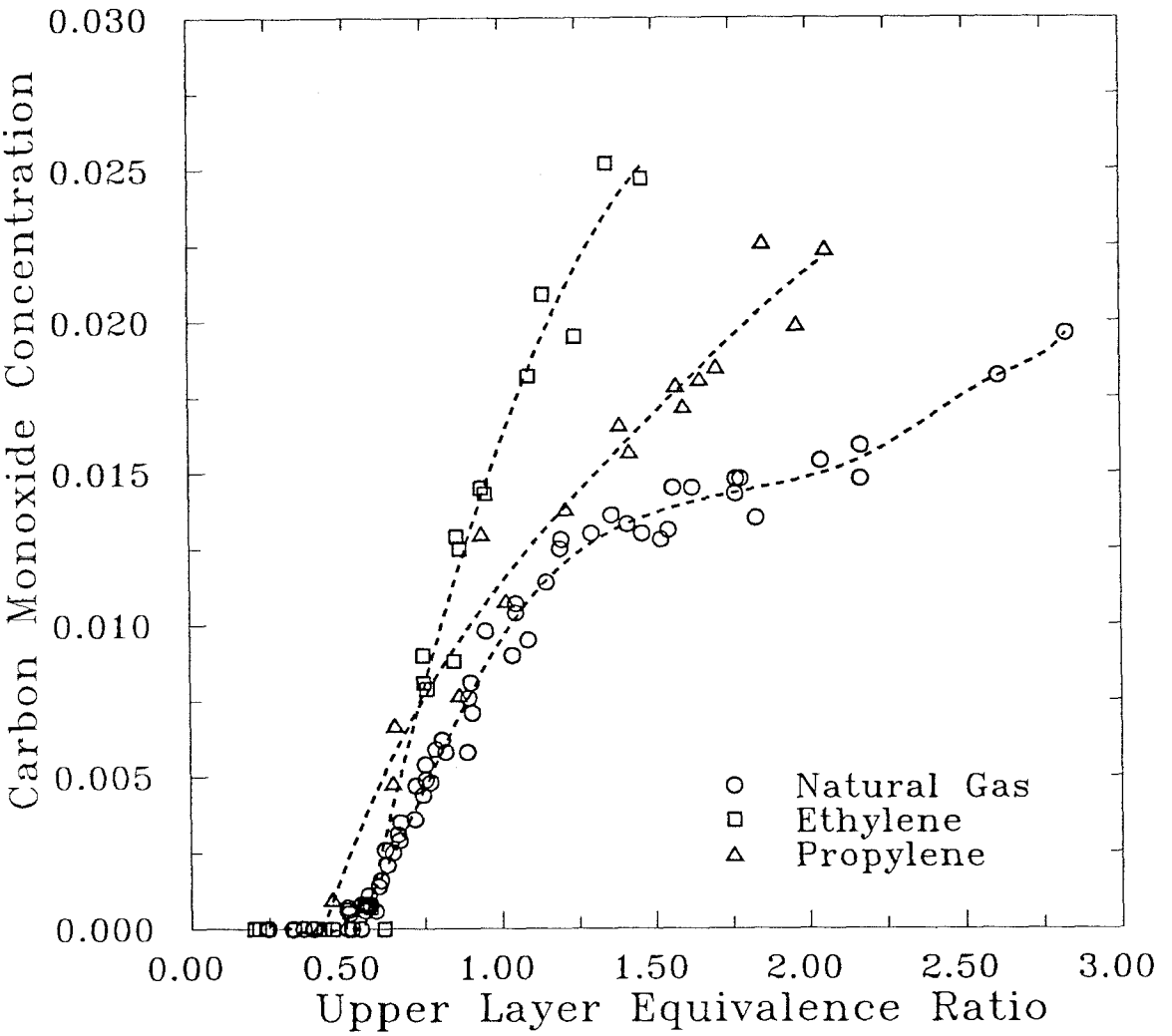

Figure 6.18: Comparison of carbon monoxide measurements in two-layered fires stabilized on a 19 cm diameter burner

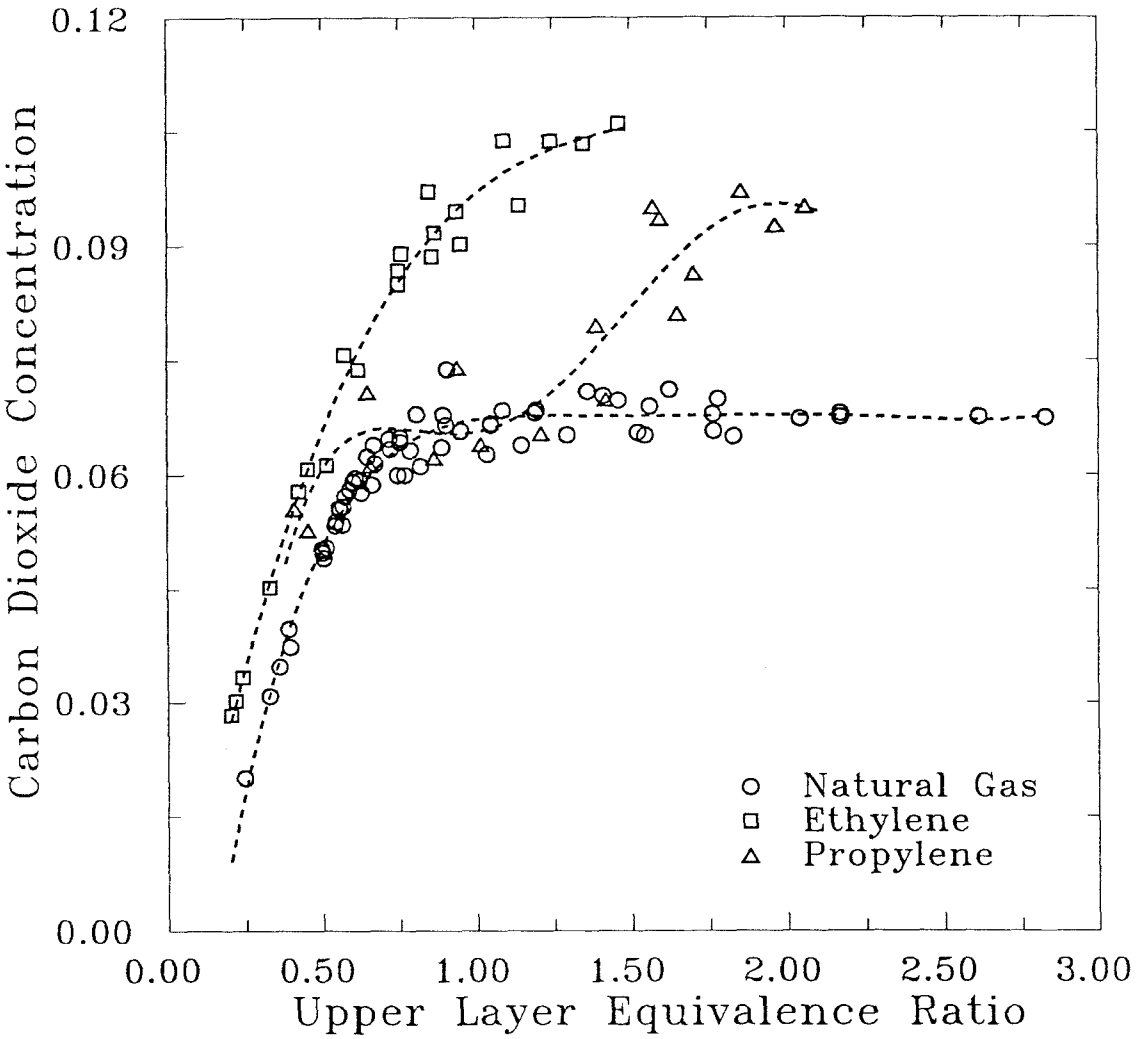

Figure 6.19: Comparison of carbon dioxide measurements in two-layered fires stabilized on a 19 cm diameter burner

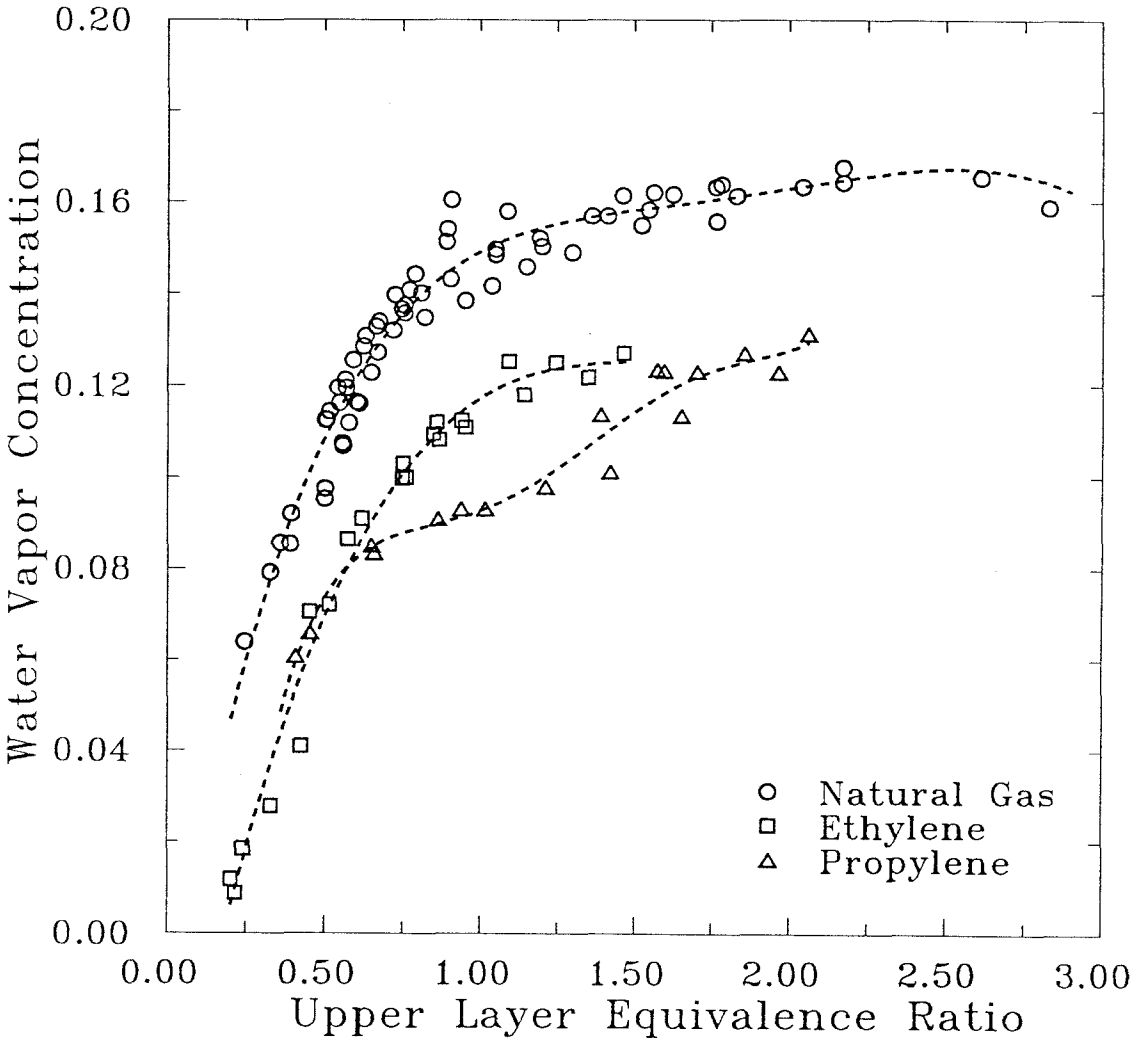

Figure 6.20: Comparison of water vapor measurements in two-layered fires stabilized on a 19 cm diameter burner

Chapter 7

Chemical Species Produced in Fires near the Limit of Flammability

When the oxygen concentration in a gas mixture is below some critical value, no burning of a combustible in the mixture is possible. The borderline composition, known as the limit of flammability (a slight modification to the oxygen content of the mixture will produce flammable or nonflammable conditions), is strongly dependent on the fuel and the diluent(s) present.

Previous investigators have measured the oxygen concentration at the limit of flammability for a wide variety of fuels with several different inert gas diluents using many different burner configurations and experimental techniques. These studies include work with premixed fuel/oxygen/diluent combinations (Jones and Kennedy, 1935; Coward and Jones, 1952), experiments with diffusion flames in nitrogen diluted atmospheres (Simmons and Wolfhard, 1957), oxygen index tests performed on a wide variety of combustibles (Fenimore and Martin, 1966; Nelson and Webb, 1973), investigations of organic liquid and complex solid fuels (Tewarson and Pion, 1976), and a recent study of the extinction of liquid pool and gas fires using an inert pressurization technique (Lockwood, 1986). The present study uses a modified "residual atmosphere" approach. Oxygen reduction is accomplished by the fire's consumption of the air in the environment, leaving the combustion products as the diluent. An incoming, distributed air supply allows conditions to be precisely controlled, thus the chemical species produced under limiting conditions can be investigated in a steady manner.

7.1 Development of Homogeneous, Vitiated Conditions in an Enclosure Fire

A fire burning in an enclosure with restricted ventilation produces a layer of warm products of combustion mixed with entrained air which accumulates adjacent to the ceiling. During this initial phase of the fire, the flames are exposed only to the unvitiated air. Eventually, the depth of the ceiling layer can extend to occupy a significant portion of the volume of the enclosure. When the ventilation is sufficiently restricted, the layer of combustion products can extend to occupy the entire volume of the enclosure, resulting in the complete immersion of the fire in a

vitiated atmosphere. Burning can continue provided the vitiated gases contain a sufficient concentration of oxygen to support the combustion processes. Here we will focus on the determination of the minimum oxygen concentration necessary to continue the burning of some typical fuels in an environment of gases vitiated with combustion products. Also of interest is the examination of the chemical species produced in these fires, especially when conditions are near the limit of flammability.

The experimental technique used in the work of Jones et al. (1935) and Coward et al. (1952) was directed at investigating the flammability of a fuel/oxygen/diluent mixture in a cylindrical tube. Although the measurement of the minimum oxygen percentage for the combustibility of these premixed gases certainly provides some fundamental information about the flammability of a gas mixture, it is not clear that these measurements are applicable to the full-scale diffusion flames encountered during an enclosure fire burning in a reduced oxygen atmosphere. Other investigators have used air supplies diluted with nitrogen to quench diffusion flames where the burners had small characteristic dimensions (Simmons and Wolfhard reported measurements from a range of hemispherical burners with diameters from 1.6 to 4.1 cm; Nelson and Webb presented results using an experimental technique with a 2 mL ceramic reservoir in which liquid and solid fuels were burned). Again, the applicability of these flammability measurements for small-scale, laminar fires to the large-scale phenomenon of interest has not been demonstrated. Slightly larger fires were used by Tewarson and Pion (1976) who reported measurements from pool fires with a 10 cm diameter, however, the experimental technique was to reduce the oxygen concentration in a nitrogen/air oxidizer stream until extinction conditions were reached. In contrast, an enclosure fire burning in a vitiated layer will be exposed to a combination of diluents including significant levels of carbon dioxide and water vapor. In the experiments of Lockwood (1986), a fire chamber was pressurized with an inert gas (nitrogen, carbon dioxide, or argon) until extinction occurred. Since the experiments were performed in a transient manner, questions arise regarding the accuracy of the oxygen measurements and the homogeneity of the atmosphere which caused extinction. The rates of inert gas addition in these tests were sufficiently large so that an insignificant amount of combustion products were present in the extinguishing environment. Because of the differences between the inert-diluted atmosphere of this pressurizable vessel and the fire-vitiated gases produced in an enclosure fire, the applicability of these measurements toward the scenario described above is

also unclear.

Many of these studies and those of other investigators, albeit considering closely-related but different problems, have presented measurements of flammability limits of combustibles (or mixtures of combustibles). In order for any such measurements to be applicable to a full-scale enclosure fire burning in a vitiated environment, both the scale of the experiment and the combination of diluents used to achieve the reduction in the oxygen content of the oxidant must simulate actual conditions. A preferable arrangement would be a steady experiment so that a sufficient accumulation of combustion products from fires near the flammability limit could be examined in a consistent, repeatable manner.

7.2 Experimental Method

A schematic of the experimental apparatus is shown in Figure 7.1. A simple modification to the equipment described in Chapter 2, namely the addition of an extending "curtain," relocated the position of the interface to below the surface of the burner. This curtain was made of heavy gauge aluminum foil and extended 40 cm below the bottom edges of the hood. The effect of its presence was to eliminate entrainment into the fire plume of room air, hence the only source of air to support the combustion was via the air addition network. With this arrangement, the fire consumes the available oxygen within the hood, but instead of quickly depleting the air supply, the air addition network replenishes the oxygen at a rate just large enough to maintain the burning.

The fuel is supplied to the 19 cm diameter burner where the fire is stabilized on a 5 cm deep porous bed of 6.3 mm diameter spherical glass beads. Data is also presented from experiments conducted with 8.9 and 50 cm diameter burners of similar construction using natural gas fuel. Excess combustion products mixed with the added air are allowed to spill out beneath the edges of the curtain and are caught in the larger exhaust hood. This creates a well-defined interface between the recirculating vitiated gases in the hood and the cool uncontaminated room air, positioned well below the burner surface. The chemical composition of the product gases is again measured using the chromatographic technique described in Chapter 2. Results of tests with methane (natural gas) and ethylene will be reported here. In addition, the observations from experiments attempted with propylene fuel will also be described.

7.3 Results for Natural Gas and Ethylene Fuels

Measurements were taken in natural gas fires ranging from 15 to 31 kW and ethylene fires from 14 to 20 kW. The experimental technique was to adjust the fuel flow rate to provide the largest flame height which would not extend into the air addition region of the hood. The air addition rate was set to provide more than enough air to support the combustion of the fuel. After allowing the composition and temperature inside the hood to reach a steady state (about 25 to 30 minutes), the fuel flow rate was incrementally increased. If burning continued in the new environment, the fuel flow rate was again increased after a waiting period of 20 minutes. This procedure was continued until any further increases in the fuel flow rate would cause the extinction of the fire. After holding conditions very close to extinction for 20 minutes, the gases in the hood were sampled and analyzed. Additional samples were also taken at intermediate conditions with the same procedure.

As conditions approached the limit of flammability, some changes were observed in the character of the fire. The flame heights were continually reduced as conditions became more fuel-rich, and in some cases the flame height at the limiting condition was roughly half of the original flame height. For the most fuel-lean conditions, the fire was stabilized on the entire surface of the burner. At conditions near the limit, however, the burning was stabilized on a small portion of the burner's surface, usually near the edge of the burner. In the case of the ethylene fires it was possible to adjust the fuel flow rate so that the burning was no longer stabilized on the burner bed, but was stabilized at a distance of 10 to 15 cm above the burner surface.

The most striking observation of these fires near the limit of flammability is that radiation from soot in the reaction zone becomes imperceptible, and the regions of combustion are marked only by a weakly-luminous blue flame. Even extended periods of burning at these conditions do not produce an observable deposit of soot on the hood's interior, nor is the presence of soot detected in the 0.1 μm filter of the sample line. This behavior has been documented in previous studies for both diffusion flames (Simmons and Wolfhard, 1957) and premixed flames near extinction (Tewarson, 1977). Measurements of the heat release rates in premixed methane and ethane fires by Tewarson (1977) show that 93 to 95 percent of the heat release is convective when the flames are "non-luminous," in comparison with values of 50% to 75% convective heat release when soot is

produced. The absence of visible radiation from soot in the flames, and perhaps the complete suppression of soot production, may be due to a decrease in the temperature of the reaction zone. If it is assumed that fuel and oxidant meet in stoichiometric proportions in the reaction zone of a diffusion flame, the lowered oxygen content of a vitiated environment will cause a reduction in the reaction zone temperature, since more of the inert gases are heated by the combustion of the same amount of fuel. This temperature reduction is apparently sufficient to "freeze out" the reaction steps responsible for the soot production in the flames.

Flow visualization techniques show that no significant mixing takes place at the interface between the vitiated gases in the hood and the room air below. The stoichiometry of the gases in the hood can now be described by a single equivalence ratio, φ, defined as the ratio of the rate of fuel mass addition to the rate of air mass addition, normalized by the stoichiometric ratio. Measurements of the oxygen and carbon dioxide mole fractions, along with values for water vapor determined by differencing, are shown from experiments using natural gas and ethylene fuels (see Figures 7.2 and 7.3, respectively). The experimental measurements, which are correlated with the equivalence ratio, are compared to equilibrium values (shown as solid lines) determined for reactants in the same proportions. Equilibrium species concentrations are computed assuming the temperature of the products is 400 K, however, for the range of conditions investigated ($\varphi < 0.55$), the composition of equilibrium products is not dependent on temperature.

In the experiments using natural gas fuel, the products of combustion (even for cases nearest the limit of flammability) are present in stoichiometric proportions, i.e., identical to the products of a stoichiometric reaction with components of air added but unreacted. When the oxygen concentration is reduced to levels below 0.132 mole fraction, as measured in experiments with the 19 cm diameter burner, the fire is extinguished. The conditions nearest the flammability limit where the burning was sustained correspond to an equivalence ratio of 0.357. Note that the measurements at these limiting conditions show *no detectable levels of carbon monoxide or residual fuel* in the vitiated gases. The chromatographic technique employed here allows the measurement of concentrations less than 250 parts per million for these species. Tewarson (1977) also found negligibly small amounts of carbon monoxide and total hydrocarbons in the product gases of premixed methane and ethane flames near extinction. This indicates that despite the changes observed in the character of the fire, the combustion of the natural gas is complete.

Measurements of product layer gas temperatures in the experiments using natural gas fuel ranged from 390 to 515 K. As the fuel flow rate is increased and limiting conditions are approached, the temperature of the product gases within the hood continues to increase. We believe this is due not only to an increase in the rate of chemical energy release, from the increase in the fuel flow rate, but also from a reduction in energy losses by radiation from the soot.

Experiments using ethylene fuel were performed with only the 19 cm diameter burner. As shown in Figure 7.3, the combustion products appear in approximately stoichiometric proportions for all conditions investigated, up to the limit of flammability. As with the experiments using natural gas, the ethylene flames become a weakly-luminous blue color at conditions near extinction, and no residual fuel or carbon monoxide is detected in the product gases. Burning is extinguished when the oxygen mole fraction falls below 0.106, a limit which corresponds to an equivalence ratio of 0.515. The deviation between the amounts of water vapor determined experimentally and the equilibrium levels is due to the excess oxygen measured. Product gas temperatures ranged from 375 to 430 K for these experiments, and displayed the same increasing temperature behavior as in the tests with natural gas.

At conditions nearest extinction, it was possible to adjust the fuel flow rate so that the flames were balanced 10 to 15 cm above the burner surface. With no alteration to the fuel or air addition rates, this limiting condition could be maintained much longer than the residence time of the gas within the hood (based on fluid-mechanical considerations). In contrast, when natural gas fires near the limiting conditions detach from the burner surface, the flames travel slowly upward away from the burner by as much as 3 to 4 burner diameters (for the 19 cm diameter burner) before complete extinction occurs. Lockwood (1986) reported similar observations for gas fires (methane and propane fuels) very near extinction and attributed this behavior to the flame following a region of hot gas with greater oxygen content.

Additional tests were performed using 8.9 and 50 cm diameter burners with natural gas fuel. As shown in Figure 7.2, our limiting measurements are a weak function of burner size. Although the initial momentum flux of the fuel varied by a factor of 12 for the different burners (highlighting the role of flame stability), the limiting oxygen concentrations remained comparable (reinforcing the dominant role of the composition of the environment). It is possible that the observed dependence on burner diameter is related to the attachment of the flames near

the perimeter of the burner's surface when limiting conditions are approached. The larger gas velocity induced by entrainment at the rim of the smaller burners may have assisted in detaching the flames, thereby promoting extinction. The radiant heat transfer to the burner surface also plays an important role by influencing the fuel's initial buoyancy. However, it was not our aim to investigate or quantify these effects.

It has been noted that the moisture content and the temperature of the ambient gases have an effect on the results (Coward and Jones, 1952). This dependence may be due to the large specific heat of H_2O in comparison to the other species present. In our experiments, the water vapor concentrations were a function of the degree of vitiation in the hood, and were not dependent on the moisture content of the laboratory air. Differences in the limiting oxygen concentrations due to changes in temperature are expected after our discussion of the flamesheet model (cf. Section 5.2). An increased ambient temperature has a significant impact on the limiting flame temperature and the effective reaction zone thickness. The vitiated gas temperatures in the experiments using natural gas fuel showed relatively small deviations (all within 50°C).

Comparisons of the measurements of the present study to those of other investigations are found in Tables 7.1 and 7.2 for methane and ethylene fuels, respectively. The limiting oxygen measurements are expressed in terms of mole fractions and correspond to the most fuel-rich conditions which continued to support the combustion process. Assuming that under limiting conditions the fuel and oxidant meet in stoichiometric proportions in the reaction zone of a diffusion flame, a limiting flame temperature can be approximated by the adiabatic flame temperature for a stoichiometric mixture of fuel and vitiated gases. Experiments by Diedrichsen and Wolfhard (1956) have shown that the error introduced by this approximation is small.

Our limiting oxygen measurements for the methane fires show good agreement with the other measurements taken in nitrogen diluted environments. This result is reasonable since the composition of the diluent gases in our vitiated environment is primarily nitrogen (85% N_2, 10% H_2O, 4% CO_2, and 1% Ar for the limiting experiment with the 19 cm diameter burner). Differences in the limiting flame temperatures are due to the presence of some water vapor and carbon dioxide in the oxidant supporting the combustion here. The results of the experiments with ethylene fuel agree remarkably well for all of the studies listed in Table 7.2, despite the widely varying experimental techniques. Again, differences in the limiting

flame temperatures are due to the water vapor and carbon dioxide content of our vitiated environment.

These results suggest that there is some applicability of measurements taken in small-scale laminar flames to the full-scale burning phenomenon which occurs in the later stages of an enclosure fire. The extent of the agreement between the measurements in this study and those of other experimental approaches is encouraging, however, the limited evidence with these simple fuels may not be indicative of more complex fuels, and small-scale measurements for the purposes of predicting large-scale behavior should be used with caution.

7.4 Observations from Experiments with Propylene Fuel

Using the same approach as with the natural gas and ethylene fuels, initial experiments were conducted with propylene fuel, where the flames were stabilized on the 19 cm diameter burner. Once the effects of oxygen reduction in the supporting environment became significant, the flames behaved differently from the previous tests. The fuel flow and air addition rates were approximately the same as those for the natural gas tests, with fire strengths from 23 to 28 kW, but even with these initial settings (not yet near extinction), the fire's unusual behavior was apparent.

Because the propylene fuel is negatively buoyant in air (molecular weight of 42.08), an upright, stabilized flame occurs only when the radiant feedback to the burner bed is sufficient to heat the exiting fuel. For example, if the environment is composed of warm air at 425 K, the fuel must be heated to nearly 620 K before it is no longer negatively buoyant. As with the previous fuels, when the oxygen concentration is reduced, there is also a decline in the radiant intensity of the flames. In these tests with continually sooting flames, the radiant heating is sufficiently reduced to cause the fuel to spill down the sides of the burner before being ignited. Such an arrangement is tolerable in that it presents no difficulties to the measurement technique and it does not change the rate of air addition to the environment within the hood.

Unfortunately, further increases in the fuel flow rate, in order to push conditions closer to the flammability limit, cause the fuel spilling down the burner's side to reach the interface where mixing and ignition take place. This observation is sketched in Figure 7.4, which highlights the difficulties presented by this behavior. Clearly this arrangement is unacceptable for determining the minimum

oxygen concentration necessary to support the combustion process. Not only is it unclear at what rate air is being added to the hood's interior (due to mixing at the interface), it is also not possible to control (reduce) the oxygen content of the environment in order to find the limiting condition.

There are several methods for dealing with this limitation. One idea is to premix the fuel with helium so that the resulting mixture is buoyant in the gases within the hood. The presence of helium in the gas sample will have the same effect as a reduction in the size of the chromatographic sample loop, since helium is the carrier gas here. Because we use a peak area normalization technique, only the relative amounts of the species in the sample are important, not the sample volume. Also, we do not expect the helium to interfere with the processes occurring in the flame, but the increase in the initial momentum may have an impact on the stability of the flame, particularly when conditions are close to extinction. Based on the measurements for natural gas fires with varying burner sizes, some concern does exist with respect to the role of flame stability in determining the limiting conditions.

Another approach that may allow this experimental procedure to be extended to fuels which are heavier than air is the use of fuel preheating. Before the burner outlet, the fuel supply stream can be heated to temperatures necessary for positive buoyancy in air, e.g., using heating tape with insulation. As mentioned previously, with some heavier gases this may require a significant amount of heating since the fuel's temperature (to achieve non-negative buoyancy) must reach:

$$T_{fuel} = T_{gas} \times \frac{W_{fuel}}{W_{gas}}. \tag{7.1}$$

This amount of temperature increase may cause problems with thermal degradation of the fuel's structure, especially for long-chained molecules and complex structures (e.g., aromatic hydrocarbons). A potential strategy for investigating these fuels with this experimental approach might be to employ a combination of these techniques. Since neither method interferes with the accuracy of the chemistry measurements, combining helium premixing and fuel preheating may provide a suitable approach for investigating these heavier fuels.

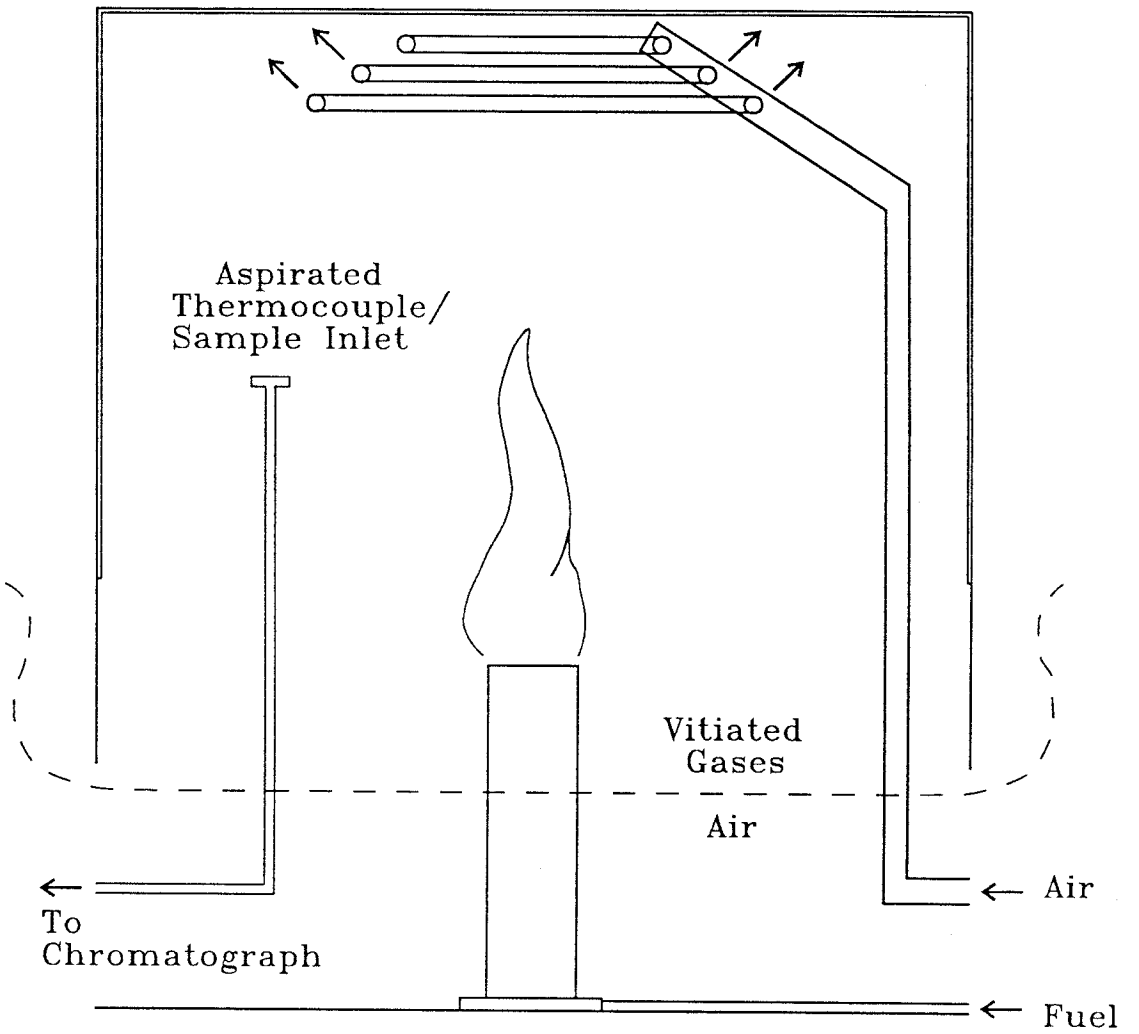

Figure 7.1: Schematic of experiment showing extending curtain which prevents entrainment

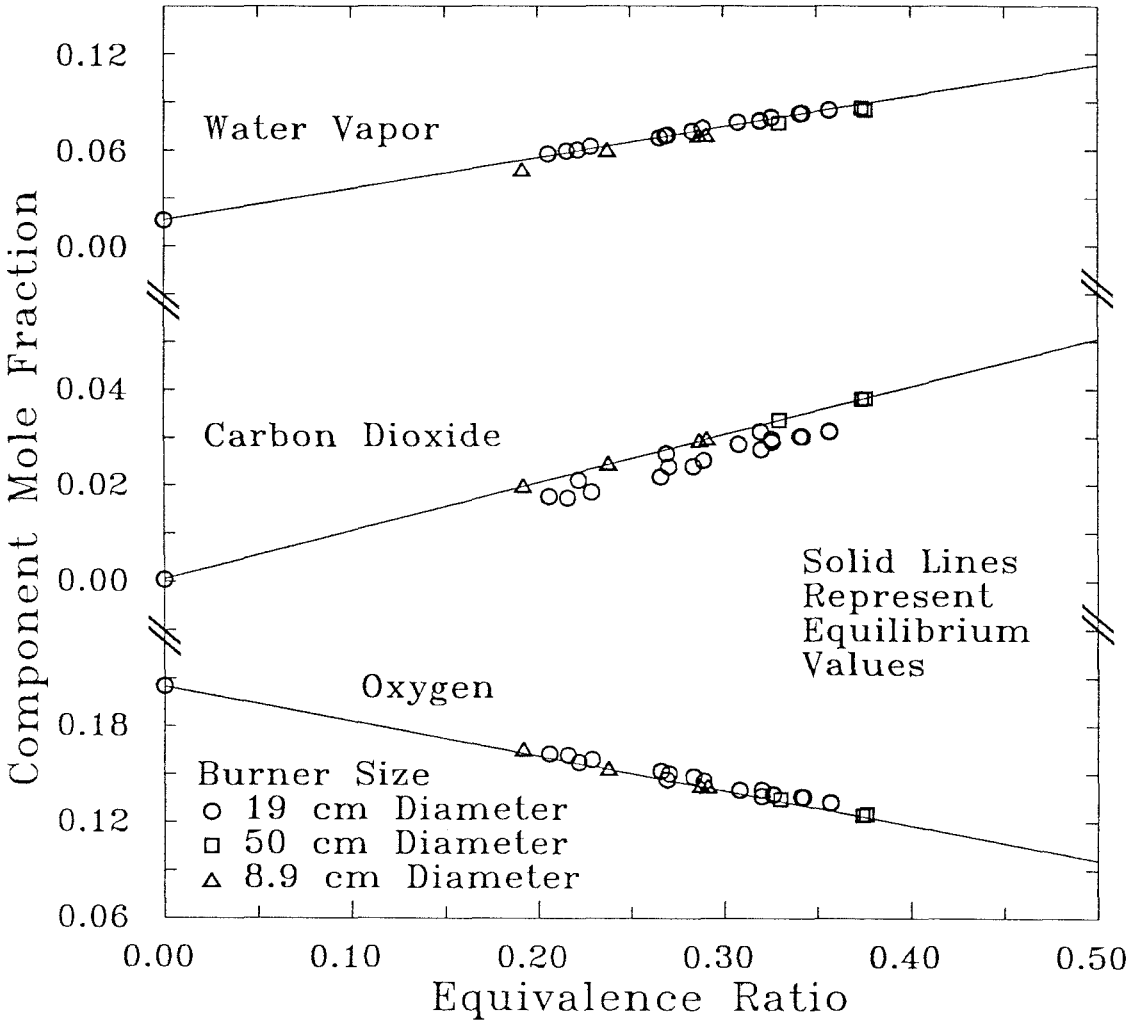

Figure 7.2: Measurements of species in natural gas fires as conditions approach the limit of flammability

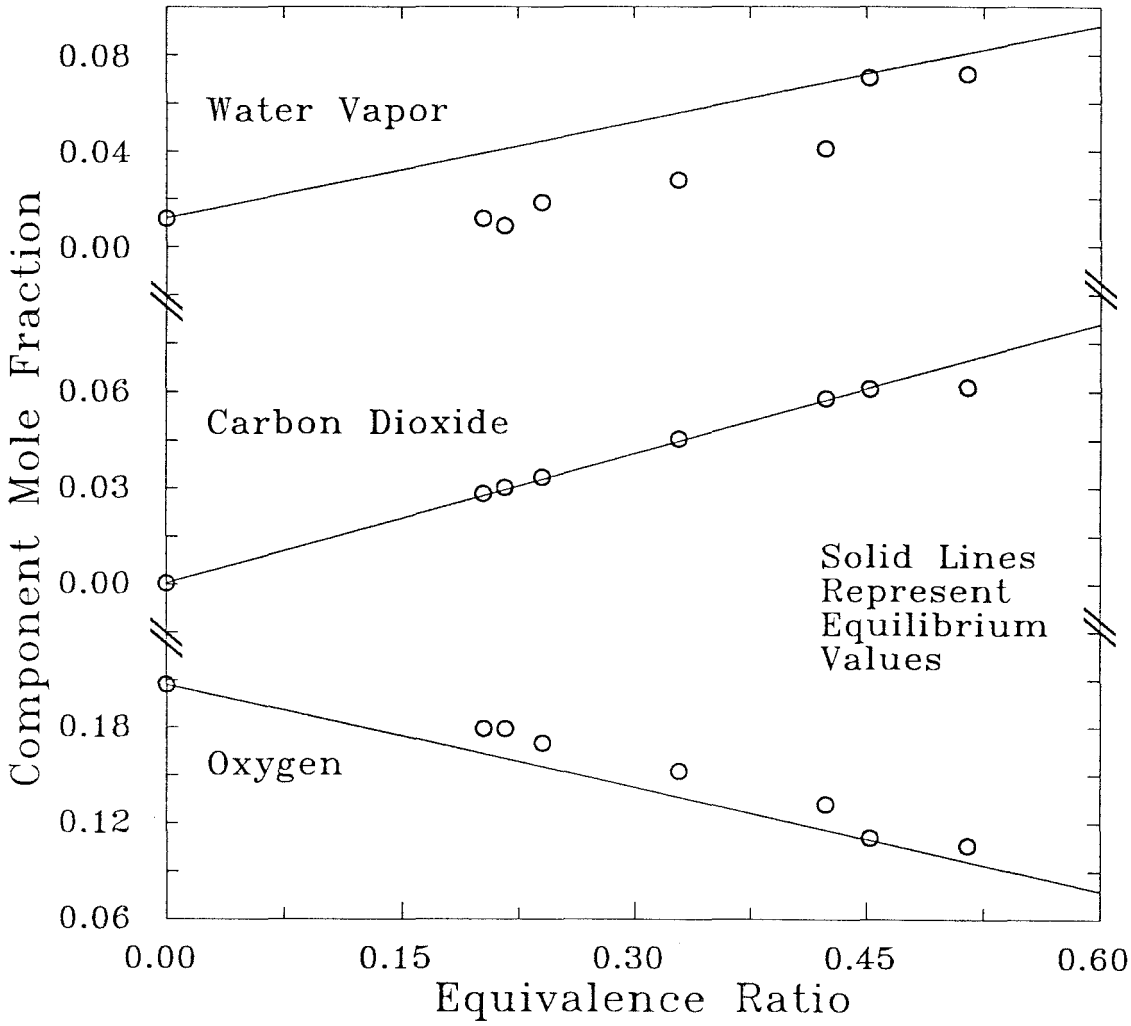

Figure 7.3: Measurements of species in ethylene fires as the conditions approach the limit of flammability

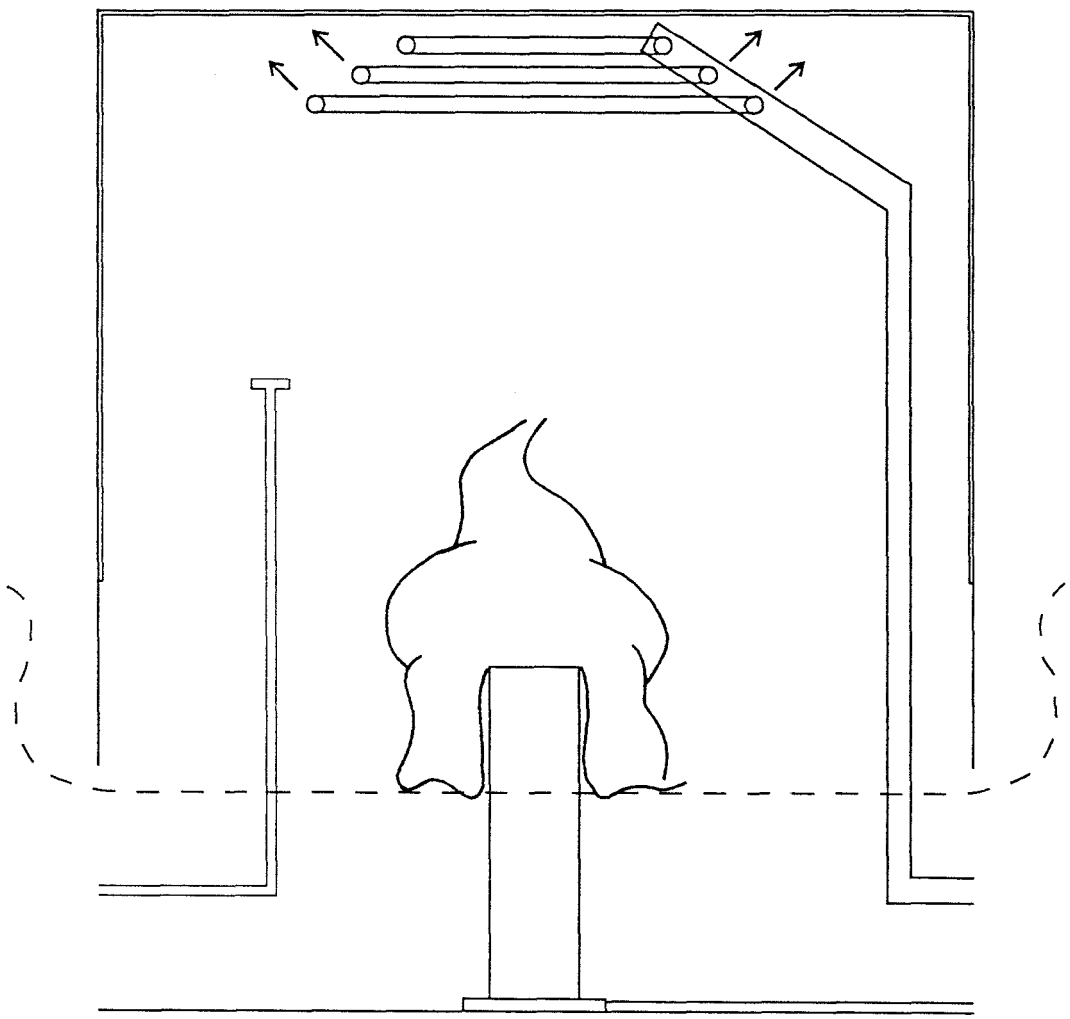

Figure 7.4: Schematic of experiment showing behavior of fire when burning propylene fuel

Table 7.1

Comparison of Measurements for Methane Fires

Diluent	Limit O_2	Limit Temp	Burner Size	Ref
Combustion Products	0.1242	1765 K	50 cm dia	
	0.1321	1837 K	19 cm dia	(*a*)
	0.1428	1928 K	8.9 cm dia	
Nitrogen	0.121		Premixed	(*b*)
	0.129		Premixed	(*c*)
	0.139	1791 K	1.6 to 4.1 cm dia	(*d*)
	0.1446	1811 K	25 to 30 cm dia	(*e*)
Carbon Dioxide	0.146		Premixed	(*b*)
	0.157		Premixed	(*c*)
	0.1789	1773 K	25 to 30 cm dia	(*e*)
Argon	0.1275	1847 K	25 to 30 cm dia	(*e*)

(*a*) Present Study
(*b*) Jones and Kennedy (1935)
(*c*) Coward and Jones (1952)
(*d*) Simmons and Wolfhard (1957)
(*e*) Lockwood (1986)

Table 7.2

Comparison of Measurements for Ethylene Fires

Diluent	Limit O_2	Limit Temp	Burner Size	Ref
Combustion Products	0.1060	1763 K	19 cm dia	(*a*)
Nitrogen	0.100		Premixed	(*b*)
	0.100		Premixed	(*c*)
	0.105	1608 K	1.6 to 4.1 cm dia	(*d*)
Carbon Dioxide	0.117		Premixed	(*b*)
	0.124		Premixed	(*c*)

Chapter 8

Conclusions

The chemical species produced by a buoyant, turbulent diffusion flame burning partially in fresh air and extending into a layer of oxygen-reduced gases vitiated with combustion products have been examined. A unique experimental approach allowed the investigation of the conditions which can occur during the transient development of a fire within an enclosure. When the strength of the fire or the depth of the ceiling layer are rapidly increasing, the fuel-air ratio of the material in the fire plume being transported into the ceiling layer can be substantially higher than that of the layer gases. The experiments performed in this study have modeled these conditions by directly injecting air into the upper portion of a catch-hood which accumulates the plume gases from fires placed below, hence the essential features of the transient development are preserved in a steady flow experiment.

The measurements of the gas composition in the upper layer of our experiment show uniform values for all species over a wide range of positions , both with and without air addition to the hood. This indicates that the experimental model did indeed produce a well stirred, homogeneous upper layer. Hence, the chemistry measurements were insensitive to the location of the sample inlet on the probe arm, provided it was not directly in the plume flow. A vertical temperature gradient was found, however, with gas temperatures varying by more than 10% between the highest and lowest elevations within the hood. This was true for experiments performed with and without air addition.

The residence time for the gases within the hood ranged from 25 seconds to several minutes, depending on the experimental configuration. Thus, the upper layer gases could be recirculated through the fire plume many times before escaping via the exiting flow beneath the edges of the hood. Although the product gas composition reached a steady state, these concentrations did not match the corresponding equilibrium values, except for very fuel-lean conditions. The species produced in fires burning in the two-layered arrangement are primarily a function of the upper layer's stoichiometry, and are not dependent on that of the plume flow entering the upper layer. From this we conclude that it is the global description of the upper layer which is important (the complete time history of the plume flow creating the upper layer), not the instantaneous influx.

A weak dependence of species concentrations on the temperature of the gas in the upper layer was observed over the range 500 to 900 K. This behavior accounts for a large part of the differences between the measurements of this study and those of Toner (1986), who reported results for a similar experimental approach using natural gas fuel. Higher temperatures in the oxidant supporting the diffusion flame may have reduced conductive heat losses from the reaction zone, effectively increasing its thickness and assisting the combustion to continue towards further completion.

Using a detailed chemical kinetics model, the stability (i.e., the propensity for reactions between the gas phase species) of the upper layer composition was investigated for a sample case taken from an experiment with a fuel-rich upper layer stoichiometry. For the range of temperatures measured in the experiments (550 to 700 K), no changes were found for the major stable species when the gas mixture was input into an isothermal plug flow reactor for a 20 second period. At higher temperatures (800 to 1034 K), reactions do occur between the species, while the rate of consumption of the available oxygen and the steady state species concentrations depend largely on the reactor temperature. These results indicate that for the time frames of interest here, the upper layer composition is stable, but if the gases are re-entrained into the chemically reacting regions of the flame, further reactions may occur.

The experiments in this study with fires burning in two-layered environments were conducted with three different gaseous fuels: natural gas (primarily methane), ethylene, and propylene. The molecular structure of the fuel had an impact on the measurements of the composition of the product layer. The presence of a double bond between carbon atoms in the fuel was accompanied by an increase in the amount of carbon monoxide measured. This may have been caused by the more complete consumption of fuel species with this reactive bonding arrangement, leading to a reduced supply of oxygen necessary for the oxidation of the CO to CO_2. The propylene structure contains both single and double carbon-carbon bonds, and as expected its behavior was between that of the methane (simplest alkane) and the ethylene (simplest alkene). Thus, the conduct of the fuel appears to be influenced by the bonding arrangements between the carbon atoms.

Natural gas and ethylene fires burning in homogeneous vitiated environments with conditions near the limit of flammability were also investigated. As extinction conditions were approached, the flame heights were reduced, the yellowish luminosity disappeared, and the soot production was apparently suppressed. Measure-

ments of chemical species produced in these fires showed that levels of incomplete combustion products were negligible. Despite the significant changes in the behavior of the flames, even under limiting conditions, the combustion process was essentially complete. A comparison of experimental measurements of the limiting oxygen concentrations for premixed flames, small-scale diffusion flames, and large-scale diffusion flames indicates that the minimum oxygen levels necessary to sustain the combustion reactions are primarily dependent on fuel type and diluents present, and are less sensitive to the burner design. Some applicability of the measurements taken in small-scale tests to large-scale fires has been demonstrated for these simple fuels, but any such interpretation of small-scale measurements should be used with caution.

References

Babrauskas, V. (1989) CO Prediction In Fires—Current Needs, Executive Summary for the Workshop on Developing a Predictive Capability for CO Formation in Fires, NISTIR 89-4093, National Institute of Standards and Technology, Department of Commerce, Gaithersburg, MD.

Beers, Y. (1957) *Introduction to the Theory of Error*, Addison Wesley, Reading MA.

Beyler, C. L. (1983) Development and Burning of a Layer of Products of Incomplete Combustion Generated by a Buoyant Diffusion Flame, Ph.D. Thesis, Harvard University, Cambridge, MA.

Brown, T. L. and LeMay, H. E. (1977) *Chemistry—The Central Science,* Prentice-Hall, Englewood Cliffs, NJ.

Cetegen, B. M. (1982) Entrainment and Flame Geometry of Fire Plumes, Ph.D. Thesis, California Institute of Technology, Pasadena, CA.

Coward, H. F. and Jones, G.W. (1952) Limits of Flammability of Gases and Vapors, *Bull. U. S. Bur. Min. No. 503.*

Diedrichsen, J. and Wolfhard, H. G. (1965) Spectrographic Examination of Gaseous Flames at High Pressure, *Proc. Roy. Soc.*, **A** 236, 89-103.

Dietz, W. A. (1967) Response Factors for Gas Chromatographic Analyses, *J. Gas Chrom.*, **5**, 68-71.

Faeth, G. M. (1989) Carbon Monoxide Formation in Flames: A Laminar Flamelet Perspective, included with NISTIR 89-4093, National Institute of Standards and Technology, Department of Commerce, Gaithersburg, MD.

Fenimore, C. P. and Martin, F. J. (1966) Flammability of Polymers, *Comb. and Fl.*, **10**, 135-139.

Glassman, I. (1987) *Combustion, 2nd ed.*, Academic Press, New York, NY.

Huggett, C. (1980) Estimation of Rate of Heat Release by Means of Oxygen Consumption Measurements, *Fire and Mat.*, **4**:2, 61-65.

Jones, G. W. and Kennedy, R. E. (1935) Prevention of Gas Explosions by Controlling Oxygen Concentration, *Ind. Eng. Chem.*, **27**, 1344-46.

Karter, M. J. (1989) Fire Loss in the United States in 1988, *Fire J.*, **83**:5, 24-32.

Kawagoe, K. (1958) Fire Behavior in Rooms, Report No. 27, Building Research Institute, Japan.

Kee, R. J., Miller, J. A., and Jefferson, T. H. (1980) CHEMKIN: A General- Purpose, Problem-Independent, Transportable, FORTRAN Chemical Kinetics Code Package, Report SAND 80-8003, Sandia National Laboratories, Livermore, CA.

Knuth, D. E. (1986) *The TEXbook*, Addison Wesley, Reading, MA.

Lim, C. (1984) Entrainment In Fire Plumes, Part 2, Aeronautical Engineer Thesis, California Institute of Technology, Pasadena, CA.

Lockwood, W. R. (1986) Inert Suppression of Enclosure Fires, Ph.D. Thesis, University of Washington, Seattle, WA.

McCaffrey, B. J. (1979) Purely Buoyant Diffusion Flames: Some Experimental Results, NBSIR 79-1910, National Bureau of Standards, Department of Commerce, Washington, DC.

McCaffrey, B. J. and Harkleroad, M. (1988) Combustion Efficiency, Radiation, CO and Soot Yield from a Variety of Gaseous, Liquid, and Solid Fueled Buoyant Diffusion Flames, *22nd Symp. (Int'l) on Comb.*, The Combustion Institute, Pittsburgh, PA, 1251-61.

Morton, B. R., Taylor, G. I., and Turner, J. S. (1956) Turbulent Gravitational Convection from Maintained and Instantaneous Sources, *Proc. Roy. Soc.*, **A** 234, 1-23.

Nelson, G. L. and Webb, J. L. (1973) Oxygen Index of Liquids Technique and Application, *J. Fire and Flamm.*, **4**, 210-226.

Orloff, L., deRis, J., and Delichatsios, M. A. (1985) Chemical Modeling of Gaseous Species in Turbulent Fires, FMRC Technical Report RC 85-BT-4.

Palmer, H. B., and Cullis, C. F. (1965) *Chemistry and Physics of Carbon*, (P. L. Walker, editor), **1**, Dekker, New York, NY.

Pitts, W. M. (1989) Executive Summary, NISTIR 89-4093, National Institute of Standards and Technology, Department of Commerce, Gaithersburg, MD.

Reid, R. C., Prausnitz, J. M., and Sherwood, T. K. (1977) *The Properties of Gases and Liquids, 3rd ed.*, McGraw-Hill, New York, NY.

Reynolds, W. C. (1989) STANJAN version 3.31: The Element Potential Method for Chemical Equilibrium Analysis, Stanford University, Menlo Park, CA.

Ricou, F. P., and Spalding, D. B. (1961) Measurements of Entrainment By Axisymmetric Turbulent Jets, *J. Fluid Mech.*, **11**, 21-32.

Rouse, H., Yih, C. S., and Humphreys, H. W. (1952) Gravitational Convection from a Boundary Source, *Tellus*, **4**, 201.

Schmidt, W. Z. (1941) Turbulente Ausbreitung eines Stromes erhitzter Luft *Z. Angew. Math. Mech.*, **21**, 351-363.

Senkan, S. M. (1989) Detailed Chemical Kinetic Modeling of Complex Chemically Reacting Systems: The Plug Flow and Stirred Tank Reactor Programs, Department of Chemical Engr., Illinois Institute of Technology, Chicago, IL.

Simmons, R. F., and Wolfhard, H. G. (1957) Some Limiting Oxygen Concentrations for Diffusion Flames in Air Diluted With Nitrogen, *Comb. and Fl.*, **1**, 155-161.

Smithsonian Institute (1939) *Smithsonian Meteorological Tables, 5th ed.*, Pub. 3116, Smithsonian Institute, Washington, DC.

Tewarson, A., and Pion, R. F. (1976) Flammability of Plastics—I. Burning Intensity, *Comb and Fl.*, **26**, 85-103.

Tewarson, A. (1977) Heat Release Rates from Burning Plastics, *J. Fire and Flamm.*, **8**, 115-130.

Toner, S. J. (1986) Entrainment, Chemistry and Structure of Fire Plumes, Ph.D. Thesis, California Institute of Technology, Pasadena, CA.

Tsuji, H. and Yamaoka, I. (1967) The Structure of Counterflow Diffusion Flames in the Forward Stagnation Region of a Porous Cylinder, *12th Symp (Int'l) on Comb.*, The Combustion Institute, Pittsburgh, PA, 997.

Yokoi, S. (1961) *The Use of Models in Fire Research*, Pub. No. 786, National Academy of Sciences, National Research Council, Washington, DC., 186-206.

Zukoski, E. E., Kubota, T., and Cetegen, B. M. (1980) Entrainment in Fire Plumes, *Fire Safety J.*, **3**, 107-121.

Zukoski, E. E., Morehart, J. H., Kubota, T., and Toner, S. J. (1990) Species Production and Heat Release Rates in Two-Layered Natural Gas Fires, to be published *Comb. and Fl.*

Appendix A

Gas Analysis Data Reduction Programs

Data reduction for the experiments using natural gas fuel was performed with the following set of programs.

- DATAIN—This is the data file creation program which allows the direct input of the experimentally measured quantities. When this program is run, a sequential file is created. This raw data file is named EX##DDMM.RAW, where ## is the specific experiment identification number, and DDMM is the day and month when the experiment was performed.

- CRUNCHER—This program reads the raw data file and performs the bulk of the computations. Subroutines are called to perform each phase of the solution method, and the output data file is created. In a fashion similar to above, the output file is named EX##DDMM.OUT.

- PRINTOUT—The final program reads in both of the data files for the experiment, performs some additional computations, and writes a formatted output file. This file, named with an extention .TEX can then be processed directly with the TEX typesetting program to produce a formatted data report sheet (see Appendix B).

```
      PROGRAM DATAIN
C     DATA FILE CREATION PROGRAM
      INTEGER RUNNUMBR,THOOD,TSAMPLE
      INTEGER A1,A2,A3,A4,A5
      INTEGER A6,A9,A10,A11
      INTEGER DA1,DA2,DA3,DA4,DA5
      INTEGER DA6,DA9,DA10,DA11
      CHARACTER * 2 EXPNO
      CHARACTER * 8 RUNDATE
      CHARACTER * 5 RUNTIME
      CHARACTER * 12 FILENAME
      PRINT *,'INPUT EXPERIMENT NUMBER, NN   '
      READ '(A2)',EXPNO
C     ***************  TEST CONDITIONS  ********************
      DATA RUNDATE,RUNTIME,RUNNUMBR  / '03-26-88','14:18',
     2240/
      DATA PRESS,TDRY,TWET             / 738.4,24.0,12.8 /
      DATA FUELFLOW,AIRFLOW            / 0.00350,0.00000 /
      DATA UPSTRMPF,UPSTRMPA           / 0.10000,0.14500 /
      DATA BOXHITE,TSAMPLE,THOOD       / 10.0,673,470 /
      DATA DIAMETER,ENTRAIN,DENTRAIN / 19.0,10.2854,
     200.2685 /
      DATA DPRESS,DTDRY,DTWET          / 0.5,0.2,0.2 /
      DATA DFUELFL,DAIRFL              / 0.00010,0.00010 /
      DATA DUPSTMPF,DUPSTMPA           / 0.01000,0.01000 /
C     ***************  FUEL MOLE FRACTIONS  ***************
      DATA X1,X2,X3,X4      / 0.93800,0.03020,0.00520,
     20.01680 /
      DATA X5,X6,X7,X8      / 0.00710,0.00050,0.00060,
     20.00100 /
      DATA X9,X10           / 0.00030,0.00030 /
      DATA DX1,DX2,DX3,DX4 / 0.01000,0.00500,0.00200,
     20.00200/
      DATA DX5,DX6,DX7,DX8 / 0.00200,0.00010,0.00010,
     20.00010/
      DATA DX9,DX10         / 0.00010,0.00010 /
C     ***************  RESPONSE FACTORS  ******************
      DATA F1,F2,F3,F4       / 186.525,1.54794,1.50821,
     22.82073/
      DATA F5,F6,F9,F10      / 1.47558,1.22502,1.50896,
     21.19242/
      DATA F11,F12           / 1.12456,1.47422 /
      DATA DF1,DF2,DF3,DF4   / -.07347,-.01814,-.00980,
     2-.05240/
      DATA DF5,DF6,DF9,DF10 / -.02230,-.00480,-.02350,
     2-.00576/
      DATA DF11,DF12         / -.00595,-.02327 /
C     ***************  PEAK AREAS  ************************
      DATA A1,A6,A10,A11,A9       / 000,320920,00000,0000,
     20000/
      DATA A2,A3,A4,A5            / 464920,3534600,00000,
     23796 /
      DATA DA1,DA6,DA10,DA11,DA9 / 0001,0010,0001,0010,
```

```
     20010 /
      DATA DA2,DA3,DA4,DA5        / 0010,0100,0010,0010 /
C     ***************************************************
      FILENAME='EX' // EXPNO(1:2) // RUNDATE(1:2) //
     2RUNDATE(4:5) // '.RAW'
      OPEN(UNIT=1,FILE=FILENAME)
      WRITE(1,10) RUNDATE,RUNTIME,EXPNO,FUELFLOW,AIRFLOW,
     2UPSTRMPF
      WRITE(1,20) UPSTRMPA,PRESS,TDRY,TWET,DPRESS,DTDRY,
     2DTWET
      WRITE(1,30) BOXHITE,TSAMPLE,RUNNUMBR,DIAMETER,ENTRAIN
     2,THOOD
      WRITE(1,40) DFUELFL,DAIRFL,DUPSTMPF,DUPSTMPA,DENTRAIN
      WRITE(1,40) X1,X2,X3,X4,X5
      WRITE(1,40) X6,X7,X8,X9,X10
      WRITE(1,40) DX1,DX2,DX3,DX4,DX5
      WRITE(1,40) DX6,DX7,DX8,DX9,DX10
      WRITE(1,50) F1,F2,F3,F4,F5
      WRITE(1,40) F6,F9,F10,F11,F12
      WRITE(1,40) DF1,DF2,DF3,DF4,DF5
      WRITE(1,40) DF6,DF9,DF10,DF11,DF12
      WRITE(1,60) A1,A6,A10,A11,A9
      WRITE(1,70) A2,A3,A4,A5
      WRITE(1,80) DA1,DA6,DA10,DA11,DA9
      WRITE(1,90) DA2,DA3,DA4,DA5
 10   FORMAT(A8,1X,A5,1X,A2,3(1X,F7.5)/)
 20   FORMAT(F7.5,1X,F5.1,2(1X,F4.1),3(1X,F3.1)/)
 30   FORMAT(F4.1,2(1X,I4),1X,F4.1,1X,F6.3,1X,I4/)
 40   FORMAT(5(F7.5,1X)/)
 50   FORMAT(F7.3,4(1X,F7.5)/)
 60   FORMAT(I4,1X,I6,3(1X,I5)/)
 70   FORMAT(I6,1X,I7,2(1X,I6)/)
 80   FORMAT(5(I4,1X)/)
 90   FORMAT(4(I4,1X)/)
      CLOSE(UNIT=1)
      STOP
      END


      PROGRAM CRUNCHER
C     ******  DATA REDUCTION PROGRAM FOR GAS ANALYSIS  ****
C     FORTRAN VERSION WRITTEN IN MARCH 1989 BY JIM MOREHART
C     FASHIONED AFTER A REDUCTION PROGRAM 'REV6@16.BAS'
C     WRITTEN IN MAY 1985 BY STEPHEN TONER (ALONG WITH SEV-
C     ERAL REVISIONS BY JHM).
C          THIS PROGRAM IS THE COMPLETE DATA REDUCTION PRGM
C     FOR DATA OBTAINED FROM GAS ANALYSIS USING A GAS CHRO-
C     MATOGRAPH.  THE ANALYZED GAS IS THE PRODUCT OF A NAT-
C     URAL GAS AND AIR FIRE WITH THE WATER REMOVED AND THE
C     SOOT FILTERED OUT.  THE PROGRAM CALCULATES THE WATER
C     CONTENT OF AIR USING THE PRESSURE, DRY-BULB TEMPERA-
C     TURE, AND WET-BULB TEMPERATURE.  FROM THIS, WITH A
C     STANDARD DRY AIR COMPOSITION ASSUMED, THE COMPONENTS
```

```
C     OF THE AIR ARE KNOWN.  FUEL COMPOSITION OBTAINED FROM
C     WEEKLY ANALYSES PERFORMED BY THE SOUTHERN CALIFORNIA
C     GAS COMPANY IS ALSO INPUT.  A MEASURED FUEL FLOW RATE
C     IS INPUT.  STOICHIOMETRIC EQUATIONS ALLOW THE CALCU-
C     LATION OF THE ENTRAINMENT AND PRODUCT COMPOSITION DUE
C     TO A COMPLETE STOICHIOMETRIC REACTION.  THE ACTUAL
C     ENTRAINMENT IS CALCULATED FROM A SET OF FOUR LINEAR
C     EQUATIONS DERIVED FROM THE CONSERVATION OF SPECIES
C     EQUATIONS.  FROM THE ENTRAINMENT, THE EQUIVALENCE
C     RATIOS FOR THE PRODUCT LAYER AND FOR THE PLUME AT
C     INTERFACE HEIGHT ARE OBTAINED.  THROUGHOUT THE PROG-
C     RAM, ERROR ANALYSIS IS CARRIED OUT SIDE-BY-SIDE WITH
C     THE CALCULATIONS.  THE ERROR ANALYSIS FOLLOWS FROM
C     "INTRODUCTION TO THE THEORY OF ERRORS, 2nd EDITION"
C     BY YARDLEY BEERS.
C     ************************  MAIN DRIVER  **************
C     THE EXPERIMENTAL DATA IS READ IN FROM A SEQUENTIAL
C     DATA FILE NAMED 'EX######.RAW', WHERE THE #'S REPRE-
C     SENT THE EXPERIMENT NUMBER AND DATE.  UNCERTAINTIES
C     ARE ALSO READ, HOWEVER, IF THE VALUE OF AN UNCERTAIN-
C     TY IS NEGATIVE, IT IS TAKEN TO BE A VALUE OF THE
C     RELATIVE ERROR.
      CHARACTER * 2 EXPNO
      CHARACTER * 8 RUNDATE
      CHARACTER * 5 RUNTIME
      CHARACTER * 12 FILENAME
      INTEGER AREA,DAREA,RUNNUMBR,THOOD,TSAMPLE
      REAL I,IS,LHEATM,MOLWTM,KW,MDOTA,MDOTF
      COMMON /AELEMS/ AC,AH,AO,AN,DAC,DAH,DAO,DAN
      COMMON /AIRADD/ I,IS,DI,DIS
      COMMON /AREAS/  AREA(11),DAREA(11)
      COMMON /BELEMS/ BC,BH,BO,BN,DBC,DBH,DBO,DBN
      COMMON /CHROM/  C1,DC1,Y2PLUS,DY2PLUS
      COMMON /DFLOW/  DAIMATCH,DENTRAIN,DKW,DMDOTA,DMDOTF,
     2DQNG
      COMMON /FLOWS/  AIRMATCH,ENTRAIN,KW,MDOTA,MDOTF,QNG
      COMMON /FRACT/  X(12),XM(12),XMA(12),XS(12),YM(12),
     2YMS(12),DYM(12)
      COMMON /FUEL/   FUELX(10),DFUELX(10)
      COMMON /HEATS/  HEATA,HEATF,HEATP,HEATSP
      COMMON /HRXN/   HRXNA,HRXNS,RATIO,RATIOAM
      COMMON /LABEL/ BOXHITE,RUNNUMBR,DIAMETER
      COMMON /MEAS1/ AIRFLOW,FUELFLOW,DAIRFL,DFUELFL,PRESS,
     2DPRESS
      COMMON /MEAS2/ PVAP,TDRY,TWET,DPVAP,DTDRY,DTWET,
     2TSAMPLE,THOOD
      COMMON /MEAS3/ UPSTRMPA,UPSTRMPF,DUPSTMPA,DUPSTMPF
      COMMON /MOLES/ A(5),B(5),Y(12),DA(5),DB(5),DY(12)
      COMMON /PHIS/  DPHIL,DPHIP,PHIRATIO,PLUMEPHI,ULAYERPH
      COMMON /PROPS/ LHEATM,MOLWTM,VISCM,CTSAMPLE,CTHOOD
      COMMON /RESPONSE/ F(12),DF(12)
      COMMON /YELEMS/ YC,YH,YO,YN,DYC,DYH,DYO,DYN
      PRINT *,'INPUT EXPERIMENT NUMBER   '
```

```
      READ '(A2)',EXPNO
      PRINT *,'INPUT DATE OF EXPERIMENT , MM-DD-YY    '
      READ '(A8)',RUNDATE
      FILENAME='EX' // EXPNO(1:2) // RUNDATE(1:2) //
     2  RUNDATE(4:5) //* '.RAW'
      OPEN(UNIT=1,FILE=FILENAME,STATUS='OLD')
      READ(1,10) RUNDATE,RUNTIME,EXPNO,FUELFLOW,AIRFLOW,
     2UPSTRMPF
      READ(1,20) UPSTRMPA,PRESS,TDRY,TWET,DPRESS,DTDRY,
     2DTWET
      READ(1,30) BOXHITE,TSAMPLE,RUNNUMBR,DIAMETER,ENTRAIN,
     2THOOD
      READ(1,40) DFUELFL,DAIRFL,DUPSTMPF,DUPSTMPA,DENTRAIN
      READ(1,40) FUELX(1),FUELX(2),FUELX(3),FUELX(4),
     2FUELX(5)
      READ(1,40) FUELX(6),FUELX(7),FUELX(8),FUELX(9),
     2FUELX(10)
      READ(1,40) DFUELX(1),DFUELX(2),DFUELX(3),DFUELX(4),
     2DFUELX(5)
      READ(1,40) DFUELX(6),DFUELX(7),DFUELX(8),DFUELX(9),
     2DFUELX(10)
      READ(1,50) F(1),F(2),F(3),F(4),F(5)
      READ(1,40) F(6),F(9),F(10),F(11),F(12)
      READ(1,40) DF(1),DF(2),DF(3),DF(4),DF(5)
      READ(1,40) DF(6),DF(9),DF(10),DF(11),DF(12)
      READ(1,60) AREA(1),AREA(6),AREA(10),AREA(11),AREA(9)
      READ(1,70) AREA(2),AREA(3),AREA(4),AREA(5)
      READ(1,80) DAREA(1),DAREA(6),DAREA(10),DAREA(11),
     2DAREA(9)
      READ(1,90) DAREA(2),DAREA(3),DAREA(4),DAREA(5)
10    FORMAT(A8,1X,A5,1X,A2,3(1X,F7.5)/)
20    FORMAT(F7.5,1X,F5.1,2(1X,F4.1),3(1X,F3.1)/)
30    FORMAT(F4.1,2(1X,I4),1X,F4.1,1X,F6.3,1X,I4/)
40    FORMAT(5(F7.5,1X)/)
50    FORMAT(F7.3,4(1X,F7.5)/)
60    FORMAT(I4,1X,I6,3(1X,I5)/)
70    FORMAT(I6,1X,I7,2(1X,I6)/)
80    FORMAT(5(I4,1X)/)
90    FORMAT(4(I4,1X)/)
      CLOSE(UNIT=1)
      CALL NATGAS
      CALL FLOWRATE
      CALL PSCHOMET
      CALL ASPECIES
      CALL BSPECIES
      CALL ELEMENTS
      CALL YSPECIES
      CALL YELEMENT
      CALL SOLUTION
      CALL FRACTION
      CALL STOICH
      CALL EQUIVLNT
      CALL OUTPUT(FILENAME,RUNDATE,RUNTIME,EXPNO)
```

```
      PRINT *,'SUBROUTINE SEQUENCE COMPLETE  '
      STOP
      END


      SUBROUTINE NATGAS
C     THIS SUBROUTINE CALCULATES THE LOWER HEATING VALUE,
C     MOLECULAR WEIGHT, AND VISCOSITY OF NATURAL GAS FOR A
C     SPECIFIED COMPOSITION.  THE COMPONENT MOLECULAR
C     WEIGHTS, LOWER HEATING VALUES, AND VISCOSITIES ARE
C     INCLUDED IN THE PROGRAM.  THE HEATING VALUE IS GIVEN
C     IN BTU/SCF AND THE VISCOSITY IN MICROPOISE.  THE VIS-
C     COSITY IS CALCULATED FROM COMPONENT MOLE FRACTIONS,
C     MOLECULAR WEIGHTS, AND VISCOSITIES FOLLOWING EQUA-
C     TIONS 9-5.1 AND 9-5.2 FROM THE BOOK "THE PROPERTIES
C     OF GASES AND LIQUIDS, 3rd EDITION" BY REID, PRAUS-
C     NITZ, AND SHERWOOD, PUBLISHED BY McGRAW-HILL, NY,
C     1977.  THESE EQUATIONS USE AN EXTENSION OF THE
C     KINETIC THEORY OF CHAPMAN-ENSKOG AND WILKE'S APPROXI-
C     MATION FOR THE COLLISION INTEGRAL PARAMETER.
      COMMON /FUEL/ FUELX(10),DFUELX(10)
      COMMON /PROPS/ LHEATM,MOLWTM,VISCM,CTSAMPLE,CTHOOD
      DIMENSION CH(10),CM(10),CV(10),PHI(10,10)
      REAL LHEATM,MOLWTM,NUM
      DATA CH(1),CM(1),CV(1)     /  913,16.041,109  /
      DATA CH(2),CM(2),CV(2)     / 1641,30.067, 90.1/
      DATA CH(3),CM(3),CV(3)     / 2385,44.092, 80.6/
      DATA CH(4),CM(4),CV(4)     /    0,28.016,175.8/
      DATA CH(5),CM(5),CV(5)     /    0,44.01 ,146.6/
      DATA CH(6),CM(6),CV(6)     / 4412,86.169, 69.2/
      DATA CH(7),CM(7),CV(7)     / 3105,58.118, 74.4/
      DATA CH(8),CM(8),CV(8)     / 3113,58.118, 73.9/
      DATA CH(9),CM(9),CV(9)     / 3716,72.144, 93  /
      DATA CH(10),CM(10),CV(10) / 3709,72.144, 91.7/
      DO 20 I=1,10
           DO 10 J=1,10
                NUM=1.+SQRT(CV(I)/CV(J))*SQRT(SQRT(CM(J)/
     2              CM(I)))
                PHI(I,J)=NUM*NUM/SQRT(8.*(1.+CM(I)/CM(J)))
10         CONTINUE
20    CONTINUE

      VISCM=0.
      DO 40 I=1,10
           SUM=0.
           DO 30 J=1,10
                SUM=SUM+FUELX(J)*PHI(I,J)
30         CONTINUE
           VISCM=VISCM+FUELX(I)*CV(I)/SUM
40    CONTINUE

      MOLWTM=0.
      LHEATM=0.
```

```
      DO 50 I=1,10
           MOLWTM=MOLWTM+FUELX(I)*CM(I)
           LHEATM=LHEATM+FUELX(I)*CH(I)
50    CONTINUE
      RETURN
      END


      SUBROUTINE FLOWRATE
C     THIS SUBROUTINE CALCULATES THE FLOWRATE IN SCFM AND
C     FUEL HEATING VALUE FOR NATURAL GAS FLOW THROUGH THE
C     MERRIAM LAMINAR FLOWMETER MODEL NO. 50MC2-2P, SERIAL
C     NO.T-6405 1.  IT ALSO CALCULATES THE FLOWRATE OF AIR
C     IN SCFM FOR AIR FLOW THROUGH THE MERRIAM LAMINAR
C     FLOWMETER MODEL NO. 50MC2-4, SERIAL NO. 719080-A3.
      REAL LHEATM,MOLWTM,KW,MDOTA,MDOTF
      INTEGER TSAMPLE,THOOD
      COMMON /FLOWS/ AIRMATCH,ENTRAIN,KW,MDOTA,MDOTF,QNG
      COMMON /DFLOW/ DAIMATCH,DENTRAIN,DKW,DMDOTA,DMDOTF,
     2DQNG
      COMMON /MEAS1/ AIRFLOW,FUELFLOW,DAIRFL,DFUELFL,PRESS,
     2DPRESS
      COMMON /MEAS2/ PVAP,TDRY,TWET,DPVAP,DTDRY,DTWET,
     2TSAMPLE,THOOD
      COMMON /MEAS3/ UPSTRMPA,UPSTRMPF,DUPSTMPA,DUPSTMPF
      COMMON /PROPS/ LHEATM,MOLWTM,VISCM,CTSAMPLE,CTHOOD
      FF1=181.87/VISCM
      FFMPRESS=UPSTRMPF*760./14.69595
      DFFMPR=FFMPRESS*DUPSTMPF/UPSTRMPF
      FF2=(PRESS+FFMPRESS)/760.
      DFF2=SQRT((DPRESS**2+DFFMPR**2)/760.**2)
      FF3=529.67/(1.8*TDRY+491.67)
      DFF3=FF3*1.8*DTDRY/(1.8*TDRY+491.67)
      FF4=181.87/(.4757*(TDRY+273.15)+41.889)
      DFF4=FF4*.4757*DTDRY/(.4757*(TDRY+273.15)+41.889)
      FLOWFACT=FF1*FF2*FF3*FF4
      DFLOWFCT=FLOWFACT*SQRT((DFF2/FF2)**2+(DFF3/FF3)**2+
      2(DFF4/FF4)**2)
      QNG=FLOWFACT*629.35*FUELFLOW
      DQNG=QNG*SQRT((DFLOWFCT/FLOWFACT)**2+(DFUELFL/
     2FUELFLOW)**2)
      EDOTFUEL=LHEATM*QNG/60.
      DEDOTF=EDOTFUEL*DQNG/QNG
      KW=EDOTFUEL/.9481
      DKW=KW*DEDOTF/EDOTFUEL
      DENSITYF=(PRESS+FFMPRESS)*MOLWTM*.016035/
     2(TDRY+273.15)
      DDENSTYF=DENSITYF*SQRT((DPRESS**2+DFFMPR**2)/
     2    (PRESS+FFMPRESS)**2+(DTDRY/(TDRY+273.15))**2)
      MDOTF=0.47195*QNG*DENSITYF
      DMDOTF=MDOTF*SQRT((DQNG/QNG)**2+(DDENSTYF/DENSITYF)
     2**2)
      CTSAMPLE=(TSAMPLE-32.)/1.8
```

```
      CTHOOD=(THOOD-32.)/1.8
      AFMPRESS=UPSTRMPA*760./14.69595
      IF(UPSTRMPA .EQ. 0.) THEN
        DAFMPR=0.
      ELSE
        DAFMPR=AFMPRESS*DUPSTMPA/UPSTRMPA
      ENDIF
      AF1=(PRESS+AFMPRESS)/760.
      DAF1=AF1*(DPRESS+DAFMPR)/(PRESS+AFMPRESS)
      AF2=FF3
      DAF2=DFF3
      AF3=FF4
      DAF3=DFF4
      AIRFACT=AF1*AF2*AF3
      DAIRFACT=AIRFACT*SQRT((DAF1/AF1)**2+(DAF2/AF2)**2+
      2(DAF3/AF3)**2)
      QAIR=AIRFACT*(55.0*53.4252)*AIRFLOW
      IF(AIRFLOW .EQ. 0.) THEN
        DQAIR=0.
      ELSE
        DQAIR=QAIR*SQRT((DAIRFACT/AIRFACT)**2+(DAIRFL/
     2AIRFLOW)**2)
      ENDIF
      DENSITYA=1.1614
      MDOTA=0.47195*QAIR*DENSITYA
      IF(QAIR .EQ. 0.) THEN
        DMDOTA=0.
      ELSE
        DMDOTA=MDOTA*DQAIR/QAIR
      ENDIF
      RETURN
      END


      SUBROUTINE PSCHOMET
C     THIS SUBROUTINE CALCULATES THE VAPOR PRESSURE OF
C     WATER IN LAB AIR BY USING A SIX-PARAMETER LEAST-
C     SQUARES POLYNOMIAL FIT TO THE SMITHSONIAN VAPOR PRES-
C     SURE DATA.  GIVEN THE WET BULB TEMPERATURE (TWET),
C     THE VAPOR PRESSURE AT THIS TEMPERATURE IS CALCULATED.
C     IT IS THEN CORRECTED USING THE ATMOSPHERIC PRESSURE
C     (P), AND DRY-BULB TEMPERATURE (TDRY) TO GIVE THE
C     VAPOR PRESSURE OF WATER (PVAP) AT ATMOSPHERIC CONDI-
C     TIONS.  TWET AND TDRY ARE TO BE SUPPLIED IN DEGREES
C     CELSIUS, PRESSURES IN TORR.  THESE EQUATIONS HOLD FOR
C     -19C < TWET < 30C, .861 < PVAP < 32 TORR.  AN ERROR
C     ANALYSIS IS ALSO DONE IN THIS SUBROUTINE BY VARYING
C     THE INPUT VALUES.  THESE ERRORS MUST BE COMBINED WITH
C     THE 0.02 TORR ERROR DUE TO THE NUMERICAL FIT.
      INTEGER THOOD,TSAMPLE
      LOGICAL L1,L2
      COMMON /MEAS1/ AIRFLOW,FUELFLOW,DAIRFL,DFUELFL,PRESS,
     2DPRESS
```

```
      COMMON /MEAS2/ PVAP,TDRY,TWET,DPVAP,DTDRY,DTWET,
     2TSAMPLE,THOOD
      COMMON /MEAS3/ UPSTRMPA,UPSTRMPF,DUPSTMPA,DUPSTMPF
      DIMENSION D(5),DELTA(3)
      DATA D(1),D(2),D(3)   / 4.53582,.344087,.010243/
      DATA D(4),D(5)        /  .0001841,3.47926E-06  /
      PR=PRESS
      TD=TDRY
      TW=TWET
      J=0
    5 R=1.
      PVAP=0.
      DO 10 I=1,5
           PVAP=PVAP+D(I)*R
           R=R*TW
   10 CONTINUE
      PVAP=PVAP-.00066*PR*(TD-TW)*(1.+.00115*TW)
      IF(J.EQ.0) THEN
        PVAP0=PVAP
      ELSE
        GOTO 20
      ENDIF
      J=1
      TD=TDRY+DTDRY
      GO TO 5
   20 IF(J.EQ.1) THEN
        DELTA(1)=PVAP-PVAP0
      ELSE
        GOTO 30
      ENDIF
      J=2
      TD=TDRY
      PR=PR+DPRESS
      GOTO 5
   30 IF(J.EQ.2) THEN
        DELTA(2)=PVAP-PVAP0
      ELSE
        GOTO 40
      ENDIF
      J=3
      PR=PRESS
      TW=TWET+DTWET
      GOTO 5
   40 IF(J.EQ.3) THEN
        DELTA(3)=PVAP-PVAP0
      ELSE
        GOTO 50
      ENDIF
      PVAP=PVAP0
      TW=TWET
C     NOW COMBINE THE ERRORS FOR EACH VARIED INPUT VALUE
      DPVAP=SQRT(.0004+DELTA(1)**2+DELTA(2)**2+DELTA(3)**2)
      L1=PVAP .GT. 0.861
```

```
      L2=PVAP .LT. 31.86
      IF(L1 .AND. L2) THEN
        RETURN
      ELSE
        PRINT *,'PVAP IS OUT OF LIMITS'
      ENDIF
 50   PRINT *,'ERROR IN SUBROUTINE PSCHOMET'
      RETURN
      END


      SUBROUTINE ASPECIES
C     THIS SUBROUTINE CALCULATES THE VALUES OF THE MOLE
C     FRACTIONS OF METHANE, ETHANE, PROPANE, NITROGEN, AND
C     CARBON DIOXIDE IN THE SUPPLIED NATURAL GAS.  THE DATA
C     IS OBTAINED FROM THE SOUTHERN CALIFORNIA GAS COMPANY
C     FROM VALUES MEASURED AT THE PASADENA
C     POWER PLANT.  ALSO, AN UNCERTAINTY IS COMPUTED.
      COMMON /FUEL/ FUELX(10),DFUELX(10)
      COMMON /MOLES/ A(5),B(5),Y(12),DA(5),DB(5),DY(12)
      A(1)=FUELX(1)
      A(2)=FUELX(2)
      A(3)=FUELX(3)
      A(4)=FUELX(4)
      A(5)=FUELX(5)
C     FUEL COMPONENTS FOR TRACE HYDROCARBONS ARE CHARGED TO
C     PROPANE
      DO 10 I=6,10
           A(3)=A(3)+FUELX(I)
 10   CONTINUE
      ACHECK=A(1)+A(2)+A(3)+A(4)+A(5)
      DELTA=ABS(1.-ACHECK)
      IF(DELTA .GT. 0.0001) THEN
        PRINT *,'INCOMPLETE SPECIFICATION OF FUEL'
      ENDIF
      DO 20 I=1,10
           IF(DFUELX(I) .LT. 0.) THEN
             DFUELX(I)=-FUELX(I)*DFUELX(I)
           ENDIF
 20   CONTINUE
      DA(1)=DFUELX(1)
      DA(2)=DFUELX(2)
      DA(3)=DFUELX(3)
      DA(4)=DFUELX(4)
      DA(5)=DFUELX(5)
      RETURN
      END


      SUBROUTINE BSPECIES
C     THIS SUBROUTINE CALCULATES THE VALUES OF THE MOLE
C     FRACTIONS OF OXYGEN, NITROGEN, WATER VAPOR, CARBON
C     DIOXIDE, AND ARGON IN THE LAB AIR.  USING THE NBS
```

```
C       STANDARD, DRY AIR IS ASSUMED TO BE 78.09% NITROGEN,
C       20.95% OXYGEN, .03% CARBON DIOXIDE, AND 0.93%
C       ARGON.  ALSO, AN UNCERTAINTY IS COMPUTED.
        INTEGER THOOD,TSAMPLE
        COMMON /MEAS1/ AIRFLOW,FUELFLOW,DAIRFL,DFUELFL,PRESS,
            2DPRESS
        COMMON /MEAS2/ PVAP,TDRY,TWET,DPVAP,DTDRY,DTWET,
       2TSAMPLE,THOOD
        COMMON /MEAS3/ UPSTRMPA,UPSTRMPF,DUPSTMPA,DUPSTMPF
        COMMON /MOLES/ A(5),B(5),Y(12),DA(5),DB(5),DY(12)
        B(3)=PVAP/PRESS
        B(1)=(1.-B(3))*.2095
        B(2)=(1.-B(3))*.7809
        B(4)=(1.-B(3))*.0003
        B(5)=(1.-B(3))*.0093
        DB(3)=B(3)*SQRT((DPVAP/PVAP)**2+(DPRESS/PRESS)**2)
        DB(1)=.001
        DB(2)=.002
        DB(4)=.00008
        DB(5)=.0006
        RETURN
        END


        SUBROUTINE ELEMENTS
C       THIS SUBROUTINE CALCULATES THE VALUES AND UNCERTAIN-
C       TIES OF THE A AND B COEFFICIENTS IN TERMS OF THE
C       ELEMENTS C, H, O, AND N.
        COMMON /AELEMS/ AC,AH,AO,AN,DAC,DAH,DAO,DAN
        COMMON /BELEMS/ BC,BH,BO,BN,DBC,DBH,DBO,DBN
        COMMON /CHROM/  C1,DC1,Y2PLUS,DY2PLUS
        COMMON /MOLES/  A(5),B(5),Y(12),DA(5),DB(5),DY(12)
        COMMON /RESPONSE/ F(12),DF(12)
        C1=F(2)/F(12)
        DC1=C1*SQRT((DF(2)/F(2))**2+(DF(12)/F(12))**2)
        AC=A(1)+2.*A(2)+3.*A(3)+A(5)
        AH=2.*A(1)+3.*A(2)+4.*A(3)
        AO=2.*A(5)
        AN=A(4)
        DAC=SQRT(DA(1)**2+4.*DA(2)**2+9.*DA(3)**2+DA(5)**2)
        DAH=SQRT(4.*DA(1)**2+9.*DA(2)**2+16.*DA(3)**2)
        DAO=2.*DA(5)
        DAN=DA(4)
        BC=B(4)
        BH=B(3)
        BO=2.*(B(1)+C1*B(5))+B(3)+2.*B(4)
        BN=B(2)
        DBC=DB(4)
        DBH=DB(3)
        DBO=SQRT(4.*DB(1)**2+4.*(C1*DB(5))**2+4.*(B(5)*DC1)
                **2+DB(3)**2+4.*DB(4)**2)
        DBN=DB(2)
        RETURN
```

```
      END


      SUBROUTINE YSPECIES
C     THIS SUBROUTINE CALCULATES THE VALUES AND UNCERTAIN-
C     TIES OF THE MOLE FRACTIONS MEASURED BY THE GAS CHROM-
C     ATOGRAPH, NORMALIZED BY THE NITROGEN MEASUREMENTS.
      REAL MISC,DAREA(11)
      INTEGER AREA,DIAREA
      COMMON /AREAS/ AREA(11),DIAREA(11)
      COMMON /CHROM/ C1,DC1,Y2PLUS,DY2PLUS
      COMMON /MOLES/ A(5),B(5),Y(12),DA(5),DB(5),DY(12)
      COMMON /RESPONSE/ F(12),DF(12)
      DO 10 I=1,11
           IF(AREA(I) .EQ. 0) GOTO 10
           IF(DIAREA(I) .GT. 0) THEN
             DAREA(I)=DIAREA(I)/FLOAT(AREA(I))
           ELSE
             DAREA(I)=-DIAREA(I)
           ENDIF
 10   CONTINUE
      DO 20 I=1,12
           IF(F(I) .EQ. 0.) GOTO 20
           IF(DF(I) .GE. 0.) THEN
             DF(I)=DF(I)/F(I)
           ELSE
             DF(I)=-DF(I)
           ENDIF
 20   CONTINUE
      DEN=F(3)*AREA(3)
      Y(1)=F(1)*AREA(1)/DEN
      Y(4)=F(4)*AREA(4)/DEN
      Y(5)=F(5)*AREA(5)/DEN
      Y(6)=F(6)*AREA(6)/DEN
      Y(9)=F(9)*AREA(9)/DEN
      Y(10)=F(10)*AREA(10)/DEN
      Y(11)=F(11)*AREA(11)/DEN
      Y2PLUS=F(2)*AREA(2)/DEN
      MISC=DAREA(3)**2+DF(3)**2
      DY(1)=Y(1)*SQRT(DF(1)**2+DAREA(1)**2+MISC)
      DY(4)=Y(4)*SQRT(DF(4)**2+DAREA(4)**2+MISC)
      DY(5)=Y(5)*SQRT(DF(5)**2+DAREA(5)**2+MISC)
      DY(6)=Y(6)*SQRT(DF(6)**2+DAREA(6)**2+MISC)
      DY(9)=Y(9)*SQRT(DF(9)**2+DAREA(9)**2+MISC)
      DY(10)=Y(10)*SQRT(DF(10)**2+DAREA(10)**2+MISC)
      DY(11)=Y(11)*SQRT(DF(11)**2+DAREA(11)**2+MISC)
      DY2PLUS=Y2PLUS*SQRT(DF(2)**2+DAREA(2)**2+MISC)
      RETURN
      END


      SUBROUTINE YELEMENT
C     THIS SUBROUTINE CALCULATES THE VALUES AND UNCERTAIN-
```

```
C      TIES OF THE Y COEFFICIENTS IN TERMS OF THE ELEMENTS
C      C, H, O, AND N.
       COMMON /CHROM/ C1,DC1,Y2PLUS,DY2PLUS
       COMMON /MOLES/ A(5),B(5),Y(12),DA(5),DB(5),DY(12)
       COMMON /YELEMS/ YC,YH,YO,YN,DYC,DYH,DYO,DYN
       YC=Y(4)+Y(5)+Y(6)+2.*Y(9)+2.*Y(10)+2.*Y(11)
       YH=Y(1)+2.*Y(4)+Y(9)+2.*Y(10)+3.*Y(11)
       YO=2.*Y2PLUS+Y(5)+2.*Y(6)
       YN=1.
       DYC=SQRT(DY(4)**2+DY(5)**2+DY(6)**2+4.*(DY(9)**2+
     2      DY(10)**2
     *          +DY(11)**2))
       DYH=SQRT(DY(1)**2+4.*DY(4)**2+DY(9)**2+4.*DY(10)**2
     *          +9.*DY(11)**2)
       DYO=SQRT(4.*DY2PLUS**2+DY(5)**2+4.*DY(6)**2)
       DYN=0.
       RETURN
       END


       SUBROUTINE SOLUTION
C      THIS SUBROUTINE SOLVES FOR THE FOUR UNKNOWNS I, X3,
C      X7, AND X8. ALSO, UNCERTAINTIES ARE COMPUTED.  THE
C      COMPOSITION OF SOOT IS TAKEN AS C8H.
       COMMON /AELEMS/ AC,AH,AO,AN,DAC,DAH,DAO,DAN
       COMMON /AIRADD/ I,IS,DI,DIS
       COMMON /BELEMS/ BC,BH,BO,BN,DBC,DBH,DBO,DBN
       COMMON /CHROM/ C1,DC1,Y2PLUS,DY2PLUS
       COMMON /FRACT/ X(12),XM(12),XMA(12),XS(12),YM(12),
     2YMS(12),DYM(12)
       COMMON /MOLES/ A(5),B(5),Y(12),DA(5),DB(5),DY(5)
       COMMON /YELEMS/ YC,YH,YO,YN,DYC,DYH,DYO,DYN
       REAL MISCA,MISCB,MISCY,MISCDEN,MISCNUM1,MISCNUM2
       REAL I,IS
       DIMENSION DX(12)
       MISCA=16.*(AH-AO)-AC
       MISCB=16.*(BH-BO)-BC
       MISCY=16.*(YH-YO)-YC
       I=(YN*MISCA-AN*MISCY)/(BN*MISCY-YN*MISCB)
       X(3)=(AN+I*BN)/YN
       X(7)=AO+I*BO-X(3)*YO
       X(8)=(AC+I*BC-X(3)*YC)/8.
       DMISCA=(16.*DAH)**2+(16.*DAO)**2+DAC**2
       DMISCB=(16.*DBH)**2+(16.*DBO)**2+DBC**2
       DMISCY=(16.*DYH)**2+(16.*DYO)**2+DYC**2
       MISCDEN=(BN*MISCY-YN*MISCB)**2
       MISCNUM1=(YN*DMISCA)**2+(AN*DMISCY)**2
     $         +(MISCA*DYN)**2+(MISCY*DAN)**2
       MISCNUM2=(YN*DMISCB)**2+(BN*DMISCY)**2
     $         +(MISCB*DYN)**2+(MISCY*DBN)**2
       DI=SQRT((I**2*MISCNUM2+MISCNUM1)/MISCDEN)
       DX(3)=X(3)*SQRT((DYN/YN)**2+(DAN**2+(I*DBN)**2+
     2          (BN*DI)**2)/(AN+I*BN)**2)
```

```
      DX(7)=SQRT(DAO**2+(I*DBO)**2+(BO*DI)**2+(YO*DX(3))**2
     *           +(X(3)*DYO)**2)
      DX(8)=SQRT(DAC**2+(I*DBC)**2+(BC*DI)**2+(YC*DX(3))**2
     *           +(X(3)*DYC)**2)
      X(12)=I*B(5)
      Y(7)=X(7)/X(3)
      Y(3)=1.
      IF(X(8) .GT. 0.)THEN
        Y(8)=X(8)/X(3)
      ELSE
        Y(8)=0.
      ENDIF
      Y(12)=X(12)/X(3)
      Y(2)=Y2PLUS-C1*Y(12)
      DY(3)=0.
      DY(7)=Y(7)*SQRT((DX(7)/X(7))**2+(DX(3)/X(3))**2)
      IF(X(8) .GT. 0.) THEN
        DY(8)=Y(8)*SQRT((DX(8)/X(8))**2+(DX(3)/X(3))**2)
      ELSE
        DY(8)=0.
      ENDIF
      DY(12)=Y(12)*SQRT((DX(3)/X(3))**2+(DB(5)/B(5))**2+
     2(DI/I)**2)
      DY(2)=SQRT(DY2PLUS**2+(C1*DY(12))**2+(Y(12)*DC1)**2)
C     NOW CHECK THE MOLE FRACTION OF SOOT, WHICH IS OFTEN
C     SMALL, TO SEE THAT IT IS POSITIVE.  IF IT IS NEGA-
C     TIVE, THEN ITS VALUE IS SET TO ZERO AND THE CALCULA-
C     TIONS ARE CARRIED OUT AGAIN.
      IF(X(8) .GE. 0.) GO TO 10
      PRINT *,'SETTING SOOT MOLE FRACTION TO ZERO   '
      X(8)=0.
      I=(AC*YN-AN*YC)/(BN*YC-BC*YN)
      X(3)=(AN+BN*I)/YN
      X(7)=AO+BO*I-YO*X(3)
 10   RETURN
      END


      SUBROUTINE FRACTION
C     THIS SUBROUTINE CALCULATES THE MOLE FRACTIONS AND
C     MASS FRACTIONS OF THE PRODUCT GAS DUE TO THE COMBUS-
C     TION OF NATURAL GAS FUEL. ALSO, UNCERTAINTIES ARE
C     COMPUTED FOR THE MOLE FRACTIONS.
      COMMON /FRACT/ X(12),XM(12),XMA(12),XS(12),YM(12),
     2YMS(12),DYM(12)
      COMMON /MOLES/ A(5),B(5),Y(12),DA(5),DB(5),DY(12)
      DIMENSION MASS(12)
      REAL MASS
      SUMMOLES=0.
      DSUMMOLES=0.
      DO 10 J=1,12
           SUMMOLES=SUMMOLES+Y(J)
           DSUMMOLES=DSUMMOLES+DY(J)**2
```

```
 10   CONTINUE
      DO 20 J=1,12
           IF(Y(J) .GT. 0.) THEN
             YM(J)=Y(J)/SUMMOLES
             DYM(J)=YM(J)*SQRT((DY(J)/Y(J))**2+DSUMMOLES/
     2               SUMMOLES**2)
           ELSE
             YM(J)=0.
             DYM(J)=0.
           ENDIF
 20   CONTINUE
      DATA MASS(1),MASS(2),MASS(3) / 2.016,31.999,28.013/
      DATA MASS(4),MASS(5),MASS(6) / 16.043,28.011,44.01/
      DATA MASS(7),MASS(8),MASS(9) / 18.015,97.097,26.038/
      DATA MASS(10),MASS(11),MASS(12) /28.054,30.07,39.948/
      SUMMASS=0.
      DO 30 J=1,12
           SUMMASS=SUMMASS+YM(J)*MASS(J)
 30   CONTINUE
      DO 40 J=1,12
           XM(J)=YM(J)*MASS(J)/SUMMASS
 40   CONTINUE
      RETURN
      END


      SUBROUTINE STOICH
C     THIS SUBROUTINE CALCULATES THE STOICHIOMETRIC FUEL-
C     AIR RATIO AND THE PRODUCTS OF A STOICHIOMETRIC REAC-
C     TION.  THE ENTRAINMENT AND THE EQUIVALENCE RATIOS ARE
C     CALCULATED.  ALSO, UNCERTAINTIES FOR THESE ARE
C     COMPUTED.
      COMMON /AIRADD/ I,IS,DI,DIS
      COMMON /CHROM/ C1,DC1,Y2PLUS,DY2PLUS
      COMMON /DFLOW/ DAIMATCH,DENTRAIN,DKW,DMDOTA,DMDOTF,
     2DQNG
      COMMON /FLOWS/ AIRMATCH,ENTRAIN,KW,MDOTA,MDOTF,QNG
      COMMON /FRACT/ X(12),XM(12),XMA(12),XS(12),YM(12),
     2YMS(12),DYM(12)
      COMMON /HEATS/ HEATA,HEATF,HEATP,HEATSP
      COMMON /HRXN/  HRXNA,HRXNS,RATIO,RATIOAM
      COMMON /MOLES/ A(5),B(5),Y(12),DA(5),DB(5),DY(12)
      COMMON /PHIS/  DPHIL,DPHIP,PHIRATIO,PLUMEPHI,ULAYERPH
      COMMON /PROPS/ LHEATM,MOLWTM,VISCM,CTSAMPLE,CTHOOD
      REAL I,IS,KW,MDOTA,MDOTATOT,MDOTF,LHEATM,MOLWTM
C     ENTRAINMENT AND MOLES OF PRODUCT FOR A STOICHIOMETRIC
C     REACTION
      IS=(4.*A(1)+7.*A(2)+10.*A(3))/(2.*B(1))
      XS(3)=A(4)+B(2)*IS
      XS(6)=A(1)+2.*A(2)+3.*A(3)+A(5)+B(4)*IS
      XS(7)=2.*A(1)+3.*A(2)+4.*A(3)+B(3)*IS
      XS(12)=B(5)*IS
      DIS=SQRT(((4.*DA(1))**2+(7.*DA(2))**2+(10.*DA(3))**2
```

```
     $          +(2.*DB(1))**2)/(2.*B(1))**2)
      SUMSTMOL=XS(3)+XS(6)+XS(7)+XS(12)
      YMS(3)=XS(3)/SUMSTMOL
      YMS(6)=XS(6)/SUMSTMOL
      YMS(7)=XS(7)/SUMSTMOL
      YMS(12)=XS(12)/SUMSTMOL
C     EQUIVALENCE RATIO OF THE UPPER LAYER
      ULAYERPH=IS/I
      DPHIL=ULAYERPH*SQRT((DIS/IS)**2+(DI/I)**2)
      MDOTATOT=MDOTF*I*28.9/MOLWTM
      DMDOTATT=MDOTATOT*SQRT((DMDOTF/MDOTF)**2+(DI/I)**2)
C     MDOTA IS THE AIR ADDITION RATE GIVEN BY THE FLOWMETER
C     ANALYSIS, AIRMATCH IS THE AIR ADDITION RATE DERIVED
C     FROM THE CHEMISTRY
      IF (MDOTA .GT. 0.) THEN
        AIRMATCH=MDOTATOT-ENTRAIN
        DAIMATCH=SQRT(DMDOTATT**2+DENTRAIN**2)
      ELSE
        AIRMATCH=0.
        DAIMATCH=0.
        ENTRAIN=MDOTATOT
        DENTRAIN=DMDOTATT
      ENDIF
      IF(ENTRAIN .GE. 0.1) THEN
C       CALCULATIONS FOR TWO LAYERED CONFIGURATIONS
        PLUMEPHI=IS/(ENTRAIN/MDOTF)*28.9/MOLWTM
        DPHIP=PLUMEPHI*SQRT((DIS/IS)**2+(DMDOTF/MDOTF)**2
     $                      +(DENTRAIN/ENTRAIN)**2)
      ELSE
C       CALCULATIONS FOR EXTINCTION LIMIT EXPERIMENTS
        PLUMEPHI=0.0000
        DPHIP=0.0000
      ENDIF
C     HEATS OF FORMATION CALCULATIONS
      HEATF=-17.89*A(1)+12.5*A(2)-24.82*A(3)-94.05*A(5)
      HEATA=-57.8*B(3)-94.05*B(4)
      HEATP=-17.89*YM(4)-26.42*YM(5)-94.05*YM(6)-57.8*YM(7)
     *      +54.19*YM(9)+.881*YM(10)+1.073*YM(11)
      HEATSP=-94.05*YMS(6)-57.8*YMS(7)
      SUMMOLES=0.
      DO 10 J=1,12
           SUMMOLES=SUMMOLES+Y(J)
 10   CONTINUE
      PRODN=X(3)*SUMMOLES
      HRXNA=PRODN*HEATP-I*HEATA-HEATF
      HRXNS=SUMSTMOL*HEATSP-IS*HEATA-HEATF
      RATIO=HRXNA/HRXNS
      IF(ULAYERPH .LT. 1.) THEN
        RATIOAM=RATIO
      ELSE
        RATIOAM=ULAYERPH*RATIO
      ENDIF
      RETURN
```

```
      END


      SUBROUTINE EQUIVLNT
C     THIS SUBROUTINE COMPUTES THE MASS FRACTIONS OF AN
C     EQUIVALENT SOURCE FOR THE PLUME, ONE WHICH PROVIDES
C     THE SAME RATE OF SPECIES ADDITION TO THE UPPER LAYER.
      COMMON /AIRADD/ I,IS,DI,DIS
      COMMON /FRACT/ X(12),XM(12),XMA(12),XS(12),YM(12),
     2YMS(12),DYM(12)
      COMMON /MOLES/ A(5),B(5),Y(12),DA(5),DB(5),DY(12)
      COMMON /PHIS/ DPHIL,DPHIP,PHIRATIO,PLUMEPHI,ULAYERPH
      COMMON /PROPS/ LHEATM,MOLWTM,VISCM,CTSAMPLE,CTHOOD
      REAL I,IS,LHEATM,MOLWTM
      SUMAIR=B(1)*31.999+B(2)*28.013+B(3)*18.015+B(4)*44.01
     *       +B(5)*39.948
      XMA(2)=B(1)*31.999/SUMAIR
      XMA(3)=B(2)*28.013/SUMAIR
      XMA(7)=B(3)*18.015/SUMAIR
      XMA(6)=B(4)*44.01/SUMAIR
      XMA(12)=B(5)*39.948/SUMAIR
      FS=MOLWTM/(IS*28.9)
      PHIRATIO=(PLUMEPHI-ULAYERPH)/(ULAYERPH*
     2(1.+FS*PLUMEPHI))
      XS(1)=XM(1)*(1.+PHIRATIO)
      XS(2)=XM(2)+PHIRATIO*(XM(2)-XMA(2))
      XS(3)=XM(3)+PHIRATIO*(XM(3)-XMA(3))
      XS(4)=XM(4)*(1.+PHIRATIO)
      XS(5)=XM(5)*(1.+PHIRATIO)
      XS(6)=XM(6)+PHIRATIO*(XM(6)-XMA(6))
      XS(7)=XM(7)+PHIRATIO*(XM(7)-XMA(7))
      XS(8)=XM(8)*(1.+PHIRATIO)
      XS(9)=XM(9)*(1.+PHIRATIO)
      XS(10)=XM(10)*(1.+PHIRATIO)
      XS(11)=XM(11)*(1.+PHIRATIO)
      XS(12)=XM(12)+PHIRATIO*(XM(12)-XMA(12))
      XMA(1)=0.
      XMA(4)=0.
      XMA(5)=0.
      XMA(8)=0.
      XMA(9)=0.
      XMA(10)=0.
      XMA(11)=0.
      RETURN
      END


      SUBROUTINE OUTPUT(FILENAME,RUNDATE,RUNTIME,EXPNO)
C     THIS SUBROUTINE SENDS ALL OF THE COMPUTED VALUES INTO
C     A FILE CALLED 'EX######.OUT', WHERE THE #'S REPRESENT
C     THE EXPERIMENT NUMBER AND THE DATE.
      COMMON /AIRADD/ I,IS,DI,DIS
      COMMON /DFLOW/ DAIMATCH,DENTRAIN,DKW,DMDOTA,DMDOTF,
```

```
     2DQNG
      COMMON /FLOWS/ AIRMATCH,ENTRAIN,KW,MDOTA,MDOTF,QNG
      COMMON /FRACT/ X(12),XM(12),XMA(12),XS(12),YM(12),
     2YMS(12),DYM(12)
      COMMON /HEATS/ HEATA,HEATF,HEATP,HEATSP
      COMMON /HRXN/  HRXNA,HRXNS,RATIO,RATIOAM
      COMMON /LABEL/ BOXHITE,RUNNUMBR,DIAMETER
      COMMON /MOLES/ A(5),B(5),Y(12),DA(5),DB(5),DY(12)
      COMMON /PHIS/  DPHIL,DPHIP,PHIRATIO,PLUMEPHI,ULAYERPH
      COMMON /PROPS/ LHEATM,MOLWTM,VISCM,CTSAMPLE,CTHOOD
      CHARACTER * 2 EXPNO
      CHARACTER * 8 RUNDATE
      CHARACTER * 5 RUNTIME
      CHARACTER * 12 FILENAME
      CHARACTER * 12 FILEOUT
      INTEGER RUNNUMBR
      REAL I,IS,LHEATM,MOLWTM,KW,MDOTA,MDOTF
      FILEOUT=FILENAME(1:9) // 'OUT'
      OPEN(UNIT=1,FILE=FILEOUT)
      WRITE(1,10) RUNDATE,RUNTIME,EXPNO,RUNNUMBR
      WRITE(1,20) BOXHITE,DIAMETER,CTSAMPLE,CTHOOD
      WRITE(1,30) MDOTF,KW,QNG,MDOTA,AIRMATCH,ENTRAIN
      WRITE(1,35) DAIMATCH,DENTRAIN,DKW,DMDOTA,DMDOTF,DQNG
      WRITE(1,40) LHEATM,MOLWTM,VISCM
      WRITE(1,50) I,IS,DI,DIS
      WRITE(1,60) ULAYERPH,DPHIL,PLUMEPHI,DPHIP
      WRITE(1,70) HEATF,HEATA,HEATP,HEATSP
      WRITE(1,70) HRXNA,HRXNS,RATIO,RATIOAM
      WRITE(1,80) A(1),A(2),A(3),A(4),A(5)
      WRITE(1,80) DA(1),DA(2),DA(3),DA(4),DA(5)
      WRITE(1,80) B(1),B(2),B(3),B(4),B(5)
      WRITE(1,80) DB(1),DB(2),DB(3),DB(4),DB(5)
      WRITE(1,90) Y(1),Y(2),Y(3),Y(4),Y(5),Y(6)
      WRITE(1,90) Y(7),Y(8),Y(9),Y(10),Y(11),Y(12)
      WRITE(1,90) DY(1),DY(2),DY(3),DY(4),DY(5),DY(6)
      WRITE(1,90) DY(7),DY(8),DY(9),DY(10),DY(11),DY(12)
      WRITE(1,90) YMS(1),YMS(2),YMS(3),YMS(4),YMS(5),YMS(6)
      WRITE(1,90) YMS(7),YMS(8),YMS(9),YMS(10),YMS(11),
     2YMS(12)
      WRITE(1,90) YM(1),YM(2),YM(3),YM(4),YM(5),YM(6)
      WRITE(1,90) YM(7),YM(8),YM(9),YM(10),YM(11),YM(12)
      WRITE(1,90) DYM(1),DYM(2),DYM(3),DYM(4),DYM(5),DYM(6)
      WRITE(1,90) DYM(7),DYM(8),DYM(9),DYM(10),DYM(11),
     2DYM(12)
      WRITE(1,90) XM(1),XM(2),XM(3),XM(4),XM(5),XM(6)
      WRITE(1,90) XM(7),XM(8),XM(9),XM(10),XM(11),XM(12)
      WRITE(1,90) XS(1),XS(2),XS(3),XS(4),XS(5),XS(6)
      WRITE(1,90) XS(7),XS(8),XS(9),XS(10),XS(11),XS(12)
      WRITE(1,90) XMA(1),XMA(2),XMA(3),XMA(4),XMA(5),XMA(6)
      WRITE(1,90) XMA(7),XMA(8),XMA(9),XMA(10),XMA(11),
     2XMA(12)
10    FORMAT(A8,1X,A5,1X,A2,1X,I4/)
20    FORMAT(F4.1,1X,F4.1,1X,F5.1,1X,F5.1/)
```

```
 30    FORMAT(F7.4,1X,F5.1,1X,F8.4,3(1X,F8.4)/)
 35    FORMAT(2(F6.4,1X),F4.2,3(F6.4,1X)/)
 40    FORMAT(F8.4,1X,F7.4,1X,F8.4/)
 50    FORMAT(2(F8.4,1X),2(F6.4,1X)/)
 60    FORMAT(4(F6.4,1X)/)
 70    FORMAT(4(F9.4,1X)/)
 80    FORMAT(5(F6.4,1X)/)
 90    FORMAT(6(F7.4,1X)/)
       RETURN
       END


       PROGRAM PRINTOUT
C      THIS PROGRAM READS THE RAW DATA FILE CREATED BY THE
C      DATAIN PROGRAM "EX##DDMM.RAW" AND THE SEQUENTIAL OUT-
C      PUT FILE FROM THE DATA REDUCTION PROGRAM (CRUNCHER)
C      CALLED "EX##DDMM.OUT".  THESE MEASURED AND CALCULATED
C      VALUES ARE ARRANGED INTO A PAGE OUTPUT FORMAT AND
C      WRITTEN INTO A FILE CALLED "EX##DDMM.TEX" WHICH CAN
C      BE DIRECTLY TeX'ED USING THE TeX TYPESETTING PROGRAM
C      WITH HARD COPY AVAILABLE BY OUTPUTTING THE "EX##DDMM.
C      DVI" FILE CREATED BY THE TeX PROGRAM BY DONALD E.
C      KNUTH.
       CHARACTER * 2 EXPNO
       CHARACTER * 8 RUNDATE
       CHARACTER * 5 RUNTIME
       CHARACTER * 12 FILENAME
       CHARACTER * 12 FILEOUT
       CHARACTER * 12 PRNTFIL
       INTEGER AREA,DAREA,TSAMPLE,THOOD,RUNNUMBR
       REAL I,IS,LHEATM,MOLWTM,KW,MDOTA,MDOTF
       DIMENSION FUELX(10),DFUELX(10),F(12),DF(12),AREA(11),
      2DAREA(11)
       DIMENSION A(5),DA(5),B(5),DB(5),Y(12),DY(12),YMS(12),
      2YM(12)
       DIMENSION DYM(12),XM(12),XS(12),XMA(12)
       PRINT *,'INPUT EXPERIMENT NUMBER   '
       READ '(A2)',EXPNO
       PRINT *,'INPUT DATE OF EXPERIMENT , MM-DD-YY   '
       READ '(A8)',RUNDATE
       FILENAME='EX' // EXPNO(1:2) // RUNDATE(1:2) //
      2RUNDATE(4:5) //* '.RAW'
       OPEN(UNIT=1,FILE=FILENAME,STATUS='OLD')
       READ(1,10) RUNDATE,RUNTIME,EXPNO,FUELFLOW,AIRFLOW,
      2UPSTRMPF
       READ(1,20) UPSTRMPA,PRESS,TDRY,TWET,DPRESS,DTDRY,
      2DTWET
       READ(1,30) BOXHITE,TSAMPLE,RUNNUMBR,DIAMETER,ENTRAIN,
      2THOOD
       READ(1,40) DFUELFL,DAIRFL,DUPSTMPF,DUPSTMPA,DENTRAIN
       READ(1,40) FUELX(1),FUELX(2),FUELX(3),FUELX(4),
      2FUELX(5)
       READ(1,40) FUELX(6),FUELX(7),FUELX(8),FUELX(9),
```

```
     2FUELX(10)
      READ(1,40) DFUELX(1),DFUELX(2),DFUELX(3),DFUELX(4),
     2DFUELX(5)
      READ(1,40) DFUELX(6),DFUELX(7),DFUELX(8),DFUELX(9),
     2DFUELX(10)
      READ(1,50) F(1),F(2),F(3),F(4),F(5)
      READ(1,40) F(6),F(9),F(10),F(11),F(12)
      READ(1,40) DF(1),DF(2),DF(3),DF(4),DF(5)
      READ(1,40) DF(6),DF(9),DF(10),DF(11),DF(12)
      READ(1,60) AREA(1),AREA(6),AREA(10),AREA(11),AREA(9)
      READ(1,70) AREA(2),AREA(3),AREA(4),AREA(5)
      READ(1,80) DAREA(1),DAREA(6),DAREA(10),DAREA(11),
     2DAREA(9)
      READ(1,90) DAREA(2),DAREA(3),DAREA(4),DAREA(5)
10    FORMAT(A8,1X,A5,1X,A2,3(1X,F7.5)/)
20    FORMAT(F7.5,1X,F5.1,2(1X,F4.1),3(1X,F3.1)/)
30    FORMAT(F4.1,2(1X,I4),1X,F4.1,1X,F6.3,1X,I4/)
40    FORMAT(5(F7.5,1X)/)
50    FORMAT(F7.3,4(1X,F7.5)/)
60    FORMAT(I4,1X,I6,3(1X,I5)/)
70    FORMAT(I6,1X,I7,2(1X,I6)/)
80    FORMAT(5(I4,1X)/)
90    FORMAT(4(I4,1X)/)
      CLOSE(UNIT=1)
      FILEOUT=FILENAME(1:9) // 'OUT'
      OPEN(UNIT=1,FILE=FILEOUT,STATUS='OLD')
      READ(1,110) RUNDATE,RUNTIME,EXPNO,RUNNUMBR
      READ(1,120) BOXHITE,DIAMETER,CTSAMPLE,CTHOOD
      READ(1,130) MDOTF,KW,QNG,MDOTA,AIRMATCH,ENTRAIN
      READ(1,135) DAIMATCH,DENTRAIN,DKW,DMDOTA,DMDOTF,DQNG
      READ(1,140) LHEATM,MOLWTM,VISCM
      READ(1,150) I,IS,DI,DIS
      READ(1,160) ULAYERPH,DPHIL,PLUMEPHI,DPHIP
      READ(1,170) HEATF,HEATA,HEATP,HEATSP
      READ(1,170) HRXNA,HRXNS,RATIO,RATIOAM
      READ(1,180) A(1),A(2),A(3),A(4),A(5)
      READ(1,180) DA(1),DA(2),DA(3),DA(4),DA(5)
      READ(1,180) B(1),B(2),B(3),B(4),B(5)
      READ(1,180) DB(1),DB(2),DB(3),DB(4),DB(5)
      READ(1,190) Y(1),Y(2),Y(3),Y(4),Y(5),Y(6)
      READ(1,190) Y(7),Y(8),Y(9),Y(10),Y(11),Y(12)
      READ(1,190) DY(1),DY(2),DY(3),DY(4),DY(5),DY(6)
      READ(1,190) DY(7),DY(8),DY(9),DY(10),DY(11),DY(12)
      READ(1,190) YMS(1),YMS(2),YMS(3),YMS(4),YMS(5),YMS(6)
      READ(1,190) YMS(7),YMS(8),YMS(9),YMS(10),YMS(11),
     2YMS(12)
      READ(1,190) YM(1),YM(2),YM(3),YM(4),YM(5),YM(6)
      READ(1,190) YM(7),YM(8),YM(9),YM(10),YM(11),YM(12)
      READ(1,190) DYM(1),DYM(2),DYM(3),DYM(4),DYM(5),DYM(6)
      READ(1,190) DYM(7),DYM(8),DYM(9),DYM(10),DYM(11),
     2DYM(12)
      READ(1,190) XM(1),XM(2),XM(3),XM(4),XM(5),XM(6)
      READ(1,190) XM(7),XM(8),XM(9),XM(10),XM(11),XM(12)
```

```
      READ(1,190) XS(1),XS(2),XS(3),XS(4),XS(5),XS(6)
      READ(1,190) XS(7),XS(8),XS(9),XS(10),XS(11),XS(12)
      READ(1,190) XMA(1),XMA(2),XMA(3),XMA(4),XMA(5),XMA(6)
      READ(1,190) XMA(7),XMA(8),XMA(9),XMA(10),XMA(11),
     2XMA(12)
110   FORMAT(A8,1X,A5,1X,A2,1X,I4/)
120   FORMAT(F4.1,1X,F4.1,1X,F5.1,1X,F5.1/)
130   FORMAT(F7.4,1X,F5.1,1X,F8.4,3(1X,F8.4)/)
135   FORMAT(2(F6.4,1X),F4.2,3(F6.4,1X)/)
140   FORMAT(F8.4,1X,F7.4,1X,F8.4/)
150   FORMAT(2(F8.4,1X),2(F6.4,1X)/)
160   FORMAT(4(F6.4,1X)/)
170   FORMAT(4(F9.4,1X)/)
180   FORMAT(5(F6.4,1X)/)
190   FORMAT(6(F7.4,1X)/)
      CLOSE(UNIT=1)
      PRNTFIL=FILENAME(1:9) // 'TEX'
      OPEN(UNIT=2,FILE=PRNTFIL)
      WRITE(2,300)
300   FORMAT(18H\magnification=875)
      WRITE(2,310)
310   FORMAT(14H\hoffset .95in)
      WRITE(2,320)
320   FORMAT(14H\nopagenumbers)
      WRITE(2,330)
330   FORMAT(23H\centerline{$\underline)
      WRITE(2,340)
340   FORMAT(38H{\bf DATA\ REDUCTION\ PROGRAM\ OUTPUT})
      WRITE(2,350)
350   FORMAT(14H\hskip 1.6in$},/,12H\vskip .25in)
      WRITE(2,360)
360   FORMAT(49H\settabs\+INTERFACE HEIGHT:&x&NN.N&&+&x&
     2N.NN&&kW&)
      WRITE(2,370)
370   FORMAT(54Hxxxx&INTEGRATER RUN NUMBER:&&NNN.N&x&+&x&
     2N.N&&torr&\cr)
      WRITE(2,380) RUNDATE
380   FORMAT(13H\+RUN DATE:&&,A8,8H&&&&&&&&)
      WRITE(2,390) EXPNO
390   FORMAT(27HEXPERIMENT NUMBER:&&\hfill ,A2,
     210H&&&&&&&\cr)
      WRITE(2,400) RUNTIME
400   FORMAT(13H\+RUN TIME:&&,A5,8H&&&&&&&&)
      WRITE(2,410) RUNNUMBR
410   FORMAT(31HINTEGRATER RUN NUMBER:&&\hfill ,I4,
     210H&&&&&&&\cr)
      WRITE(2,420)
420   FORMAT(12H\vskip .15in)
      WRITE(2,470) BOXHITE
470   FORMAT(21H\+INTERFACE HEIGHT:&&,F5.1,10H&cm&&&&&&&)
      WRITE(2,480) PRESS
480   FORMAT(22HLAB PRESSURE:&&\hfill ,F5.1,9H&&$\pm$&&)
      WRITE(2,490) DPRESS
```

```
490   FORMAT(F3.1,10H&&torr&\cr)
      WRITE(2,500) DIAMETER
500   FORMAT(20H\+BURNER DIAMETER:&&,F4.1,10H&cm&&&&&&&)
      WRITE(2,510) TDRY
510   FORMAT(30HDRY-BULB TEMPERATURE:&&\hfill ,F4.1,9H&&
     2$\pm$&&)
      WRITE(2,520) DTDRY
520   FORMAT(F3.1,18H&&${ }^\circ$C&\cr)
      WRITE(2,530) KW,DKW
530   FORMAT(14H\+FIRE SIZE:&&,F5.1,9H&&$\pm$&&,F4.2,
     26H&&kW&&)
      WRITE(2,540) TWET
540   FORMAT(30HWET-BULB TEMPERATURE:&&\hfill ,F4.1,9H&&
     2$\pm$&&)
      WRITE(2,550) DTWET
550   FORMAT(F3.1,18H&&${ }^\circ$C&\cr)
      WRITE(2,560)
560   FORMAT(11H\vskip .2in,/,9H\noindent)
      WRITE(2,570)
570   FORMAT(36H$\underline{\rm SUPPLY\ FLOWRATES:}$)
      WRITE(2,580)
580   FORMAT(11H\vskip .1in)
      WRITE(2,590)
590   FORMAT(50H\settabs\+AIR ADDED TO UPPER LAYER:&x&
     2NN.NNNN&x&+&)
      WRITE(2,600)
600   FORMAT(19Hx&N.NNNN&&g/sec&\cr)
      WRITE(2,620) MDOTF
620   FORMAT(28H\+NATURAL GAS FUEL:&&\hfill ,F7.4,
     29H&&$\pm$&&)
      WRITE(2,630) DMDOTF
630   FORMAT(F6.4,11H&&g/sec&\cr)
      WRITE(2,650) ENTRAIN
650   FORMAT(34H\+AIR ENTRAINED BY PLUME:&&\hfill ,F8.4,
     29H&&$\pm$&&)
      WRITE(2,660) DENTRAIN
660   FORMAT(F6.4,11H&&g/sec&\cr)
      WRITE(2,680) AIRMATCH
680   FORMAT(36H\+AIR ADDED TO UPPER LAYER:&&\hfill ,F8.4,
     29H&&$\pm$&&)
      WRITE(2,690) DAIMATCH
690   FORMAT(F6.4,11H&&g/sec&\cr)
      WRITE(2,740)
740   FORMAT(12H\vskip .05in)
      TOTAL=MDOTF+ENTRAIN+AIRMATCH
      DTOTAL=DMDOTF+DENTRAIN+DAIMATCH
      WRITE(2,750) TOTAL,DTOTAL
750   FORMAT(17H\+TOTAL:&&\hfill ,F8.4,9H&&$\pm$&&,F6.4,
     211H&&g/sec&\cr)
      WRITE(2,780)
780   FORMAT(12H\vskip .15in)
      WRITE(2,790)
      PI=ACOS(-1.)
```

```
      RE=(MDOTF/(DIAMETER*VISCM))*4.*1000000/PI
      TBED=673.15
      TINF=TDRY+273.15
      RI=(28.9*TBED/(MOLWTM*TINF))*(TINF/TBED)**2*
     2(PI**2/16.)*32.*(10./12.)**5/(QNG**2)
790   FORMAT(37H\settabs\+Is&=&&N.NNNN&x&+&x&N.NNNN&&)
      WRITE(2,810)
810   FORMAT(55Hmoles Air/mole Fuel&xxxx&FUEL INLET
     2RICHARDSON NUMBER:&)
      WRITE(2,815)
815   FORMAT(11Hx&N.NNN&\cr)
      WRITE(2,820) I,DI
820   FORMAT(14H\+I&=&&\hfill ,F8.4,9H&&$\pm$&&,F6.4,2H&&)
      WRITE(2,830)
830   FORMAT(50Hmoles Air/mole Fuel&&FUEL INLET REYNOLDS
     2NUMBER:&&)
      WRITE(2,840) RE
840   FORMAT(7H\hfill ,F6.1,4H&\cr)
      WRITE(2,850) IS,DIS
850   FORMAT(24H\+${\rm I_s}$&=&&\hfill ,F8.4,9H&&$\pm$&&,
     2F6.4,2H&&)
      WRITE(2,860)
860   FORMAT(52Hmoles Air/mole Fuel&&FUEL INLET RICHARDSON
     2NUMBER:&&)
      WRITE(2,870) RI
870   FORMAT(7H\hfill ,f6.4,4H&\cr)
      WRITE(2,985)
985   FORMAT(12H\vskip .15in)
      WRITE(2,990)
990   FORMAT(48H\settabs\+CARBON DIOXIDE&xx&N.NNNN&x&+&x&
     2N.NNNN&)
      WRITE(2,995)
995   FORMAT(54H\hskip .75in&CARBON DIOXIDE&xx&N.NNNN&x&+
     2&x&N.NNNN&\cr)
      WRITE(2,1000)
1000  FORMAT(40H\+$\underline{\rm FUEL\ COMPOSITION:}$\ )
      WRITE(2,1002)
1002  FORMAT(45H(mole fractions)&&&&&&&&$\underline
     2{\rm AIR\ )
      WRITE(2,1004)
1004  FORMAT(42HCOMPOSITION:}$\ (mole fractions)&&&&&&&\cr)
      WRITE(2,1006)
1006  FORMAT(11H\vskip .1in)
      WRITE(2,1010) A(1),DA(1)
1010  FORMAT(18H\+METHANE&&\hfill ,F6.4,9H&&$\pm$&&,F6.4)
      WRITE(2,1015) B(1),DB(1)
1015  FORMAT(17H&&OXYGEN&&\hfill ,F6.4,9H&&$\pm$&&,F6.4,
     24H&\cr)
      WRITE(2,1020) A(2),DA(2)
1020  FORMAT(17H\+ETHANE&&\hfill ,F6.4,9H&&$\pm$&&,F6.4)
      WRITE(2,1025) B(2),DB(2)
1025  FORMAT(19H&&NITROGEN&&\hfill ,F6.4,9H&&$\pm$&&,F6.4,
     24H&\cr)
```

```
      WRITE(2,1030) A(3),DA(3)
1030  FORMAT(18H\+PROPANE&&\hfill ,F6.4,9H&&$\pm$&&,F6.4)
      WRITE(2,1035) B(3),DB(3)
1035  FORMAT(22H&&WATER VAPOR&&\hfill ,F6.4,9H&&$\pm$&&,
     2F6.4,4H&\cr)
      WRITE(2,1040) A(4),DA(4)
1040  FORMAT(19H\+NITROGEN&&\hfill ,F6.4,9H&&$\pm$&&,F6.4)
      WRITE(2,1045) B(4),DB(4)
1045  FORMAT(25H&&CARBON DIOXIDE&&\hfill ,F6.4,9H&&$\pm$&&,
     2F6.4,4H&\cr)
      WRITE(2,1050) A(5),DA(5)
1050  FORMAT(25H\+CARBON DIOXIDE&&\hfill ,F6.4,9H&&$\pm$&&,
     2F6.4)
      WRITE(2,1055) B(5),DB(5)
1055  FORMAT(16H&&ARGON&&\hfill ,F6.4,9H&&$\pm$&&,F6.4,
     24H&\cr)
      WRITE(2,1056)
1056  FORMAT(12H\vskip .15in)
      DENSITYF=(PRESS+100.*FUELFLOW)*MOLWTM*.016035/
     2(TDRY+273.15)
      VALUELH=LHEATM*1.055*35.31467/DENSITYF
      VALUELHM=VALUELH/1000.
      WRITE(2,1060)
1060  FORMAT(45H\settabs\+FUEL LOWER HEATING VALUE:&x&
     2NNN.NN&)
      WRITE(2,1065)
1065  FORMAT(13Hx&MJ/mole&\cr)
      WRITE(2,1070) VISCM
1070  FORMAT(26H\+FUEL VISCOSITY:&&\hfill ,F6.2,16H&&$\mu$
     2Poise&\cr)
      WRITE(2,1080) MOLWTM
1080  FORMAT(33H\+FUEL MOLECULAR WEIGHT:&&\hfill ,F6.2,
     212H&&g/mole&\cr)
      WRITE(2,1090) VALUELHM
1090  FORMAT(36H\+FUEL LOWER HEATING VALUE:&&\hfill ,F6.2,
     27H&&MJ/kg)
      WRITE(2,1095)
1095  FORMAT(4H&\cr,/,12H\vskip .15in)
      WRITE(2,1100)
1100  FORMAT(50H\settabs\+CARBON MONOXIDE&xx&N.NNNN&x&+&x&
     2N.NNNNN&)
      WRITE(2,1105)
1105  FORMAT(43H\hskip .75in&N.NNNN&\hskip .85in&
     2N.NNNN&\cr)
      WRITE(2,1110)
1110  FORMAT(48H\+$\underline{\rm PRODUCT\ LAYER\
     2ANALYSIS:}$\cr)
      WRITE(2,1120)
1120  FORMAT(44H\+&&&&&&&&&\hskip .55in mass fraction
     2of&\cr)
      WRITE(2,1130)
1130  FORMAT(49H\+&&\hskip .32in mole fractions \hskip
     2.74in mass)
```

```
      WRITE(2,1135)
1135  FORMAT(49Hfractions \hskip .22in plume equivalent
     2source\cr)
      WRITE(2,1136)
1136  FORMAT(12H\vskip .05in)
      WRITE(2,1140) YM(1),DYM(1)
1140  FORMAT(19H\+HYDROGEN&&\hfill ,F6.4,9H&&$\pm$&&,F7.5)
      WRITE(2,1145) XM(1),XS(1)
1145  FORMAT(2H&&,F6.4,2H&&,F6.4,4H&\cr)
      WRITE(2,1150) YM(2),DYM(2)
1150  FORMAT(17H\+OXYGEN&&\hfill ,F6.4,9H&&$\pm$&&,F7.5)
      WRITE(2,1145) XM(2),XS(2)
      WRITE(2,1160) YM(3),DYM(3)
1160  FORMAT(19H\+NITROGEN&&\hfill ,F6.4,9H&&$\pm$&&,F7.5)
      WRITE(2,1145) XM(3),XS(3)
      WRITE(2,1170) YM(4),DYM(4)
1170  FORMAT(18H\+METHANE&&\hfill ,F6.4,9H&&$\pm$&&,F7.5)
      WRITE(2,1145) XM(4),XS(4)
      WRITE(2,1180) YM(5),DYM(5)
1180  FORMAT(26H\+CARBON MONOXIDE&&\hfill ,F6.4,9H&&
     2$\pm$&&,F7.5)
      WRITE(2,1145) XM(5),XS(5)
      WRITE(2,1190) YM(6),DYM(6)
1190  FORMAT(25H\+CARBON DIOXIDE&&\hfill ,F6.4,9H&&$\pm$&&,
     2F7.5)
      WRITE(2,1145) XM(6),XS(6)
      WRITE(2,1200) YM(7),DYM(7)
1200  FORMAT(22H\+WATER VAPOR&&\hfill ,F6.4,9H&&$\pm$&&,
     2F7.5)
      WRITE(2,1145) XM(7),XS(7)
      WRITE(2,1210) YM(8),DYM(8)
1210  FORMAT(27H\+SOOT (C${ }_8$H)&&\hfill ,F6.4,9H&&
     2$\pm$&&,F7.5)
      WRITE(2,1145) XM(8),XS(8)
      WRITE(2,1220) YM(9),DYM(9)
1220  FORMAT(20H\+ACETYLENE&&\hfill ,F6.4,9H&&$\pm$&&,F7.5)
      WRITE(2,1145) XM(9),XS(9)
      WRITE(2,1230) YM(10),DYM(10)
1230  FORMAT(19H\+ETHYLENE&&\hfill ,F6.4,9H&&$\pm$&&,F7.5)
      WRITE(2,1145) XM(10),XS(10)
      WRITE(2,1240) YM(11),DYM(11)
1240  FORMAT(17H\+ETHANE&&\hfill ,F6.4,9H&&$\pm$&&,F7.5)
      WRITE(2,1145) XM(11),XS(11)
      WRITE(2,1250) YM(12),DYM(12)
1250  FORMAT(16H\+ARGON&&\hfill ,F6.4,9H&&$\pm$&&,F7.5)
      WRITE(2,1145) XM(12),XS(12)
      WRITE(2,1255)
1255  FORMAT(12H\vskip .15in)
      FS=MOLWTM/(28.9*IS)
      WRITE(2,1260)
1260  FORMAT(55H\settabs\+PLUME EQUIVALENCE RATIO AT
     2INTERFACE HEIGHT:&)
      WRITE(2,1265)
```

```
1265 FORMAT(23Hxx&N.NN&&+&x&N.NNNN&\cr)
     WRITE(2,1270) ULAYERPH
1270 FORMAT(34H\+UPPER LAYER EQUIVALENCE RATIO:&&,F5.3,
    29H&&$\pm$&&)
     WRITE(2,1275) DPHIL
1275 FORMAT(F6.4,4H&\cr)
     WRITE(2,1280) PLUMEPHI
1280 FORMAT(48H\+PLUME EQUIVALENCE RATIO AT INTERFACE
    2HEIGHT:&&,F5.3)
     WRITE(2,1285) DPHIP
1285 FORMAT(9H&&$\pm$&&,F6.4,4H&\cr)
     WRITE(2,1290) FS
1290 FORMAT(39H\+STOICHIOMETRIC FUEL/AIR MASS RATIO:&&,
    2F6.4,4H&\cr)
     WRITE(2,1295) CTSAMPLE
1295 FORMAT(23H\+SAMPLE TEMPERATURE:&&,F5.1,
        218H\ ${ }^\circ$C&\cr)
     WRITE(2,1300) CTHOOD
1300 FORMAT(21H\+HOOD TEMPERATURE:&&,F5.1,
    218H\ ${ }^\circ$C&\cr)
     WRITE(2,1310)
1310 FORMAT(12H\vskip .15in)
     WRITE(2,1315)
1315 FORMAT(55H\settabs\+HEAT OF FORMATION PER MOLE OF
    2STOICHIOMETRIC )
     WRITE(2,1316)
1316 FORMAT(36HPRODUCTS:&xx&NNN.NNN&x&kcal/mole&\cr)
     WRITE(2,1320) HEATF
1320 FORMAT(46H\+HEAT OF FORMATION PER MOLE OF FUEL:&&
    2\hfill ,F7.3)
     WRITE(2,1325)
1325 FORMAT(15H&&kcal/mole&\cr)
     WRITE(2,1330) HEATA
1330 FORMAT(45H\+HEAT OF FORMATION PER MOLE OF AIR:&&
       2\hfill ,F7.3)
     WRITE(2,1325)
     WRITE(2,1340) HEATP
1340 FORMAT(50H\+HEAT OF FORMATION PER MOLE OF PRODUCTS:&&
    2\hfill ,F7.3)
     WRITE(2,1325)
     WRITE(2,1350)
1350 FORMAT(55H\+HEAT OF FORMATION PER MOLE OF
    2STOICHIOMETRIC PRODUCTS)
     WRITE(2,1355) HEATSP
1355 FORMAT(10H:&&\hfill ,F7.3)
     WRITE(2,1325)
     WRITE(2,1360)
1360 FORMAT(52H\settabs\+(ACTUAL/STOICHIOMETRIC) HEAT OF
    2REACTION:&)
     WRITE(2,1365)
1365 FORMAT(34Hx&NNNN.NNN&x&kcal/mole of fuel&\cr)
     WRITE(2,1370) HRXNA
1370 FORMAT(35H\+ACTUAL HEAT OF REACTION:&&\hfill ,F8.3)
```

```
      WRITE(2,1375)
1375  FORMAT(23H&&kcal/mole of fuel&\cr)
      WRITE(2,1380) HRXNS
1380  FORMAT(42H\+HEAT OF STOICHIOMETRIC REACTION:&&
     2\hfill ,F8.3)
      WRITE(2,1375)
      WRITE(2,1390)
1390  FORMAT(44H\+(ACTUAL/STOICHIOMETRIC) HEAT OF REACTION:
     2&)
      WRITE(2,1395) RATIO
1395  FORMAT(8H&\hfill ,F5.3,4H&\cr)
      WRITE(2,1400)
1400  FORMAT(37H\+(ACTUAL/MAXIMUM) HEAT OF REACTION:&)
      WRITE(2,1395) RATIOAM
      WRITE(2,1410)
1410  FORMAT(16H\vfill\eject\end)
      STOP
      END
```

Appendix B

Data Reduction Program Output Sheets

Included here are the report sheets for the eight series of experiments discussed in Chapter 4. Information on 64 separate tests are reported here, all performed using a 19 cm diameter burner with natural gas fuel. The order of the series are organized as follows:

1) $\dot{Q} = 67$ kW, $Z_i = 10$ cm
2) $\dot{Q} = 57$ kW, $Z_i = 10$ cm
3) $\dot{Q} = 49$ kW, $Z_i = 10$ cm
4) $\dot{Q} = 41$ kW, $Z_i = 10$ cm
5) $\dot{Q} = 67$ kW, $Z_i = 23$ cm
6) $\dot{Q} = 41$ kW, $Z_i = 23$ cm
7) $\dot{Q} = 67$ kW, $Z_i = 5$ cm
8) $\dot{Q} = 41$ kW, $Z_i = 5$ cm

In an effort to characterize the fuel flow and its initial buoyancy, approximations are made for the Reynolds number (Re) and Richardson number (Ri) assuming the temperature of the fuel exiting the burner is constant at 673 K. Throughout the calculations, a side-by-side uncertainty analysis is carried along with the calculations. This procedure follows the approach of Beers (1957).

DATA REDUCTION PROGRAM OUTPUT

RUN DATE:	03-22-88	EXPERIMENT NUMBER:	01
RUN TIME:	17:20	INTEGRATER RUN NUMBER:	191
INTERFACE HEIGHT:	10.0 cm	LAB PRESSURE:	742.0 ± 0.5 torr
BURNER DIAMETER:	19.0 cm	DRY-BULB TEMPERATURE:	23.4 ± 0.2 °C
FIRE SIZE:	67.7 ± 1.65 kW	WET-BULB TEMPERATURE:	15.8 ± 0.2 °C

SUPPLY FLOWRATES :

NATURAL GAS FUEL:	1.3581 ± 0.0332	g/sec
AIR ENTRAINED BY PLUME:	10.2972 ± 0.2696	g/sec
AIR ADDED TO UPPER LAYER:	0.0000 ± 0.0000	g/sec
TOTAL:	11.6553 ± 0.3028	g/sec

I =	4.5020 ± 0.0421 moles Air/mole Fuel	FUEL INLET REYNOLDS NUMBER:	830.7
I_s =	9.7705 ± 0.1374 moles Air/mole Fuel	FUEL INLET RICHARDSON NUMBER:	0.3414

FUEL COMPOSITION : (mole fractions)

METHANE	0.9382 ± 0.0100
ETHANE	0.0298 ± 0.0050
PROPANE	0.0079 ± 0.0020
NITROGEN	0.0162 ± 0.0020
CARBON DIOXIDE	0.0079 ± 0.0020

AIR COMPOSITION : (mole fractions)

OXYGEN	0.2068 ± 0.0010
NITROGEN	0.7707 ± 0.0020
WATER VAPOR	0.0130 ± 0.0004
CARBON DIOXIDE	0.0003 ± 0.0001
ARGON	0.0092 ± 0.0006

FUEL VISCOSITY:	109.56 μPoise
FUEL MOLECULAR WEIGHT:	17.16 g/mole
FUEL LOWER HEATING VALUE:	50.16 MJ/kg

PRODUCT LAYER ANALYSIS :

	mole fractions	mass fractions	mass fraction of plume equivalent source
HYDROGEN	0.0195 ± 0.00090	0.0015	0.0015
OXYGEN	0.0143 ± 0.00070	0.0174	0.0174
NITROGEN	0.6168 ± 0.00570	0.6635	0.6635
METHANE	0.0905 ± 0.00490	0.0554	0.0554
CARBON MONOXIDE	0.0148 ± 0.00040	0.0159	0.0159
CARBON DIOXIDE	0.0675 ± 0.00100	0.1134	0.1134
WATER VAPOR	0.1676 ± 0.00520	0.1152	0.1152
SOOT (C_8H)	0.0006 ± 0.00590	0.0022	0.0022
ACETYLENE	0.0017 ± 0.00000	0.0017	0.0017
ETHYLENE	0.0000 ± 0.00000	0.0000	0.0000
ETHANE	0.0014 ± 0.00000	0.0016	0.0016
ARGON	0.0074 ± 0.00050	0.0112	0.0112

UPPER LAYER EQUIVALENCE RATIO:	2.170 ± 0.0367
PLUME EQUIVALENCE RATIO AT INTERFACE HEIGHT:	2.170 ± 0.0835
STOICHIOMETRIC FUEL/AIR MASS RATIO:	0.0608
SAMPLE TEMPERATURE:	256.7 °C
HOOD TEMPERATURE:	208.3 °C

HEAT OF FORMATION PER MOLE OF FUEL:		-17.351 kcal/mole
HEAT OF FORMATION PER MOLE OF AIR:		-0.782 kcal/mole
HEAT OF FORMATION PER MOLE OF PRODUCTS:		-17.950 kcal/mole
HEAT OF FORMATION PER MOLE OF STOICHIOMETRIC PRODUCTS :		-20.374 kcal/mole
ACTUAL HEAT OF REACTION:	-79.715 kcal/mole of fuel	
HEAT OF STOICHIOMETRIC REACTION:	-194.914 kcal/mole of fuel	
(ACTUAL/STOICHIOMETRIC) HEAT OF REACTION:	0.409	
(ACTUAL/MAXIMUM) HEAT OF REACTION:	0.888	

DATA REDUCTION PROGRAM OUTPUT

RUN DATE:	03-22-88	EXPERIMENT NUMBER:	02
RUN TIME:	17:47	INTEGRATER RUN NUMBER:	192
INTERFACE HEIGHT:	10.0 cm	LAB PRESSURE:	742.0 ± 0.5 torr
BURNER DIAMETER:	19.0 cm	DRY-BULB TEMPERATURE:	23.4 ± 0.2 °C
FIRE SIZE:	67.7 ± 1.65 kW	WET-BULB TEMPERATURE:	15.8 ± 0.2 °C

SUPPLY FLOWRATES :

NATURAL GAS FUEL:	1.3581 ± 0.0332	g/sec
AIR ENTRAINED BY PLUME:	10.2970 ± 0.2696	g/sec
AIR ADDED TO UPPER LAYER:	1.9073 ± 0.4128	g/sec
TOTAL:	13.5624 ± 0.7156	g/sec

I =	5.3358 ± 0.0407 moles Air/mole Fuel	FUEL INLET REYNOLDS NUMBER:	830.7
I_s =	9.7705 ± 0.1374 moles Air/mole Fuel	FUEL INLET RICHARDSON NUMBER:	0.3414

FUEL COMPOSITION : (mole fractions)

METHANE	0.9382 ± 0.0100
ETHANE	0.0298 ± 0.0050
PROPANE	0.0079 ± 0.0020
NITROGEN	0.0162 ± 0.0020
CARBON DIOXIDE	0.0079 ± 0.0020

AIR COMPOSITION : (mole fractions)

OXYGEN	0.2068 ± 0.0010
NITROGEN	0.7707 ± 0.0020
WATER VAPOR	0.0130 ± 0.0004
CARBON DIOXIDE	0.0003 ± 0.0001
ARGON	0.0092 ± 0.0006

FUEL VISCOSITY:	109.56 μPoise
FUEL MOLECULAR WEIGHT:	17.16 g/mole
FUEL LOWER HEATING VALUE:	50.16 MJ/kg

PRODUCT LAYER ANALYSIS :

	mole fractions	mass fractions	mass fraction of plume equivalent source
HYDROGEN	0.0193 ± 0.00140	0.0015	0.0017
OXYGEN	0.0249 ± 0.00090	0.0302	-.0024
NITROGEN	0.6380 ± 0.00480	0.6768	0.6650
METHANE	0.0671 ± 0.00360	0.0407	0.0474
CARBON MONOXIDE	0.0135 ± 0.00030	0.0143	0.0167
CARBON DIOXIDE	0.0650 ± 0.00090	0.1084	0.1260
WATER VAPOR	0.1613 ± 0.00470	0.1100	0.1267
SOOT (C_8H)	0.0012 ± 0.00450	0.0042	0.0049
ACETYLENE	0.0013 ± 0.00000	0.0013	0.0015
ETHYLENE	0.0000 ± 0.00000	0.0000	0.0000
ETHANE	0.0010 ± 0.00000	0.0011	0.0013
ARGON	0.0076 ± 0.00050	0.0114	0.0112

UPPER LAYER EQUIVALENCE RATIO:	1.831 ± 0.0293
PLUME EQUIVALENCE RATIO AT INTERFACE HEIGHT:	2.170 ± 0.0835
STOICHIOMETRIC FUEL/AIR MASS RATIO:	0.0608
SAMPLE TEMPERATURE:	270.0 °C
HOOD TEMPERATURE:	219.4 °C

HEAT OF FORMATION PER MOLE OF FUEL:		-17.351 kcal/mole
HEAT OF FORMATION PER MOLE OF AIR:		-0.782 kcal/mole
HEAT OF FORMATION PER MOLE OF PRODUCTS:		-16.920 kcal/mole
HEAT OF FORMATION PER MOLE OF STOICHIOMETRIC PRODUCTS :		-20.374 kcal/mole
ACTUAL HEAT OF REACTION:	-87.969 kcal/mole of fuel	
HEAT OF STOICHIOMETRIC REACTION:	-194.914 kcal/mole of fuel	
(ACTUAL/STOICHIOMETRIC) HEAT OF REACTION:	0.451	
(ACTUAL/MAXIMUM) HEAT OF REACTION:	0.826	

DATA REDUCTION PROGRAM OUTPUT

RUN DATE:	03-22-88	EXPERIMENT NUMBER:	03
RUN TIME:	18:31	INTEGRATER RUN NUMBER:	194
INTERFACE HEIGHT:	10.0 cm	LAB PRESSURE:	742.0 ± 0.5 torr
BURNER DIAMETER:	19.0 cm	DRY-BULB TEMPERATURE:	23.4 ± 0.2 °C
FIRE SIZE:	67.7 ± 1.65 kW	WET-BULB TEMPERATURE:	15.8 ± 0.2 °C

SUPPLY FLOWRATES :

NATURAL GAS FUEL:	1.3581 ± 0.0332	g/sec
AIR ENTRAINED BY PLUME:	10.2970 ± 0.2696	g/sec
AIR ADDED TO UPPER LAYER:	4.1602 ± 0.4560	g/sec
TOTAL:	15.8153 ± 0.7588	g/sec

I = 6.3208 ± 0.0444 moles Air/mole Fuel
I_s = 9.7705 ± 0.1374 moles Air/mole Fuel

FUEL INLET REYNOLDS NUMBER: 830.7
FUEL INLET RICHARDSON NUMBER: 0.3414

FUEL COMPOSITION : (mole fractions)		AIR COMPOSITION : (mole fractions)	
METHANE	0.9382 ± 0.0100	OXYGEN	0.2068 ± 0.0010
ETHANE	0.0298 ± 0.0050	NITROGEN	0.7707 ± 0.0020
PROPANE	0.0079 ± 0.0020	WATER VAPOR	0.0130 ± 0.0004
NITROGEN	0.0162 ± 0.0020	CARBON DIOXIDE	0.0003 ± 0.0001
CARBON DIOXIDE	0.0079 ± 0.0020	ARGON	0.0092 ± 0.0006

FUEL VISCOSITY:	109.56 μPoise
FUEL MOLECULAR WEIGHT:	17.16 g/mole
FUEL LOWER HEATING VALUE:	50.16 MJ/kg

PRODUCT LAYER ANALYSIS :

	mole fractions	mass fractions	mass fraction of plume equivalent source
HYDROGEN	0.0092 ± 0.00070	0.0007	0.0009
OXYGEN	0.0321 ± 0.00100	0.0383	-.0300
NITROGEN	0.6580 ± 0.00450	0.6871	0.6650
METHANE	0.0543 ± 0.00290	0.0325	0.0441
CARBON MONOXIDE	0.0131 ± 0.00030	0.0136	0.0185
CARBON DIOXIDE	0.0651 ± 0.00080	0.1068	0.1448
WATER VAPOR	0.1582 ± 0.00470	0.1062	0.1412
SOOT (C_8H)	0.0003 ± 0.00380	0.0011	0.0015
ACETYLENE	0.0010 ± 0.00000	0.0010	0.0013
ETHYLENE	0.0000 ± 0.00000	0.0000	0.0000
ETHANE	0.0009 ± 0.00000	0.0010	0.0014
ARGON	0.0078 ± 0.00050	0.0116	0.0112

UPPER LAYER EQUIVALENCE RATIO:	1.546 ± 0.0243
PLUME EQUIVALENCE RATIO AT INTERFACE HEIGHT:	2.170 ± 0.0835
STOICHIOMETRIC FUEL/AIR MASS RATIO:	0.0608
SAMPLE TEMPERATURE:	277.2 °C
HOOD TEMPERATURE:	232.8 °C

HEAT OF FORMATION PER MOLE OF FUEL:	-17.351	kcal/mole
HEAT OF FORMATION PER MOLE OF AIR:	-0.782	kcal/mole
HEAT OF FORMATION PER MOLE OF PRODUCTS:	-16.528	kcal/mole
HEAT OF FORMATION PER MOLE OF STOICHIOMETRIC PRODUCTS :	-20.374	kcal/mole
ACTUAL HEAT OF REACTION:	-100.479	kcal/mole of fuel
HEAT OF STOICHIOMETRIC REACTION:	-194.914	kcal/mole of fuel
(ACTUAL/STOICHIOMETRIC) HEAT OF REACTION:	0.516	
(ACTUAL/MAXIMUM) HEAT OF REACTION:	0.797	

DATA REDUCTION PROGRAM OUTPUT

RUN DATE:	04-30-88	EXPERIMENT NUMBER:	04
RUN TIME:	14:25	INTEGRATER RUN NUMBER:	308
INTERFACE HEIGHT:	10.0 cm	LAB PRESSURE:	740.7 ± 0.5 torr
BURNER DIAMETER:	19.0 cm	DRY-BULB TEMPERATURE:	23.1 ± 0.2 °C
FIRE SIZE:	67.8 ± 1.65 kW	WET-BULB TEMPERATURE:	14.8 ± 0.2 °C

SUPPLY FLOWRATES :

NATURAL GAS FUEL:	1.3573 ± 0.0332	g/sec
AIR ENTRAINED BY PLUME:	10.2854 ± 0.2685	g/sec
AIR ADDED TO UPPER LAYER:	0.0000 ± 0.0000	g/sec
TOTAL:	11.6427 ± 0.3017	g/sec

I =	4.4960 ± 0.0411 moles Air/mole Fuel	FUEL INLET REYNOLDS NUMBER:	830.3
I_s =	9.7599 ± 0.1372 moles Air/mole Fuel	FUEL INLET RICHARDSON NUMBER:	0.3409

FUEL COMPOSITION : (mole fractions)		AIR COMPOSITION : (mole fractions)	
METHANE	0.9380 ± 0.0100	OXYGEN	0.2071 ± 0.0010
ETHANE	0.0302 ± 0.0050	NITROGEN	0.7719 ± 0.0020
PROPANE	0.0079 ± 0.0020	WATER VAPOR	0.0115 ± 0.0004
NITROGEN	0.0168 ± 0.0020	CARBON DIOXIDE	0.0003 ± 0.0001
CARBON DIOXIDE	0.0071 ± 0.0020	ARGON	0.0092 ± 0.0006

FUEL VISCOSITY:	109.54	μPoise
FUEL MOLECULAR WEIGHT:	17.15	g/mole
FUEL LOWER HEATING VALUE:	50.26	MJ/kg

PRODUCT LAYER ANALYSIS :

	mole fractions	mass fractions	mass fraction of plume equivalent source
HYDROGEN	0.0183 ± 0.00140	0.0014	0.0014
OXYGEN	0.0137 ± 0.00070	0.0168	0.0168
NITROGEN	0.6205 ± 0.00560	0.6657	0.6657
METHANE	0.0881 ± 0.00480	0.0541	0.0541
CARBON MONOXIDE	0.0159 ± 0.00040	0.0171	0.0171
CARBON DIOXIDE	0.0680 ± 0.00100	0.1146	0.1146
WATER VAPOR	0.1643 ± 0.00510	0.1133	0.1133
SOOT (C_8H)	0.0006 ± 0.00580	0.0022	0.0022
ACETYLENE	0.0021 ± 0.00010	0.0021	0.0021
ETHYLENE	0.0000 ± 0.00000	0.0000	0.0000
ETHANE	0.0012 ± 0.00000	0.0014	0.0014
ARGON	0.0074 ± 0.00050	0.0113	0.0113

UPPER LAYER EQUIVALENCE RATIO:	2.171 ± 0.0364
PLUME EQUIVALENCE RATIO AT INTERFACE HEIGHT:	2.171 ± 0.0834
STOICHIOMETRIC FUEL/AIR MASS RATIO:	0.0608
SAMPLE TEMPERATURE:	261.7 °C
HOOD TEMPERATURE:	199.4 °C

HEAT OF FORMATION PER MOLE OF FUEL:	-17.267	kcal/mole
HEAT OF FORMATION PER MOLE OF AIR:	-0.692	kcal/mole
HEAT OF FORMATION PER MOLE OF PRODUCTS:	-17.771	kcal/mole
HEAT OF FORMATION PER MOLE OF STOICHIOMETRIC PRODUCTS :	-20.314	kcal/mole
ACTUAL HEAT OF REACTION:	-79.501	kcal/mole of fuel
HEAT OF STOICHIOMETRIC REACTION:	-195.025	kcal/mole of fuel
(ACTUAL/STOICHIOMETRIC) HEAT OF REACTION:	0.408	
(ACTUAL/MAXIMUM) HEAT OF REACTION:	0.885	

DATA REDUCTION PROGRAM OUTPUT

RUN DATE:	04-30-88	EXPERIMENT NUMBER:	05
RUN TIME:	14:44	INTEGRATER RUN NUMBER:	309
INTERFACE HEIGHT:	10.0 cm	LAB PRESSURE:	740.7 ± 0.5 torr
BURNER DIAMETER:	19.0 cm	DRY-BULB TEMPERATURE:	23.1 ± 0.2 °C
FIRE SIZE:	67.8 ± 1.65 kW	WET-BULB TEMPERATURE:	14.8 ± 0.2 °C

SUPPLY FLOWRATES :

NATURAL GAS FUEL:	1.3573 ± 0.0332	g/sec
AIR ENTRAINED BY PLUME:	10.2850 ± 0.2685	g/sec
AIR ADDED TO UPPER LAYER:	0.6521 ± 0.3904	g/sec
TOTAL:	12.2944 ± 0.6921	g/sec

I = 4.7809 ± 0.0410 moles Air/mole Fuel
I_s = 9.7599 ± 0.1372 moles Air/mole Fuel

FUEL INLET REYNOLDS NUMBER: 830.3
FUEL INLET RICHARDSON NUMBER: 0.3409

FUEL COMPOSITION : (mole fractions)		AIR COMPOSITION : (mole fractions)	
METHANE	0.9380 ± 0.0100	OXYGEN	0.2071 ± 0.0010
ETHANE	0.0302 ± 0.0050	NITROGEN	0.7719 ± 0.0020
PROPANE	0.0079 ± 0.0020	WATER VAPOR	0.0115 ± 0.0004
NITROGEN	0.0168 ± 0.0020	CARBON DIOXIDE	0.0003 ± 0.0001
CARBON DIOXIDE	0.0071 ± 0.0020	ARGON	0.0092 ± 0.0006

FUEL VISCOSITY:	109.54 μPoise
FUEL MOLECULAR WEIGHT:	17.15 g/mole
FUEL LOWER HEATING VALUE:	50.26 MJ/kg

PRODUCT LAYER ANALYSIS :

	mole fractions	mass fractions	mass fraction of plume equivalent source
HYDROGEN	0.0170 ± 0.00130	0.0013	0.0014
OXYGEN	0.0172 ± 0.00080	0.0210	0.0093
NITROGEN	0.6280 ± 0.00540	0.6702	0.6657
METHANE	0.0811 ± 0.00440	0.0496	0.0523
CARBON MONOXIDE	0.0154 ± 0.00040	0.0164	0.0173
CARBON DIOXIDE	0.0673 ± 0.00090	0.1128	0.1191
WATER VAPOR	0.1633 ± 0.00490	0.1121	0.1179
SOOT (C_8H)	0.0007 ± 0.00530	0.0025	0.0027
ACETYLENE	0.0016 ± 0.00000	0.0016	0.0017
ETHYLENE	0.0000 ± 0.00000	0.0000	0.0000
ETHANE	0.0011 ± 0.00000	0.0013	0.0014
ARGON	0.0074 ± 0.00050	0.0113	0.0113

UPPER LAYER EQUIVALENCE RATIO:	2.041 ± 0.0336
PLUME EQUIVALENCE RATIO AT INTERFACE HEIGHT:	2.171 ± 0.0834
STOICHIOMETRIC FUEL/AIR MASS RATIO:	0.0608
SAMPLE TEMPERATURE:	265.6 °C
HOOD TEMPERATURE:	202.8 °C

HEAT OF FORMATION PER MOLE OF FUEL:	-17.267	kcal/mole
HEAT OF FORMATION PER MOLE OF AIR:	-0.692	kcal/mole
HEAT OF FORMATION PER MOLE OF PRODUCTS:	-17.533	kcal/mole
HEAT OF FORMATION PER MOLE OF STOICHIOMETRIC PRODUCTS :	-20.314	kcal/mole
ACTUAL HEAT OF REACTION:	-82.938	kcal/mole of fuel
HEAT OF STOICHIOMETRIC REACTION:	-195.025	kcal/mole of fuel
(ACTUAL/STOICHIOMETRIC) HEAT OF REACTION:	0.425	
(ACTUAL/MAXIMUM) HEAT OF REACTION:	0.868	

DATA REDUCTION PROGRAM OUTPUT

RUN DATE:	04-30-88	EXPERIMENT NUMBER:	06
RUN TIME:	15:02	INTEGRATER RUN NUMBER:	310
INTERFACE HEIGHT:	10.0 cm	LAB PRESSURE:	740.7 ± 0.5 torr
BURNER DIAMETER:	19.0 cm	DRY-BULB TEMPERATURE:	23.1 ± 0.2 °C
FIRE SIZE:	67.8 ± 1.65 kW	WET-BULB TEMPERATURE:	14.8 ± 0.2 °C

SUPPLY FLOWRATES :

NATURAL GAS FUEL:	1.3573 ± 0.0332	g/sec
AIR ENTRAINED BY PLUME:	10.2850 ± 0.2685	g/sec
AIR ADDED TO UPPER LAYER:	2.2437 ± 0.4176	g/sec
TOTAL:	13.8860 ± 0.7193	g/sec

I =	5.4766 ± 0.0402 moles Air/mole Fuel	FUEL INLET REYNOLDS NUMBER:	830.3
I_s =	9.7599 ± 0.1372 moles Air/mole Fuel	FUEL INLET RICHARDSON NUMBER:	0.3409

FUEL COMPOSITION : (mole fractions)		AIR COMPOSITION : (mole fractions)	
METHANE	0.9380 ± 0.0100	OXYGEN	0.2071 ± 0.0010
ETHANE	0.0302 ± 0.0050	NITROGEN	0.7719 ± 0.0020
PROPANE	0.0079 ± 0.0020	WATER VAPOR	0.0115 ± 0.0004
NITROGEN	0.0168 ± 0.0020	CARBON DIOXIDE	0.0003 ± 0.0001
CARBON DIOXIDE	0.0071 ± 0.0020	ARGON	0.0092 ± 0.0006

FUEL VISCOSITY:	109.54 μPoise
FUEL MOLECULAR WEIGHT:	17.15 g/mole
FUEL LOWER HEATING VALUE:	50.26 MJ/kg

PRODUCT LAYER ANALYSIS :

	mole fractions	mass fractions	mass fraction of plume equivalent source
HYDROGEN	0.0166 ± 0.00120	0.0013	0.0015
OXYGEN	0.0185 ± 0.00080	0.0223	-.0176
NITROGEN	0.6424 ± 0.00470	0.6793	0.6657
METHANE	0.0634 ± 0.00340	0.0384	0.0458
CARBON MONOXIDE	0.0148 ± 0.00040	0.0157	0.0187
CARBON DIOXIDE	0.0699 ± 0.00090	0.1162	0.1385
WATER VAPOR	0.1638 ± 0.00460	0.1114	0.1315
SOOT (C_8H)	0.0003 ± 0.00440	0.0013	0.0015
ACETYLENE	0.0015 ± 0.00000	0.0015	0.0018
ETHYLENE	0.0000 ± 0.00000	0.0000	0.0000
ETHANE	0.0010 ± 0.00000	0.0011	0.0013
ARGON	0.0076 ± 0.00050	0.0115	0.0113

UPPER LAYER EQUIVALENCE RATIO:	1.782 ± 0.0283
PLUME EQUIVALENCE RATIO AT INTERFACE HEIGHT:	2.171 ± 0.0834
STOICHIOMETRIC FUEL/AIR MASS RATIO:	0.0608
SAMPLE TEMPERATURE:	268.9 °C
HOOD TEMPERATURE:	205.0 °C

HEAT OF FORMATION PER MOLE OF FUEL:	-17.267	kcal/mole
HEAT OF FORMATION PER MOLE OF AIR:	-0.692	kcal/mole
HEAT OF FORMATION PER MOLE OF PRODUCTS:	-17.487	kcal/mole
HEAT OF FORMATION PER MOLE OF STOICHIOMETRIC PRODUCTS :	-20.314	kcal/mole
ACTUAL HEAT OF REACTION:	-94.483	kcal/mole of fuel
HEAT OF STOICHIOMETRIC REACTION:	-195.025	kcal/mole of fuel
(ACTUAL/STOICHIOMETRIC) HEAT OF REACTION:	0.484	
(ACTUAL/MAXIMUM) HEAT OF REACTION:	0.863	

DATA REDUCTION PROGRAM OUTPUT

RUN DATE:	04-30-88	EXPERIMENT NUMBER:	07
RUN TIME:	15:22	INTEGRATER RUN NUMBER:	311
INTERFACE HEIGHT:	10.0 cm	LAB PRESSURE:	740.7 ± 0.5 torr
BURNER DIAMETER:	19.0 cm	DRY-BULB TEMPERATURE:	23.1 ± 0.2 °C
FIRE SIZE:	67.8 ± 1.65 kW	WET-BULB TEMPERATURE:	14.8 ± 0.2 °C

SUPPLY FLOWRATES :

NATURAL GAS FUEL:	1.3573 ± 0.0332	g/sec
AIR ENTRAINED BY PLUME:	10.2850 ± 0.2685	g/sec
AIR ADDED TO UPPER LAYER:	2.3736 ± 0.4203	g/sec
TOTAL:	14.0159 ± 0.7220	g/sec

I =	5.5334 ± 0.0409 moles Air/mole Fuel	FUEL INLET REYNOLDS NUMBER:	830.3
I_s =	9.7599 ± 0.1372 moles Air/mole Fuel	FUEL INLET RICHARDSON NUMBER:	0.3409

FUEL COMPOSITION : (mole fractions)

METHANE	0.9380 ± 0.0100
ETHANE	0.0302 ± 0.0050
PROPANE	0.0079 ± 0.0020
NITROGEN	0.0168 ± 0.0020
CARBON DIOXIDE	0.0071 ± 0.0020

AIR COMPOSITION : (mole fractions)

OXYGEN	0.2071 ± 0.0010
NITROGEN	0.7719 ± 0.0020
WATER VAPOR	0.0115 ± 0.0004
CARBON DIOXIDE	0.0003 ± 0.0001
ARGON	0.0092 ± 0.0006

FUEL VISCOSITY:	109.54 μPoise
FUEL MOLECULAR WEIGHT:	17.15 g/mole
FUEL LOWER HEATING VALUE:	50.26 MJ/kg

PRODUCT LAYER ANALYSIS :

	mole fractions	mass fractions	mass fraction of plume equivalent source
HYDROGEN	0.0132 ± 0.00100	0.0010	0.0012
OXYGEN	0.0216 ± 0.00080	0.0261	-.0155
NITROGEN	0.6445 ± 0.00470	0.6800	0.6657
METHANE	0.0643 ± 0.00350	0.0388	0.0468
CARBON MONOXIDE	0.0143 ± 0.00040	0.0151	0.0181
CARBON DIOXIDE	0.0679 ± 0.00090	0.1126	0.1355
WATER VAPOR	0.1632 ± 0.00460	0.1107	0.1318
SOOT (C_8H)	0.0003 ± 0.00440	0.0011	0.0013
ACETYLENE	0.0022 ± 0.00010	0.0021	0.0026
ETHYLENE	0.0000 ± 0.00000	0.0000	0.0000
ETHANE	0.0009 ± 0.00000	0.0010	0.0012
ARGON	0.0076 ± 0.00050	0.0115	0.0113

UPPER LAYER EQUIVALENCE RATIO:	1.764 ± 0.0280
PLUME EQUIVALENCE RATIO AT INTERFACE HEIGHT:	2.171 ± 0.0834
STOICHIOMETRIC FUEL/AIR MASS RATIO:	0.0608
SAMPLE TEMPERATURE:	272.8 °C
HOOD TEMPERATURE:	206.1 °C

HEAT OF FORMATION PER MOLE OF FUEL:	-17.267	kcal/mole
HEAT OF FORMATION PER MOLE OF AIR:	-0.692	kcal/mole
HEAT OF FORMATION PER MOLE OF PRODUCTS:	-17.231	kcal/mole
HEAT OF FORMATION PER MOLE OF STOICHIOMETRIC PRODUCTS :	-20.314	kcal/mole
ACTUAL HEAT OF REACTION:	-93.554	kcal/mole of fuel
HEAT OF STOICHIOMETRIC REACTION:	-195.025	kcal/mole of fuel
(ACTUAL/STOICHIOMETRIC) HEAT OF REACTION:	0.480	
(ACTUAL/MAXIMUM) HEAT OF REACTION:	0.846	

DATA REDUCTION PROGRAM OUTPUT

RUN DATE:	04-30-88	EXPERIMENT NUMBER:	08
RUN TIME:	15:41	INTEGRATER RUN NUMBER:	312
INTERFACE HEIGHT:	10.0 cm	LAB PRESSURE:	740.7 ± 0.5 torr
BURNER DIAMETER:	19.0 cm	DRY-BULB TEMPERATURE:	23.1 ± 0.2 °C
FIRE SIZE:	67.8 ± 1.65 kW	WET-BULB TEMPERATURE:	14.8 ± 0.2 °C

SUPPLY FLOWRATES :

NATURAL GAS FUEL:	1.3573 ± 0.0332	g/sec
AIR ENTRAINED BY PLUME:	10.2850 ± 0.2685	g/sec
AIR ADDED TO UPPER LAYER:	4.0075 ± 0.4515	g/sec
TOTAL:	15.6498 ± 0.7532	g/sec

I =	6.2476 ± 0.0429 moles Air/mole Fuel	FUEL INLET REYNOLDS NUMBER:	830.3
I_s =	9.7599 ± 0.1372 moles Air/mole Fuel	FUEL INLET RICHARDSON NUMBER:	0.3409

FUEL COMPOSITION : (mole fractions)

METHANE	0.9380 ± 0.0100
ETHANE	0.0302 ± 0.0050
PROPANE	0.0079 ± 0.0020
NITROGEN	0.0168 ± 0.0020
CARBON DIOXIDE	0.0071 ± 0.0020

AIR COMPOSITION : (mole fractions)

OXYGEN	0.2071 ± 0.0010
NITROGEN	0.7719 ± 0.0020
WATER VAPOR	0.0115 ± 0.0004
CARBON DIOXIDE	0.0003 ± 0.0001
ARGON	0.0092 ± 0.0006

FUEL VISCOSITY:	109.54 μPoise
FUEL MOLECULAR WEIGHT:	17.15 g/mole
FUEL LOWER HEATING VALUE:	50.26 MJ/kg

PRODUCT LAYER ANALYSIS :

	mole fractions	mass fractions	mass fraction of plume equivalent source
HYDROGEN	0.0101 ± 0.00070	0.0008	0.0010
OXYGEN	0.0248 ± 0.00090	0.0296	-.0393
NITROGEN	0.6577 ± 0.00360	0.6873	0.6658
METHANE	0.0519 ± 0.00280	0.0311	0.0417
CARBON MONOXIDE	0.0145 ± 0.00040	0.0151	0.0203
CARBON DIOXIDE	0.0689 ± 0.00080	0.1131	0.1519
WATER VAPOR	0.1620 ± 0.00450	0.1089	0.1439
SOOT (C_8H)	0.0000 ± 0.00000	0.0000	0.0000
ACETYLENE	0.0016 ± 0.00000	0.0015	0.0021
ETHYLENE	0.0000 ± 0.00000	0.0000	0.0000
ETHANE	0.0008 ± 0.00000	0.0009	0.0013
ARGON	0.0078 ± 0.00050	0.0116	0.0113

UPPER LAYER EQUIVALENCE RATIO:	1.562 ± 0.0244
PLUME EQUIVALENCE RATIO AT INTERFACE HEIGHT:	2.171 ± 0.0834
STOICHIOMETRIC FUEL/AIR MASS RATIO:	0.0608
SAMPLE TEMPERATURE:	273.3 °C
HOOD TEMPERATURE:	208.9 °C

HEAT OF FORMATION PER MOLE OF FUEL:	-17.267	kcal/mole
HEAT OF FORMATION PER MOLE OF AIR:	-0.692	kcal/mole
HEAT OF FORMATION PER MOLE OF PRODUCTS:	-17.066	kcal/mole
HEAT OF FORMATION PER MOLE OF STOICHIOMETRIC PRODUCTS :	-20.314	kcal/mole
ACTUAL HEAT OF REACTION:	-103.989	kcal/mole of fuel
HEAT OF STOICHIOMETRIC REACTION:	-195.025	kcal/mole of fuel
(ACTUAL/STOICHIOMETRIC) HEAT OF REACTION:	0.533	
(ACTUAL/MAXIMUM) HEAT OF REACTION:	0.833	

DATA REDUCTION PROGRAM OUTPUT

RUN DATE:	04-30-88	EXPERIMENT NUMBER:	09
RUN TIME:	16:01	INTEGRATER RUN NUMBER:	313
INTERFACE HEIGHT:	10.0 cm	LAB PRESSURE:	740.7 ± 0.5 torr
BURNER DIAMETER:	19.0 cm	DRY-BULB TEMPERATURE:	23.1 ± 0.2 °C
FIRE SIZE:	67.8 ± 1.65 kW	WET-BULB TEMPERATURE:	14.8 ± 0.2 °C

SUPPLY FLOWRATES :

NATURAL GAS FUEL:	1.3573 ± 0.0332	g/sec
AIR ENTRAINED BY PLUME:	10.2850 ± 0.2685	g/sec
AIR ADDED TO UPPER LAYER:	4.3810 ± 0.4597	g/sec
TOTAL:	16.0233 ± 0.7614	g/sec

I =	6.4108 ± 0.0450 moles Air/mole Fuel	FUEL INLET REYNOLDS NUMBER:	830.3
I_s =	9.7599 ± 0.1372 moles Air/mole Fuel	FUEL INLET RICHARDSON NUMBER:	0.3409

FUEL COMPOSITION : (mole fractions)		AIR COMPOSITION : (mole fractions)	
METHANE	0.9380 ± 0.0100	OXYGEN	0.2071 ± 0.0010
ETHANE	0.0302 ± 0.0050	NITROGEN	0.7719 ± 0.0020
PROPANE	0.0079 ± 0.0020	WATER VAPOR	0.0115 ± 0.0004
NITROGEN	0.0168 ± 0.0020	CARBON DIOXIDE	0.0003 ± 0.0001
CARBON DIOXIDE	0.0071 ± 0.0020	ARGON	0.0092 ± 0.0006

FUEL VISCOSITY:	109.54	μPoise
FUEL MOLECULAR WEIGHT:	17.15	g/mole
FUEL LOWER HEATING VALUE:	50.26	MJ/kg

PRODUCT LAYER ANALYSIS :

	mole fractions	mass fractions	mass fraction of plume equivalent source
HYDROGEN	0.0097 ± 0.00070	0.0007	0.0010
OXYGEN	0.0334 ± 0.00110	0.0398	-.0317
NITROGEN	0.6602 ± 0.00450	0.6887	0.6657
METHANE	0.0538 ± 0.00290	0.0321	0.0442
CARBON MONOXIDE	0.0128 ± 0.00030	0.0133	0.0183
CARBON DIOXIDE	0.0655 ± 0.00080	0.1073	0.1475
WATER VAPOR	0.1548 ± 0.00470	0.1038	0.1402
SOOT (C_8H)	0.0001 ± 0.00380	0.0005	0.0007
ACETYLENE	0.0013 ± 0.00000	0.0013	0.0018
ETHYLENE	0.0000 ± 0.00000	0.0000	0.0000
ETHANE	0.0007 ± 0.00000	0.0007	0.0010
ARGON	0.0078 ± 0.00050	0.0117	0.0113

UPPER LAYER EQUIVALENCE RATIO:	1.522 ± 0.0239
PLUME EQUIVALENCE RATIO AT INTERFACE HEIGHT:	2.171 ± 0.0834
STOICHIOMETRIC FUEL/AIR MASS RATIO:	0.0608
SAMPLE TEMPERATURE:	277.2 °C
HOOD TEMPERATURE:	211.7 °C

HEAT OF FORMATION PER MOLE OF FUEL:	-17.267	kcal/mole
HEAT OF FORMATION PER MOLE OF AIR:	-0.692	kcal/mole
HEAT OF FORMATION PER MOLE OF PRODUCTS:	-16.328	kcal/mole
HEAT OF FORMATION PER MOLE OF STOICHIOMETRIC PRODUCTS :	-20.314	kcal/mole
ACTUAL HEAT OF REACTION:	-101.112	kcal/mole of fuel
HEAT OF STOICHIOMETRIC REACTION:	-195.025	kcal/mole of fuel
(ACTUAL/STOICHIOMETRIC) HEAT OF REACTION:	0.518	
(ACTUAL/MAXIMUM) HEAT OF REACTION:	0.789	

DATA REDUCTION PROGRAM OUTPUT

RUN DATE:	04-30-88	EXPERIMENT NUMBER:	10
RUN TIME:	16:20	INTEGRATER RUN NUMBER:	314
INTERFACE HEIGHT:	10.0 cm	LAB PRESSURE:	740.7 ± 0.5 torr
BURNER DIAMETER:	19.0 cm	DRY-BULB TEMPERATURE:	23.1 ± 0.2 °C
FIRE SIZE:	67.8 ± 1.65 kW	WET-BULB TEMPERATURE:	14.8 ± 0.2 °C

SUPPLY FLOWRATES :

NATURAL GAS FUEL:	1.3573 ± 0.0332	g/sec
AIR ENTRAINED BY PLUME:	10.2850 ± 0.2685	g/sec
AIR ADDED TO UPPER LAYER:	6.9460 ± 0.5133	g/sec
TOTAL:	18.5883 ± 0.8150	g/sec

I = 7.5321 ± 0.0515 moles Air/mole Fuel
I_s = 9.7599 ± 0.1372 moles Air/mole Fuel

FUEL INLET REYNOLDS NUMBER: 830.3
FUEL INLET RICHARDSON NUMBER: 0.3409

FUEL COMPOSITION : (mole fractions)

METHANE	0.9380 ± 0.0100
ETHANE	0.0302 ± 0.0050
PROPANE	0.0079 ± 0.0020
NITROGEN	0.0168 ± 0.0020
CARBON DIOXIDE	0.0071 ± 0.0020

AIR COMPOSITION : (mole fractions)

OXYGEN	0.2071 ± 0.0010
NITROGEN	0.7719 ± 0.0020
WATER VAPOR	0.0115 ± 0.0004
CARBON DIOXIDE	0.0003 ± 0.0001
ARGON	0.0092 ± 0.0006

FUEL VISCOSITY:	109.54 μPoise
FUEL MOLECULAR WEIGHT:	17.15 g/mole
FUEL LOWER HEATING VALUE:	50.26 MJ/kg

PRODUCT LAYER ANALYSIS :

	mole fractions	mass fractions	mass fraction of plume equivalent source
HYDROGEN	0.0088 ± 0.00070	0.0007	0.0010
OXYGEN	0.0407 ± 0.00120	0.0479	-.0606
NITROGEN	0.6758 ± 0.00360	0.6974	0.6662
METHANE	0.0377 ± 0.00200	0.0223	0.0356
CARBON MONOXIDE	0.0130 ± 0.00030	0.0134	0.0214
CARBON DIOXIDE	0.0652 ± 0.00080	0.1058	0.1686
WATER VAPOR	0.1489 ± 0.00470	0.0988	0.1535
SOOT (C_8H)	0.0000 ± 0.00000	0.0000	0.0000
ACETYLENE	0.0011 ± 0.00000	0.0010	0.0017
ETHYLENE	0.0000 ± 0.00000	0.0000	0.0000
ETHANE	0.0007 ± 0.00000	0.0008	0.0013
ARGON	0.0080 ± 0.00050	0.0118	0.0113

UPPER LAYER EQUIVALENCE RATIO:	1.296 ± 0.0203
PLUME EQUIVALENCE RATIO AT INTERFACE HEIGHT:	2.171 ± 0.0834
STOICHIOMETRIC FUEL/AIR MASS RATIO:	0.0608
SAMPLE TEMPERATURE:	279.4 °C
HOOD TEMPERATURE:	213.9 °C

HEAT OF FORMATION PER MOLE OF FUEL:	-17.267	kcal/mole
HEAT OF FORMATION PER MOLE OF AIR:	-0.692	kcal/mole
HEAT OF FORMATION PER MOLE OF PRODUCTS:	-15.704	kcal/mole
HEAT OF FORMATION PER MOLE OF STOICHIOMETRIC PRODUCTS :	-20.314	kcal/mole
ACTUAL HEAT OF REACTION:	-113.009	kcal/mole of fuel
HEAT OF STOICHIOMETRIC REACTION:	-195.025	kcal/mole of fuel
(ACTUAL/STOICHIOMETRIC) HEAT OF REACTION:	0.580	
(ACTUAL/MAXIMUM) HEAT OF REACTION:	0.751	

DATA REDUCTION PROGRAM OUTPUT

RUN DATE:	04-30-88	EXPERIMENT NUMBER:	11
RUN TIME:	16:39	INTEGRATER RUN NUMBER:	315
INTERFACE HEIGHT:	10.0 cm	LAB PRESSURE:	740.7 ± 0.5 torr
BURNER DIAMETER:	19.0 cm	DRY-BULB TEMPERATURE:	23.1 ± 0.2 °C
FIRE SIZE:	67.8 ± 1.65 kW	WET-BULB TEMPERATURE:	14.8 ± 0.2 °C

SUPPLY FLOWRATES :

NATURAL GAS FUEL:	1.3573 ± 0.0332	g/sec
AIR ENTRAINED BY PLUME:	10.2850 ± 0.2685	g/sec
AIR ADDED TO UPPER LAYER:	9.1642 ± 0.5629	g/sec
TOTAL:	20.8065 ± 0.8646	g/sec

I = 8.5017 ± 0.0596 moles Air/mole Fuel
I_s = 9.7599 ± 0.1372 moles Air/mole Fuel

FUEL INLET REYNOLDS NUMBER: 830.3
FUEL INLET RICHARDSON NUMBER: 0.3409

FUEL COMPOSITION : (mole fractions)

METHANE	0.9380 ± 0.0100
ETHANE	0.0302 ± 0.0050
PROPANE	0.0079 ± 0.0020
NITROGEN	0.0168 ± 0.0020
CARBON DIOXIDE	0.0071 ± 0.0020

AIR COMPOSITION : (mole fractions)

OXYGEN	0.2071 ± 0.0010
NITROGEN	0.7719 ± 0.0020
WATER VAPOR	0.0115 ± 0.0004
CARBON DIOXIDE	0.0003 ± 0.0001
ARGON	0.0092 ± 0.0006

FUEL VISCOSITY:	109.54 μPoise
FUEL MOLECULAR WEIGHT:	17.15 g/mole
FUEL LOWER HEATING VALUE:	50.26 MJ/kg

PRODUCT LAYER ANALYSIS :

	mole fractions	mass fractions	mass fraction of plume equivalent source
HYDROGEN	0.0043 ± 0.00030	0.0003	0.0006
OXYGEN	0.0476 ± 0.00130	0.0556	-.0814
NITROGEN	0.6878 ± 0.00370	0.7032	0.6664
METHANE	0.0294 ± 0.00160	0.0172	0.0308
CARBON MONOXIDE	0.0114 ± 0.00030	0.0116	0.0208
CARBON DIOXIDE	0.0639 ± 0.00080	0.1026	0.1831
WATER VAPOR	0.1458 ± 0.00490	0.0959	0.1657
SOOT (C_8H)	0.0000 ± 0.00000	0.0000	0.0000
ACETYLENE	0.0010 ± 0.00000	0.0009	0.0016
ETHYLENE	0.0000 ± 0.00000	0.0000	0.0000
ETHANE	0.0006 ± 0.00000	0.0007	0.0012
ARGON	0.0082 ± 0.00050	0.0119	0.0113

UPPER LAYER EQUIVALENCE RATIO:	1.148 ± 0.0180
PLUME EQUIVALENCE RATIO AT INTERFACE HEIGHT:	2.171 ± 0.0834
STOICHIOMETRIC FUEL/AIR MASS RATIO:	0.0608
SAMPLE TEMPERATURE:	286.7 °C
HOOD TEMPERATURE:	221.1 °C

HEAT OF FORMATION PER MOLE OF FUEL:	-17.267	kcal/mole
HEAT OF FORMATION PER MOLE OF AIR:	-0.692	kcal/mole
HEAT OF FORMATION PER MOLE OF PRODUCTS:	-15.213	kcal/mole
HEAT OF FORMATION PER MOLE OF STOICHIOMETRIC PRODUCTS :	-20.314	kcal/mole
ACTUAL HEAT OF REACTION:	-122.373	kcal/mole of fuel
HEAT OF STOICHIOMETRIC REACTION:	-195.025	kcal/mole of fuel
(ACTUAL/STOICHIOMETRIC) HEAT OF REACTION:	0.627	
(ACTUAL/MAXIMUM) HEAT OF REACTION:	0.720	

DATA REDUCTION PROGRAM OUTPUT

RUN DATE:	04-30-88	EXPERIMENT NUMBER:	12
RUN TIME:	16:58	INTEGRATER RUN NUMBER:	316
INTERFACE HEIGHT:	10.0 cm	LAB PRESSURE:	740.7 ± 0.5 torr
BURNER DIAMETER:	19.0 cm	DRY-BULB TEMPERATURE:	23.1 ± 0.2 °C
FIRE SIZE:	67.8 ± 1.65 kW	WET-BULB TEMPERATURE:	14.8 ± 0.2 °C

SUPPLY FLOWRATES :

NATURAL GAS FUEL:	1.3573 ± 0.0332	g/sec
AIR ENTRAINED BY PLUME:	10.2850 ± 0.2685	g/sec
AIR ADDED TO UPPER LAYER:	11.2514 ± 0.6114	g/sec
TOTAL:	22.8937 ± 0.9131	g/sec

I =	9.4141 ± 0.0683 moles Air/mole Fuel	FUEL INLET REYNOLDS NUMBER:	830.3
I_s =	9.7599 ± 0.1372 moles Air/mole Fuel	FUEL INLET RICHARDSON NUMBER:	0.3409

FUEL COMPOSITION : (mole fractions)

METHANE	0.9380 ± 0.0100
ETHANE	0.0302 ± 0.0050
PROPANE	0.0079 ± 0.0020
NITROGEN	0.0168 ± 0.0020
CARBON DIOXIDE	0.0071 ± 0.0020

AIR COMPOSITION : (mole fractions)

OXYGEN	0.2071 ± 0.0010
NITROGEN	0.7719 ± 0.0020
WATER VAPOR	0.0115 ± 0.0004
CARBON DIOXIDE	0.0003 ± 0.0001
ARGON	0.0092 ± 0.0006

FUEL VISCOSITY:	109.54 μPoise
FUEL MOLECULAR WEIGHT:	17.15 g/mole
FUEL LOWER HEATING VALUE:	50.26 MJ/kg

PRODUCT LAYER ANALYSIS :

	mole fractions	mass fractions	mass fraction of plume equivalent source
HYDROGEN	0.0016 ± 0.00010	0.0001	0.0002
OXYGEN	0.0544 ± 0.00150	0.0632	-.0979
NITROGEN	0.6963 ± 0.00390	0.7074	0.6665
METHANE	0.0251 ± 0.00130	0.0146	0.0287
CARBON MONOXIDE	0.0090 ± 0.00020	0.0091	0.0180
CARBON DIOXIDE	0.0627 ± 0.00080	0.1002	0.1965
WATER VAPOR	0.1416 ± 0.00520	0.0925	0.1750
SOOT (C_8H)	0.0000 ± 0.00000	0.0000	0.0000
ACETYLENE	0.0009 ± 0.00000	0.0008	0.0017
ETHYLENE	0.0000 ± 0.00000	0.0000	0.0000
ETHANE	0.0000 ± 0.00000	0.0000	0.0000
ARGON	0.0083 ± 0.00050	0.0120	0.0113

UPPER LAYER EQUIVALENCE RATIO:	1.037 ± 0.0164
PLUME EQUIVALENCE RATIO AT INTERFACE HEIGHT:	2.171 ± 0.0834
STOICHIOMETRIC FUEL/AIR MASS RATIO:	0.0608
SAMPLE TEMPERATURE:	302.8 °C
HOOD TEMPERATURE:	230.0 °C

HEAT OF FORMATION PER MOLE OF FUEL:	-17.267	kcal/mole
HEAT OF FORMATION PER MOLE OF AIR:	-0.692	kcal/mole
HEAT OF FORMATION PER MOLE OF PRODUCTS:	-14.727	kcal/mole
HEAT OF FORMATION PER MOLE OF STOICHIOMETRIC PRODUCTS :	-20.314	kcal/mole
ACTUAL HEAT OF REACTION:	-130.267	kcal/mole of fuel
HEAT OF STOICHIOMETRIC REACTION:	-195.025	kcal/mole of fuel
(ACTUAL/STOICHIOMETRIC) HEAT OF REACTION:	0.668	
(ACTUAL/MAXIMUM) HEAT OF REACTION:	0.692	

DATA REDUCTION PROGRAM OUTPUT

RUN DATE:	04-30-88	EXPERIMENT NUMBER:	13
RUN TIME:	17:17	INTEGRATER RUN NUMBER:	317
INTERFACE HEIGHT:	10.0 cm	LAB PRESSURE:	740.7 ± 0.5 torr
BURNER DIAMETER:	19.0 cm	DRY-BULB TEMPERATURE:	23.1 ± 0.2 °C
FIRE SIZE:	67.8 ± 1.65 kW	WET-BULB TEMPERATURE:	14.8 ± 0.2 °C

SUPPLY FLOWRATES :

NATURAL GAS FUEL:	1.3573 ± 0.0332	g/sec
AIR ENTRAINED BY PLUME:	10.2850 ± 0.2685	g/sec
AIR ADDED TO UPPER LAYER:	16.9568 ± 0.7509	g/sec
TOTAL:	28.5991 ± 1.0526	g/sec

I =	11.9080 ± 0.0958	moles Air/mole Fuel	FUEL INLET REYNOLDS NUMBER: 830.3
I_s =	9.7599 ± 0.1372	moles Air/mole Fuel	FUEL INLET RICHARDSON NUMBER: 0.3409

FUEL COMPOSITION : (mole fractions)		AIR COMPOSITION : (mole fractions)	
METHANE	0.9380 ± 0.0100	OXYGEN	0.2071 ± 0.0010
ETHANE	0.0302 ± 0.0050	NITROGEN	0.7719 ± 0.0020
PROPANE	0.0079 ± 0.0020	WATER VAPOR	0.0115 ± 0.0004
NITROGEN	0.0168 ± 0.0020	CARBON DIOXIDE	0.0003 ± 0.0001
CARBON DIOXIDE	0.0071 ± 0.0020	ARGON	0.0092 ± 0.0006

FUEL VISCOSITY:	109.54	μPoise
FUEL MOLECULAR WEIGHT:	17.15	g/mole
FUEL LOWER HEATING VALUE:	50.26	MJ/kg

PRODUCT LAYER ANALYSIS :

	mole fractions	mass fractions	mass fraction of plume equivalent source
HYDROGEN	0.0000 ± 0.00000	0.0000	0.0000
OXYGEN	0.0654 ± 0.00170	0.0751	-.1502
NITROGEN	0.7118 ± 0.00430	0.7159	0.6664
METHANE	0.0123 ± 0.00070	0.0071	0.0174
CARBON MONOXIDE	0.0058 ± 0.00010	0.0058	0.0143
CARBON DIOXIDE	0.0611 ± 0.00080	0.0965	0.2363
WATER VAPOR	0.1348 ± 0.00580	0.0872	0.2038
SOOT (C_8H)	0.0000 ± 0.00000	0.0000	0.0000
ACETYLENE	0.0003 ± 0.00000	0.0003	0.0008
ETHYLENE	0.0000 ± 0.00000	0.0000	0.0000
ETHANE	0.0000 ± 0.00000	0.0000	0.0000
ARGON	0.0085 ± 0.00060	0.0121	0.0113

UPPER LAYER EQUIVALENCE RATIO:	0.820 ± 0.0133
PLUME EQUIVALENCE RATIO AT INTERFACE HEIGHT:	2.171 ± 0.0834
STOICHIOMETRIC FUEL/AIR MASS RATIO:	0.0608
SAMPLE TEMPERATURE:	318.9 °C
HOOD TEMPERATURE:	235.6 °C

HEAT OF FORMATION PER MOLE OF FUEL:	-17.267	kcal/mole
HEAT OF FORMATION PER MOLE OF AIR:	-0.692	kcal/mole
HEAT OF FORMATION PER MOLE OF PRODUCTS:	-13.891	kcal/mole
HEAT OF FORMATION PER MOLE OF STOICHIOMETRIC PRODUCTS :	-20.314	kcal/mole
ACTUAL HEAT OF REACTION:	-154.200	kcal/mole of fuel
HEAT OF STOICHIOMETRIC REACTION:	-195.025	kcal/mole of fuel
(ACTUAL/STOICHIOMETRIC) HEAT OF REACTION:	0.791	
(ACTUAL/MAXIMUM) HEAT OF REACTION:	0.791	

DATA REDUCTION PROGRAM OUTPUT

RUN DATE:	04-30-88	EXPERIMENT NUMBER:	14
RUN TIME:	17:37	INTEGRATER RUN NUMBER:	318
INTERFACE HEIGHT:	10.0 cm	LAB PRESSURE:	740.7 ± 0.5 torr
BURNER DIAMETER:	19.0 cm	DRY-BULB TEMPERATURE:	23.1 ± 0.2 °C
FIRE SIZE:	67.8 ± 1.65 kW	WET-BULB TEMPERATURE:	14.8 ± 0.2 °C

SUPPLY FLOWRATES :

NATURAL GAS FUEL:	1.3573 ± 0.0332	g/sec
AIR ENTRAINED BY PLUME:	10.2850 ± 0.2685	g/sec
AIR ADDED TO UPPER LAYER:	28.9421 ± 1.0757	g/sec
TOTAL:	40.5844 ± 1.3774	g/sec

I = 17.1471 ± 0.1775 moles Air/mole Fuel
I_s = 9.7599 ± 0.1372 moles Air/mole Fuel

FUEL INLET REYNOLDS NUMBER: 830.3
FUEL INLET RICHARDSON NUMBER: 0.3409

FUEL COMPOSITION : (mole fractions)		AIR COMPOSITION : (mole fractions)	
METHANE	0.9380 ± 0.0100	OXYGEN	0.2071 ± 0.0010
ETHANE	0.0302 ± 0.0050	NITROGEN	0.7719 ± 0.0020
PROPANE	0.0079 ± 0.0020	WATER VAPOR	0.0115 ± 0.0004
NITROGEN	0.0168 ± 0.0020	CARBON DIOXIDE	0.0003 ± 0.0001
CARBON DIOXIDE	0.0071 ± 0.0020	ARGON	0.0092 ± 0.0006

FUEL VISCOSITY:	109.54 μPoise
FUEL MOLECULAR WEIGHT:	17.15 g/mole
FUEL LOWER HEATING VALUE:	50.26 MJ/kg

PRODUCT LAYER ANALYSIS :

	mole fractions	mass fractions	mass fraction of plume equivalent source
HYDROGEN	0.0000 ± 0.00000	0.0000	0.0000
OXYGEN	0.0854 ± 0.00210	0.0971	-.2328
NITROGEN	0.7295 ± 0.00550	0.7258	0.6660
METHANE	0.0000 ± 0.00000	0.0000	0.0000
CARBON MONOXIDE	0.0011 ± 0.00000	0.0011	0.0037
CARBON DIOXIDE	0.0559 ± 0.00070	0.0873	0.3033
WATER VAPOR	0.1195 ± 0.00730	0.0764	0.2486
SOOT (C_8H)	0.0000 ± 0.00000	0.0000	0.0000
ACETYLENE	0.0000 ± 0.00000	0.0000	0.0000
ETHYLENE	0.0000 ± 0.00000	0.0000	0.0000
ETHANE	0.0000 ± 0.00000	0.0000	0.0000
ARGON	0.0087 ± 0.00060	0.0123	0.0113

UPPER LAYER EQUIVALENCE RATIO:	0.569 ± 0.0099
PLUME EQUIVALENCE RATIO AT INTERFACE HEIGHT:	2.171 ± 0.0834
STOICHIOMETRIC FUEL/AIR MASS RATIO:	0.0608
SAMPLE TEMPERATURE:	357.2 °C
HOOD TEMPERATURE:	245.0 °C

HEAT OF FORMATION PER MOLE OF FUEL:	-17.267	kcal/mole
HEAT OF FORMATION PER MOLE OF AIR:	-0.692	kcal/mole
HEAT OF FORMATION PER MOLE OF PRODUCTS:	-12.188	kcal/mole
HEAT OF FORMATION PER MOLE OF STOICHIOMETRIC PRODUCTS :	-20.314	kcal/mole
ACTUAL HEAT OF REACTION:	-192.288	kcal/mole of fuel
HEAT OF STOICHIOMETRIC REACTION:	-195.025	kcal/mole of fuel
(ACTUAL/STOICHIOMETRIC) HEAT OF REACTION:	0.986	
(ACTUAL/MAXIMUM) HEAT OF REACTION:	0.986	

DATA REDUCTION PROGRAM OUTPUT

RUN DATE:	04-30-88	EXPERIMENT NUMBER:	15
RUN TIME:	18:04	INTEGRATER RUN NUMBER:	320
INTERFACE HEIGHT:	10.0 cm	LAB PRESSURE:	740.7 ± 0.5 torr
BURNER DIAMETER:	19.0 cm	DRY-BULB TEMPERATURE:	23.1 ± 0.2 °C
FIRE SIZE:	67.8 ± 1.65 kW	WET-BULB TEMPERATURE:	14.8 ± 0.2 °C

SUPPLY FLOWRATES :

NATURAL GAS FUEL:	1.3573 ± 0.0332	g/sec
AIR ENTRAINED BY PLUME:	10.2850 ± 0.2685	g/sec
AIR ADDED TO UPPER LAYER:	30.6544 ± 1.1240	g/sec
TOTAL:	42.2967 ± 1.4257	g/sec

I =	17.8956 ± 0.1902 moles Air/mole Fuel	FUEL INLET REYNOLDS NUMBER:	830.3
I_s =	9.7599 ± 0.1372 moles Air/mole Fuel	FUEL INLET RICHARDSON NUMBER:	0.3409

FUEL COMPOSITION : (mole fractions)

METHANE	0.9380 ± 0.0100
ETHANE	0.0302 ± 0.0050
PROPANE	0.0079 ± 0.0020
NITROGEN	0.0168 ± 0.0020
CARBON DIOXIDE	0.0071 ± 0.0020

AIR COMPOSITION : (mole fractions)

OXYGEN	0.2071 ± 0.0010
NITROGEN	0.7719 ± 0.0020
WATER VAPOR	0.0115 ± 0.0004
CARBON DIOXIDE	0.0003 ± 0.0001
ARGON	0.0092 ± 0.0006

FUEL VISCOSITY:	109.54 μPoise
FUEL MOLECULAR WEIGHT:	17.15 g/mole
FUEL LOWER HEATING VALUE:	50.26 MJ/kg

PRODUCT LAYER ANALYSIS :

	mole fractions	mass fractions	mass fraction of plume equivalent source
HYDROGEN	0.0000 ± 0.00000	0.0000	0.0000
OXYGEN	0.0895 ± 0.00220	0.1017	-.2356
NITROGEN	0.7309 ± 0.00570	0.7267	0.6658
METHANE	0.0000 ± 0.00000	0.0000	0.0000
CARBON MONOXIDE	0.0008 ± 0.00000	0.0008	0.0028
CARBON DIOXIDE	0.0539 ± 0.00070	0.0842	0.3047
WATER VAPOR	0.1162 ± 0.00750	0.0743	0.2511
SOOT (C_8H)	0.0000 ± 0.00000	0.0000	0.0000
ACETYLENE	0.0000 ± 0.00000	0.0000	0.0000
ETHYLENE	0.0000 ± 0.00000	0.0000	0.0000
ETHANE	0.0000 ± 0.00000	0.0000	0.0000
ARGON	0.0087 ± 0.00060	0.0123	0.0113

UPPER LAYER EQUIVALENCE RATIO:	0.545 ± 0.0096
PLUME EQUIVALENCE RATIO AT INTERFACE HEIGHT:	2.171 ± 0.0834
STOICHIOMETRIC FUEL/AIR MASS RATIO:	0.0608
SAMPLE TEMPERATURE:	356.1 °C
HOOD TEMPERATURE:	243.3 °C

HEAT OF FORMATION PER MOLE OF FUEL:	-17.267	kcal/mole
HEAT OF FORMATION PER MOLE OF AIR:	-0.692	kcal/mole
HEAT OF FORMATION PER MOLE OF PRODUCTS:	-11.807	kcal/mole
HEAT OF FORMATION PER MOLE OF STOICHIOMETRIC PRODUCTS :	-20.314	kcal/mole
ACTUAL HEAT OF REACTION:	-193.777	kcal/mole of fuel
HEAT OF STOICHIOMETRIC REACTION:	-195.025	kcal/mole of fuel
(ACTUAL/STOICHIOMETRIC) HEAT OF REACTION:	0.994	
(ACTUAL/MAXIMUM) HEAT OF REACTION:	0.994	

DATA REDUCTION PROGRAM OUTPUT

RUN DATE:	03-26-88	EXPERIMENT NUMBER:	16
RUN TIME:	14:18	INTEGRATER RUN NUMBER:	240
INTERFACE HEIGHT:	10.0 cm	LAB PRESSURE:	738.4 ± 0.5 torr
BURNER DIAMETER:	19.0 cm	DRY-BULB TEMPERATURE:	24.0 ± 0.2 °C
FIRE SIZE:	57.3 ± 1.64 kW	WET-BULB TEMPERATURE:	12.8 ± 0.2 °C

SUPPLY FLOWRATES :

NATURAL GAS FUEL:	1.1399 ± 0.0326	g/sec
AIR ENTRAINED BY PLUME:	11.4829 ± 0.3382	g/sec
AIR ADDED TO UPPER LAYER:	0.0000 ± 0.0000	g/sec
TOTAL:	12.6228 ± 0.3708	g/sec

I = 5.9815 ± 0.0414 moles Air/mole Fuel
I_s = 9.7161 ± 0.1366 moles Air/mole Fuel

FUEL INLET REYNOLDS NUMBER: 697.2
FUEL INLET RICHARDSON NUMBER: 0.4782

FUEL COMPOSITION : (mole fractions)

METHANE	0.9382 ± 0.0100
ETHANE	0.0298 ± 0.0050
PROPANE	0.0079 ± 0.0020
NITROGEN	0.0162 ± 0.0020
CARBON DIOXIDE	0.0079 ± 0.0020

AIR COMPOSITION : (mole fractions)

OXYGEN	0.2079 ± 0.0010
NITROGEN	0.7750 ± 0.0020
WATER VAPOR	0.0075 ± 0.0004
CARBON DIOXIDE	0.0003 ± 0.0001
ARGON	0.0092 ± 0.0006

FUEL VISCOSITY:	109.56 μPoise
FUEL MOLECULAR WEIGHT:	17.16 g/mole
FUEL LOWER HEATING VALUE:	50.51 MJ/kg

PRODUCT LAYER ANALYSIS :

	mole fractions	mass fractions	mass fraction of plume equivalent source
HYDROGEN	0.0117 ± 0.00090	0.0009	0.0009
OXYGEN	0.0206 ± 0.00080	0.0247	0.0247
NITROGEN	0.6557 ± 0.00360	0.6865	0.6865
METHANE	0.0544 ± 0.00290	0.0326	0.0326
CARBON MONOXIDE	0.0145 ± 0.00040	0.0152	0.0152
CARBON DIOXIDE	0.0711 ± 0.00090	0.1170	0.1170
WATER VAPOR	0.1616 ± 0.00440	0.1088	0.1088
SOOT (C_8H)	0.0000 ± 0.00000	0.0000	0.0000
ACETYLENE	0.0016 ± 0.00000	0.0015	0.0015
ETHYLENE	0.0000 ± 0.00000	0.0000	0.0000
ETHANE	0.0011 ± 0.00000	0.0012	0.0012
ARGON	0.0078 ± 0.00050	0.0116	0.0116

UPPER LAYER EQUIVALENCE RATIO:	1.624 ± 0.0255
PLUME EQUIVALENCE RATIO AT INTERFACE HEIGHT:	1.624 ± 0.0705
STOICHIOMETRIC FUEL/AIR MASS RATIO:	0.0611
SAMPLE TEMPERATURE:	256.7 °C
HOOD TEMPERATURE:	203.9 °C

HEAT OF FORMATION PER MOLE OF FUEL:	-17.351	kcal/mole
HEAT OF FORMATION PER MOLE OF AIR:	-0.463	kcal/mole
HEAT OF FORMATION PER MOLE OF PRODUCTS:	-17.301	kcal/mole
HEAT OF FORMATION PER MOLE OF STOICHIOMETRIC PRODUCTS :	-20.185	kcal/mole
ACTUAL HEAT OF REACTION:	-102.634	kcal/mole of fuel
HEAT OF STOICHIOMETRIC REACTION:	-194.914	kcal/mole of fuel
(ACTUAL/STOICHIOMETRIC) HEAT OF REACTION:	0.527	
(ACTUAL/MAXIMUM) HEAT OF REACTION:	0.855	

DATA REDUCTION PROGRAM OUTPUT

RUN DATE:	03-26-88	EXPERIMENT NUMBER:	17
RUN TIME:	15:09	INTEGRATER RUN NUMBER:	243
INTERFACE HEIGHT:	10.0 cm	LAB PRESSURE:	738.4 ± 0.5 torr
BURNER DIAMETER:	19.0 cm	DRY-BULB TEMPERATURE:	24.0 ± 0.2 °C
FIRE SIZE:	57.3 ± 1.64 kW	WET-BULB TEMPERATURE:	12.8 ± 0.2 °C

SUPPLY FLOWRATES :

NATURAL GAS FUEL:	1.1399 ± 0.0326	g/sec
AIR ENTRAINED BY PLUME:	11.4830 ± 0.3382	g/sec
AIR ADDED TO UPPER LAYER:	1.7180 ± 0.5146	g/sec
TOTAL:	14.3409 ± 0.8854	g/sec

I = 6.8765 ± 0.0454 moles Air/mole Fuel
I_s = 9.7161 ± 0.1366 moles Air/mole Fuel

FUEL INLET REYNOLDS NUMBER: 697.2
FUEL INLET RICHARDSON NUMBER: 0.4782

FUEL COMPOSITION : (mole fractions)

METHANE	0.9382 ± 0.0100
ETHANE	0.0298 ± 0.0050
PROPANE	0.0079 ± 0.0020
NITROGEN	0.0162 ± 0.0020
CARBON DIOXIDE	0.0079 ± 0.0020

AIR COMPOSITION : (mole fractions)

OXYGEN	0.2079 ± 0.0010
NITROGEN	0.7750 ± 0.0020
WATER VAPOR	0.0075 ± 0.0004
CARBON DIOXIDE	0.0003 ± 0.0001
ARGON	0.0092 ± 0.0006

FUEL VISCOSITY:	109.56 μPoise
FUEL MOLECULAR WEIGHT:	17.16 g/mole
FUEL LOWER HEATING VALUE:	50.51 MJ/kg

PRODUCT LAYER ANALYSIS :

	mole fractions	mass fractions	mass fraction of plume equivalent source
HYDROGEN	0.0119 ± 0.00090	0.0009	0.0010
OXYGEN	0.0279 ± 0.00100	0.0331	0.0063
NITROGEN	0.6687 ± 0.00340	0.6944	0.6865
METHANE	0.0407 ± 0.00220	0.0242	0.0275
CARBON MONOXIDE	0.0133 ± 0.00030	0.0138	0.0157
CARBON DIOXIDE	0.0703 ± 0.00080	0.1146	0.1302
WATER VAPOR	0.1569 ± 0.00450	0.1048	0.1184
SOOT (C_8H)	0.0000 ± 0.00000	0.0000	0.0000
ACETYLENE	0.0016 ± 0.00000	0.0015	0.0017
ETHYLENE	0.0000 ± 0.00000	0.0000	0.0000
ETHANE	0.0008 ± 0.00000	0.0009	0.0010
ARGON	0.0079 ± 0.00050	0.0118	0.0116

UPPER LAYER EQUIVALENCE RATIO:	1.413 ± 0.0220
PLUME EQUIVALENCE RATIO AT INTERFACE HEIGHT:	1.624 ± 0.0705
STOICHIOMETRIC FUEL/AIR MASS RATIO:	0.0611
SAMPLE TEMPERATURE:	264.4 °C
HOOD TEMPERATURE:	211.1 °C

HEAT OF FORMATION PER MOLE OF FUEL:	-17.351	kcal/mole
HEAT OF FORMATION PER MOLE OF AIR:	-0.463	kcal/mole
HEAT OF FORMATION PER MOLE OF PRODUCTS:	-16.672	kcal/mole
HEAT OF FORMATION PER MOLE OF STOICHIOMETRIC PRODUCTS :	-20.185	kcal/mole
ACTUAL HEAT OF REACTION:	-112.749	kcal/mole of fuel
HEAT OF STOICHIOMETRIC REACTION:	-194.914	kcal/mole of fuel
(ACTUAL/STOICHIOMETRIC) HEAT OF REACTION:	0.578	
(ACTUAL/MAXIMUM) HEAT OF REACTION:	0.817	

DATA REDUCTION PROGRAM OUTPUT

RUN DATE:	03-26-88	EXPERIMENT NUMBER:	18
RUN TIME:	15:31	INTEGRATER RUN NUMBER:	244
INTERFACE HEIGHT:	10.0 cm	LAB PRESSURE:	738.4 ± 0.5 torr
BURNER DIAMETER:	19.0 cm	DRY-BULB TEMPERATURE:	24.0 ± 0.2 °C
FIRE SIZE:	57.3 ± 1.64 kW	WET-BULB TEMPERATURE:	12.8 ± 0.2 °C

SUPPLY FLOWRATES :

NATURAL GAS FUEL:	1.1399 ± 0.0326	g/sec
AIR ENTRAINED BY PLUME:	11.4830 ± 0.3382	g/sec
AIR ADDED TO UPPER LAYER:	2.2152 ± 0.5258	g/sec
TOTAL:	14.8381 ± 0.8966	g/sec

I =	7.1355 ± 0.0476 moles Air/mole Fuel	FUEL INLET REYNOLDS NUMBER:	697.2
I_s =	9.7161 ± 0.1366 moles Air/mole Fuel	FUEL INLET RICHARDSON NUMBER:	0.4782

FUEL COMPOSITION : (mole fractions)		AIR COMPOSITION : (mole fractions)	
METHANE	0.9382 ± 0.0100	OXYGEN	0.2079 ± 0.0010
ETHANE	0.0298 ± 0.0050	NITROGEN	0.7750 ± 0.0020
PROPANE	0.0079 ± 0.0020	WATER VAPOR	0.0075 ± 0.0004
NITROGEN	0.0162 ± 0.0020	CARBON DIOXIDE	0.0003 ± 0.0001
CARBON DIOXIDE	0.0079 ± 0.0020	ARGON	0.0092 ± 0.0006

FUEL VISCOSITY:	109.56	μPoise
FUEL MOLECULAR WEIGHT:	17.16	g/mole
FUEL LOWER HEATING VALUE:	50.51	MJ/kg

PRODUCT LAYER ANALYSIS :

	mole fractions	mass fractions	mass fraction of plume equivalent source
HYDROGEN	0.0093 ± 0.00070	0.0007	0.0008
OXYGEN	0.0286 ± 0.00100	0.0338	-.0007
NITROGEN	0.6740 ± 0.00340	0.6965	0.6868
METHANE	0.0367 ± 0.00200	0.0217	0.0255
CARBON MONOXIDE	0.0136 ± 0.00030	0.0140	0.0165
CARBON DIOXIDE	0.0709 ± 0.00090	0.1152	0.1353
WATER VAPOR	0.1569 ± 0.00450	0.1042	0.1217
SOOT (C_8H)	0.0000 ± 0.00000	0.0000	0.0000
ACETYLENE	0.0012 ± 0.00000	0.0012	0.0014
ETHYLENE	0.0000 ± 0.00000	0.0000	0.0000
ETHANE	0.0009 ± 0.00000	0.0010	0.0011
ARGON	0.0080 ± 0.00050	0.0118	0.0116

UPPER LAYER EQUIVALENCE RATIO:	1.362 ± 0.0212	
PLUME EQUIVALENCE RATIO AT INTERFACE HEIGHT:	1.624 ± 0.0705	
STOICHIOMETRIC FUEL/AIR MASS RATIO:	0.0611	
SAMPLE TEMPERATURE:	267.2 °C	
HOOD TEMPERATURE:	209.4 °C	
HEAT OF FORMATION PER MOLE OF FUEL:	-17.351	kcal/mole
HEAT OF FORMATION PER MOLE OF AIR:	-0.463	kcal/mole
HEAT OF FORMATION PER MOLE OF PRODUCTS:	-16.688	kcal/mole
HEAT OF FORMATION PER MOLE OF STOICHIOMETRIC PRODUCTS :	-20.185	kcal/mole
ACTUAL HEAT OF REACTION:	-116.677	kcal/mole of fuel
HEAT OF STOICHIOMETRIC REACTION:	-194.914	kcal/mole of fuel
(ACTUAL/STOICHIOMETRIC) HEAT OF REACTION:	0.599	
(ACTUAL/MAXIMUM) HEAT OF REACTION:	0.815	

DATA REDUCTION PROGRAM OUTPUT

RUN DATE:	03-26-88	EXPERIMENT NUMBER:	19
RUN TIME:	15:50	INTEGRATER RUN NUMBER:	245
INTERFACE HEIGHT:	10.0 cm	LAB PRESSURE:	738.4 ± 0.5 torr
BURNER DIAMETER:	19.0 cm	DRY-BULB TEMPERATURE:	24.0 ± 0.2 °C
FIRE SIZE:	57.3 ± 1.64 kW	WET-BULB TEMPERATURE:	12.8 ± 0.2 °C

SUPPLY FLOWRATES :

NATURAL GAS FUEL:	1.1399 ± 0.0326	g/sec
AIR ENTRAINED BY PLUME:	11.4830 ± 0.3382	g/sec
AIR ADDED TO UPPER LAYER:	4.1637 ± 0.5712	g/sec
TOTAL:	16.7866 ± 0.9420	g/sec

I = 8.1505 ± 0.0553 moles Air/mole Fuel
I_s = 9.7161 ± 0.1366 moles Air/mole Fuel

FUEL INLET REYNOLDS NUMBER: 697.2
FUEL INLET RICHARDSON NUMBER: 0.4782

FUEL COMPOSITION : (mole fractions)

METHANE	0.9382 ± 0.0100
ETHANE	0.0298 ± 0.0050
PROPANE	0.0079 ± 0.0020
NITROGEN	0.0162 ± 0.0020
CARBON DIOXIDE	0.0079 ± 0.0020

AIR COMPOSITION : (mole fractions)

OXYGEN	0.2079 ± 0.0010
NITROGEN	0.7750 ± 0.0020
WATER VAPOR	0.0075 ± 0.0004
CARBON DIOXIDE	0.0003 ± 0.0001
ARGON	0.0092 ± 0.0006

FUEL VISCOSITY:	109.56 μPoise
FUEL MOLECULAR WEIGHT:	17.16 g/mole
FUEL LOWER HEATING VALUE:	50.51 MJ/kg

PRODUCT LAYER ANALYSIS :

	mole fractions	mass fractions	mass fraction of plume equivalent source
HYDROGEN	0.0057 ± 0.00040	0.0004	0.0006
OXYGEN	0.0375 ± 0.00110	0.0439	-.0175
NITROGEN	0.6857 ± 0.00350	0.7029	0.6868
METHANE	0.0293 ± 0.00160	0.0172	0.0228
CARBON MONOXIDE	0.0125 ± 0.00030	0.0128	0.0170
CARBON DIOXIDE	0.0681 ± 0.00080	0.1097	0.1458
WATER VAPOR	0.1520 ± 0.00470	0.1002	0.1317
SOOT (C_8H)	0.0000 ± 0.00000	0.0000	0.0000
ACETYLENE	0.0009 ± 0.00000	0.0009	0.0012
ETHYLENE	0.0000 ± 0.00000	0.0000	0.0000
ETHANE	0.0000 ± 0.00000	0.0000	0.0000
ARGON	0.0081 ± 0.00050	0.0119	0.0116

UPPER LAYER EQUIVALENCE RATIO:	1.192 ± 0.0186
PLUME EQUIVALENCE RATIO AT INTERFACE HEIGHT:	1.624 ± 0.0705
STOICHIOMETRIC FUEL/AIR MASS RATIO:	0.0611
SAMPLE TEMPERATURE:	272.2 °C
HOOD TEMPERATURE:	217.2 °C

HEAT OF FORMATION PER MOLE OF FUEL:	-17.351	kcal/mole
HEAT OF FORMATION PER MOLE OF AIR:	-0.463	kcal/mole
HEAT OF FORMATION PER MOLE OF PRODUCTS:	-15.999	kcal/mole
HEAT OF FORMATION PER MOLE OF STOICHIOMETRIC PRODUCTS :	-20.185	kcal/mole
ACTUAL HEAT OF REACTION:	-126.629	kcal/mole of fuel
HEAT OF STOICHIOMETRIC REACTION:	-194.914	kcal/mole of fuel
(ACTUAL/STOICHIOMETRIC) HEAT OF REACTION:	0.650	
(ACTUAL/MAXIMUM) HEAT OF REACTION:	0.775	

DATA REDUCTION PROGRAM OUTPUT

RUN DATE:	03-26-88	EXPERIMENT NUMBER:	20
RUN TIME:	16:10	INTEGRATER RUN NUMBER:	246
INTERFACE HEIGHT:	10.0 cm	LAB PRESSURE:	738.4 ± 0.5 torr
BURNER DIAMETER:	19.0 cm	DRY-BULB TEMPERATURE:	24.0 ± 0.2 °C
FIRE SIZE:	57.3 ± 1.64 kW	WET-BULB TEMPERATURE:	12.8 ± 0.2 °C

SUPPLY FLOWRATES :

NATURAL GAS FUEL:	1.1399 ± 0.0326	g/sec
AIR ENTRAINED BY PLUME:	11.4830 ± 0.3382	g/sec
AIR ADDED TO UPPER LAYER:	4.0942 ± 0.5699	g/sec
TOTAL:	16.7171 ± 0.9407	g/sec

I =	8.1143 ± 0.0562 moles Air/mole Fuel	FUEL INLET REYNOLDS NUMBER:	697.2
I_s =	9.7161 ± 0.1366 moles Air/mole Fuel	FUEL INLET RICHARDSON NUMBER:	0.4782

FUEL COMPOSITION : (mole fractions)

METHANE	0.9382 ± 0.0100
ETHANE	0.0298 ± 0.0050
PROPANE	0.0079 ± 0.0020
NITROGEN	0.0162 ± 0.0020
CARBON DIOXIDE	0.0079 ± 0.0020

AIR COMPOSITION : (mole fractions)

OXYGEN	0.2079 ± 0.0010
NITROGEN	0.7750 ± 0.0020
WATER VAPOR	0.0075 ± 0.0004
CARBON DIOXIDE	0.0003 ± 0.0001
ARGON	0.0092 ± 0.0006

FUEL VISCOSITY:	109.56 μPoise
FUEL MOLECULAR WEIGHT:	17.16 g/mole
FUEL LOWER HEATING VALUE:	50.51 MJ/kg

PRODUCT LAYER ANALYSIS :

	mole fractions	mass fractions	mass fraction of plume equivalent source
HYDROGEN	0.0058 ± 0.00040	0.0004	0.0006
OXYGEN	0.0381 ± 0.00110	0.0446	-.0157
NITROGEN	0.6864 ± 0.00350	0.7029	0.6871
METHANE	0.0290 ± 0.00160	0.0170	0.0226
CARBON MONOXIDE	0.0128 ± 0.00030	0.0131	0.0173
CARBON DIOXIDE	0.0685 ± 0.00080	0.1102	0.1459
WATER VAPOR	0.1502 ± 0.00470	0.0989	0.1295
SOOT (C_8H)	0.0000 ± 0.00000	0.0000	0.0000
ACETYLENE	0.0010 ± 0.00000	0.0009	0.0013
ETHYLENE	0.0000 ± 0.00000	0.0000	0.0000
ETHANE	0.0000 ± 0.00000	0.0000	0.0000
ARGON	0.0082 ± 0.00050	0.0119	0.0116

UPPER LAYER EQUIVALENCE RATIO:	1.197 ± 0.0188
PLUME EQUIVALENCE RATIO AT INTERFACE HEIGHT:	1.624 ± 0.0705
STOICHIOMETRIC FUEL/AIR MASS RATIO:	0.0611
SAMPLE TEMPERATURE:	273.9 °C
HOOD TEMPERATURE:	216.1 °C

HEAT OF FORMATION PER MOLE OF FUEL:	-17.351	kcal/mole
HEAT OF FORMATION PER MOLE OF AIR:	-0.463	kcal/mole
HEAT OF FORMATION PER MOLE OF PRODUCTS:	-15.930	kcal/mole
HEAT OF FORMATION PER MOLE OF STOICHIOMETRIC PRODUCTS :	-20.185	kcal/mole
ACTUAL HEAT OF REACTION:	-125.208	kcal/mole of fuel
HEAT OF STOICHIOMETRIC REACTION:	-194.914	kcal/mole of fuel
(ACTUAL/STOICHIOMETRIC) HEAT OF REACTION:	0.642	
(ACTUAL/MAXIMUM) HEAT OF REACTION:	0.769	

DATA REDUCTION PROGRAM OUTPUT

RUN DATE:	03-26-88	EXPERIMENT NUMBER:	21
RUN TIME:	16:29	INTEGRATER RUN NUMBER:	247
INTERFACE HEIGHT:	10.0 cm	LAB PRESSURE:	738.4 ± 0.5 torr
BURNER DIAMETER:	19.0 cm	DRY-BULB TEMPERATURE:	24.0 ± 0.2 °C
FIRE SIZE:	57.3 ± 1.64 kW	WET-BULB TEMPERATURE:	12.8 ± 0.2 °C

SUPPLY FLOWRATES :

NATURAL GAS FUEL:	1.1399 ± 0.0326	g/sec
AIR ENTRAINED BY PLUME:	11.4830 ± 0.3382	g/sec
AIR ADDED TO UPPER LAYER:	6.3130 ± 0.6247	g/sec
TOTAL:	18.9359 ± 0.9955	g/sec

I =	9.2701 ± 0.0666 moles Air/mole Fuel	FUEL INLET REYNOLDS NUMBER:	697.2
I_s =	9.7161 ± 0.1366 moles Air/mole Fuel	FUEL INLET RICHARDSON NUMBER:	0.4782

FUEL COMPOSITION : (mole fractions)		AIR COMPOSITION : (mole fractions)	
METHANE	0.9382 ± 0.0100	OXYGEN	0.2079 ± 0.0010
ETHANE	0.0298 ± 0.0050	NITROGEN	0.7750 ± 0.0020
PROPANE	0.0079 ± 0.0020	WATER VAPOR	0.0075 ± 0.0004
NITROGEN	0.0162 ± 0.0020	CARBON DIOXIDE	0.0003 ± 0.0001
CARBON DIOXIDE	0.0079 ± 0.0020	ARGON	0.0092 ± 0.0006

FUEL VISCOSITY:	109.56 μPoise
FUEL MOLECULAR WEIGHT:	17.16 g/mole
FUEL LOWER HEATING VALUE:	50.51 MJ/kg

PRODUCT LAYER ANALYSIS :

	mole fractions	mass fractions	mass fraction of plume equivalent source
HYDROGEN	0.0000 ± 0.00000	0.0000	0.0000
OXYGEN	0.0454 ± 0.00130	0.0526	-.0363
NITROGEN	0.6986 ± 0.00370	0.7086	0.6871
METHANE	0.0215 ± 0.00120	0.0125	0.0187
CARBON MONOXIDE	0.0107 ± 0.00030	0.0108	0.0162
CARBON DIOXIDE	0.0665 ± 0.00080	0.1059	0.1587
WATER VAPOR	0.1484 ± 0.00500	0.0968	0.1429
SOOT (C_8H)	0.0000 ± 0.00000	0.0000	0.0000
ACETYLENE	0.0008 ± 0.00000	0.0007	0.0011
ETHYLENE	0.0000 ± 0.00000	0.0000	0.0000
ETHANE	0.0000 ± 0.00000	0.0000	0.0000
ARGON	0.0083 ± 0.00050	0.0120	0.0116

UPPER LAYER EQUIVALENCE RATIO:	1.048 ± 0.0166
PLUME EQUIVALENCE RATIO AT INTERFACE HEIGHT:	1.624 ± 0.0705
STOICHIOMETRIC FUEL/AIR MASS RATIO:	0.0611
SAMPLE TEMPERATURE:	278.9 °C
HOOD TEMPERATURE:	222.8 °C

HEAT OF FORMATION PER MOLE OF FUEL:	-17.351	kcal/mole
HEAT OF FORMATION PER MOLE OF AIR:	-0.463	kcal/mole
HEAT OF FORMATION PER MOLE OF PRODUCTS:	-15.451	kcal/mole
HEAT OF FORMATION PER MOLE OF STOICHIOMETRIC PRODUCTS :	-20.185	kcal/mole
ACTUAL HEAT OF REACTION:	-137.624	kcal/mole of fuel
HEAT OF STOICHIOMETRIC REACTION:	-194.914	kcal/mole of fuel
(ACTUAL/STOICHIOMETRIC) HEAT OF REACTION:	0.706	
(ACTUAL/MAXIMUM) HEAT OF REACTION:	0.740	

DATA REDUCTION PROGRAM OUTPUT

RUN DATE:	03-26-88	EXPERIMENT NUMBER:	22
RUN TIME:	16:48	INTEGRATER RUN NUMBER:	248
INTERFACE HEIGHT:	10.0 cm	LAB PRESSURE:	738.4 ± 0.5 torr
BURNER DIAMETER:	19.0 cm	DRY-BULB TEMPERATURE:	24.0 ± 0.2 °C
FIRE SIZE:	57.3 ± 1.64 kW	WET-BULB TEMPERATURE:	12.8 ± 0.2 °C

SUPPLY FLOWRATES :

NATURAL GAS FUEL:	1.1399 ± 0.0326	g/sec
AIR ENTRAINED BY PLUME:	11.4830 ± 0.3382	g/sec
AIR ADDED TO UPPER LAYER:	6.3120 ± 0.6244	g/sec
TOTAL:	18.9349 ± 0.9952	g/sec

I = 9.2696 ± 0.0659 moles Air/mole Fuel
I_s = 9.7161 ± 0.1366 moles Air/mole Fuel

FUEL INLET REYNOLDS NUMBER: 697.2
FUEL INLET RICHARDSON NUMBER: 0.4782

FUEL COMPOSITION : (mole fractions)

METHANE	0.9382 ± 0.0100
ETHANE	0.0298 ± 0.0050
PROPANE	0.0079 ± 0.0020
NITROGEN	0.0162 ± 0.0020
CARBON DIOXIDE	0.0079 ± 0.0020

AIR COMPOSITION : (mole fractions)

OXYGEN	0.2079 ± 0.0010
NITROGEN	0.7750 ± 0.0020
WATER VAPOR	0.0075 ± 0.0004
CARBON DIOXIDE	0.0003 ± 0.0001
ARGON	0.0092 ± 0.0006

FUEL VISCOSITY:	109.56 μPoise
FUEL MOLECULAR WEIGHT:	17.16 g/mole
FUEL LOWER HEATING VALUE:	50.51 MJ/kg

PRODUCT LAYER ANALYSIS :

	mole fractions	mass fractions	mass fraction of plume equivalent source
HYDROGEN	0.0000 ± 0.00000	0.0000	0.0000
OXYGEN	0.0446 ± 0.00130	0.0517	-.0377
NITROGEN	0.6982 ± 0.00370	0.7086	0.6870
METHANE	0.0213 ± 0.00110	0.0124	0.0186
CARBON MONOXIDE	0.0104 ± 0.00030	0.0106	0.0158
CARBON DIOXIDE	0.0667 ± 0.00080	0.1064	0.1594
WATER VAPOR	0.1496 ± 0.00490	0.0976	0.1441
SOOT (C_8H)	0.0000 ± 0.00000	0.0000	0.0000
ACETYLENE	0.0008 ± 0.00000	0.0008	0.0011
ETHYLENE	0.0000 ± 0.00000	0.0000	0.0000
ETHANE	0.0000 ± 0.00000	0.0000	0.0000
ARGON	0.0083 ± 0.00050	0.0120	0.0116

UPPER LAYER EQUIVALENCE RATIO:	1.048 ± 0.0165
PLUME EQUIVALENCE RATIO AT INTERFACE HEIGHT:	1.624 ± 0.0705
STOICHIOMETRIC FUEL/AIR MASS RATIO:	0.0611
SAMPLE TEMPERATURE:	279.4 °C
HOOD TEMPERATURE:	222.8 °C

HEAT OF FORMATION PER MOLE OF FUEL:	-17.351	kcal/mole
HEAT OF FORMATION PER MOLE OF AIR:	-0.463	kcal/mole
HEAT OF FORMATION PER MOLE OF PRODUCTS:	-15.538	kcal/mole
HEAT OF FORMATION PER MOLE OF STOICHIOMETRIC PRODUCTS :	-20.185	kcal/mole
ACTUAL HEAT OF REACTION:	-138.582	kcal/mole of fuel
HEAT OF STOICHIOMETRIC REACTION:	-194.914	kcal/mole of fuel
(ACTUAL/STOICHIOMETRIC) HEAT OF REACTION:	0.711	
(ACTUAL/MAXIMUM) HEAT OF REACTION:	0.745	

DATA REDUCTION PROGRAM OUTPUT

RUN DATE:	03-26-88	EXPERIMENT NUMBER:	23
RUN TIME:	17:08	INTEGRATER RUN NUMBER:	249
INTERFACE HEIGHT:	10.0 cm	LAB PRESSURE:	738.4 ± 0.5 torr
BURNER DIAMETER:	19.0 cm	DRY-BULB TEMPERATURE:	24.0 ± 0.2 °C
FIRE SIZE:	57.3 ± 1.64 kW	WET-BULB TEMPERATURE:	12.8 ± 0.2 °C

SUPPLY FLOWRATES :

NATURAL GAS FUEL:	1.1399 ± 0.0326	g/sec
AIR ENTRAINED BY PLUME:	11.4830 ± 0.3382	g/sec
AIR ADDED TO UPPER LAYER:	9.1937 ± 0.6998	g/sec
TOTAL:	21.8166 ± 1.0706	g/sec

I =	10.7707 ± 0.0824	moles Air/mole Fuel	FUEL INLET REYNOLDS NUMBER: 697.2
I_s =	9.7161 ± 0.1366	moles Air/mole Fuel	FUEL INLET RICHARDSON NUMBER: 0.4782

FUEL COMPOSITION : (mole fractions)

METHANE	0.9382 ± 0.0100
ETHANE	0.0298 ± 0.0050
PROPANE	0.0079 ± 0.0020
NITROGEN	0.0162 ± 0.0020
CARBON DIOXIDE	0.0079 ± 0.0020

AIR COMPOSITION : (mole fractions)

OXYGEN	0.2079 ± 0.0010
NITROGEN	0.7750 ± 0.0020
WATER VAPOR	0.0075 ± 0.0004
CARBON DIOXIDE	0.0003 ± 0.0001
ARGON	0.0092 ± 0.0006

FUEL VISCOSITY:	109.56 μPoise
FUEL MOLECULAR WEIGHT:	17.16 g/mole
FUEL LOWER HEATING VALUE:	50.51 MJ/kg

PRODUCT LAYER ANALYSIS :

	mole fractions	mass fractions	mass fraction of plume equivalent source
HYDROGEN	0.0000 ± 0.00000	0.0000	0.0000
OXYGEN	0.0521 ± 0.00140	0.0599	-.0642
NITROGEN	0.7089 ± 0.00390	0.7143	0.6871
METHANE	0.0129 ± 0.00070	0.0074	0.0128
CARBON MONOXIDE	0.0081 ± 0.00020	0.0082	0.0142
CARBON DIOXIDE	0.0665 ± 0.00080	0.1053	0.1816
WATER VAPOR	0.1431 ± 0.00530	0.0927	0.1568
SOOT (C_8H)	0.0000 ± 0.00000	0.0000	0.0000
ACETYLENE	0.0000 ± 0.00000	0.0000	0.0000
ETHYLENE	0.0000 ± 0.00000	0.0000	0.0000
ETHANE	0.0000 ± 0.00000	0.0000	0.0000
ARGON	0.0084 ± 0.00060	0.0121	0.0116

UPPER LAYER EQUIVALENCE RATIO:	0.902 ± 0.0144
PLUME EQUIVALENCE RATIO AT INTERFACE HEIGHT:	1.624 ± 0.0705
STOICHIOMETRIC FUEL/AIR MASS RATIO:	0.0611
SAMPLE TEMPERATURE:	290.6 °C
HOOD TEMPERATURE:	231.7 °C

HEAT OF FORMATION PER MOLE OF FUEL:	-17.351	kcal/mole
HEAT OF FORMATION PER MOLE OF AIR:	-0.463	kcal/mole
HEAT OF FORMATION PER MOLE OF PRODUCTS:	-14.970	kcal/mole
HEAT OF FORMATION PER MOLE OF STOICHIOMETRIC PRODUCTS :	-20.185	kcal/mole
ACTUAL HEAT OF REACTION:	-154.275	kcal/mole of fuel
HEAT OF STOICHIOMETRIC REACTION:	-194.914	kcal/mole of fuel
(ACTUAL/STOICHIOMETRIC) HEAT OF REACTION:	0.791	
(ACTUAL/MAXIMUM) HEAT OF REACTION:	0.791	

DATA REDUCTION PROGRAM OUTPUT

RUN DATE:	03-26-88	EXPERIMENT NUMBER:	24
RUN TIME:	17:26	INTEGRATER RUN NUMBER:	250
INTERFACE HEIGHT:	10.0 cm	LAB PRESSURE:	738.4 ± 0.5 torr
BURNER DIAMETER:	19.0 cm	DRY-BULB TEMPERATURE:	24.0 ± 0.2 °C
FIRE SIZE:	57.3 ± 1.64 kW	WET-BULB TEMPERATURE:	12.8 ± 0.2 °C

SUPPLY FLOWRATES :

NATURAL GAS FUEL:	1.1399 ± 0.0326	g/sec
AIR ENTRAINED BY PLUME:	11.4830 ± 0.3382	g/sec
AIR ADDED TO UPPER LAYER:	8.1442 ± 0.6745	g/sec
TOTAL:	20.7671 ± 1.0453	g/sec

I = 10.2239 ± 0.0823 moles Air/mole Fuel
I_s = 9.7161 ± 0.1366 moles Air/mole Fuel

FUEL INLET REYNOLDS NUMBER: 697.2
FUEL INLET RICHARDSON NUMBER: 0.4782

FUEL COMPOSITION : (mole fractions)

METHANE	0.9382 ± 0.0100
ETHANE	0.0298 ± 0.0050
PROPANE	0.0079 ± 0.0020
NITROGEN	0.0162 ± 0.0020
CARBON DIOXIDE	0.0079 ± 0.0020

AIR COMPOSITION : (mole fractions)

OXYGEN	0.2079 ± 0.0010
NITROGEN	0.7750 ± 0.0020
WATER VAPOR	0.0075 ± 0.0004
CARBON DIOXIDE	0.0003 ± 0.0001
ARGON	0.0092 ± 0.0006

FUEL VISCOSITY:	109.56 μPoise
FUEL MOLECULAR WEIGHT:	17.16 g/mole
FUEL LOWER HEATING VALUE:	50.51 MJ/kg

PRODUCT LAYER ANALYSIS :

	mole fractions	mass fractions	mass fraction of plume equivalent source
HYDROGEN	0.0000 ± 0.00000	0.0000	0.0000
OXYGEN	0.0540 ± 0.00150	0.0622	-.0463
NITROGEN	0.7078 ± 0.00400	0.7129	0.6878
METHANE	0.0151 ± 0.00080	0.0087	0.0144
CARBON MONOXIDE	0.0098 ± 0.00020	0.0098	0.0162
CARBON DIOXIDE	0.0657 ± 0.00080	0.1040	0.1708
WATER VAPOR	0.1384 ± 0.00540	0.0896	0.1445
SOOT (C_8H)	0.0000 ± 0.00000	0.0000	0.0000
ACETYLENE	0.0007 ± 0.00000	0.0006	0.0011
ETHYLENE	0.0000 ± 0.00000	0.0000	0.0000
ETHANE	0.0000 ± 0.00000	0.0000	0.0000
ARGON	0.0084 ± 0.00060	0.0121	0.0116

UPPER LAYER EQUIVALENCE RATIO:	0.950 ± 0.0154
PLUME EQUIVALENCE RATIO AT INTERFACE HEIGHT:	1.624 ± 0.0705
STOICHIOMETRIC FUEL/AIR MASS RATIO:	0.0611
SAMPLE TEMPERATURE:	291.1 °C
HOOD TEMPERATURE:	231.7 °C

HEAT OF FORMATION PER MOLE OF FUEL:	-17.351	kcal/mole
HEAT OF FORMATION PER MOLE OF AIR:	-0.463	kcal/mole
HEAT OF FORMATION PER MOLE OF PRODUCTS:	-14.675	kcal/mole
HEAT OF FORMATION PER MOLE OF STOICHIOMETRIC PRODUCTS :	-20.185	kcal/mole
ACTUAL HEAT OF REACTION:	-142.538	kcal/mole of fuel
HEAT OF STOICHIOMETRIC REACTION:	-194.914	kcal/mole of fuel
(ACTUAL/STOICHIOMETRIC) HEAT OF REACTION:	0.731	
(ACTUAL/MAXIMUM) HEAT OF REACTION:	0.731	

DATA REDUCTION PROGRAM OUTPUT

RUN DATE:	03-26-88	EXPERIMENT NUMBER:	25
RUN TIME:	17:45	INTEGRATER RUN NUMBER:	251
INTERFACE HEIGHT:	10.0 cm	LAB PRESSURE:	738.4 ± 0.5 torr
BURNER DIAMETER:	19.0 cm	DRY-BULB TEMPERATURE:	24.0 ± 0.2 °C
FIRE SIZE:	57.3 ± 1.64 kW	WET-BULB TEMPERATURE:	12.8 ± 0.2 °C

SUPPLY FLOWRATES :

NATURAL GAS FUEL:	1.1399 ± 0.0326	g/sec
AIR ENTRAINED BY PLUME:	11.4830 ± 0.3382	g/sec
AIR ADDED TO UPPER LAYER:	13.2443 ± 0.8103	g/sec
TOTAL:	25.8672 ± 1.1811	g/sec

I = 12.8806 ± 0.1058 moles Air/mole Fuel
I_s = 9.7161 ± 0.1366 moles Air/mole Fuel

FUEL INLET REYNOLDS NUMBER: 697.2
FUEL INLET RICHARDSON NUMBER: 0.4782

FUEL COMPOSITION : (mole fractions)		AIR COMPOSITION : (mole fractions)	
METHANE	0.9382 ± 0.0100	OXYGEN	0.2079 ± 0.0010
ETHANE	0.0298 ± 0.0050	NITROGEN	0.7750 ± 0.0020
PROPANE	0.0079 ± 0.0020	WATER VAPOR	0.0075 ± 0.0004
NITROGEN	0.0162 ± 0.0020	CARBON DIOXIDE	0.0003 ± 0.0001
CARBON DIOXIDE	0.0079 ± 0.0020	ARGON	0.0092 ± 0.0006

FUEL VISCOSITY:	109.56 μPoise
FUEL MOLECULAR WEIGHT:	17.16 g/mole
FUEL LOWER HEATING VALUE:	50.51 MJ/kg

PRODUCT LAYER ANALYSIS :

	mole fractions	mass fractions	mass fraction of plume equivalent source
HYDROGEN	0.0000 ± 0.00000	0.0000	0.0000
OXYGEN	0.0613 ± 0.00160	0.0702	-.0979
NITROGEN	0.7185 ± 0.00430	0.7200	0.6868
METHANE	0.0050 ± 0.00030	0.0029	0.0059
CARBON MONOXIDE	0.0049 ± 0.00010	0.0049	0.0101
CARBON DIOXIDE	0.0643 ± 0.00080	0.1013	0.2070
WATER VAPOR	0.1374 ± 0.00580	0.0885	0.1765
SOOT (C_8H)	0.0000 ± 0.00000	0.0000	0.0000
ACETYLENE	0.0000 ± 0.00000	0.0000	0.0000
ETHYLENE	0.0000 ± 0.00000	0.0000	0.0000
ETHANE	0.0000 ± 0.00000	0.0000	0.0000
ARGON	0.0085 ± 0.00060	0.0122	0.0116

UPPER LAYER EQUIVALENCE RATIO:	0.754 ± 0.0123
PLUME EQUIVALENCE RATIO AT INTERFACE HEIGHT:	1.624 ± 0.0705
STOICHIOMETRIC FUEL/AIR MASS RATIO:	0.0611
SAMPLE TEMPERATURE:	307.8 °C
HOOD TEMPERATURE:	236.1 °C

HEAT OF FORMATION PER MOLE OF FUEL:	-17.351	kcal/mole
HEAT OF FORMATION PER MOLE OF AIR:	-0.463	kcal/mole
HEAT OF FORMATION PER MOLE OF PRODUCTS:	-14.208	kcal/mole
HEAT OF FORMATION PER MOLE OF STOICHIOMETRIC PRODUCTS :	-20.185	kcal/mole
ACTUAL HEAT OF REACTION:	-174.404	kcal/mole of fuel
HEAT OF STOICHIOMETRIC REACTION:	-194.914	kcal/mole of fuel
(ACTUAL/STOICHIOMETRIC) HEAT OF REACTION:	0.895	
(ACTUAL/MAXIMUM) HEAT OF REACTION:	0.895	

DATA REDUCTION PROGRAM OUTPUT

RUN DATE:	03-26-88	EXPERIMENT NUMBER:	26
RUN TIME:	18:04	INTEGRATER RUN NUMBER:	252
INTERFACE HEIGHT:	10.0 cm	LAB PRESSURE:	738.4 ± 0.5 torr
BURNER DIAMETER:	19.0 cm	DRY-BULB TEMPERATURE:	24.0 ± 0.2 °C
FIRE SIZE:	57.3 ± 1.64 kW	WET-BULB TEMPERATURE:	12.8 ± 0.2 °C

SUPPLY FLOWRATES :

NATURAL GAS FUEL:	1.1399 ± 0.0326	g/sec
AIR ENTRAINED BY PLUME:	11.4830 ± 0.3382	g/sec
AIR ADDED TO UPPER LAYER:	13.2432 ± 0.8129	g/sec
TOTAL:	25.8661 ± 1.1837	g/sec

I = 12.8801 ± 0.1110 moles Air/mole Fuel
I_s = 9.7161 ± 0.1366 moles Air/mole Fuel

FUEL INLET REYNOLDS NUMBER: 697.2
FUEL INLET RICHARDSON NUMBER: 0.4782

FUEL COMPOSITION : (mole fractions)

METHANE	0.9382 ± 0.0100
ETHANE	0.0298 ± 0.0050
PROPANE	0.0079 ± 0.0020
NITROGEN	0.0162 ± 0.0020
CARBON DIOXIDE	0.0079 ± 0.0020

AIR COMPOSITION : (mole fractions)

OXYGEN	0.2079 ± 0.0010
NITROGEN	0.7750 ± 0.0020
WATER VAPOR	0.0075 ± 0.0004
CARBON DIOXIDE	0.0003 ± 0.0001
ARGON	0.0092 ± 0.0006

FUEL VISCOSITY:	109.56 μPoise
FUEL MOLECULAR WEIGHT:	17.16 g/mole
FUEL LOWER HEATING VALUE:	50.51 MJ/kg

PRODUCT LAYER ANALYSIS :

	mole fractions	mass fractions	mass fraction of plume equivalent source
HYDROGEN	0.0000 ± 0.00000	0.0000	0.0000
OXYGEN	0.0617 ± 0.00160	0.0705	-.0973
NITROGEN	0.7197 ± 0.00440	0.7202	0.6872
METHANE	0.0040 ± 0.00020	0.0023	0.0048
CARBON MONOXIDE	0.0054 ± 0.00010	0.0054	0.0112
CARBON DIOXIDE	0.0649 ± 0.00080	0.1020	0.2086
WATER VAPOR	0.1357 ± 0.00590	0.0873	0.1740
SOOT (C_8H)	0.0000 ± 0.00000	0.0000	0.0000
ACETYLENE	0.0000 ± 0.00000	0.0000	0.0000
ETHYLENE	0.0000 ± 0.00000	0.0000	0.0000
ETHANE	0.0000 ± 0.00000	0.0000	0.0000
ARGON	0.0086 ± 0.00060	0.0122	0.0116

UPPER LAYER EQUIVALENCE RATIO:	0.754 ± 0.0124
PLUME EQUIVALENCE RATIO AT INTERFACE HEIGHT:	1.624 ± 0.0705
STOICHIOMETRIC FUEL/AIR MASS RATIO:	0.0611
SAMPLE TEMPERATURE:	308.9 °C
HOOD TEMPERATURE:	237.8 °C

HEAT OF FORMATION PER MOLE OF FUEL:		-17.351 kcal/mole
HEAT OF FORMATION PER MOLE OF AIR:		-0.463 kcal/mole
HEAT OF FORMATION PER MOLE OF PRODUCTS:		-14.160 kcal/mole
HEAT OF FORMATION PER MOLE OF STOICHIOMETRIC PRODUCTS :		-20.185 kcal/mole
ACTUAL HEAT OF REACTION:	-173.392 kcal/mole of fuel	
HEAT OF STOICHIOMETRIC REACTION:	-194.914 kcal/mole of fuel	
(ACTUAL/STOICHIOMETRIC) HEAT OF REACTION:	0.890	
(ACTUAL/MAXIMUM) HEAT OF REACTION:	0.890	

DATA REDUCTION PROGRAM OUTPUT

RUN DATE:	04-13-88	EXPERIMENT NUMBER:	27
RUN TIME:	22:08	INTEGRATER RUN NUMBER:	290
INTERFACE HEIGHT:	10.0 cm	LAB PRESSURE:	738.0 ± 0.5 torr
BURNER DIAMETER:	19.0 cm	DRY-BULB TEMPERATURE:	22.9 ± 0.2 °C
FIRE SIZE:	49.5 ± 1.65 kW	WET-BULB TEMPERATURE:	15.4 ± 0.2 °C

SUPPLY FLOWRATES :

NATURAL GAS FUEL:	0.9820 ± 0.0328	g/sec
AIR ENTRAINED BY PLUME:	14.9256 ± 0.5079	g/sec
AIR ADDED TO UPPER LAYER:	0.0000 ± 0.0000	g/sec
TOTAL:	15.9076 ± 0.5407	g/sec

I = 8.9986 ± 0.0594 moles Air/mole Fuel
I_s = 9.7857 ± 0.1374 moles Air/mole Fuel

FUEL INLET REYNOLDS NUMBER: 601.5
FUEL INLET RICHARDSON NUMBER: 0.6424

FUEL COMPOSITION : (mole fractions)

METHANE	0.9423 ± 0.0100
ETHANE	0.0281 ± 0.0050
PROPANE	0.0082 ± 0.0020
NITROGEN	0.0140 ± 0.0020
CARBON DIOXIDE	0.0075 ± 0.0020

AIR COMPOSITION : (mole fractions)

OXYGEN	0.2068 ± 0.0010
NITROGEN	0.7709 ± 0.0020
WATER VAPOR	0.0128 ± 0.0004
CARBON DIOXIDE	0.0003 ± 0.0001
ARGON	0.0092 ± 0.0006

FUEL VISCOSITY:	109.41 μPoise
FUEL MOLECULAR WEIGHT:	17.11 g/mole
FUEL LOWER HEATING VALUE:	50.60 MJ/kg

PRODUCT LAYER ANALYSIS :

	mole fractions	mass fractions	mass fraction of plume equivalent source
HYDROGEN	0.0041 ± 0.00070	0.0003	0.0007
OXYGEN	0.0387 ± 0.00120	0.0451	0.0451
NITROGEN	0.6907 ± 0.00380	0.7049	0.7045
METHANE	0.0202 ± 0.00110	0.0118	0.0118
CARBON MONOXIDE	0.0095 ± 0.00020	0.0097	0.0097
CARBON DIOXIDE	0.0687 ± 0.00080	0.1102	0.1102
WATER VAPOR	0.1588 ± 0.00480	0.1042	0.1042
SOOT (C_8H)	0.0003 ± 0.00210	0.0012	0.0012
ACETYLENE	0.0007 ± 0.00000	0.0007	0.0007
ETHYLENE	0.0000 ± 0.00000	0.0000	0.0000
ETHANE	0.0000 ± 0.00000	0.0000	0.0000
ARGON	0.0082 ± 0.00050	0.0119	0.0119

UPPER LAYER EQUIVALENCE RATIO:	1.087 ± 0.0169
PLUME EQUIVALENCE RATIO AT INTERFACE HEIGHT:	1.087 ± 0.0540
STOICHIOMETRIC FUEL/AIR MASS RATIO:	0.0605
SAMPLE TEMPERATURE:	260.6 °C
HOOD TEMPERATURE:	198.9 °C

HEAT OF FORMATION PER MOLE OF FUEL:		-17.415 kcal/mole
HEAT OF FORMATION PER MOLE OF AIR:		-0.765 kcal/mole
HEAT OF FORMATION PER MOLE OF PRODUCTS:		-16.125 kcal/mole
HEAT OF FORMATION PER MOLE OF STOICHIOMETRIC PRODUCTS :		-20.366 kcal/mole
ACTUAL HEAT OF REACTION:	-138.966 kcal/mole of fuel	
HEAT OF STOICHIOMETRIC REACTION:	-195.211 kcal/mole of fuel	
(ACTUAL/STOICHIOMETRIC) HEAT OF REACTION:	0.712	
(ACTUAL/MAXIMUM) HEAT OF REACTION:	0.774	

DATA REDUCTION PROGRAM OUTPUT

RUN DATE:	04-13-88	EXPERIMENT NUMBER:	28
RUN TIME:	22:48	INTEGRATER RUN NUMBER:	292
INTERFACE HEIGHT:	10.0 cm	LAB PRESSURE:	738.0 ± 0.5 torr
BURNER DIAMETER:	19.0 cm	DRY-BULB TEMPERATURE:	22.9 ± 0.2 °C
FIRE SIZE:	49.5 ± 1.65 kW	WET-BULB TEMPERATURE:	15.4 ± 0.2 °C

SUPPLY FLOWRATES :

NATURAL GAS FUEL:	0.9820 ± 0.0328	g/sec
AIR ENTRAINED BY PLUME:	14.9260 ± 0.5079	g/sec
AIR ADDED TO UPPER LAYER:	3.2328 ± 0.8022	g/sec
TOTAL:	19.1408 ± 1.3429	g/sec

I = 10.9479 ± 0.0813 moles Air/mole Fuel
I_s = 9.7857 ± 0.1374 moles Air/mole Fuel

FUEL INLET REYNOLDS NUMBER: 601.5
FUEL INLET RICHARDSON NUMBER: 0.6424

FUEL COMPOSITION : (mole fractions)

METHANE	0.9423 ± 0.0100
ETHANE	0.0281 ± 0.0050
PROPANE	0.0082 ± 0.0020
NITROGEN	0.0140 ± 0.0020
CARBON DIOXIDE	0.0075 ± 0.0020

AIR COMPOSITION : (mole fractions)

OXYGEN	0.2068 ± 0.0010
NITROGEN	0.7709 ± 0.0020
WATER VAPOR	0.0128 ± 0.0004
CARBON DIOXIDE	0.0003 ± 0.0001
ARGON	0.0092 ± 0.0006

FUEL VISCOSITY:	109.41 μPoise
FUEL MOLECULAR WEIGHT:	17.11 g/mole
FUEL LOWER HEATING VALUE:	50.60 MJ/kg

PRODUCT LAYER ANALYSIS :

	mole fractions	mass fractions	mass fraction of plume equivalent source
HYDROGEN	0.0000 ± 0.00000	0.0000	0.0000
OXYGEN	0.0470 ± 0.00130	0.0542	0.0185
NITROGEN	0.7050 ± 0.00380	0.7123	0.7047
METHANE	0.0098 ± 0.00050	0.0057	0.0069
CARBON MONOXIDE	0.0076 ± 0.00020	0.0077	0.0093
CARBON DIOXIDE	0.0678 ± 0.00080	0.1076	0.1293
WATER VAPOR	0.1540 ± 0.00520	0.1001	0.1188
SOOT (C_8H)	0.0000 ± 0.00000	0.0000	0.0000
ACETYLENE	0.0005 ± 0.00000	0.0005	0.0006
ETHYLENE	0.0000 ± 0.00000	0.0000	0.0000
ETHANE	0.0000 ± 0.00000	0.0000	0.0000
ARGON	0.0084 ± 0.00060	0.0121	0.0119

UPPER LAYER EQUIVALENCE RATIO:	0.894 ± 0.0142
PLUME EQUIVALENCE RATIO AT INTERFACE HEIGHT:	1.087 ± 0.0540
STOICHIOMETRIC FUEL/AIR MASS RATIO:	0.0605
SAMPLE TEMPERATURE:	270.6 °C
HOOD TEMPERATURE:	209.4 °C

HEAT OF FORMATION PER MOLE OF FUEL:	-17.415	kcal/mole
HEAT OF FORMATION PER MOLE OF AIR:	-0.765	kcal/mole
HEAT OF FORMATION PER MOLE OF PRODUCTS:	-15.625	kcal/mole
HEAT OF FORMATION PER MOLE OF STOICHIOMETRIC PRODUCTS :	-20.366	kcal/mole
ACTUAL HEAT OF REACTION:	-161.585	kcal/mole of fuel
HEAT OF STOICHIOMETRIC REACTION:	-195.211	kcal/mole of fuel
(ACTUAL/STOICHIOMETRIC) HEAT OF REACTION:	0.828	
(ACTUAL/MAXIMUM) HEAT OF REACTION:	0.828	

DATA REDUCTION PROGRAM OUTPUT

RUN DATE:	04-13-88	EXPERIMENT NUMBER:	29
RUN TIME:	23:20	INTEGRATER RUN NUMBER:	294
INTERFACE HEIGHT:	10.0 cm	LAB PRESSURE:	738.0 ± 0.5 torr
BURNER DIAMETER:	19.0 cm	DRY-BULB TEMPERATURE:	22.9 ± 0.2 °C
FIRE SIZE:	49.5 ± 1.65 kW	WET-BULB TEMPERATURE:	15.4 ± 0.2 °C

SUPPLY FLOWRATES :

NATURAL GAS FUEL:	0.9820 ± 0.0328	g/sec
AIR ENTRAINED BY PLUME:	14.9260 ± 0.5079	g/sec
AIR ADDED TO UPPER LAYER:	3.3264 ± 0.8040	g/sec
TOTAL:	19.2344 ± 1.3447	g/sec

I = 11.0043 ± 0.0791 moles Air/mole Fuel
I_s = 9.7857 ± 0.1374 moles Air/mole Fuel

FUEL INLET REYNOLDS NUMBER: 601.5
FUEL INLET RICHARDSON NUMBER: 0.6424

FUEL COMPOSITION : (mole fractions)

METHANE	0.9423 ± 0.0100
ETHANE	0.0281 ± 0.0050
PROPANE	0.0082 ± 0.0020
NITROGEN	0.0140 ± 0.0020
CARBON DIOXIDE	0.0075 ± 0.0020

AIR COMPOSITION : (mole fractions)

OXYGEN	0.2068 ± 0.0010
NITROGEN	0.7709 ± 0.0020
WATER VAPOR	0.0128 ± 0.0004
CARBON DIOXIDE	0.0003 ± 0.0001
ARGON	0.0092 ± 0.0006

FUEL VISCOSITY:	109.41 μPoise
FUEL MOLECULAR WEIGHT:	17.11 g/mole
FUEL LOWER HEATING VALUE:	50.60 MJ/kg

PRODUCT LAYER ANALYSIS :

	mole fractions	mass fractions	mass fraction of plume equivalent source
HYDROGEN	0.0000 ± 0.00000	0.0000	0.0000
OXYGEN	0.0532 ± 0.00140	0.0615	0.0263
NITROGEN	0.7042 ± 0.00410	0.7122	0.7045
METHANE	0.0129 ± 0.00070	0.0075	0.0090
CARBON MONOXIDE	0.0058 ± 0.00010	0.0059	0.0072
CARBON DIOXIDE	0.0636 ± 0.00080	0.1010	0.1220
WATER VAPOR	0.1512 ± 0.00530	0.0983	0.1172
SOOT (C_8H)	0.0003 ± 0.00170	0.0011	0.0014
ACETYLENE	0.0004 ± 0.00000	0.0004	0.0004
ETHYLENE	0.0000 ± 0.00000	0.0000	0.0000
ETHANE	0.0000 ± 0.00000	0.0000	0.0000
ARGON	0.0084 ± 0.00060	0.0121	0.0119

UPPER LAYER EQUIVALENCE RATIO:	0.889 ± 0.0140
PLUME EQUIVALENCE RATIO AT INTERFACE HEIGHT:	1.087 ± 0.0540
STOICHIOMETRIC FUEL/AIR MASS RATIO:	0.0605
SAMPLE TEMPERATURE:	273.3 °C
HOOD TEMPERATURE:	212.8 °C

HEAT OF FORMATION PER MOLE OF FUEL:	-17.415	kcal/mole
HEAT OF FORMATION PER MOLE OF AIR:	-0.765	kcal/mole
HEAT OF FORMATION PER MOLE OF PRODUCTS:	-15.082	kcal/mole
HEAT OF FORMATION PER MOLE OF STOICHIOMETRIC PRODUCTS :	-20.366	kcal/mole
ACTUAL HEAT OF REACTION:	-156.163	kcal/mole of fuel
HEAT OF STOICHIOMETRIC REACTION:	-195.211	kcal/mole of fuel
(ACTUAL/STOICHIOMETRIC) HEAT OF REACTION:	0.800	
(ACTUAL/MAXIMUM) HEAT OF REACTION:	0.800	

DATA REDUCTION PROGRAM OUTPUT

RUN DATE:	04-13-88	EXPERIMENT NUMBER:	30
RUN TIME:	23:38	INTEGRATER RUN NUMBER:	295
INTERFACE HEIGHT:	10.0 cm	LAB PRESSURE:	738.0 ± 0.5 torr
BURNER DIAMETER:	19.0 cm	DRY-BULB TEMPERATURE:	22.9 ± 0.2 °C
FIRE SIZE:	49.5 ± 1.65 kW	WET-BULB TEMPERATURE:	15.4 ± 0.2 °C

SUPPLY FLOWRATES :

NATURAL GAS FUEL:	0.9820 ± 0.0328	g/sec
AIR ENTRAINED BY PLUME:	14.9260 ± 0.5079	g/sec
AIR ADDED TO UPPER LAYER:	7.5167 ± 0.9258	g/sec
TOTAL:	23.4247 ± 1.4665	g/sec

I =	13.5306 ± 0.1175 moles Air/mole Fuel	FUEL INLET REYNOLDS NUMBER:	601.5
I_s =	9.7857 ± 0.1374 moles Air/mole Fuel	FUEL INLET RICHARDSON NUMBER:	0.6424

FUEL COMPOSITION : (mole fractions)		AIR COMPOSITION : (mole fractions)	
METHANE	0.9423 ± 0.0100	OXYGEN	0.2068 ± 0.0010
ETHANE	0.0281 ± 0.0050	NITROGEN	0.7709 ± 0.0020
PROPANE	0.0082 ± 0.0020	WATER VAPOR	0.0128 ± 0.0004
NITROGEN	0.0140 ± 0.0020	CARBON DIOXIDE	0.0003 ± 0.0001
CARBON DIOXIDE	0.0075 ± 0.0020	ARGON	0.0092 ± 0.0006

FUEL VISCOSITY:	109.41	μPoise
FUEL MOLECULAR WEIGHT:	17.11	g/mole
FUEL LOWER HEATING VALUE:	50.60	MJ/kg

PRODUCT LAYER ANALYSIS :

	mole fractions	mass fractions	mass fraction of plume equivalent source
HYDROGEN	0.0000 ± 0.00000	0.0000	0.0000
OXYGEN	0.0634 ± 0.00170	0.0726	-.0016
NITROGEN	0.7177 ± 0.00450	0.7191	0.7048
METHANE	0.0022 ± 0.00010	0.0013	0.0019
CARBON MONOXIDE	0.0047 ± 0.00010	0.0048	0.0070
CARBON DIOXIDE	0.0634 ± 0.00080	0.0998	0.1467
WATER VAPOR	0.1397 ± 0.00600	0.0900	0.1288
SOOT (C_8H)	0.0000 ± 0.00000	0.0000	0.0000
ACETYLENE	0.0004 ± 0.00000	0.0003	0.0005
ETHYLENE	0.0000 ± 0.00000	0.0000	0.0000
ETHANE	0.0000 ± 0.00000	0.0000	0.0000
ARGON	0.0085 ± 0.00060	0.0122	0.0119

UPPER LAYER EQUIVALENCE RATIO:	0.723 ± 0.0119	
PLUME EQUIVALENCE RATIO AT INTERFACE HEIGHT:	1.087 ± 0.0540	
STOICHIOMETRIC FUEL/AIR MASS RATIO:	0.0605	
SAMPLE TEMPERATURE:	275.6 °C	
HOOD TEMPERATURE:	216.7 °C	
HEAT OF FORMATION PER MOLE OF FUEL:		-17.415 kcal/mole
HEAT OF FORMATION PER MOLE OF AIR:		-0.765 kcal/mole
HEAT OF FORMATION PER MOLE OF PRODUCTS:		-14.180 kcal/mole
HEAT OF FORMATION PER MOLE OF STOICHIOMETRIC PRODUCTS :		-20.366 kcal/mole
ACTUAL HEAT OF REACTION:	-178.613 kcal/mole of fuel	
HEAT OF STOICHIOMETRIC REACTION:	-195.211 kcal/mole of fuel	
(ACTUAL/STOICHIOMETRIC) HEAT OF REACTION:	0.915	
(ACTUAL/MAXIMUM) HEAT OF REACTION:	0.915	

DATA REDUCTION PROGRAM OUTPUT

RUN DATE:	04-13-88	EXPERIMENT NUMBER:	31
RUN TIME:	23:56	INTEGRATER RUN NUMBER:	296
INTERFACE HEIGHT:	10.0 cm	LAB PRESSURE:	738.0 ± 0.5 torr
BURNER DIAMETER:	19.0 cm	DRY-BULB TEMPERATURE:	22.9 ± 0.2 °C
FIRE SIZE:	49.5 ± 1.65 kW	WET-BULB TEMPERATURE:	15.4 ± 0.2 °C

SUPPLY FLOWRATES :

NATURAL GAS FUEL:	0.9820 ± 0.0328	g/sec
AIR ENTRAINED BY PLUME:	14.9260 ± 0.5079	g/sec
AIR ADDED TO UPPER LAYER:	9.2139 ± 0.9775	g/sec
TOTAL:	25.1219 ± 1.5182	g/sec

I = 14.5539 ± 0.1325 moles Air/mole Fuel
I_s = 9.7857 ± 0.1374 moles Air/mole Fuel

FUEL INLET REYNOLDS NUMBER: 601.5
FUEL INLET RICHARDSON NUMBER: 0.6424

FUEL COMPOSITION : (mole fractions)

METHANE	0.9423 ± 0.0100
ETHANE	0.0281 ± 0.0050
PROPANE	0.0082 ± 0.0020
NITROGEN	0.0140 ± 0.0020
CARBON DIOXIDE	0.0075 ± 0.0020

AIR COMPOSITION : (mole fractions)

OXYGEN	0.2068 ± 0.0010
NITROGEN	0.7709 ± 0.0020
WATER VAPOR	0.0128 ± 0.0004
CARBON DIOXIDE	0.0003 ± 0.0001
ARGON	0.0092 ± 0.0006

FUEL VISCOSITY:	109.41 μPoise
FUEL MOLECULAR WEIGHT:	17.11 g/mole
FUEL LOWER HEATING VALUE:	50.60 MJ/kg

PRODUCT LAYER ANALYSIS :

	mole fractions	mass fractions	mass fraction of plume equivalent source
HYDROGEN	0.0000 ± 0.00000	0.0000	0.0000
OXYGEN	0.0697 ± 0.00180	0.0796	-.0072
NITROGEN	0.7213 ± 0.00470	0.7211	0.7048
METHANE	0.0014 ± 0.00010	0.0008	0.0013
CARBON MONOXIDE	0.0035 ± 0.00010	0.0035	0.0055
CARBON DIOXIDE	0.0615 ± 0.00080	0.0966	0.1523
WATER VAPOR	0.1339 ± 0.00630	0.0861	0.1314
SOOT (C_8H)	0.0000 ± 0.00000	0.0000	0.0000
ACETYLENE	0.0000 ± 0.00000	0.0000	0.0000
ETHYLENE	0.0000 ± 0.00000	0.0000	0.0000
ETHANE	0.0000 ± 0.00000	0.0000	0.0000
ARGON	0.0086 ± 0.00060	0.0122	0.0119

UPPER LAYER EQUIVALENCE RATIO:	0.672 ± 0.0112
PLUME EQUIVALENCE RATIO AT INTERFACE HEIGHT:	1.087 ± 0.0540
STOICHIOMETRIC FUEL/AIR MASS RATIO:	0.0605
SAMPLE TEMPERATURE:	276.1 °C
HOOD TEMPERATURE:	218.9 °C

HEAT OF FORMATION PER MOLE OF FUEL:	-17.415	kcal/mole
HEAT OF FORMATION PER MOLE OF AIR:	-0.765	kcal/mole
HEAT OF FORMATION PER MOLE OF PRODUCTS:	-13.645	kcal/mole
HEAT OF FORMATION PER MOLE OF STOICHIOMETRIC PRODUCTS :	-20.366	kcal/mole
ACTUAL HEAT OF REACTION:	-183.978	kcal/mole of fuel
HEAT OF STOICHIOMETRIC REACTION:	-195.211	kcal/mole of fuel
(ACTUAL/STOICHIOMETRIC) HEAT OF REACTION:	0.942	
(ACTUAL/MAXIMUM) HEAT OF REACTION:	0.942	

DATA REDUCTION PROGRAM OUTPUT

RUN DATE:	04-14-88	EXPERIMENT NUMBER:	32
RUN TIME:	00:15	INTEGRATER RUN NUMBER:	297
INTERFACE HEIGHT:	10.0 cm	LAB PRESSURE:	738.0 ± 0.5 torr
BURNER DIAMETER:	19.0 cm	DRY-BULB TEMPERATURE:	22.9 ± 0.2 °C
FIRE SIZE:	49.5 ± 1.65 kW	WET-BULB TEMPERATURE:	15.4 ± 0.2 °C

SUPPLY FLOWRATES :

NATURAL GAS FUEL:	0.9820 ± 0.0328	g/sec
AIR ENTRAINED BY PLUME:	14.9260 ± 0.5079	g/sec
AIR ADDED TO UPPER LAYER:	11.1171 ± 1.0382	g/sec
TOTAL:	27.0251 ± 1.5789	g/sec

I =	15.7013 ± 0.1527 moles Air/mole Fuel	FUEL INLET REYNOLDS NUMBER:	601.5
I_s =	9.7857 ± 0.1374 moles Air/mole Fuel	FUEL INLET RICHARDSON NUMBER:	0.6424

FUEL COMPOSITION : (mole fractions)

METHANE	0.9423 ± 0.0100
ETHANE	0.0281 ± 0.0050
PROPANE	0.0082 ± 0.0020
NITROGEN	0.0140 ± 0.0020
CARBON DIOXIDE	0.0075 ± 0.0020

AIR COMPOSITION : (mole fractions)

OXYGEN	0.2068 ± 0.0010
NITROGEN	0.7709 ± 0.0020
WATER VAPOR	0.0128 ± 0.0004
CARBON DIOXIDE	0.0003 ± 0.0001
ARGON	0.0092 ± 0.0006

FUEL VISCOSITY:	109.41 μPoise
FUEL MOLECULAR WEIGHT:	17.11 g/mole
FUEL LOWER HEATING VALUE:	50.60 MJ/kg

PRODUCT LAYER ANALYSIS :

	mole fractions	mass fractions	mass fraction of plume equivalent source
HYDROGEN	0.0000 ± 0.00000	0.0000	0.0000
OXYGEN	0.0761 ± 0.00190	0.0867	-.0132
NITROGEN	0.7249 ± 0.00510	0.7231	0.7048
METHANE	0.0000 ± 0.00000	0.0000	0.0000
CARBON MONOXIDE	0.0026 ± 0.00010	0.0026	0.0044
CARBON DIOXIDE	0.0593 ± 0.00080	0.0929	0.1576
WATER VAPOR	0.1285 ± 0.00670	0.0824	0.1344
SOOT (C_8H)	0.0000 ± 0.00000	0.0000	0.0000
ACETYLENE	0.0000 ± 0.00000	0.0000	0.0000
ETHYLENE	0.0000 ± 0.00000	0.0000	0.0000
ETHANE	0.0000 ± 0.00000	0.0000	0.0000
ARGON	0.0086 ± 0.00060	0.0123	0.0119

UPPER LAYER EQUIVALENCE RATIO:	0.623 ± 0.0106
PLUME EQUIVALENCE RATIO AT INTERFACE HEIGHT:	1.087 ± 0.0540
STOICHIOMETRIC FUEL/AIR MASS RATIO:	0.0605
SAMPLE TEMPERATURE:	276.1 °C
HOOD TEMPERATURE:	221.7 °C

HEAT OF FORMATION PER MOLE OF FUEL:	-17.415	kcal/mole
HEAT OF FORMATION PER MOLE OF AIR:	-0.765	kcal/mole
HEAT OF FORMATION PER MOLE OF PRODUCTS:	-13.073	kcal/mole
HEAT OF FORMATION PER MOLE OF STOICHIOMETRIC PRODUCTS :	-20.366	kcal/mole
ACTUAL HEAT OF REACTION:	-189.131	kcal/mole of fuel
HEAT OF STOICHIOMETRIC REACTION:	-195.211	kcal/mole of fuel
(ACTUAL/STOICHIOMETRIC) HEAT OF REACTION:	0.969	
(ACTUAL/MAXIMUM) HEAT OF REACTION:	0.969	

DATA REDUCTION PROGRAM OUTPUT

RUN DATE:	04-14-88	EXPERIMENT NUMBER:	33
RUN TIME:	00:43	INTEGRATER RUN NUMBER:	299
INTERFACE HEIGHT:	10.0 cm	LAB PRESSURE:	738.0 ± 0.5 torr
BURNER DIAMETER:	19.0 cm	DRY-BULB TEMPERATURE:	22.9 ± 0.2 °C
FIRE SIZE:	49.5 ± 1.65 kW	WET-BULB TEMPERATURE:	15.4 ± 0.2 °C

SUPPLY FLOWRATES :

NATURAL GAS FUEL:	0.9820 ± 0.0328	g/sec
AIR ENTRAINED BY PLUME:	14.9260 ± 0.5079	g/sec
AIR ADDED TO UPPER LAYER:	13.7395 ± 1.1221	g/sec
TOTAL:	29.6475 ± 1.6628	g/sec

I = 17.2823 ± 0.1764 moles Air/mole Fuel
I_s = 9.7857 ± 0.1374 moles Air/mole Fuel

FUEL INLET REYNOLDS NUMBER: 601.5
FUEL INLET RICHARDSON NUMBER: 0.6424

FUEL COMPOSITION : (mole fractions)		AIR COMPOSITION : (mole fractions)	
METHANE	0.9423 ± 0.0100	OXYGEN	0.2068 ± 0.0010
ETHANE	0.0281 ± 0.0050	NITROGEN	0.7709 ± 0.0020
PROPANE	0.0082 ± 0.0020	WATER VAPOR	0.0128 ± 0.0004
NITROGEN	0.0140 ± 0.0020	CARBON DIOXIDE	0.0003 ± 0.0001
CARBON DIOXIDE	0.0075 ± 0.0020	ARGON	0.0092 ± 0.0006

FUEL VISCOSITY:	109.41	μPoise
FUEL MOLECULAR WEIGHT:	17.11	g/mole
FUEL LOWER HEATING VALUE:	50.60	MJ/kg

PRODUCT LAYER ANALYSIS :

	mole fractions	mass fractions	mass fraction of plume equivalent source
HYDROGEN	0.0000 ± 0.00000	0.0000	0.0000
OXYGEN	0.0873 ± 0.00220	0.0994	-.0131
NITROGEN	0.7282 ± 0.00560	0.7252	0.7045
METHANE	0.0000 ± 0.00000	0.0000	0.0000
CARBON MONOXIDE	0.0008 ± 0.00000	0.0008	0.0015
CARBON DIOXIDE	0.0535 ± 0.00070	0.0837	0.1557
WATER VAPOR	0.1212 ± 0.00730	0.0776	0.1378
SOOT (C_8H)	0.0003 ± 0.00120	0.0010	0.0018
ACETYLENE	0.0000 ± 0.00000	0.0000	0.0000
ETHYLENE	0.0000 ± 0.00000	0.0000	0.0000
ETHANE	0.0000 ± 0.00000	0.0000	0.0000
ARGON	0.0087 ± 0.00060	0.0123	0.0119

UPPER LAYER EQUIVALENCE RATIO:	0.566 ± 0.0098	
PLUME EQUIVALENCE RATIO AT INTERFACE HEIGHT:	1.087 ± 0.0540	
STOICHIOMETRIC FUEL/AIR MASS RATIO:	0.0605	
SAMPLE TEMPERATURE:	275.6 °C	
HOOD TEMPERATURE:	220.0 °C	
HEAT OF FORMATION PER MOLE OF FUEL:	-17.415	kcal/mole
HEAT OF FORMATION PER MOLE OF AIR:	-0.765	kcal/mole
HEAT OF FORMATION PER MOLE OF PRODUCTS:	-12.060	kcal/mole
HEAT OF FORMATION PER MOLE OF STOICHIOMETRIC PRODUCTS :	-20.366	kcal/mole
ACTUAL HEAT OF REACTION:	-190.245	kcal/mole of fuel
HEAT OF STOICHIOMETRIC REACTION:	-195.211	kcal/mole of fuel
(ACTUAL/STOICHIOMETRIC) HEAT OF REACTION:	0.975	
(ACTUAL/MAXIMUM) HEAT OF REACTION:	0.975	

DATA REDUCTION PROGRAM OUTPUT

RUN DATE:	04-14-88	EXPERIMENT NUMBER:	34
RUN TIME:	01:00	INTEGRATER RUN NUMBER:	300
INTERFACE HEIGHT:	10.0 cm	LAB PRESSURE:	738.0 ± 0.5 torr
BURNER DIAMETER:	19.0 cm	DRY-BULB TEMPERATURE:	22.9 ± 0.2 °C
FIRE SIZE:	49.5 ± 1.65 kW	WET-BULB TEMPERATURE:	15.4 ± 0.2 °C

SUPPLY FLOWRATES :

NATURAL GAS FUEL:	0.9820 ± 0.0328	g/sec
AIR ENTRAINED BY PLUME:	14.9260 ± 0.5079	g/sec
AIR ADDED TO UPPER LAYER:	26.6717 ± 1.6549	g/sec
TOTAL:	42.5797 ± 2.1956	g/sec

I =	25.0791 ± 0.4483 moles Air/mole Fuel	FUEL INLET REYNOLDS NUMBER:	601.5
I_s =	9.7857 ± 0.1374 moles Air/mole Fuel	FUEL INLET RICHARDSON NUMBER:	0.6424

FUEL COMPOSITION : (mole fractions)		AIR COMPOSITION : (mole fractions)	
METHANE	0.9423 ± 0.0100	OXYGEN	0.2068 ± 0.0010
ETHANE	0.0281 ± 0.0050	NITROGEN	0.7709 ± 0.0020
PROPANE	0.0082 ± 0.0020	WATER VAPOR	0.0128 ± 0.0004
NITROGEN	0.0140 ± 0.0020	CARBON DIOXIDE	0.0003 ± 0.0001
CARBON DIOXIDE	0.0075 ± 0.0020	ARGON	0.0092 ± 0.0006

FUEL VISCOSITY:	109.41 μPoise
FUEL MOLECULAR WEIGHT:	17.11 g/mole
FUEL LOWER HEATING VALUE:	50.60 MJ/kg

PRODUCT LAYER ANALYSIS :

	mole fractions	mass fractions	mass fraction of plume equivalent source
HYDROGEN	0.0000 ± 0.00000	0.0000	0.0000
OXYGEN	0.1233 ± 0.00320	0.1389	-.0131
NITROGEN	0.7427 ± 0.00860	0.7327	0.7050
METHANE	0.0000 ± 0.00000	0.0000	0.0000
CARBON MONOXIDE	0.0000 ± 0.00000	0.0000	0.0000
CARBON DIOXIDE	0.0398 ± 0.00060	0.0618	0.1645
WATER VAPOR	0.0854 ± 0.01130	0.0542	0.1316
SOOT (C_8H)	0.0000 ± 0.00000	0.0000	0.0000
ACETYLENE	0.0000 ± 0.00000	0.0000	0.0000
ETHYLENE	0.0000 ± 0.00000	0.0000	0.0000
ETHANE	0.0000 ± 0.00000	0.0000	0.0000
ARGON	0.0088 ± 0.00060	0.0124	0.0120

UPPER LAYER EQUIVALENCE RATIO:	0.390 ± 0.0089
PLUME EQUIVALENCE RATIO AT INTERFACE HEIGHT:	1.087 ± 0.0540
STOICHIOMETRIC FUEL/AIR MASS RATIO:	0.0605
SAMPLE TEMPERATURE:	254.4 °C
HOOD TEMPERATURE:	191.7 °C

HEAT OF FORMATION PER MOLE OF FUEL:	-17.415	kcal/mole
HEAT OF FORMATION PER MOLE OF AIR:	-0.765	kcal/mole
HEAT OF FORMATION PER MOLE OF PRODUCTS:	-8.682	kcal/mole
HEAT OF FORMATION PER MOLE OF STOICHIOMETRIC PRODUCTS :	-20.366	kcal/mole
ACTUAL HEAT OF REACTION:	-189.590	kcal/mole of fuel
HEAT OF STOICHIOMETRIC REACTION:	-195.211	kcal/mole of fuel
(ACTUAL/STOICHIOMETRIC) HEAT OF REACTION:	0.971	
(ACTUAL/MAXIMUM) HEAT OF REACTION:	0.971	

DATA REDUCTION PROGRAM OUTPUT

RUN DATE:	04-01-88	EXPERIMENT NUMBER:	35
RUN TIME:	17:16	INTEGRATER RUN NUMBER:	262
INTERFACE HEIGHT:	10.0 cm	LAB PRESSURE:	741.4 ± 0.5 torr
BURNER DIAMETER:	19.0 cm	DRY-BULB TEMPERATURE:	22.9 ± 0.2 °C
FIRE SIZE:	41.2 ± 1.65 kW	WET-BULB TEMPERATURE:	10.5 ± 0.2 °C

SUPPLY FLOWRATES :

NATURAL GAS FUEL:	0.8250 ± 0.0330	g/sec
AIR ENTRAINED BY PLUME:	16.6687 ± 0.6812	g/sec
AIR ADDED TO UPPER LAYER:	0.0000 ± 0.0000	g/sec
TOTAL:	17.4937 ± 0.7142	g/sec

I = 11.9966 ± 0.0981 moles Air/mole Fuel
I_s = 9.6873 ± 0.1362 moles Air/mole Fuel

FUEL INLET REYNOLDS NUMBER: 504.6
FUEL INLET RICHARDSON NUMBER: 0.9189

FUEL COMPOSITION : (mole fractions)

METHANE	0.9382 ± 0.0100
ETHANE	0.0298 ± 0.0050
PROPANE	0.0079 ± 0.0020
NITROGEN	0.0162 ± 0.0020
CARBON DIOXIDE	0.0079 ± 0.0020

AIR COMPOSITION : (mole fractions)

OXYGEN	0.2085 ± 0.0010
NITROGEN	0.7773 ± 0.0020
WATER VAPOR	0.0046 ± 0.0003
CARBON DIOXIDE	0.0003 ± 0.0001
ARGON	0.0093 ± 0.0006

FUEL VISCOSITY:	109.56 μPoise
FUEL MOLECULAR WEIGHT:	17.16 g/mole
FUEL LOWER HEATING VALUE:	50.13 MJ/kg

PRODUCT LAYER ANALYSIS :

	mole fractions	mass fractions	mass fraction of plume equivalent source
HYDROGEN	0.0000 ± 0.00000	0.0000	0.0000
OXYGEN	0.0542 ± 0.00150	0.0620	0.0620
NITROGEN	0.7179 ± 0.00410	0.7194	0.7194
METHANE	0.0050 ± 0.00030	0.0029	0.0029
CARBON MONOXIDE	0.0062 ± 0.00020	0.0062	0.0062
CARBON DIOXIDE	0.0679 ± 0.00080	0.1069	0.1069
WATER VAPOR	0.1401 ± 0.00560	0.0903	0.0903
SOOT (C_8H)	0.0000 ± 0.00000	0.0000	0.0000
ACETYLENE	0.0001 ± 0.00000	0.0001	0.0001
ETHYLENE	0.0000 ± 0.00000	0.0000	0.0000
ETHANE	0.0000 ± 0.00000	0.0000	0.0000
ARGON	0.0085 ± 0.00060	0.0122	0.0122

UPPER LAYER EQUIVALENCE RATIO:	0.808 ± 0.0131
PLUME EQUIVALENCE RATIO AT INTERFACE HEIGHT:	0.808 ± 0.0476
STOICHIOMETRIC FUEL/AIR MASS RATIO:	0.0613
SAMPLE TEMPERATURE:	252.8 °C
HOOD TEMPERATURE:	191.7 °C

HEAT OF FORMATION PER MOLE OF FUEL:	-17.351	kcal/mole
HEAT OF FORMATION PER MOLE OF AIR:	-0.293	kcal/mole
HEAT OF FORMATION PER MOLE OF PRODUCTS:	-14.733	kcal/mole
HEAT OF FORMATION PER MOLE OF STOICHIOMETRIC PRODUCTS :	-20.084	kcal/mole
ACTUAL HEAT OF REACTION:	-170.841	kcal/mole of fuel
HEAT OF STOICHIOMETRIC REACTION:	-194.914	kcal/mole of fuel
(ACTUAL/STOICHIOMETRIC) HEAT OF REACTION:	0.877	
(ACTUAL/MAXIMUM) HEAT OF REACTION:	0.877	

DATA REDUCTION PROGRAM OUTPUT

RUN DATE:	04-01-88	EXPERIMENT NUMBER:	36
RUN TIME:	17:54	INTEGRATER RUN NUMBER:	264
INTERFACE HEIGHT:	10.0 cm	LAB PRESSURE:	741.4 ± 0.5 torr
BURNER DIAMETER:	19.0 cm	DRY-BULB TEMPERATURE:	22.9 ± 0.2 °C
FIRE SIZE:	41.2 ± 1.65 kW	WET-BULB TEMPERATURE:	10.5 ± 0.2 °C

SUPPLY FLOWRATES :

NATURAL GAS FUEL:	0.8250 ± 0.0330	g/sec
AIR ENTRAINED BY PLUME:	16.6690 ± 0.6812	g/sec
AIR ADDED TO UPPER LAYER:	2.0683 ± 1.0262	g/sec
TOTAL:	19.5623 ± 1.7404	g/sec

I =	13.4854 ± 0.1167 moles Air/mole Fuel	FUEL INLET REYNOLDS NUMBER:	504.6
I_s =	9.6873 ± 0.1362 moles Air/mole Fuel	FUEL INLET RICHARDSON NUMBER:	0.9189

FUEL COMPOSITION : (mole fractions)

METHANE	0.9382 ± 0.0100
ETHANE	0.0298 ± 0.0050
PROPANE	0.0079 ± 0.0020
NITROGEN	0.0162 ± 0.0020
CARBON DIOXIDE	0.0079 ± 0.0020

AIR COMPOSITION : (mole fractions)

OXYGEN	0.2085 ± 0.0010
NITROGEN	0.7773 ± 0.0020
WATER VAPOR	0.0046 ± 0.0003
CARBON DIOXIDE	0.0003 ± 0.0001
ARGON	0.0093 ± 0.0006

FUEL VISCOSITY:	109.56 μPoise
FUEL MOLECULAR WEIGHT:	17.16 g/mole
FUEL LOWER HEATING VALUE:	50.13 MJ/kg

PRODUCT LAYER ANALYSIS :

	mole fractions	mass fractions	mass fraction of plume equivalent source
HYDROGEN	0.0000 ± 0.00000	0.0000	0.0000
OXYGEN	0.0644 ± 0.00170	0.0734	0.0548
NITROGEN	0.7239 ± 0.00450	0.7228	0.7192
METHANE	0.0028 ± 0.00010	0.0016	0.0018
CARBON MONOXIDE	0.0036 ± 0.00010	0.0036	0.0040
CARBON DIOXIDE	0.0647 ± 0.00080	0.1015	0.1134
WATER VAPOR	0.1320 ± 0.00600	0.0847	0.0944
SOOT (C_8H)	0.0000 ± 0.00000	0.0000	0.0000
ACETYLENE	0.0001 ± 0.00000	0.0001	0.0001
ETHYLENE	0.0000 ± 0.00000	0.0000	0.0000
ETHANE	0.0000 ± 0.00000	0.0000	0.0000
ARGON	0.0086 ± 0.00060	0.0123	0.0122

UPPER LAYER EQUIVALENCE RATIO:	0.718 ± 0.0119
PLUME EQUIVALENCE RATIO AT INTERFACE HEIGHT:	0.808 ± 0.0476
STOICHIOMETRIC FUEL/AIR MASS RATIO:	0.0613
SAMPLE TEMPERATURE:	257.2 °C
HOOD TEMPERATURE:	196.1 °C

HEAT OF FORMATION PER MOLE OF FUEL:	-17.351	kcal/mole
HEAT OF FORMATION PER MOLE OF AIR:	-0.293	kcal/mole
HEAT OF FORMATION PER MOLE OF PRODUCTS:	-13.849	kcal/mole
HEAT OF FORMATION PER MOLE OF STOICHIOMETRIC PRODUCTS :	-20.084	kcal/mole
ACTUAL HEAT OF REACTION:	-179.553	kcal/mole of fuel
HEAT OF STOICHIOMETRIC REACTION:	-194.914	kcal/mole of fuel
(ACTUAL/STOICHIOMETRIC) HEAT OF REACTION:	0.921	
(ACTUAL/MAXIMUM) HEAT OF REACTION:	0.921	

DATA REDUCTION PROGRAM OUTPUT

RUN DATE:	04-01-88	EXPERIMENT NUMBER:	37
RUN TIME:	18:35	INTEGRATER RUN NUMBER:	266
INTERFACE HEIGHT:	10.0 cm	LAB PRESSURE:	741.4 ± 0.5 torr
BURNER DIAMETER:	19.0 cm	DRY-BULB TEMPERATURE:	22.9 ± 0.2 °C
FIRE SIZE:	41.2 ± 1.65 kW	WET-BULB TEMPERATURE:	10.5 ± 0.2 °C

SUPPLY FLOWRATES :

NATURAL GAS FUEL:	0.8250 ± 0.0330	g/sec
AIR ENTRAINED BY PLUME:	16.6690 ± 0.6812	g/sec
AIR ADDED TO UPPER LAYER:	3.4445 ± 1.0718	g/sec
TOTAL:	20.9385 ± 1.7860	g/sec

I = 14.4758 ± 0.1367 moles Air/mole Fuel
I_s = 9.6873 ± 0.1362 moles Air/mole Fuel

FUEL INLET REYNOLDS NUMBER: 504.6
FUEL INLET RICHARDSON NUMBER: 0.9189

FUEL COMPOSITION : (mole fractions)

METHANE	0.9382 ± 0.0100
ETHANE	0.0298 ± 0.0050
PROPANE	0.0079 ± 0.0020
NITROGEN	0.0162 ± 0.0020
CARBON DIOXIDE	0.0079 ± 0.0020

AIR COMPOSITION : (mole fractions)

OXYGEN	0.2085 ± 0.0010
NITROGEN	0.7773 ± 0.0020
WATER VAPOR	0.0046 ± 0.0003
CARBON DIOXIDE	0.0003 ± 0.0001
ARGON	0.0093 ± 0.0006

FUEL VISCOSITY:	109.56 μPoise
FUEL MOLECULAR WEIGHT:	17.16 g/mole
FUEL LOWER HEATING VALUE:	50.13 MJ/kg

PRODUCT LAYER ANALYSIS :

	mole fractions	mass fractions	mass fraction of plume equivalent source
HYDROGEN	0.0000 ± 0.00000	0.0000	0.0000
OXYGEN	0.0691 ± 0.00180	0.0786	0.0486
NITROGEN	0.7283 ± 0.00480	0.7249	0.7194
METHANE	0.0000 ± 0.00000	0.0000	0.0000
CARBON MONOXIDE	0.0029 ± 0.00010	0.0029	0.0035
CARBON DIOXIDE	0.0639 ± 0.00080	0.0999	0.1195
WATER VAPOR	0.1272 ± 0.00640	0.0814	0.0969
SOOT (C_8H)	0.0000 ± 0.00000	0.0000	0.0000
ACETYLENE	0.0000 ± 0.00000	0.0000	0.0000
ETHYLENE	0.0000 ± 0.00000	0.0000	0.0000
ETHANE	0.0000 ± 0.00000	0.0000	0.0000
ARGON	0.0087 ± 0.00060	0.0123	0.0122

UPPER LAYER EQUIVALENCE RATIO:	0.669 ± 0.0113
PLUME EQUIVALENCE RATIO AT INTERFACE HEIGHT:	0.808 ± 0.0476
STOICHIOMETRIC FUEL/AIR MASS RATIO:	0.0613
SAMPLE TEMPERATURE:	257.2 °C
HOOD TEMPERATURE:	195.6 °C

HEAT OF FORMATION PER MOLE OF FUEL:	-17.351	kcal/mole
HEAT OF FORMATION PER MOLE OF AIR:	-0.293	kcal/mole
HEAT OF FORMATION PER MOLE OF PRODUCTS:	-13.435	kcal/mole
HEAT OF FORMATION PER MOLE OF STOICHIOMETRIC PRODUCTS :	-20.084	kcal/mole
ACTUAL HEAT OF REACTION:	-186.296	kcal/mole of fuel
HEAT OF STOICHIOMETRIC REACTION:	-194.914	kcal/mole of fuel
(ACTUAL/STOICHIOMETRIC) HEAT OF REACTION:	0.956	
(ACTUAL/MAXIMUM) HEAT OF REACTION:	0.956	

DATA REDUCTION PROGRAM OUTPUT

RUN DATE:	04-01-88	EXPERIMENT NUMBER:	38
RUN TIME:	18:53	INTEGRATER RUN NUMBER:	267
INTERFACE HEIGHT:	10.0 cm	LAB PRESSURE:	741.4 ± 0.5 torr
BURNER DIAMETER:	19.0 cm	DRY-BULB TEMPERATURE:	22.9 ± 0.2 °C
FIRE SIZE:	41.2 ± 1.65 kW	WET-BULB TEMPERATURE:	10.5 ± 0.2 °C

SUPPLY FLOWRATES :

NATURAL GAS FUEL:	0.8250 ± 0.0330	g/sec
AIR ENTRAINED BY PLUME:	16.6690 ± 0.6812	g/sec
AIR ADDED TO UPPER LAYER:	4.1022 ± 1.0943	g/sec
TOTAL:	21.5962 ± 1.8085	g/sec

I = 14.9492 ± 0.1474 moles Air/mole Fuel
I_s = 9.6873 ± 0.1362 moles Air/mole Fuel

FUEL INLET REYNOLDS NUMBER: 504.6
FUEL INLET RICHARDSON NUMBER: 0.9189

FUEL COMPOSITION : (mole fractions)

METHANE	0.9382 ± 0.0100
ETHANE	0.0298 ± 0.0050
PROPANE	0.0079 ± 0.0020
NITROGEN	0.0162 ± 0.0020
CARBON DIOXIDE	0.0079 ± 0.0020

AIR COMPOSITION : (mole fractions)

OXYGEN	0.2085 ± 0.0010
NITROGEN	0.7773 ± 0.0020
WATER VAPOR	0.0046 ± 0.0003
CARBON DIOXIDE	0.0003 ± 0.0001
ARGON	0.0093 ± 0.0006

FUEL VISCOSITY:	109.56 μPoise
FUEL MOLECULAR WEIGHT:	17.16 g/mole
FUEL LOWER HEATING VALUE:	50.13 MJ/kg

PRODUCT LAYER ANALYSIS :

	mole fractions	mass fractions	mass fraction of plume equivalent source
HYDROGEN	0.0000 ± 0.00000	0.0000	0.0000
OXYGEN	0.0735 ± 0.00190	0.0834	0.0489
NITROGEN	0.7301 ± 0.00500	0.7258	0.7194
METHANE	0.0000 ± 0.00000	0.0000	0.0000
CARBON MONOXIDE	0.0025 ± 0.00010	0.0025	0.0030
CARBON DIOXIDE	0.0624 ± 0.00080	0.0975	0.1202
WATER VAPOR	0.1228 ± 0.00660	0.0785	0.0963
SOOT (C_8H)	0.0000 ± 0.00000	0.0000	0.0000
ACETYLENE	0.0000 ± 0.00000	0.0000	0.0000
ETHYLENE	0.0000 ± 0.00000	0.0000	0.0000
ETHANE	0.0000 ± 0.00000	0.0000	0.0000
ARGON	0.0087 ± 0.00060	0.0123	0.0122

UPPER LAYER EQUIVALENCE RATIO:	0.648 ± 0.0111
PLUME EQUIVALENCE RATIO AT INTERFACE HEIGHT:	0.808 ± 0.0476
STOICHIOMETRIC FUEL/AIR MASS RATIO:	0.0613
SAMPLE TEMPERATURE:	255.6 °C
HOOD TEMPERATURE:	195.0 °C

HEAT OF FORMATION PER MOLE OF FUEL:	-17.351	kcal/mole
HEAT OF FORMATION PER MOLE OF AIR:	-0.293	kcal/mole
HEAT OF FORMATION PER MOLE OF PRODUCTS:	-13.034	kcal/mole
HEAT OF FORMATION PER MOLE OF STOICHIOMETRIC PRODUCTS :	-20.084	kcal/mole
ACTUAL HEAT OF REACTION:	-186.007	kcal/mole of fuel
HEAT OF STOICHIOMETRIC REACTION:	-194.914	kcal/mole of fuel
(ACTUAL/STOICHIOMETRIC) HEAT OF REACTION:	0.954	
(ACTUAL/MAXIMUM) HEAT OF REACTION:	0.954	

DATA REDUCTION PROGRAM OUTPUT

RUN DATE:	04-01-88	EXPERIMENT NUMBER:	39
RUN TIME:	19:12	INTEGRATER RUN NUMBER:	268
INTERFACE HEIGHT:	10.0 cm	LAB PRESSURE:	741.4 ± 0.5 torr
BURNER DIAMETER:	19.0 cm	DRY-BULB TEMPERATURE:	22.9 ± 0.2 °C
FIRE SIZE:	41.2 ± 1.65 kW	WET-BULB TEMPERATURE:	10.5 ± 0.2 °C

SUPPLY FLOWRATES :

NATURAL GAS FUEL:	0.8250 ± 0.0330	g/sec
AIR ENTRAINED BY PLUME:	16.6690 ± 0.6812	g/sec
AIR ADDED TO UPPER LAYER:	5.4451 ± 1.1410	g/sec
TOTAL:	22.9391 ± 1.8552	g/sec

I = 15.9157 ± 0.1670 moles Air/mole Fuel
I_s = 9.6873 ± 0.1362 moles Air/mole Fuel

FUEL INLET REYNOLDS NUMBER: 504.6
FUEL INLET RICHARDSON NUMBER: 0.9189

FUEL COMPOSITION : (mole fractions)

METHANE	0.9382 ± 0.0100
ETHANE	0.0298 ± 0.0050
PROPANE	0.0079 ± 0.0020
NITROGEN	0.0162 ± 0.0020
CARBON DIOXIDE	0.0079 ± 0.0020

AIR COMPOSITION : (mole fractions)

OXYGEN	0.2085 ± 0.0010
NITROGEN	0.7773 ± 0.0020
WATER VAPOR	0.0046 ± 0.0003
CARBON DIOXIDE	0.0003 ± 0.0001
ARGON	0.0093 ± 0.0006

FUEL VISCOSITY:	109.56 μPoise
FUEL MOLECULAR WEIGHT:	17.16 g/mole
FUEL LOWER HEATING VALUE:	50.13 MJ/kg

PRODUCT LAYER ANALYSIS :

	mole fractions	mass fractions	mass fraction of plume equivalent source
HYDROGEN	0.0000 ± 0.00000	0.0000	0.0000
OXYGEN	0.0808 ± 0.00200	0.0916	0.0483
NITROGEN	0.7331 ± 0.00530	0.7274	0.7194
METHANE	0.0000 ± 0.00000	0.0000	0.0000
CARBON MONOXIDE	0.0016 ± 0.00000	0.0016	0.0021
CARBON DIOXIDE	0.0596 ± 0.00080	0.0929	0.1217
WATER VAPOR	0.1161 ± 0.00700	0.0741	0.0963
SOOT (C_8H)	0.0000 ± 0.00000	0.0000	0.0000
ACETYLENE	0.0000 ± 0.00000	0.0000	0.0000
ETHYLENE	0.0000 ± 0.00000	0.0000	0.0000
ETHANE	0.0000 ± 0.00000	0.0000	0.0000
ARGON	0.0087 ± 0.00060	0.0123	0.0122

UPPER LAYER EQUIVALENCE RATIO:	0.609 ± 0.0107
PLUME EQUIVALENCE RATIO AT INTERFACE HEIGHT:	0.808 ± 0.0476
STOICHIOMETRIC FUEL/AIR MASS RATIO:	0.0613
SAMPLE TEMPERATURE:	255.0 °C
HOOD TEMPERATURE:	195.6 °C

HEAT OF FORMATION PER MOLE OF FUEL:	-17.351	kcal/mole
HEAT OF FORMATION PER MOLE OF AIR:	-0.293	kcal/mole
HEAT OF FORMATION PER MOLE OF PRODUCTS:	-12.360	kcal/mole
HEAT OF FORMATION PER MOLE OF STOICHIOMETRIC PRODUCTS :	-20.084	kcal/mole
ACTUAL HEAT OF REACTION:	-186.855	kcal/mole of fuel
HEAT OF STOICHIOMETRIC REACTION:	-194.914	kcal/mole of fuel
(ACTUAL/STOICHIOMETRIC) HEAT OF REACTION:	0.959	
(ACTUAL/MAXIMUM) HEAT OF REACTION:	0.959	

DATA REDUCTION PROGRAM OUTPUT

RUN DATE:	04-01-88	EXPERIMENT NUMBER:	40
RUN TIME:	19:32	INTEGRATER RUN NUMBER:	269
INTERFACE HEIGHT:	10.0 cm	LAB PRESSURE:	741.4 ± 0.5 torr
BURNER DIAMETER:	19.0 cm	DRY-BULB TEMPERATURE:	22.9 ± 0.2 °C
FIRE SIZE:	41.2 ± 1.65 kW	WET-BULB TEMPERATURE:	10.5 ± 0.2 °C

SUPPLY FLOWRATES :

NATURAL GAS FUEL:	0.8250 ± 0.0330	g/sec
AIR ENTRAINED BY PLUME:	16.6690 ± 0.6812	g/sec
AIR ADDED TO UPPER LAYER:	5.7192 ± 1.1494	g/sec
TOTAL:	23.2132 ± 1.8636	g/sec

I =	16.1130 ± 0.1664 moles Air/mole Fuel	FUEL INLET REYNOLDS NUMBER:	504.6
I_s =	9.6873 ± 0.1362 moles Air/mole Fuel	FUEL INLET RICHARDSON NUMBER:	0.9189

FUEL COMPOSITION : (mole fractions)		AIR COMPOSITION : (mole fractions)	
METHANE	0.9382 ± 0.0100	OXYGEN	0.2085 ± 0.0010
ETHANE	0.0298 ± 0.0050	NITROGEN	0.7773 ± 0.0020
PROPANE	0.0079 ± 0.0020	WATER VAPOR	0.0046 ± 0.0003
NITROGEN	0.0162 ± 0.0020	CARBON DIOXIDE	0.0003 ± 0.0001
CARBON DIOXIDE	0.0079 ± 0.0020	ARGON	0.0093 ± 0.0006

FUEL VISCOSITY:	109.56	μPoise
FUEL MOLECULAR WEIGHT:	17.16	g/mole
FUEL LOWER HEATING VALUE:	50.13	MJ/kg

PRODUCT LAYER ANALYSIS :

	mole fractions	mass fractions	mass fraction of plume equivalent source
HYDROGEN	0.0000 ± 0.00000	0.0000	0.0000
OXYGEN	0.0814 ± 0.00210	0.0923	0.0470
NITROGEN	0.7331 ± 0.00540	0.7276	0.7193
METHANE	0.0000 ± 0.00000	0.0000	0.0000
CARBON MONOXIDE	0.0014 ± 0.00000	0.0014	0.0018
CARBON DIOXIDE	0.0591 ± 0.00080	0.0921	0.1220
WATER VAPOR	0.1164 ± 0.00700	0.0743	0.0976
SOOT (C_8H)	0.0000 ± 0.00000	0.0000	0.0000
ACETYLENE	0.0000 ± 0.00000	0.0000	0.0000
ETHYLENE	0.0000 ± 0.00000	0.0000	0.0000
ETHANE	0.0000 ± 0.00000	0.0000	0.0000
ARGON	0.0087 ± 0.00060	0.0123	0.0122

UPPER LAYER EQUIVALENCE RATIO:	0.601 ± 0.0105	
PLUME EQUIVALENCE RATIO AT INTERFACE HEIGHT:	0.808 ± 0.0476	
STOICHIOMETRIC FUEL/AIR MASS RATIO:	0.0613	
SAMPLE TEMPERATURE:	255.0 °C	
HOOD TEMPERATURE:	195.6 °C	
HEAT OF FORMATION PER MOLE OF FUEL:	-17.351	kcal/mole
HEAT OF FORMATION PER MOLE OF AIR:	-0.293	kcal/mole
HEAT OF FORMATION PER MOLE OF PRODUCTS:	-12.316	kcal/mole
HEAT OF FORMATION PER MOLE OF STOICHIOMETRIC PRODUCTS :	-20.084	kcal/mole
ACTUAL HEAT OF REACTION:	-188.637	kcal/mole of fuel
HEAT OF STOICHIOMETRIC REACTION:	-194.914	kcal/mole of fuel
(ACTUAL/STOICHIOMETRIC) HEAT OF REACTION:	0.968	
(ACTUAL/MAXIMUM) HEAT OF REACTION:	0.968	

DATA REDUCTION PROGRAM OUTPUT

RUN DATE:	04-01-88	EXPERIMENT NUMBER:	41
RUN TIME:	19:51	INTEGRATER RUN NUMBER:	270
INTERFACE HEIGHT:	10.0 cm	LAB PRESSURE:	741.4 ± 0.5 torr
BURNER DIAMETER:	19.0 cm	DRY-BULB TEMPERATURE:	22.9 ± 0.2 °C
FIRE SIZE:	41.2 ± 1.65 kW	WET-BULB TEMPERATURE:	10.5 ± 0.2 °C

SUPPLY FLOWRATES :

NATURAL GAS FUEL:	0.8250 ± 0.0330	g/sec
AIR ENTRAINED BY PLUME:	16.6690 ± 0.6812	g/sec
AIR ADDED TO UPPER LAYER:	7.4670 ± 1.2152	g/sec
TOTAL:	24.9610 ± 1.9294	g/sec

I = 17.3709 ± 0.2021 moles Air/mole Fuel
I_s = 9.6873 ± 0.1362 moles Air/mole Fuel

FUEL INLET REYNOLDS NUMBER: 504.6
FUEL INLET RICHARDSON NUMBER: 0.9189

FUEL COMPOSITION : (mole fractions)		AIR COMPOSITION : (mole fractions)	
METHANE	0.9382 ± 0.0100	OXYGEN	0.2085 ± 0.0010
ETHANE	0.0298 ± 0.0050	NITROGEN	0.7773 ± 0.0020
PROPANE	0.0079 ± 0.0020	WATER VAPOR	0.0046 ± 0.0003
NITROGEN	0.0162 ± 0.0020	CARBON DIOXIDE	0.0003 ± 0.0001
CARBON DIOXIDE	0.0079 ± 0.0020	ARGON	0.0093 ± 0.0006

FUEL VISCOSITY:	109.56 μPoise
FUEL MOLECULAR WEIGHT:	17.16 g/mole
FUEL LOWER HEATING VALUE:	50.13 MJ/kg

PRODUCT LAYER ANALYSIS :

	mole fractions	mass fractions	mass fraction of plume equivalent source
HYDROGEN	0.0000 ± 0.00000	0.0000	0.0000
OXYGEN	0.0909 ± 0.00230	0.1028	0.0481
NITROGEN	0.7370 ± 0.00590	0.7295	0.7195
METHANE	0.0000 ± 0.00000	0.0000	0.0000
CARBON MONOXIDE	0.0008 ± 0.00000	0.0008	0.0011
CARBON DIOXIDE	0.0556 ± 0.00080	0.0865	0.1232
WATER VAPOR	0.1069 ± 0.00770	0.0681	0.0959
SOOT (C_8H)	0.0000 ± 0.00000	0.0000	0.0000
ACETYLENE	0.0000 ± 0.00000	0.0000	0.0000
ETHYLENE	0.0000 ± 0.00000	0.0000	0.0000
ETHANE	0.0000 ± 0.00000	0.0000	0.0000
ARGON	0.0088 ± 0.00060	0.0124	0.0122

UPPER LAYER EQUIVALENCE RATIO:	0.558 ± 0.0102
PLUME EQUIVALENCE RATIO AT INTERFACE HEIGHT:	0.808 ± 0.0476
STOICHIOMETRIC FUEL/AIR MASS RATIO:	0.0613
SAMPLE TEMPERATURE:	251.7 °C
HOOD TEMPERATURE:	195.0 °C

HEAT OF FORMATION PER MOLE OF FUEL:	-17.351	kcal/mole
HEAT OF FORMATION PER MOLE OF AIR:	-0.293	kcal/mole
HEAT OF FORMATION PER MOLE OF PRODUCTS:	-11.432	kcal/mole
HEAT OF FORMATION PER MOLE OF STOICHIOMETRIC PRODUCTS :	-20.084	kcal/mole
ACTUAL HEAT OF REACTION:	-187.263	kcal/mole of fuel
HEAT OF STOICHIOMETRIC REACTION:	-194.914	kcal/mole of fuel
(ACTUAL/STOICHIOMETRIC) HEAT OF REACTION:	0.961	
(ACTUAL/MAXIMUM) HEAT OF REACTION:	0.961	

DATA REDUCTION PROGRAM OUTPUT

RUN DATE:	04-01-88	EXPERIMENT NUMBER:	42
RUN TIME:	20:09	INTEGRATER RUN NUMBER:	271
INTERFACE HEIGHT:	10.0 cm	LAB PRESSURE:	741.4 ± 0.5 torr
BURNER DIAMETER:	19.0 cm	DRY-BULB TEMPERATURE:	22.9 ± 0.2 °C
FIRE SIZE:	41.2 ± 1.65 kW	WET-BULB TEMPERATURE:	10.5 ± 0.2 °C

SUPPLY FLOWRATES :

NATURAL GAS FUEL:	0.8250 ± 0.0330	g/sec
AIR ENTRAINED BY PLUME:	16.6690 ± 0.6812	g/sec
AIR ADDED TO UPPER LAYER:	7.5635 ± 1.2175	g/sec
TOTAL:	25.0575 ± 1.9317	g/sec

I =	17.4403 ± 0.1997 moles Air/mole Fuel	FUEL INLET REYNOLDS NUMBER:	504.6
I_s =	9.6873 ± 0.1362 moles Air/mole Fuel	FUEL INLET RICHARDSON NUMBER:	0.9189

FUEL COMPOSITION : (mole fractions)		AIR COMPOSITION : (mole fractions)	
METHANE	0.9382 ± 0.0100	OXYGEN	0.2085 ± 0.0010
ETHANE	0.0298 ± 0.0050	NITROGEN	0.7773 ± 0.0020
PROPANE	0.0079 ± 0.0020	WATER VAPOR	0.0046 ± 0.0003
NITROGEN	0.0162 ± 0.0020	CARBON DIOXIDE	0.0003 ± 0.0001
CARBON DIOXIDE	0.0079 ± 0.0020	ARGON	0.0093 ± 0.0006

FUEL VISCOSITY:	109.56 μPoise
FUEL MOLECULAR WEIGHT:	17.16 g/mole
FUEL LOWER HEATING VALUE:	50.13 MJ/kg

PRODUCT LAYER ANALYSIS :

	mole fractions	mass fractions	mass fraction of plume equivalent source
HYDROGEN	0.0000 ± 0.00000	0.0000	0.0000
OXYGEN	0.0907 ± 0.00230	0.1026	0.0471
NITROGEN	0.7369 ± 0.00590	0.7296	0.7194
METHANE	0.0000 ± 0.00000	0.0000	0.0000
CARBON MONOXIDE	0.0006 ± 0.00000	0.0006	0.0008
CARBON DIOXIDE	0.0556 ± 0.00080	0.0865	0.1236
WATER VAPOR	0.1075 ± 0.00770	0.0685	0.0968
SOOT (C_8H)	0.0000 ± 0.00000	0.0000	0.0000
ACETYLENE	0.0000 ± 0.00000	0.0000	0.0000
ETHYLENE	0.0000 ± 0.00000	0.0000	0.0000
ETHANE	0.0000 ± 0.00000	0.0000	0.0000
ARGON	0.0088 ± 0.00060	0.0124	0.0122

UPPER LAYER EQUIVALENCE RATIO:	0.555 ± 0.0101
PLUME EQUIVALENCE RATIO AT INTERFACE HEIGHT:	0.808 ± 0.0476
STOICHIOMETRIC FUEL/AIR MASS RATIO:	0.0613
SAMPLE TEMPERATURE:	251.7 °C
HOOD TEMPERATURE:	196.7 °C

HEAT OF FORMATION PER MOLE OF FUEL:	-17.351	kcal/mole
HEAT OF FORMATION PER MOLE OF AIR:	-0.293	kcal/mole
HEAT OF FORMATION PER MOLE OF PRODUCTS:	-11.457	kcal/mole
HEAT OF FORMATION PER MOLE OF STOICHIOMETRIC PRODUCTS :	-20.084	kcal/mole
ACTUAL HEAT OF REACTION:	-188.588	kcal/mole of fuel
HEAT OF STOICHIOMETRIC REACTION:	-194.914	kcal/mole of fuel
(ACTUAL/STOICHIOMETRIC) HEAT OF REACTION:	0.967	
(ACTUAL/MAXIMUM) HEAT OF REACTION:	0.967	

DATA REDUCTION PROGRAM OUTPUT

RUN DATE:	04-01-88	EXPERIMENT NUMBER:	43
RUN TIME:	20:27	INTEGRATER RUN NUMBER:	272
INTERFACE HEIGHT:	10.0 cm	LAB PRESSURE:	741.4 ± 0.5 torr
BURNER DIAMETER:	19.0 cm	DRY-BULB TEMPERATURE:	22.9 ± 0.2 °C
FIRE SIZE:	41.2 ± 1.65 kW	WET-BULB TEMPERATURE:	10.5 ± 0.2 °C

SUPPLY FLOWRATES :

NATURAL GAS FUEL:	0.8250 ± 0.0330	g/sec
AIR ENTRAINED BY PLUME:	16.6690 ± 0.6812	g/sec
AIR ADDED TO UPPER LAYER:	10.1972 ± 1.3207	g/sec
TOTAL:	27.6912 ± 2.0349	g/sec

I = 19.3358 ± 0.2526 moles Air/mole Fuel
I_s = 9.6873 ± 0.1362 moles Air/mole Fuel

FUEL INLET REYNOLDS NUMBER: 504.6
FUEL INLET RICHARDSON NUMBER: 0.9189

FUEL COMPOSITION : (mole fractions)		AIR COMPOSITION : (mole fractions)	
METHANE	0.9382 ± 0.0100	OXYGEN	0.2085 ± 0.0010
ETHANE	0.0298 ± 0.0050	NITROGEN	0.7773 ± 0.0020
PROPANE	0.0079 ± 0.0020	WATER VAPOR	0.0046 ± 0.0003
NITROGEN	0.0162 ± 0.0020	CARBON DIOXIDE	0.0003 ± 0.0001
CARBON DIOXIDE	0.0079 ± 0.0020	ARGON	0.0093 ± 0.0006

FUEL VISCOSITY:	109.56 μPoise
FUEL MOLECULAR WEIGHT:	17.16 g/mole
FUEL LOWER HEATING VALUE:	50.13 MJ/kg

PRODUCT LAYER ANALYSIS :

	mole fractions	mass fractions	mass fraction of plume equivalent source
HYDROGEN	0.0000 ± 0.00000	0.0000	0.0000
OXYGEN	0.1020 ± 0.00260	0.1151	0.0477
NITROGEN	0.7407 ± 0.00660	0.7318	0.7194
METHANE	0.0000 ± 0.00000	0.0000	0.0000
CARBON MONOXIDE	0.0007 ± 0.00000	0.0007	0.0012
CARBON DIOXIDE	0.0502 ± 0.00070	0.0780	0.1231
WATER VAPOR	0.0975 ± 0.00860	0.0619	0.0964
SOOT (C_8H)	0.0000 ± 0.00000	0.0000	0.0000
ACETYLENE	0.0000 ± 0.00000	0.0000	0.0000
ETHYLENE	0.0000 ± 0.00000	0.0000	0.0000
ETHANE	0.0000 ± 0.00000	0.0000	0.0000
ARGON	0.0088 ± 0.00060	0.0124	0.0122

UPPER LAYER EQUIVALENCE RATIO:	0.501 ± 0.0096
PLUME EQUIVALENCE RATIO AT INTERFACE HEIGHT:	0.808 ± 0.0476
STOICHIOMETRIC FUEL/AIR MASS RATIO:	0.0613
SAMPLE TEMPERATURE:	245.0 °C
HOOD TEMPERATURE:	192.8 °C

HEAT OF FORMATION PER MOLE OF FUEL:	-17.351	kcal/mole
HEAT OF FORMATION PER MOLE OF AIR:	-0.293	kcal/mole
HEAT OF FORMATION PER MOLE OF PRODUCTS:	-10.377	kcal/mole
HEAT OF FORMATION PER MOLE OF STOICHIOMETRIC PRODUCTS :	-20.084	kcal/mole
ACTUAL HEAT OF REACTION:	-187.784	kcal/mole of fuel
HEAT OF STOICHIOMETRIC REACTION:	-194.914	kcal/mole of fuel
(ACTUAL/STOICHIOMETRIC) HEAT OF REACTION:	0.963	
(ACTUAL/MAXIMUM) HEAT OF REACTION:	0.963	

DATA REDUCTION PROGRAM OUTPUT

RUN DATE:	04-01-88	EXPERIMENT NUMBER:	44
RUN TIME:	20:46	INTEGRATER RUN NUMBER:	273
INTERFACE HEIGHT:	10.0 cm	LAB PRESSURE:	741.4 ± 0.5 torr
BURNER DIAMETER:	19.0 cm	DRY-BULB TEMPERATURE:	22.9 ± 0.2 °C
FIRE SIZE:	41.2 ± 1.65 kW	WET-BULB TEMPERATURE:	10.5 ± 0.2 °C

SUPPLY FLOWRATES :

NATURAL GAS FUEL:	0.8250 ± 0.0330	g/sec
AIR ENTRAINED BY PLUME:	16.6690 ± 0.6812	g/sec
AIR ADDED TO UPPER LAYER:	10.2218 ± 1.3269	g/sec
TOTAL:	27.7158 ± 2.0411	g/sec

I = 19.3535 ± 0.2667 moles Air/mole Fuel
I_s = 9.6873 ± 0.1362 moles Air/mole Fuel

FUEL INLET REYNOLDS NUMBER: 504.6
FUEL INLET RICHARDSON NUMBER: 0.9189

FUEL COMPOSITION : (mole fractions)

METHANE	0.9382 ± 0.0100
ETHANE	0.0298 ± 0.0050
PROPANE	0.0079 ± 0.0020
NITROGEN	0.0162 ± 0.0020
CARBON DIOXIDE	0.0079 ± 0.0020

AIR COMPOSITION : (mole fractions)

OXYGEN	0.2085 ± 0.0010
NITROGEN	0.7773 ± 0.0020
WATER VAPOR	0.0046 ± 0.0003
CARBON DIOXIDE	0.0003 ± 0.0001
ARGON	0.0093 ± 0.0006

FUEL VISCOSITY:	109.56 μPoise
FUEL MOLECULAR WEIGHT:	17.16 g/mole
FUEL LOWER HEATING VALUE:	50.13 MJ/kg

PRODUCT LAYER ANALYSIS :

	mole fractions	mass fractions	mass fraction of plume equivalent source
HYDROGEN	0.0000 ± 0.00000	0.0000	0.0000
OXYGEN	0.1033 ± 0.00260	0.1165	0.0496
NITROGEN	0.7416 ± 0.00670	0.7320	0.7196
METHANE	0.0000 ± 0.00000	0.0000	0.0000
CARBON MONOXIDE	0.0006 ± 0.00000	0.0006	0.0010
CARBON DIOXIDE	0.0503 ± 0.00070	0.0781	0.1234
WATER VAPOR	0.0953 ± 0.00880	0.0605	0.0941
SOOT (C_8H)	0.0000 ± 0.00000	0.0000	0.0000
ACETYLENE	0.0000 ± 0.00000	0.0000	0.0000
ETHYLENE	0.0000 ± 0.00000	0.0000	0.0000
ETHANE	0.0000 ± 0.00000	0.0000	0.0000
ARGON	0.0088 ± 0.00060	0.0124	0.0122

UPPER LAYER EQUIVALENCE RATIO:	0.501 ± 0.0099
PLUME EQUIVALENCE RATIO AT INTERFACE HEIGHT:	0.808 ± 0.0476
STOICHIOMETRIC FUEL/AIR MASS RATIO:	0.0613
SAMPLE TEMPERATURE:	244.4 °C
HOOD TEMPERATURE:	192.8 °C

HEAT OF FORMATION PER MOLE OF FUEL:	-17.351	kcal/mole
HEAT OF FORMATION PER MOLE OF AIR:	-0.293	kcal/mole
HEAT OF FORMATION PER MOLE OF PRODUCTS:	-10.258	kcal/mole
HEAT OF FORMATION PER MOLE OF STOICHIOMETRIC PRODUCTS :	-20.084	kcal/mole
ACTUAL HEAT OF REACTION:	-185.302	kcal/mole of fuel
HEAT OF STOICHIOMETRIC REACTION:	-194.914	kcal/mole of fuel
(ACTUAL/STOICHIOMETRIC) HEAT OF REACTION:	0.951	
(ACTUAL/MAXIMUM) HEAT OF REACTION:	0.951	

DATA REDUCTION PROGRAM OUTPUT

RUN DATE:	04-01-88	EXPERIMENT NUMBER:	45
RUN TIME:	21:05	INTEGRATER RUN NUMBER:	274
INTERFACE HEIGHT:	10.0 cm	LAB PRESSURE:	741.4 ± 0.5 torr
BURNER DIAMETER:	19.0 cm	DRY-BULB TEMPERATURE:	22.9 ± 0.2 °C
FIRE SIZE:	41.2 ± 1.65 kW	WET-BULB TEMPERATURE:	10.5 ± 0.2 °C

SUPPLY FLOWRATES :

NATURAL GAS FUEL:	0.8250 ± 0.0330	g/sec
AIR ENTRAINED BY PLUME:	16.6690 ± 0.6812	g/sec
AIR ADDED TO UPPER LAYER:	6.7146 ± 1.1851	g/sec
TOTAL:	24.2086 ± 1.8993	g/sec

I =	16.8293 ± 0.1818 moles Air/mole Fuel	FUEL INLET REYNOLDS NUMBER:	504.6
I_s =	9.6873 ± 0.1362 moles Air/mole Fuel	FUEL INLET RICHARDSON NUMBER:	0.9189

FUEL COMPOSITION : (mole fractions)

METHANE	0.9382 ± 0.0100
ETHANE	0.0298 ± 0.0050
PROPANE	0.0079 ± 0.0020
NITROGEN	0.0162 ± 0.0020
CARBON DIOXIDE	0.0079 ± 0.0020

AIR COMPOSITION : (mole fractions)

OXYGEN	0.2085 ± 0.0010
NITROGEN	0.7773 ± 0.0020
WATER VAPOR	0.0046 ± 0.0003
CARBON DIOXIDE	0.0003 ± 0.0001
ARGON	0.0093 ± 0.0006

FUEL VISCOSITY:	109.56 μPoise
FUEL MOLECULAR WEIGHT:	17.16 g/mole
FUEL LOWER HEATING VALUE:	50.13 MJ/kg

PRODUCT LAYER ANALYSIS :

	mole fractions	mass fractions	mass fraction of plume equivalent source
HYDROGEN	0.0000 ± 0.00000	0.0000	0.0000
OXYGEN	0.0862 ± 0.00220	0.0976	0.0465
NITROGEN	0.7350 ± 0.00560	0.7287	0.7193
METHANE	0.0000 ± 0.00000	0.0000	0.0000
CARBON MONOXIDE	0.0008 ± 0.00000	0.0008	0.0012
CARBON DIOXIDE	0.0572 ± 0.00080	0.0891	0.1231
WATER VAPOR	0.1119 ± 0.00730	0.0714	0.0977
SOOT (C_8H)	0.0000 ± 0.00000	0.0000	0.0000
ACETYLENE	0.0000 ± 0.00000	0.0000	0.0000
ETHYLENE	0.0000 ± 0.00000	0.0000	0.0000
ETHANE	0.0000 ± 0.00000	0.0000	0.0000
ARGON	0.0087 ± 0.00060	0.0124	0.0122

UPPER LAYER EQUIVALENCE RATIO:	0.576 ± 0.0102
PLUME EQUIVALENCE RATIO AT INTERFACE HEIGHT:	0.808 ± 0.0476
STOICHIOMETRIC FUEL/AIR MASS RATIO:	0.0613
SAMPLE TEMPERATURE:	252.2 °C
HOOD TEMPERATURE:	193.3 °C

HEAT OF FORMATION PER MOLE OF FUEL:	-17.351	kcal/mole
HEAT OF FORMATION PER MOLE OF AIR:	-0.293	kcal/mole
HEAT OF FORMATION PER MOLE OF PRODUCTS:	-11.873	kcal/mole
HEAT OF FORMATION PER MOLE OF STOICHIOMETRIC PRODUCTS :	-20.084	kcal/mole
ACTUAL HEAT OF REACTION:	-189.301	kcal/mole of fuel
HEAT OF STOICHIOMETRIC REACTION:	-194.914	kcal/mole of fuel
(ACTUAL/STOICHIOMETRIC) HEAT OF REACTION:	0.971	
(ACTUAL/MAXIMUM) HEAT OF REACTION:	0.971	

DATA REDUCTION PROGRAM OUTPUT

RUN DATE:	07-14-88	EXPERIMENT NUMBER:	46
RUN TIME:	21:23	INTEGRATER RUN NUMBER:	395
INTERFACE HEIGHT:	23.0 cm	LAB PRESSURE:	736.0 ± 0.5 torr
BURNER DIAMETER:	19.0 cm	DRY-BULB TEMPERATURE:	22.2 ± 0.2 °C
FIRE SIZE:	67.6 ± 1.65 kW	WET-BULB TEMPERATURE:	17.0 ± 0.2 °C

SUPPLY FLOWRATES :

NATURAL GAS FUEL:	1.3470 ± 0.0329	g/sec
AIR ENTRAINED BY PLUME:	24.6388 ± 0.6306	g/sec
AIR ADDED TO UPPER LAYER:	0.0000 ± 0.0000	g/sec
TOTAL:	25.9858 ± 0.6635	g/sec

I =	10.8067 ± 0.0817 moles Air/mole Fuel	FUEL INLET REYNOLDS NUMBER:	824.1
I_s =	9.7948 ± 0.1379 moles Air/mole Fuel	FUEL INLET RICHARDSON NUMBER:	0.3416

FUEL COMPOSITION : (mole fractions)		AIR COMPOSITION : (mole fractions)	
METHANE	0.9436 ± 0.0100	OXYGEN	0.2061 ± 0.0010
ETHANE	0.0267 ± 0.0050	NITROGEN	0.7682 ± 0.0020
PROPANE	0.0076 ± 0.0020	WATER VAPOR	0.0163 ± 0.0004
NITROGEN	0.0148 ± 0.0020	CARBON DIOXIDE	0.0003 ± 0.0001
CARBON DIOXIDE	0.0074 ± 0.0020	ARGON	0.0091 ± 0.0006

FUEL VISCOSITY:	109.53	μPoise
FUEL MOLECULAR WEIGHT:	17.07	g/mole
FUEL LOWER HEATING VALUE:	50.56	MJ/kg

PRODUCT LAYER ANALYSIS :

	mole fractions	mass fractions	mass fraction of plume equivalent source
HYDROGEN	0.0014 ± 0.00030	0.0001	0.0001
OXYGEN	0.0387 ± 0.00120	0.0447	0.0447
NITROGEN	0.7037 ± 0.00370	0.7107	0.7107
METHANE	0.0057 ± 0.00030	0.0033	0.0033
CARBON MONOXIDE	0.0071 ± 0.00020	0.0071	0.0071
CARBON DIOXIDE	0.0741 ± 0.00090	0.1174	0.1174
WATER VAPOR	0.1608 ± 0.00510	0.1044	0.1044
SOOT (C_8H)	0.0000 ± 0.00000	0.0000	0.0000
ACETYLENE	0.0002 ± 0.00000	0.0002	0.0002
ETHYLENE	0.0000 ± 0.00000	0.0000	0.0000
ETHANE	0.0000 ± 0.00000	0.0000	0.0000
ARGON	0.0083 ± 0.00060	0.0120	0.0120

UPPER LAYER EQUIVALENCE RATIO:	0.906 ± 0.0145	
PLUME EQUIVALENCE RATIO AT INTERFACE HEIGHT:	0.906 ± 0.0345	
STOICHIOMETRIC FUEL/AIR MASS RATIO:	0.0603	
SAMPLE TEMPERATURE:	334.4 °C	
HOOD TEMPERATURE:	265.0 °C	
HEAT OF FORMATION PER MOLE OF FUEL:		-17.432 kcal/mole
HEAT OF FORMATION PER MOLE OF AIR:		-0.967 kcal/mole
HEAT OF FORMATION PER MOLE OF PRODUCTS:		-16.488 kcal/mole
HEAT OF FORMATION PER MOLE OF STOICHIOMETRIC PRODUCTS :		-20.484 kcal/mole
ACTUAL HEAT OF REACTION:	-167.523	kcal/mole of fuel
HEAT OF STOICHIOMETRIC REACTION:	-194.643	kcal/mole of fuel
(ACTUAL/STOICHIOMETRIC) HEAT OF REACTION:	0.861	
(ACTUAL/MAXIMUM) HEAT OF REACTION:	0.861	

DATA REDUCTION PROGRAM OUTPUT

RUN DATE:	07-07-88	EXPERIMENT NUMBER:	47
RUN TIME:	19:41	INTEGRATER RUN NUMBER:	364
INTERFACE HEIGHT:	23.0 cm	LAB PRESSURE:	735.7 ± 0.5 torr
BURNER DIAMETER:	19.0 cm	DRY-BULB TEMPERATURE:	23.0 ± 0.2 °C
FIRE SIZE:	67.2 ± 1.64 kW	WET-BULB TEMPERATURE:	16.9 ± 0.2 °C

SUPPLY FLOWRATES :

NATURAL GAS FUEL:	1.3340 ± 0.0326	g/sec
AIR ENTRAINED BY PLUME:	24.6390 ± 0.6306	g/sec
AIR ADDED TO UPPER LAYER:	12.8034 ± 1.1922	g/sec
TOTAL:	38.7764 ± 1.8554	g/sec

I = 16.5658 ± 0.1906 moles Air/mole Fuel
I_s = 9.7786 ± 0.1378 moles Air/mole Fuel

FUEL INLET REYNOLDS NUMBER: 815.9
FUEL INLET RICHARDSON NUMBER: 0.3467

FUEL COMPOSITION : (mole fractions)		AIR COMPOSITION : (mole fractions)	
METHANE	0.9444 ± 0.0100	OXYGEN	0.2062 ± 0.0010
ETHANE	0.0260 ± 0.0050	NITROGEN	0.7688 ± 0.0020
PROPANE	0.0074 ± 0.0020	WATER VAPOR	0.0155 ± 0.0004
NITROGEN	0.0154 ± 0.0020	CARBON DIOXIDE	0.0003 ± 0.0001
CARBON DIOXIDE	0.0070 ± 0.0020	ARGON	0.0092 ± 0.0006

FUEL VISCOSITY:	109.57 μPoise
FUEL MOLECULAR WEIGHT:	17.06 g/mole
FUEL LOWER HEATING VALUE:	50.72 MJ/kg

PRODUCT LAYER ANALYSIS :

	mole fractions	mass fractions	mass fraction of plume equivalent source
HYDROGEN	0.0000 ± 0.00000	0.0000	0.0000
OXYGEN	0.0814 ± 0.00270	0.0926	0.0253
NITROGEN	0.7258 ± 0.00650	0.7232	0.7110
METHANE	0.0000 ± 0.00000	0.0000	0.0000
CARBON MONOXIDE	0.0006 ± 0.00000	0.0006	0.0009
CARBON DIOXIDE	0.0581 ± 0.00110	0.0909	0.1355
WATER VAPOR	0.1255 ± 0.00850	0.0804	0.1153
SOOT (C_8H)	0.0000 ± 0.00000	0.0000	0.0000
ACETYLENE	0.0000 ± 0.00000	0.0000	0.0000
ETHYLENE	0.0000 ± 0.00000	0.0000	0.0000
ETHANE	0.0000 ± 0.00000	0.0000	0.0000
ARGON	0.0086 ± 0.00060	0.0123	0.0121

UPPER LAYER EQUIVALENCE RATIO:	0.590 ± 0.0107
PLUME EQUIVALENCE RATIO AT INTERFACE HEIGHT:	0.897 ± 0.0342
STOICHIOMETRIC FUEL/AIR MASS RATIO:	0.0604
SAMPLE TEMPERATURE:	347.2 °C
HOOD TEMPERATURE:	252.2 °C

HEAT OF FORMATION PER MOLE OF FUEL:	-17.412	kcal/mole
HEAT OF FORMATION PER MOLE OF AIR:	-0.926	kcal/mole
HEAT OF FORMATION PER MOLE OF PRODUCTS:	-12.731	kcal/mole
HEAT OF FORMATION PER MOLE OF STOICHIOMETRIC PRODUCTS :	-20.455	kcal/mole
ACTUAL HEAT OF REACTION:	-190.906	kcal/mole of fuel
HEAT OF STOICHIOMETRIC REACTION:	-194.437	kcal/mole of fuel
(ACTUAL/STOICHIOMETRIC) HEAT OF REACTION:	0.982	
(ACTUAL/MAXIMUM) HEAT OF REACTION:	0.982	

DATA REDUCTION PROGRAM OUTPUT

RUN DATE:	07-07-88	EXPERIMENT NUMBER:	48
RUN TIME:	19:24	INTEGRATER RUN NUMBER:	363
INTERFACE HEIGHT:	23.0 cm	LAB PRESSURE:	735.7 ± 0.5 torr
BURNER DIAMETER:	19.0 cm	DRY-BULB TEMPERATURE:	23.0 ± 0.2 °C
FIRE SIZE:	67.2 ± 1.64 kW	WET-BULB TEMPERATURE:	16.9 ± 0.2 °C

SUPPLY FLOWRATES :

NATURAL GAS FUEL:	1.3340 ± 0.0326	g/sec
AIR ENTRAINED BY PLUME:	24.6390 ± 0.6306	g/sec
AIR ADDED TO UPPER LAYER:	16.0938 ± 1.2817	g/sec
TOTAL:	42.0668 ± 1.9449	g/sec

I = 18.0217 ± 0.2225 moles Air/mole Fuel
I_s = 9.7786 ± 0.1378 moles Air/mole Fuel

FUEL INLET REYNOLDS NUMBER: 815.9
FUEL INLET RICHARDSON NUMBER: 0.3467

FUEL COMPOSITION : (mole fractions)

METHANE	0.9444 ± 0.0100
ETHANE	0.0260 ± 0.0050
PROPANE	0.0074 ± 0.0020
NITROGEN	0.0154 ± 0.0020
CARBON DIOXIDE	0.0070 ± 0.0020

AIR COMPOSITION : (mole fractions)

OXYGEN	0.2062 ± 0.0010
NITROGEN	0.7688 ± 0.0020
WATER VAPOR	0.0155 ± 0.0004
CARBON DIOXIDE	0.0003 ± 0.0001
ARGON	0.0092 ± 0.0006

FUEL VISCOSITY:	109.57 μPoise
FUEL MOLECULAR WEIGHT:	17.06 g/mole
FUEL LOWER HEATING VALUE:	50.72 MJ/kg

PRODUCT LAYER ANALYSIS :

	mole fractions	mass fractions	mass fraction of plume equivalent source
HYDROGEN	0.0000 ± 0.00000	0.0000	0.0000
OXYGEN	0.0900 ± 0.00300	0.1023	0.0237
NITROGEN	0.7283 ± 0.00710	0.7250	0.7108
METHANE	0.0000 ± 0.00000	0.0000	0.0000
CARBON MONOXIDE	0.0000 ± 0.00000	0.0000	0.0000
CARBON DIOXIDE	0.0534 ± 0.00100	0.0836	0.1351
WATER VAPOR	0.1195 ± 0.00920	0.0765	0.1179
SOOT (C_8H)	0.0001 ± 0.00140	0.0003	0.0005
ACETYLENE	0.0000 ± 0.00000	0.0000	0.0000
ETHYLENE	0.0000 ± 0.00000	0.0000	0.0000
ETHANE	0.0000 ± 0.00000	0.0000	0.0000
ARGON	0.0087 ± 0.00060	0.0123	0.0120

UPPER LAYER EQUIVALENCE RATIO:	0.543 ± 0.0102
PLUME EQUIVALENCE RATIO AT INTERFACE HEIGHT:	0.897 ± 0.0342
STOICHIOMETRIC FUEL/AIR MASS RATIO:	0.0604
SAMPLE TEMPERATURE:	343.9 °C
HOOD TEMPERATURE:	248.9 °C

HEAT OF FORMATION PER MOLE OF FUEL:		-17.412 kcal/mole
HEAT OF FORMATION PER MOLE OF AIR:		-0.926 kcal/mole
HEAT OF FORMATION PER MOLE OF PRODUCTS:		-11.933 kcal/mole
HEAT OF FORMATION PER MOLE OF STOICHIOMETRIC PRODUCTS :		-20.455 kcal/mole
ACTUAL HEAT OF REACTION:	-193.156 kcal/mole of fuel	
HEAT OF STOICHIOMETRIC REACTION:	-194.437 kcal/mole of fuel	
(ACTUAL/STOICHIOMETRIC) HEAT OF REACTION:	0.993	
(ACTUAL/MAXIMUM) HEAT OF REACTION:	0.993	

DATA REDUCTION PROGRAM OUTPUT

RUN DATE:	07-07-88	EXPERIMENT NUMBER:	49
RUN TIME:	19:07	INTEGRATER RUN NUMBER:	362
INTERFACE HEIGHT:	23.0 cm	LAB PRESSURE:	735.7 ± 0.5 torr
BURNER DIAMETER:	19.0 cm	DRY-BULB TEMPERATURE:	23.0 ± 0.2 °C
FIRE SIZE:	67.2 ± 1.64 kW	WET-BULB TEMPERATURE:	16.9 ± 0.2 °C

SUPPLY FLOWRATES :

NATURAL GAS FUEL:	1.3340 ± 0.0326	g/sec
AIR ENTRAINED BY PLUME:	24.6390 ± 0.6306	g/sec
AIR ADDED TO UPPER LAYER:	18.3155 ± 1.3542	g/sec
TOTAL:	44.2885 ± 2.0174	g/sec

I = 19.0046 ± 0.2553 moles Air/mole Fuel
I_s = 9.7786 ± 0.1378 moles Air/mole Fuel

FUEL INLET REYNOLDS NUMBER: 815.9
FUEL INLET RICHARDSON NUMBER: 0.3467

FUEL COMPOSITION : (mole fractions)		AIR COMPOSITION : (mole fractions)	
METHANE	0.9444 ± 0.0100	OXYGEN	0.2062 ± 0.0010
ETHANE	0.0260 ± 0.0050	NITROGEN	0.7688 ± 0.0020
PROPANE	0.0074 ± 0.0020	WATER VAPOR	0.0155 ± 0.0004
NITROGEN	0.0154 ± 0.0020	CARBON DIOXIDE	0.0003 ± 0.0001
CARBON DIOXIDE	0.0070 ± 0.0020	ARGON	0.0092 ± 0.0006

FUEL VISCOSITY:	109.57 μPoise
FUEL MOLECULAR WEIGHT:	17.06 g/mole
FUEL LOWER HEATING VALUE:	50.72 MJ/kg

PRODUCT LAYER ANALYSIS :

	mole fractions	mass fractions	mass fraction of plume equivalent source
HYDROGEN	0.0000 ± 0.00000	0.0000	0.0000
OXYGEN	0.0961 ± 0.00320	0.1091	0.0244
NITROGEN	0.7303 ± 0.00760	0.7262	0.7108
METHANE	0.0000 ± 0.00000	0.0000	0.0000
CARBON MONOXIDE	0.0000 ± 0.00000	0.0000	0.0000
CARBON DIOXIDE	0.0505 ± 0.00100	0.0789	0.1341
WATER VAPOR	0.1144 ± 0.00990	0.0731	0.1178
SOOT (C_8H)	0.0001 ± 0.00130	0.0004	0.0007
ACETYLENE	0.0000 ± 0.00000	0.0000	0.0000
ETHYLENE	0.0000 ± 0.00000	0.0000	0.0000
ETHANE	0.0000 ± 0.00000	0.0000	0.0000
ARGON	0.0087 ± 0.00060	0.0123	0.0120

UPPER LAYER EQUIVALENCE RATIO:	0.515 ± 0.0100
PLUME EQUIVALENCE RATIO AT INTERFACE HEIGHT:	0.897 ± 0.0342
STOICHIOMETRIC FUEL/AIR MASS RATIO:	0.0604
SAMPLE TEMPERATURE:	355.0 °C
HOOD TEMPERATURE:	238.9 °C

HEAT OF FORMATION PER MOLE OF FUEL:	-17.412	kcal/mole
HEAT OF FORMATION PER MOLE OF AIR:	-0.926	kcal/mole
HEAT OF FORMATION PER MOLE OF PRODUCTS:	-11.358	kcal/mole
HEAT OF FORMATION PER MOLE OF STOICHIOMETRIC PRODUCTS :	-20.455	kcal/mole
ACTUAL HEAT OF REACTION:	-192.456	kcal/mole of fuel
HEAT OF STOICHIOMETRIC REACTION:	-194.437	kcal/mole of fuel
(ACTUAL/STOICHIOMETRIC) HEAT OF REACTION:	0.990	
(ACTUAL/MAXIMUM) HEAT OF REACTION:	0.990	

DATA REDUCTION PROGRAM OUTPUT

RUN DATE:	07-07-88	EXPERIMENT NUMBER:	50
RUN TIME:	18:49	INTEGRATER RUN NUMBER:	361
INTERFACE HEIGHT:	23.0 cm	LAB PRESSURE:	735.7 ± 0.5 torr
BURNER DIAMETER:	19.0 cm	DRY-BULB TEMPERATURE:	23.0 ± 0.2 °C
FIRE SIZE:	67.2 ± 1.64 kW	WET-BULB TEMPERATURE:	16.9 ± 0.2 °C

SUPPLY FLOWRATES :

NATURAL GAS FUEL:	1.3340 ± 0.0326	g/sec
AIR ENTRAINED BY PLUME:	24.6390 ± 0.6306	g/sec
AIR ADDED TO UPPER LAYER:	31.4341 ± 1.9140	g/sec
TOTAL:	57.4071 ± 2.5772	g/sec

I = 24.8087 ± 0.5208 moles Air/mole Fuel
I_s = 9.7786 ± 0.1378 moles Air/mole Fuel

FUEL INLET REYNOLDS NUMBER: 815.9
FUEL INLET RICHARDSON NUMBER: 0.3467

FUEL COMPOSITION : (mole fractions)

METHANE	0.9444 ± 0.0100
ETHANE	0.0260 ± 0.0050
PROPANE	0.0074 ± 0.0020
NITROGEN	0.0154 ± 0.0020
CARBON DIOXIDE	0.0070 ± 0.0020

AIR COMPOSITION : (mole fractions)

OXYGEN	0.2062 ± 0.0010
NITROGEN	0.7688 ± 0.0020
WATER VAPOR	0.0155 ± 0.0004
CARBON DIOXIDE	0.0003 ± 0.0001
ARGON	0.0092 ± 0.0006

FUEL VISCOSITY:	109.57 μPoise
FUEL MOLECULAR WEIGHT:	17.06 g/mole
FUEL LOWER HEATING VALUE:	50.72 MJ/kg

PRODUCT LAYER ANALYSIS :

	mole fractions	mass fractions	mass fraction of plume equivalent source
HYDROGEN	0.0000 ± 0.00000	0.0000	0.0000
OXYGEN	0.1226 ± 0.00420	0.1386	0.0289
NITROGEN	0.7388 ± 0.01080	0.7311	0.7108
METHANE	0.0000 ± 0.00000	0.0000	0.0000
CARBON MONOXIDE	0.0000 ± 0.00000	0.0000	0.0000
CARBON DIOXIDE	0.0374 ± 0.00080	0.0582	0.1281
WATER VAPOR	0.0920 ± 0.01410	0.0586	0.1177
SOOT (C_8H)	0.0003 ± 0.00120	0.0011	0.0024
ACETYLENE	0.0000 ± 0.00000	0.0000	0.0000
ETHYLENE	0.0000 ± 0.00000	0.0000	0.0000
ETHANE	0.0000 ± 0.00000	0.0000	0.0000
ARGON	0.0088 ± 0.00060	0.0124	0.0120

UPPER LAYER EQUIVALENCE RATIO:	0.394 ± 0.0100
PLUME EQUIVALENCE RATIO AT INTERFACE HEIGHT:	0.897 ± 0.0342
STOICHIOMETRIC FUEL/AIR MASS RATIO:	0.0604
SAMPLE TEMPERATURE:	343.9 °C
HOOD TEMPERATURE:	217.8 °C

HEAT OF FORMATION PER MOLE OF FUEL:	-17.412	kcal/mole
HEAT OF FORMATION PER MOLE OF AIR:	-0.926	kcal/mole
HEAT OF FORMATION PER MOLE OF PRODUCTS:	-8.842	kcal/mole
HEAT OF FORMATION PER MOLE OF STOICHIOMETRIC PRODUCTS :	-20.455	kcal/mole
ACTUAL HEAT OF REACTION:	-188.048	kcal/mole of fuel
HEAT OF STOICHIOMETRIC REACTION:	-194.437	kcal/mole of fuel
(ACTUAL/STOICHIOMETRIC) HEAT OF REACTION:	0.967	
(ACTUAL/MAXIMUM) HEAT OF REACTION:	0.967	

DATA REDUCTION PROGRAM OUTPUT

RUN DATE:	07-14-88	EXPERIMENT NUMBER:	51
RUN TIME:	20:52	INTEGRATER RUN NUMBER:	393
INTERFACE HEIGHT:	23.0 cm	LAB PRESSURE:	736.0 ± 0.5 torr
BURNER DIAMETER:	19.0 cm	DRY-BULB TEMPERATURE:	22.2 ± 0.2 °C
FIRE SIZE:	41.1 ± 1.64 kW	WET-BULB TEMPERATURE:	17.0 ± 0.2 °C

SUPPLY FLOWRATES :

NATURAL GAS FUEL:	0.8146 ± 0.0326	g/sec
AIR ENTRAINED BY PLUME:	26.9021 ± 1.1220	g/sec
AIR ADDED TO UPPER LAYER:	0.0000 ± 0.0000	g/sec
TOTAL:	27.7167 ± 1.1546	g/sec

I = 19.5113 ± 0.2278 moles Air/mole Fuel
I_s = 9.7948 ± 0.1379 moles Air/mole Fuel

FUEL INLET REYNOLDS NUMBER: 498.4
FUEL INLET RICHARDSON NUMBER: 0.9264

FUEL COMPOSITION : (mole fractions)

METHANE	0.9436 ± 0.0100
ETHANE	0.0267 ± 0.0050
PROPANE	0.0076 ± 0.0020
NITROGEN	0.0148 ± 0.0020
CARBON DIOXIDE	0.0074 ± 0.0020

AIR COMPOSITION : (mole fractions)

OXYGEN	0.2061 ± 0.0010
NITROGEN	0.7682 ± 0.0020
WATER VAPOR	0.0163 ± 0.0004
CARBON DIOXIDE	0.0003 ± 0.0001
ARGON	0.0091 ± 0.0006

FUEL VISCOSITY:	109.53 μPoise
FUEL MOLECULAR WEIGHT:	17.07 g/mole
FUEL LOWER HEATING VALUE:	50.57 MJ/kg

PRODUCT LAYER ANALYSIS :

	mole fractions	mass fractions	mass fraction of plume equivalent source
HYDROGEN	0.0000 ± 0.00000	0.0000	0.0000
OXYGEN	0.0981 ± 0.00250	0.1114	0.1114
NITROGEN	0.7307 ± 0.00630	0.7263	0.7263
METHANE	0.0000 ± 0.00000	0.0000	0.0000
CARBON MONOXIDE	0.0000 ± 0.00000	0.0000	0.0000
CARBON DIOXIDE	0.0498 ± 0.00070	0.0778	0.0778
WATER VAPOR	0.1126 ± 0.00820	0.0720	0.0720
SOOT (C_8H)	0.0000 ± 0.00110	0.0001	0.0001
ACETYLENE	0.0001 ± 0.00000	0.0001	0.0001
ETHYLENE	0.0000 ± 0.00000	0.0000	0.0000
ETHANE	0.0000 ± 0.00000	0.0000	0.0000
ARGON	0.0087 ± 0.00060	0.0123	0.0123

UPPER LAYER EQUIVALENCE RATIO:	0.502 ± 0.0092
PLUME EQUIVALENCE RATIO AT INTERFACE HEIGHT:	0.502 ± 0.0299
STOICHIOMETRIC FUEL/AIR MASS RATIO:	0.0603
SAMPLE TEMPERATURE:	273.9 °C
HOOD TEMPERATURE:	204.4 °C

HEAT OF FORMATION PER MOLE OF FUEL:	-17.432	kcal/mole
HEAT OF FORMATION PER MOLE OF AIR:	-0.967	kcal/mole
HEAT OF FORMATION PER MOLE OF PRODUCTS:	-11.189	kcal/mole
HEAT OF FORMATION PER MOLE OF STOICHIOMETRIC PRODUCTS :	-20.484	kcal/mole
ACTUAL HEAT OF REACTION:	-193.438	kcal/mole of fuel
HEAT OF STOICHIOMETRIC REACTION:	-194.643	kcal/mole of fuel
(ACTUAL/STOICHIOMETRIC) HEAT OF REACTION:	0.994	
(ACTUAL/MAXIMUM) HEAT OF REACTION:	0.994	

DATA REDUCTION PROGRAM OUTPUT

RUN DATE:	07-07-88	EXPERIMENT NUMBER:	52
RUN TIME:	18:12	INTEGRATER RUN NUMBER:	359
INTERFACE HEIGHT:	23.0 cm	LAB PRESSURE:	735.7 ± 0.5 torr
BURNER DIAMETER:	19.0 cm	DRY-BULB TEMPERATURE:	23.0 ± 0.2 °C
FIRE SIZE:	40.8 ± 1.63 kW	WET-BULB TEMPERATURE:	16.9 ± 0.2 °C

SUPPLY FLOWRATES :

NATURAL GAS FUEL:	0.8067 ± 0.0323	g/sec
AIR ENTRAINED BY PLUME:	26.9020 ± 1.1220	g/sec
AIR ADDED TO UPPER LAYER:	14.1204 ± 2.3074	g/sec
TOTAL:	41.8291 ± 3.4617	g/sec

I = 30.0122 ± 0.8555 moles Air/mole Fuel
I_s = 9.7786 ± 0.1378 moles Air/mole Fuel

FUEL INLET REYNOLDS NUMBER: 493.4
FUEL INLET RICHARDSON NUMBER: 0.9403

FUEL COMPOSITION : (mole fractions)

METHANE	0.9444 ± 0.0100
ETHANE	0.0260 ± 0.0050
PROPANE	0.0074 ± 0.0020
NITROGEN	0.0154 ± 0.0020
CARBON DIOXIDE	0.0070 ± 0.0020

AIR COMPOSITION : (mole fractions)

OXYGEN	0.2062 ± 0.0010
NITROGEN	0.7688 ± 0.0020
WATER VAPOR	0.0155 ± 0.0004
CARBON DIOXIDE	0.0003 ± 0.0001
ARGON	0.0092 ± 0.0006

FUEL VISCOSITY:	109.57 μPoise
FUEL MOLECULAR WEIGHT:	17.06 g/mole
FUEL LOWER HEATING VALUE:	50.73 MJ/kg

PRODUCT LAYER ANALYSIS :

	mole fractions	mass fractions	mass fraction of plume equivalent source
HYDROGEN	0.0000 ± 0.00000	0.0000	0.0000
OXYGEN	0.1369 ± 0.00490	0.1543	0.1162
NITROGEN	0.7438 ± 0.01400	0.7340	0.7269
METHANE	0.0000 ± 0.00000	0.0000	0.0000
CARBON MONOXIDE	0.0000 ± 0.00000	0.0000	0.0000
CARBON DIOXIDE	0.0309 ± 0.00080	0.0480	0.0722
WATER VAPOR	0.0792 ± 0.01830	0.0503	0.0709
SOOT (C_8H)	0.0003 ± 0.00110	0.0010	0.0015
ACETYLENE	0.0000 ± 0.00000	0.0000	0.0000
ETHYLENE	0.0000 ± 0.00000	0.0000	0.0000
ETHANE	0.0000 ± 0.00000	0.0000	0.0000
ARGON	0.0089 ± 0.00070	0.0125	0.0123

UPPER LAYER EQUIVALENCE RATIO:	0.326 ± 0.0104
PLUME EQUIVALENCE RATIO AT INTERFACE HEIGHT:	0.497 ± 0.0296
STOICHIOMETRIC FUEL/AIR MASS RATIO:	0.0604
SAMPLE TEMPERATURE:	253.3 °C
HOOD TEMPERATURE:	172.2 °C

HEAT OF FORMATION PER MOLE OF FUEL:		-17.412 kcal/mole
HEAT OF FORMATION PER MOLE OF AIR:		-0.926 kcal/mole
HEAT OF FORMATION PER MOLE OF PRODUCTS:		-7.487 kcal/mole
HEAT OF FORMATION PER MOLE OF STOICHIOMETRIC PRODUCTS :		-20.455 kcal/mole
ACTUAL HEAT OF REACTION:	-187.194 kcal/mole of fuel	
HEAT OF STOICHIOMETRIC REACTION:	-194.437 kcal/mole of fuel	
(ACTUAL/STOICHIOMETRIC) HEAT OF REACTION:	0.963	
(ACTUAL/MAXIMUM) HEAT OF REACTION:	0.963	

DATA REDUCTION PROGRAM OUTPUT

RUN DATE:	07-07-88	EXPERIMENT NUMBER:	53
RUN TIME:	17:54	INTEGRATER RUN NUMBER:	358
INTERFACE HEIGHT:	23.0 cm	LAB PRESSURE:	735.7 ± 0.5 torr
BURNER DIAMETER:	19.0 cm	DRY-BULB TEMPERATURE:	23.0 ± 0.2 °C
FIRE SIZE:	40.8 ± 1.63 kW	WET-BULB TEMPERATURE:	16.9 ± 0.2 °C

SUPPLY FLOWRATES :

NATURAL GAS FUEL:	0.8067 ± 0.0323	g/sec
AIR ENTRAINED BY PLUME:	26.9020 ± 1.1220	g/sec
AIR ADDED TO UPPER LAYER:	27.1684 ± 3.4284	g/sec
TOTAL:	54.8771 ± 4.5827	g/sec

I = 39.5582 ± 1.7632 moles Air/mole Fuel
I_s = 9.7786 ± 0.1378 moles Air/mole Fuel

FUEL INLET REYNOLDS NUMBER: 493.4
FUEL INLET RICHARDSON NUMBER: 0.9403

FUEL COMPOSITION : (mole fractions)

METHANE	0.9444 ± 0.0100
ETHANE	0.0260 ± 0.0050
PROPANE	0.0074 ± 0.0020
NITROGEN	0.0154 ± 0.0020
CARBON DIOXIDE	0.0070 ± 0.0020

AIR COMPOSITION : (mole fractions)

OXYGEN	0.2062 ± 0.0010
NITROGEN	0.7688 ± 0.0020
WATER VAPOR	0.0155 ± 0.0004
CARBON DIOXIDE	0.0003 ± 0.0001
ARGON	0.0092 ± 0.0006

FUEL VISCOSITY:	109.57 μPoise
FUEL MOLECULAR WEIGHT:	17.06 g/mole
FUEL LOWER HEATING VALUE:	50.73 MJ/kg

PRODUCT LAYER ANALYSIS :

	mole fractions	mass fractions	mass fraction of plume equivalent source
HYDROGEN	0.0000 ± 0.00000	0.0000	0.0000
OXYGEN	0.1570 ± 0.00640	0.1764	0.1247
NITROGEN	0.7494 ± 0.02090	0.7373	0.7269
METHANE	0.0000 ± 0.00000	0.0000	0.0000
CARBON MONOXIDE	0.0000 ± 0.00000	0.0000	0.0000
CARBON DIOXIDE	0.0200 ± 0.00070	0.0309	0.0608
WATER VAPOR	0.0640 ± 0.02750	0.0405	0.0706
SOOT (C_8H)	0.0007 ± 0.00100	0.0024	0.0047
ACETYLENE	0.0000 ± 0.00000	0.0000	0.0000
ETHYLENE	0.0000 ± 0.00000	0.0000	0.0000
ETHANE	0.0000 ± 0.00000	0.0000	0.0000
ARGON	0.0089 ± 0.00080	0.0125	0.0123

UPPER LAYER EQUIVALENCE RATIO:	0.247 ± 0.0116
PLUME EQUIVALENCE RATIO AT INTERFACE HEIGHT:	0.497 ± 0.0296
STOICHIOMETRIC FUEL/AIR MASS RATIO:	0.0604
SAMPLE TEMPERATURE:	241.7 °C
HOOD TEMPERATURE:	151.1 °C

HEAT OF FORMATION PER MOLE OF FUEL:	-17.412	kcal/mole
HEAT OF FORMATION PER MOLE OF AIR:	-0.926	kcal/mole
HEAT OF FORMATION PER MOLE OF PRODUCTS:	-5.580	kcal/mole
HEAT OF FORMATION PER MOLE OF STOICHIOMETRIC PRODUCTS :	-20.455	kcal/mole
ACTUAL HEAT OF REACTION:	-172.523	kcal/mole of fuel
HEAT OF STOICHIOMETRIC REACTION:	-194.437	kcal/mole of fuel
(ACTUAL/STOICHIOMETRIC) HEAT OF REACTION:	0.887	
(ACTUAL/MAXIMUM) HEAT OF REACTION:	0.887	

DATA REDUCTION PROGRAM OUTPUT

RUN DATE:	07-12-88	EXPERIMENT NUMBER:	54
RUN TIME:	18:09	INTEGRATER RUN NUMBER:	383
INTERFACE HEIGHT:	5.0 cm	LAB PRESSURE:	737.3 ± 0.5 torr
BURNER DIAMETER:	19.0 cm	DRY-BULB TEMPERATURE:	22.5 ± 0.2 °C
FIRE SIZE:	67.5 ± 1.65 kW	WET-BULB TEMPERATURE:	17.3 ± 0.2 °C

SUPPLY FLOWRATES :

NATURAL GAS FUEL:	1.3460 ± 0.0329	g/sec
AIR ENTRAINED BY PLUME:	7.8965 ± 0.2210	g/sec
AIR ADDED TO UPPER LAYER:	0.0000 ± 0.0000	g/sec
TOTAL:	9.2425 ± 0.2539	g/sec

I = 3.4624 ± 0.0472 moles Air/mole Fuel
I_s = 9.7892 ± 0.1379 moles Air/mole Fuel

FUEL INLET REYNOLDS NUMBER: 823.2
FUEL INLET RICHARDSON NUMBER: 0.3426

FUEL COMPOSITION : (mole fractions)

METHANE	0.9444 ± 0.0100
ETHANE	0.0260 ± 0.0050
PROPANE	0.0074 ± 0.0020
NITROGEN	0.0154 ± 0.0020
CARBON DIOXIDE	0.0070 ± 0.0020

AIR COMPOSITION : (mole fractions)

OXYGEN	0.2060 ± 0.0010
NITROGEN	0.7679 ± 0.0020
WATER VAPOR	0.0166 ± 0.0004
CARBON DIOXIDE	0.0003 ± 0.0001
ARGON	0.0091 ± 0.0006

FUEL VISCOSITY:	109.57 μPoise
FUEL MOLECULAR WEIGHT:	17.06 g/mole
FUEL LOWER HEATING VALUE:	50.53 MJ/kg

PRODUCT LAYER ANALYSIS :

	mole fractions	mass fractions	mass fraction of plume equivalent source
HYDROGEN	0.0179 ± 0.00120	0.0014	0.0014
OXYGEN	0.0089 ± 0.00070	0.0111	0.0111
NITROGEN	0.5870 ± 0.00560	0.6424	0.6424
METHANE	0.1300 ± 0.00670	0.0813	0.0813
CARBON MONOXIDE	0.0196 ± 0.00060	0.0213	0.0213
CARBON DIOXIDE	0.0670 ± 0.00130	0.1153	0.1153
WATER VAPOR	0.1582 ± 0.00670	0.1113	0.1113
SOOT (C_8H)	0.0000 ± 0.00000	0.0000	0.0000
ACETYLENE	0.0021 ± 0.00010	0.0021	0.0021
ETHYLENE	0.0000 ± 0.00000	0.0000	0.0000
ETHANE	0.0025 ± 0.00000	0.0029	0.0029
ARGON	0.0070 ± 0.00050	0.0109	0.0109

UPPER LAYER EQUIVALENCE RATIO:	2.827 ± 0.0554
PLUME EQUIVALENCE RATIO AT INTERFACE HEIGHT:	2.827 ± 0.1124
STOICHIOMETRIC FUEL/AIR MASS RATIO:	0.0603
SAMPLE TEMPERATURE:	231.1 °C
HOOD TEMPERATURE:	166.7 °C

HEAT OF FORMATION PER MOLE OF FUEL:		-17.412 kcal/mole
HEAT OF FORMATION PER MOLE OF AIR:		-0.987 kcal/mole
HEAT OF FORMATION PER MOLE OF PRODUCTS:		-18.254 kcal/mole
HEAT OF FORMATION PER MOLE OF STOICHIOMETRIC PRODUCTS :		-20.492 kcal/mole
ACTUAL HEAT OF REACTION:	-61.899 kcal/mole of fuel	
HEAT OF STOICHIOMETRIC REACTION:	-194.437 kcal/mole of fuel	
(ACTUAL/STOICHIOMETRIC) HEAT OF REACTION:	0.318	
(ACTUAL/MAXIMUM) HEAT OF REACTION:	0.900	

DATA REDUCTION PROGRAM OUTPUT

RUN DATE:	07-21-88	EXPERIMENT NUMBER:	55
RUN TIME:	15:05	INTEGRATER RUN NUMBER:	441
INTERFACE HEIGHT:	5.0 cm	LAB PRESSURE:	739.6 ± 0.5 torr
BURNER DIAMETER:	19.0 cm	DRY-BULB TEMPERATURE:	22.9 ± 0.2 °C
FIRE SIZE:	67.7 ± 1.65 kW	WET-BULB TEMPERATURE:	17.7 ± 0.2 °C

SUPPLY FLOWRATES :

NATURAL GAS FUEL:	1.3513 ± 0.0330	g/sec
AIR ENTRAINED BY PLUME:	7.8970 ± 0.2210	g/sec
AIR ADDED TO UPPER LAYER:	0.6875 ± 0.3100	g/sec
TOTAL:	9.9358 ± 0.5640	g/sec

I = 3.7534 ± 0.0248 moles Air/mole Fuel
I_s = 9.8027 ± 0.1380 moles Air/mole Fuel

FUEL INLET REYNOLDS NUMBER: 826.8
FUEL INLET RICHARDSON NUMBER: 0.3420

FUEL COMPOSITION : (mole fractions)

METHANE	0.9436 ± 0.0100
ETHANE	0.0267 ± 0.0050
PROPANE	0.0076 ± 0.0020
NITROGEN	0.0148 ± 0.0020
CARBON DIOXIDE	0.0074 ± 0.0020

AIR COMPOSITION : (mole fractions)

OXYGEN	0.2059 ± 0.0010
NITROGEN	0.7676 ± 0.0020
WATER VAPOR	0.0170 ± 0.0004
CARBON DIOXIDE	0.0003 ± 0.0001
ARGON	0.0091 ± 0.0006

FUEL VISCOSITY:	109.53 μPoise
FUEL MOLECULAR WEIGHT:	17.07 g/mole
FUEL LOWER HEATING VALUE:	50.43 MJ/kg

PRODUCT LAYER ANALYSIS :

	mole fractions	mass fractions	mass fraction of plume equivalent source
HYDROGEN	0.0193 ± 0.00420	0.0015	0.0016
OXYGEN	0.0078 ± 0.00070	0.0097	-.0066
NITROGEN	0.5950 ± 0.00460	0.6488	0.6415
METHANE	0.1148 ± 0.00260	0.0717	0.0770
CARBON MONOXIDE	0.0182 ± 0.00050	0.0198	0.0213
CARBON DIOXIDE	0.0675 ± 0.00070	0.1157	0.1243
WATER VAPOR	0.1654 ± 0.00410	0.1160	0.1238
SOOT (C_8H)	0.0001 ± 0.00430	0.0004	0.0005
ACETYLENE	0.0028 ± 0.00010	0.0028	0.0030
ETHYLENE	0.0000 ± 0.00000	0.0000	0.0000
ETHANE	0.0022 ± 0.00000	0.0026	0.0027
ARGON	0.0070 ± 0.00050	0.0110	0.0108

UPPER LAYER EQUIVALENCE RATIO:	2.612 ± 0.0406
PLUME EQUIVALENCE RATIO AT INTERFACE HEIGHT:	2.839 ± 0.1128
STOICHIOMETRIC FUEL/AIR MASS RATIO:	0.0603
SAMPLE TEMPERATURE:	232.2 °C
HOOD TEMPERATURE:	168.9 °C

HEAT OF FORMATION PER MOLE OF FUEL:	-17.432	kcal/mole
HEAT OF FORMATION PER MOLE OF AIR:	-1.013	kcal/mole
HEAT OF FORMATION PER MOLE OF PRODUCTS:	-18.294	kcal/mole
HEAT OF FORMATION PER MOLE OF STOICHIOMETRIC PRODUCTS :	-20.511	kcal/mole
ACTUAL HEAT OF REACTION:	-67.809	kcal/mole of fuel
HEAT OF STOICHIOMETRIC REACTION:	-194.643	kcal/mole of fuel
(ACTUAL/STOICHIOMETRIC) HEAT OF REACTION:	0.348	
(ACTUAL/MAXIMUM) HEAT OF REACTION:	0.910	

DATA REDUCTION PROGRAM OUTPUT

RUN DATE:	07-07-88	EXPERIMENT NUMBER:	56
RUN TIME:	23:27	INTEGRATER RUN NUMBER:	375
INTERFACE HEIGHT:	5.0 cm	LAB PRESSURE:	735.7 ± 0.5 torr
BURNER DIAMETER:	19.0 cm	DRY-BULB TEMPERATURE:	23.0 ± 0.2 °C
FIRE SIZE:	67.2 ± 1.64 kW	WET-BULB TEMPERATURE:	16.9 ± 0.2 °C

SUPPLY FLOWRATES :

NATURAL GAS FUEL:	1.3340 ± 0.0326	g/sec
AIR ENTRAINED BY PLUME:	7.8970 ± 0.2210	g/sec
AIR ADDED TO UPPER LAYER:	4.6143 ± 0.3898	g/sec
TOTAL:	13.8453 ± 0.6434	g/sec

I =	5.5354 ± 0.0432 moles Air/mole Fuel	FUEL INLET REYNOLDS NUMBER:	815.9
I_s =	9.7786 ± 0.1378 moles Air/mole Fuel	FUEL INLET RICHARDSON NUMBER:	0.3467

FUEL COMPOSITION : (mole fractions)

METHANE	0.9444 ± 0.0100
ETHANE	0.0260 ± 0.0050
PROPANE	0.0074 ± 0.0020
NITROGEN	0.0154 ± 0.0020
CARBON DIOXIDE	0.0070 ± 0.0020

AIR COMPOSITION : (mole fractions)

OXYGEN	0.2062 ± 0.0010
NITROGEN	0.7688 ± 0.0020
WATER VAPOR	0.0155 ± 0.0004
CARBON DIOXIDE	0.0003 ± 0.0001
ARGON	0.0092 ± 0.0006

FUEL VISCOSITY:	109.57 μPoise
FUEL MOLECULAR WEIGHT:	17.06 g/mole
FUEL LOWER HEATING VALUE:	50.72 MJ/kg

PRODUCT LAYER ANALYSIS :

	mole fractions	mass fractions	mass fraction of plume equivalent source
HYDROGEN	0.0148 ± 0.00130	0.0011	0.0017
OXYGEN	0.0285 ± 0.00120	0.0343	-.0631
NITROGEN	0.6422 ± 0.00420	0.6784	0.6436
METHANE	0.0677 ± 0.00350	0.0409	0.0614
CARBON MONOXIDE	0.0148 ± 0.00050	0.0157	0.0235
CARBON DIOXIDE	0.0657 ± 0.00120	0.1091	0.1634
WATER VAPOR	0.1557 ± 0.00530	0.1057	0.1537
SOOT (C_8H)	0.0000 ± 0.00000	0.0000	0.0000
ACETYLENE	0.0020 ± 0.00000	0.0019	0.0029
ETHYLENE	0.0000 ± 0.00000	0.0000	0.0000
ETHANE	0.0012 ± 0.00000	0.0013	0.0020
ARGON	0.0076 ± 0.00050	0.0115	0.0109

UPPER LAYER EQUIVALENCE RATIO:	1.767 ± 0.0285
PLUME EQUIVALENCE RATIO AT INTERFACE HEIGHT:	2.799 ± 0.1112
STOICHIOMETRIC FUEL/AIR MASS RATIO:	0.0604
SAMPLE TEMPERATURE:	263.9 °C
HOOD TEMPERATURE:	190.6 °C

HEAT OF FORMATION PER MOLE OF FUEL:	-17.412	kcal/mole
HEAT OF FORMATION PER MOLE OF AIR:	-0.926	kcal/mole
HEAT OF FORMATION PER MOLE OF PRODUCTS:	-16.674	kcal/mole
HEAT OF FORMATION PER MOLE OF STOICHIOMETRIC PRODUCTS :	-20.455	kcal/mole
ACTUAL HEAT OF REACTION:	-88.352	kcal/mole of fuel
HEAT OF STOICHIOMETRIC REACTION:	-194.437	kcal/mole of fuel
(ACTUAL/STOICHIOMETRIC) HEAT OF REACTION:	0.454	
(ACTUAL/MAXIMUM) HEAT OF REACTION:	0.803	

DATA REDUCTION PROGRAM OUTPUT

RUN DATE:	07-21-88	EXPERIMENT NUMBER:	57
RUN TIME:	12:59	INTEGRATER RUN NUMBER:	435
INTERFACE HEIGHT:	5.0 cm	LAB PRESSURE:	739.6 ± 0.5 torr
BURNER DIAMETER:	19.0 cm	DRY-BULB TEMPERATURE:	22.9 ± 0.2 °C
FIRE SIZE:	67.7 ± 1.65 kW	WET-BULB TEMPERATURE:	17.7 ± 0.2 °C

SUPPLY FLOWRATES :

NATURAL GAS FUEL:	1.3513 ± 0.0330	g/sec
AIR ENTRAINED BY PLUME:	7.8970 ± 0.2210	g/sec
AIR ADDED TO UPPER LAYER:	21.2573 ± 0.7873	g/sec
TOTAL:	30.5056 ± 1.0413	g/sec

I = 12.7473 ± 0.1096 moles Air/mole Fuel
I_s = 9.8027 ± 0.1380 moles Air/mole Fuel

FUEL INLET REYNOLDS NUMBER: 826.8
FUEL INLET RICHARDSON NUMBER: 0.3420

FUEL COMPOSITION : (mole fractions)

METHANE	0.9436 ± 0.0100
ETHANE	0.0267 ± 0.0050
PROPANE	0.0076 ± 0.0020
NITROGEN	0.0148 ± 0.0020
CARBON DIOXIDE	0.0074 ± 0.0020

AIR COMPOSITION : (mole fractions)

OXYGEN	0.2059 ± 0.0010
NITROGEN	0.7676 ± 0.0020
WATER VAPOR	0.0170 ± 0.0004
CARBON DIOXIDE	0.0003 ± 0.0001
ARGON	0.0091 ± 0.0006

FUEL VISCOSITY:	109.53 μPoise
FUEL MOLECULAR WEIGHT:	17.07 g/mole
FUEL LOWER HEATING VALUE:	50.43 MJ/kg

PRODUCT LAYER ANALYSIS :

	mole fractions	mass fractions	mass fraction of plume equivalent source
HYDROGEN	0.0000 ± 0.00000	0.0000	0.0000
OXYGEN	0.0662 ± 0.00240	0.0761	-.2753
NITROGEN	0.7103 ± 0.00520	0.7152	0.6417
METHANE	0.0091 ± 0.00020	0.0052	0.0172
CARBON MONOXIDE	0.0048 ± 0.00010	0.0048	0.0160
CARBON DIOXIDE	0.0600 ± 0.00070	0.0949	0.3121
WATER VAPOR	0.1408 ± 0.00700	0.0911	0.2761
SOOT (C_8H)	0.0000 ± 0.00000	0.0000	0.0000
ACETYLENE	0.0004 ± 0.00000	0.0004	0.0013
ETHYLENE	0.0000 ± 0.00000	0.0000	0.0000
ETHANE	0.0000 ± 0.00000	0.0000	0.0000
ARGON	0.0084 ± 0.00060	0.0121	0.0108

UPPER LAYER EQUIVALENCE RATIO:	0.769 ± 0.0127
PLUME EQUIVALENCE RATIO AT INTERFACE HEIGHT:	2.839 ± 0.1128
STOICHIOMETRIC FUEL/AIR MASS RATIO:	0.0603
SAMPLE TEMPERATURE:	352.8 °C
HOOD TEMPERATURE:	214.4 °C

HEAT OF FORMATION PER MOLE OF FUEL:	-17.432	kcal/mole
HEAT OF FORMATION PER MOLE OF AIR:	-1.013	kcal/mole
HEAT OF FORMATION PER MOLE OF PRODUCTS:	-14.046	kcal/mole
HEAT OF FORMATION PER MOLE OF STOICHIOMETRIC PRODUCTS :	-20.511	kcal/mole
ACTUAL HEAT OF REACTION:	-163.434	kcal/mole of fuel
HEAT OF STOICHIOMETRIC REACTION:	-194.643	kcal/mole of fuel
(ACTUAL/STOICHIOMETRIC) HEAT OF REACTION:	0.840	
(ACTUAL/MAXIMUM) HEAT OF REACTION:	0.840	

DATA REDUCTION PROGRAM OUTPUT

RUN DATE:	07-19-88	EXPERIMENT NUMBER:	58
RUN TIME:	13:12	INTEGRATER RUN NUMBER:	410
INTERFACE HEIGHT:	5.0 cm	LAB PRESSURE:	737.3 ± 0.5 torr
BURNER DIAMETER:	19.0 cm	DRY-BULB TEMPERATURE:	22.8 ± 0.2 °C
FIRE SIZE:	67.5 ± 1.65 kW	WET-BULB TEMPERATURE:	17.7 ± 0.2 °C

SUPPLY FLOWRATES :

NATURAL GAS FUEL:	1.3442 ± 0.0329	g/sec
AIR ENTRAINED BY PLUME:	7.8970 ± 0.2210	g/sec
AIR ADDED TO UPPER LAYER:	21.9941 ± 0.8113	g/sec
TOTAL:	31.2353 ± 1.0652	g/sec

I =	13.1382 ± 0.1204 moles Air/mole Fuel	FUEL INLET REYNOLDS NUMBER:	822.4
I_s =	9.8040 ± 0.1380 moles Air/mole Fuel	FUEL INLET RICHARDSON NUMBER:	0.3436

FUEL COMPOSITION : (mole fractions)

METHANE	0.9436 ± 0.0100
ETHANE	0.0267 ± 0.0050
PROPANE	0.0076 ± 0.0020
NITROGEN	0.0148 ± 0.0020
CARBON DIOXIDE	0.0074 ± 0.0020

AIR COMPOSITION : (mole fractions)

OXYGEN	0.2059 ± 0.0010
NITROGEN	0.7675 ± 0.0020
WATER VAPOR	0.0172 ± 0.0004
CARBON DIOXIDE	0.0003 ± 0.0001
ARGON	0.0091 ± 0.0006

FUEL VISCOSITY:	109.53 μPoise
FUEL MOLECULAR WEIGHT:	17.07 g/mole
FUEL LOWER HEATING VALUE:	50.57 MJ/kg

PRODUCT LAYER ANALYSIS :

	mole fractions	mass fractions	mass fraction of plume equivalent source
HYDROGEN	0.0000 ± 0.00000	0.0000	0.0000
OXYGEN	0.0692 ± 0.00230	0.0794	-.2766
NITROGEN	0.7130 ± 0.00540	0.7162	0.6426
METHANE	0.0083 ± 0.00040	0.0048	0.0162
CARBON MONOXIDE	0.0044 ± 0.00010	0.0045	0.0151
CARBON DIOXIDE	0.0600 ± 0.00110	0.0948	0.3192
WATER VAPOR	0.1366 ± 0.00720	0.0882	0.2726
SOOT (C_8H)	0.0000 ± 0.00000	0.0000	0.0000
ACETYLENE	0.0000 ± 0.00000	0.0000	0.0000
ETHYLENE	0.0000 ± 0.00000	0.0000	0.0000
ETHANE	0.0000 ± 0.00000	0.0000	0.0000
ARGON	0.0085 ± 0.00060	0.0121	0.0109

UPPER LAYER EQUIVALENCE RATIO:	0.746 ± 0.0125
PLUME EQUIVALENCE RATIO AT INTERFACE HEIGHT:	2.825 ± 0.1122
STOICHIOMETRIC FUEL/AIR MASS RATIO:	0.0603
SAMPLE TEMPERATURE:	355.6 °C
HOOD TEMPERATURE:	220.0 °C

HEAT OF FORMATION PER MOLE OF FUEL:	-17.432	kcal/mole
HEAT OF FORMATION PER MOLE OF AIR:	-1.021	kcal/mole
HEAT OF FORMATION PER MOLE OF PRODUCTS:	-13.807	kcal/mole
HEAT OF FORMATION PER MOLE OF STOICHIOMETRIC PRODUCTS :	-20.516	kcal/mole
ACTUAL HEAT OF REACTION:	-164.724	kcal/mole of fuel
HEAT OF STOICHIOMETRIC REACTION:	-194.643	kcal/mole of fuel
(ACTUAL/STOICHIOMETRIC) HEAT OF REACTION:	0.846	
(ACTUAL/MAXIMUM) HEAT OF REACTION:	0.846	

DATA REDUCTION PROGRAM OUTPUT

RUN DATE:	07-07-88	EXPERIMENT NUMBER:	59
RUN TIME:	22:11	INTEGRATER RUN NUMBER:	371
INTERFACE HEIGHT:	5.0 cm	LAB PRESSURE:	735.7 ± 0.5 torr
BURNER DIAMETER:	19.0 cm	DRY-BULB TEMPERATURE:	23.0 ± 0.2 °C
FIRE SIZE:	67.2 ± 1.64 kW	WET-BULB TEMPERATURE:	16.9 ± 0.2 °C

SUPPLY FLOWRATES :

NATURAL GAS FUEL:	1.3340 ± 0.0326	g/sec
AIR ENTRAINED BY PLUME:	7.8970 ± 0.2210	g/sec
AIR ADDED TO UPPER LAYER:	25.4022 ± 0.9050	g/sec
TOTAL:	34.6332 ± 1.1586	g/sec

I =	14.7327 ± 0.1448 moles Air/mole Fuel	FUEL INLET REYNOLDS NUMBER:	815.9
I_s =	9.7786 ± 0.1378 moles Air/mole Fuel	FUEL INLET RICHARDSON NUMBER:	0.3467

FUEL COMPOSITION : (mole fractions)		AIR COMPOSITION : (mole fractions)	
METHANE	0.9444 ± 0.0100	OXYGEN	0.2062 ± 0.0010
ETHANE	0.0260 ± 0.0050	NITROGEN	0.7688 ± 0.0020
PROPANE	0.0074 ± 0.0020	WATER VAPOR	0.0155 ± 0.0004
NITROGEN	0.0154 ± 0.0020	CARBON DIOXIDE	0.0003 ± 0.0001
CARBON DIOXIDE	0.0070 ± 0.0020	ARGON	0.0092 ± 0.0006

FUEL VISCOSITY:	109.57	μPoise
FUEL MOLECULAR WEIGHT:	17.06	g/mole
FUEL LOWER HEATING VALUE:	50.72	MJ/kg

PRODUCT LAYER ANALYSIS :

	mole fractions	mass fractions	mass fraction of plume equivalent source
HYDROGEN	0.0000 ± 0.00000	0.0000	0.0000
OXYGEN	0.0740 ± 0.00250	0.0846	-.3132
NITROGEN	0.7193 ± 0.00580	0.7202	0.6438
METHANE	0.0035 ± 0.00020	0.0020	0.0075
CARBON MONOXIDE	0.0031 ± 0.00010	0.0031	0.0117
CARBON DIOXIDE	0.0587 ± 0.00110	0.0923	0.3452
WATER VAPOR	0.1328 ± 0.00760	0.0855	0.2941
SOOT (C_8H)	0.0000 ± 0.00000	0.0000	0.0000
ACETYLENE	0.0000 ± 0.00000	0.0000	0.0000
ETHYLENE	0.0000 ± 0.00000	0.0000	0.0000
ETHANE	0.0000 ± 0.00000	0.0000	0.0000
ARGON	0.0086 ± 0.00060	0.0122	0.0109

UPPER LAYER EQUIVALENCE RATIO:	0.664 ± 0.0114
PLUME EQUIVALENCE RATIO AT INTERFACE HEIGHT:	2.799 ± 0.1112
STOICHIOMETRIC FUEL/AIR MASS RATIO:	0.0604
SAMPLE TEMPERATURE:	393.9 °C
HOOD TEMPERATURE:	201.7 °C

HEAT OF FORMATION PER MOLE OF FUEL:	-17.412	kcal/mole
HEAT OF FORMATION PER MOLE OF AIR:	-0.926	kcal/mole
HEAT OF FORMATION PER MOLE OF PRODUCTS:	-13.343	kcal/mole
HEAT OF FORMATION PER MOLE OF STOICHIOMETRIC PRODUCTS :	-20.455	kcal/mole
ACTUAL HEAT OF REACTION:	-179.332	kcal/mole of fuel
HEAT OF STOICHIOMETRIC REACTION:	-194.437	kcal/mole of fuel
(ACTUAL/STOICHIOMETRIC) HEAT OF REACTION:	0.922	
(ACTUAL/MAXIMUM) HEAT OF REACTION:	0.922	

DATA REDUCTION PROGRAM OUTPUT

RUN DATE:	07-12-88	EXPERIMENT NUMBER:	60
RUN TIME:	17:31	INTEGRATER RUN NUMBER:	381
INTERFACE HEIGHT:	5.0 cm	LAB PRESSURE:	737.3 ± 0.5 torr
BURNER DIAMETER:	19.0 cm	DRY-BULB TEMPERATURE:	22.5 ± 0.2 °C
FIRE SIZE:	41.0 ± 1.64 kW	WET-BULB TEMPERATURE:	17.3 ± 0.2 °C

SUPPLY FLOWRATES :

NATURAL GAS FUEL:	0.8140 ± 0.0326	g/sec
AIR ENTRAINED BY PLUME:	9.2377 ± 0.3759	g/sec
AIR ADDED TO UPPER LAYER:	0.0000 ± 0.0000	g/sec
TOTAL:	10.0517 ± 0.4085	g/sec

I = 6.6977 ± 0.0487 moles Air/mole Fuel
I_s = 9.7892 ± 0.1379 moles Air/mole Fuel

FUEL INLET REYNOLDS NUMBER: 497.8
FUEL INLET RICHARDSON NUMBER: 0.9291

FUEL COMPOSITION : (mole fractions)

METHANE	0.9444 ± 0.0100
ETHANE	0.0260 ± 0.0050
PROPANE	0.0074 ± 0.0020
NITROGEN	0.0154 ± 0.0020
CARBON DIOXIDE	0.0070 ± 0.0020

AIR COMPOSITION : (mole fractions)

OXYGEN	0.2060 ± 0.0010
NITROGEN	0.7679 ± 0.0020
WATER VAPOR	0.0166 ± 0.0004
CARBON DIOXIDE	0.0003 ± 0.0001
ARGON	0.0091 ± 0.0006

FUEL VISCOSITY:	109.57 μPoise
FUEL MOLECULAR WEIGHT:	17.06 g/mole
FUEL LOWER HEATING VALUE:	50.54 MJ/kg

PRODUCT LAYER ANALYSIS :

	mole fractions	mass fractions	mass fraction of plume equivalent source
HYDROGEN	0.0068 ± 0.00030	0.0005	0.0005
OXYGEN	0.0300 ± 0.00120	0.0354	0.0354
NITROGEN	0.6646 ± 0.00390	0.6893	0.6893
METHANE	0.0449 ± 0.00230	0.0266	0.0266
CARBON MONOXIDE	0.0130 ± 0.00040	0.0135	0.0135
CARBON DIOXIDE	0.0694 ± 0.00120	0.1131	0.1131
WATER VAPOR	0.1608 ± 0.00520	0.1072	0.1072
SOOT (C_8H)	0.0000 ± 0.00000	0.0000	0.0000
ACETYLENE	0.0017 ± 0.00000	0.0017	0.0017
ETHYLENE	0.0000 ± 0.00000	0.0000	0.0000
ETHANE	0.0010 ± 0.00000	0.0011	0.0011
ARGON	0.0079 ± 0.00050	0.0117	0.0117

UPPER LAYER EQUIVALENCE RATIO:	1.462 ± 0.0232
PLUME EQUIVALENCE RATIO AT INTERFACE HEIGHT:	1.462 ± 0.0859
STOICHIOMETRIC FUEL/AIR MASS RATIO:	0.0603
SAMPLE TEMPERATURE:	230.6 °C
HOOD TEMPERATURE:	164.4 °C

HEAT OF FORMATION PER MOLE OF FUEL:	-17.412	kcal/mole
HEAT OF FORMATION PER MOLE OF AIR:	-0.987	kcal/mole
HEAT OF FORMATION PER MOLE OF PRODUCTS:	-16.930	kcal/mole
HEAT OF FORMATION PER MOLE OF STOICHIOMETRIC PRODUCTS :	-20.492	kcal/mole
ACTUAL HEAT OF REACTION:	-106.834	kcal/mole of fuel
HEAT OF STOICHIOMETRIC REACTION:	-194.437	kcal/mole of fuel
(ACTUAL/STOICHIOMETRIC) HEAT OF REACTION:	0.549	
(ACTUAL/MAXIMUM) HEAT OF REACTION:	0.803	

DATA REDUCTION PROGRAM OUTPUT

RUN DATE:	07-07-88	EXPERIMENT NUMBER:	61
RUN TIME:	21:35	INTEGRATER RUN NUMBER:	369
INTERFACE HEIGHT:	5.0 cm	LAB PRESSURE:	735.7 ± 0.5 torr
BURNER DIAMETER:	19.0 cm	DRY-BULB TEMPERATURE:	23.0 ± 0.2 °C
FIRE SIZE:	40.8 ± 1.63 kW	WET-BULB TEMPERATURE:	16.9 ± 0.2 °C

SUPPLY FLOWRATES :

NATURAL GAS FUEL:	0.8067 ± 0.0323	g/sec
AIR ENTRAINED BY PLUME:	9.2380 ± 0.3759	g/sec
AIR ADDED TO UPPER LAYER:	7.7299 ± 0.7903	g/sec
TOTAL:	17.7746 ± 1.1985	g/sec

I = 12.4138 ± 0.1079 moles Air/mole Fuel
I_s = 9.7786 ± 0.1378 moles Air/mole Fuel

FUEL INLET REYNOLDS NUMBER: 493.4
FUEL INLET RICHARDSON NUMBER: 0.9403

FUEL COMPOSITION : (mole fractions)

METHANE	0.9444 ± 0.0100
ETHANE	0.0260 ± 0.0050
PROPANE	0.0074 ± 0.0020
NITROGEN	0.0154 ± 0.0020
CARBON DIOXIDE	0.0070 ± 0.0020

AIR COMPOSITION : (mole fractions)

OXYGEN	0.2062 ± 0.0010
NITROGEN	0.7688 ± 0.0020
WATER VAPOR	0.0155 ± 0.0004
CARBON DIOXIDE	0.0003 ± 0.0001
ARGON	0.0092 ± 0.0006

FUEL VISCOSITY:	109.57 μPoise
FUEL MOLECULAR WEIGHT:	17.06 g/mole
FUEL LOWER HEATING VALUE:	50.73 MJ/kg

PRODUCT LAYER ANALYSIS :

	mole fractions	mass fractions	mass fraction of plume equivalent source
HYDROGEN	0.0000 ± 0.00000	0.0000	0.0000
OXYGEN	0.0602 ± 0.00210	0.0692	-.0540
NITROGEN	0.7112 ± 0.00500	0.7154	0.6904
METHANE	0.0063 ± 0.00030	0.0037	0.0065
CARBON MONOXIDE	0.0059 ± 0.00020	0.0059	0.0104
CARBON DIOXIDE	0.0632 ± 0.00110	0.1000	0.1765
WATER VAPOR	0.1442 ± 0.00670	0.0933	0.1576
SOOT (C_8H)	0.0000 ± 0.00000	0.0000	0.0000
ACETYLENE	0.0006 ± 0.00000	0.0005	0.0009
ETHYLENE	0.0000 ± 0.00000	0.0000	0.0000
ETHANE	0.0000 ± 0.00000	0.0000	0.0000
ARGON	0.0085 ± 0.00060	0.0121	0.0117

UPPER LAYER EQUIVALENCE RATIO:	0.788 ± 0.0130
PLUME EQUIVALENCE RATIO AT INTERFACE HEIGHT:	1.447 ± 0.0851
STOICHIOMETRIC FUEL/AIR MASS RATIO:	0.0604
SAMPLE TEMPERATURE:	265.0 °C
HOOD TEMPERATURE:	185.6 °C

HEAT OF FORMATION PER MOLE OF FUEL:	-17.412	kcal/mole
HEAT OF FORMATION PER MOLE OF AIR:	-0.926	kcal/mole
HEAT OF FORMATION PER MOLE OF PRODUCTS:	-14.519	kcal/mole
HEAT OF FORMATION PER MOLE OF STOICHIOMETRIC PRODUCTS :	-20.455	kcal/mole
ACTUAL HEAT OF REACTION:	-166.241	kcal/mole of fuel
HEAT OF STOICHIOMETRIC REACTION:	-194.437	kcal/mole of fuel
(ACTUAL/STOICHIOMETRIC) HEAT OF REACTION:	0.855	
(ACTUAL/MAXIMUM) HEAT OF REACTION:	0.855	

DATA REDUCTION PROGRAM OUTPUT

RUN DATE:	07-07-88	EXPERIMENT NUMBER:	62
RUN TIME:	21:16	INTEGRATER RUN NUMBER:	368
INTERFACE HEIGHT:	5.0 cm	LAB PRESSURE:	735.7 ± 0.5 torr
BURNER DIAMETER:	19.0 cm	DRY-BULB TEMPERATURE:	23.0 ± 0.2 °C
FIRE SIZE:	40.8 ± 1.63 kW	WET-BULB TEMPERATURE:	16.9 ± 0.2 °C

SUPPLY FLOWRATES :

NATURAL GAS FUEL:	0.8067 ± 0.0323	g/sec
AIR ENTRAINED BY PLUME:	9.2380 ± 0.3759	g/sec
AIR ADDED TO UPPER LAYER:	11.9939 ± 0.9544	g/sec
TOTAL:	22.0386 ± 1.3626	g/sec

I =	15.5334 ± 0.1585 moles Air/mole Fuel	FUEL INLET REYNOLDS NUMBER:	493.4
I_s =	9.7786 ± 0.1378 moles Air/mole Fuel	FUEL INLET RICHARDSON NUMBER:	0.9403

FUEL COMPOSITION : (mole fractions)

METHANE	0.9444 ± 0.0100
ETHANE	0.0260 ± 0.0050
PROPANE	0.0074 ± 0.0020
NITROGEN	0.0154 ± 0.0020
CARBON DIOXIDE	0.0070 ± 0.0020

AIR COMPOSITION : (mole fractions)

OXYGEN	0.2062 ± 0.0010
NITROGEN	0.7688 ± 0.0020
WATER VAPOR	0.0155 ± 0.0004
CARBON DIOXIDE	0.0003 ± 0.0001
ARGON	0.0092 ± 0.0006

FUEL VISCOSITY:	109.57 μPoise
FUEL MOLECULAR WEIGHT:	17.06 g/mole
FUEL LOWER HEATING VALUE:	50.73 MJ/kg

PRODUCT LAYER ANALYSIS :

	mole fractions	mass fractions	mass fraction of plume equivalent source
HYDROGEN	0.0000 ± 0.00000	0.0000	0.0000
OXYGEN	0.0772 ± 0.00260	0.0882	-.0802
NITROGEN	0.7215 ± 0.00600	0.7215	0.6899
METHANE	0.0020 ± 0.00010	0.0012	0.0026
CARBON MONOXIDE	0.0021 ± 0.00010	0.0021	0.0046
CARBON DIOXIDE	0.0577 ± 0.00110	0.0906	0.1983
WATER VAPOR	0.1307 ± 0.00790	0.0840	0.1727
SOOT (C_8H)	0.0000 ± 0.00000	0.0000	0.0000
ACETYLENE	0.0002 ± 0.00000	0.0002	0.0003
ETHYLENE	0.0000 ± 0.00000	0.0000	0.0000
ETHANE	0.0000 ± 0.00000	0.0000	0.0000
ARGON	0.0086 ± 0.00060	0.0122	0.0117

UPPER LAYER EQUIVALENCE RATIO:	0.629 ± 0.0110
PLUME EQUIVALENCE RATIO AT INTERFACE HEIGHT:	1.447 ± 0.0851
STOICHIOMETRIC FUEL/AIR MASS RATIO:	0.0604
SAMPLE TEMPERATURE:	272.8 °C
HOOD TEMPERATURE:	189.4 °C

HEAT OF FORMATION PER MOLE OF FUEL:	-17.412	kcal/mole
HEAT OF FORMATION PER MOLE OF AIR:	-0.926	kcal/mole
HEAT OF FORMATION PER MOLE OF PRODUCTS:	-13.062	kcal/mole
HEAT OF FORMATION PER MOLE OF STOICHIOMETRIC PRODUCTS :	-20.455	kcal/mole
ACTUAL HEAT OF REACTION:	-184.670	kcal/mole of fuel
HEAT OF STOICHIOMETRIC REACTION:	-194.437	kcal/mole of fuel
(ACTUAL/STOICHIOMETRIC) HEAT OF REACTION:	0.950	
(ACTUAL/MAXIMUM) HEAT OF REACTION:	0.950	

DATA REDUCTION PROGRAM OUTPUT

RUN DATE:	07-07-88	EXPERIMENT NUMBER:	63
RUN TIME:	20:59	INTEGRATER RUN NUMBER:	367
INTERFACE HEIGHT:	5.0 cm	LAB PRESSURE:	735.7 ± 0.5 torr
BURNER DIAMETER:	19.0 cm	DRY-BULB TEMPERATURE:	23.0 ± 0.2 °C
FIRE SIZE:	40.8 ± 1.63 kW	WET-BULB TEMPERATURE:	16.9 ± 0.2 °C

SUPPLY FLOWRATES :

NATURAL GAS FUEL:	0.8067 ± 0.0323	g/sec
AIR ENTRAINED BY PLUME:	9.2380 ± 0.3759	g/sec
AIR ADDED TO UPPER LAYER:	17.2149 ± 1.1820	g/sec
TOTAL:	27.2596 ± 1.5902	g/sec

I = 19.3531 ± 0.2678 moles Air/mole Fuel
I_s = 9.7786 ± 0.1378 moles Air/mole Fuel

FUEL INLET REYNOLDS NUMBER: 493.4
FUEL INLET RICHARDSON NUMBER: 0.9403

FUEL COMPOSITION : (mole fractions)		AIR COMPOSITION : (mole fractions)	
METHANE	0.9444 ± 0.0100	OXYGEN	0.2062 ± 0.0010
ETHANE	0.0260 ± 0.0050	NITROGEN	0.7688 ± 0.0020
PROPANE	0.0074 ± 0.0020	WATER VAPOR	0.0155 ± 0.0004
NITROGEN	0.0154 ± 0.0020	CARBON DIOXIDE	0.0003 ± 0.0001
CARBON DIOXIDE	0.0070 ± 0.0020	ARGON	0.0092 ± 0.0006

FUEL VISCOSITY:	109.57 μPoise
FUEL MOLECULAR WEIGHT:	17.06 g/mole
FUEL LOWER HEATING VALUE:	50.73 MJ/kg

PRODUCT LAYER ANALYSIS :

	mole fractions	mass fractions	mass fraction of plume equivalent source
HYDROGEN	0.0000 ± 0.00000	0.0000	0.0000
OXYGEN	0.0981 ± 0.00320	0.1114	-.0904
NITROGEN	0.7308 ± 0.00780	0.7265	0.6899
METHANE	0.0000 ± 0.00000	0.0000	0.0000
CARBON MONOXIDE	0.0005 ± 0.00000	0.0005	0.0014
CARBON DIOXIDE	0.0491 ± 0.00100	0.0768	0.2075
WATER VAPOR	0.1126 ± 0.01010	0.0720	0.1788
SOOT (C_8H)	0.0001 ± 0.00130	0.0004	0.0011
ACETYLENE	0.0000 ± 0.00000	0.0000	0.0000
ETHYLENE	0.0000 ± 0.00000	0.0000	0.0000
ETHANE	0.0000 ± 0.00000	0.0000	0.0000
ARGON	0.0087 ± 0.00060	0.0123	0.0117

UPPER LAYER EQUIVALENCE RATIO:	0.505 ± 0.0100
PLUME EQUIVALENCE RATIO AT INTERFACE HEIGHT:	1.447 ± 0.0851
STOICHIOMETRIC FUEL/AIR MASS RATIO:	0.0604
SAMPLE TEMPERATURE:	281.1 °C
HOOD TEMPERATURE:	185.6 °C

HEAT OF FORMATION PER MOLE OF FUEL:	-17.412	kcal/mole
HEAT OF FORMATION PER MOLE OF AIR:	-0.926	kcal/mole
HEAT OF FORMATION PER MOLE OF PRODUCTS:	-11.147	kcal/mole
HEAT OF FORMATION PER MOLE OF STOICHIOMETRIC PRODUCTS :	-20.455	kcal/mole
ACTUAL HEAT OF REACTION:	-191.857	kcal/mole of fuel
HEAT OF STOICHIOMETRIC REACTION:	-194.437	kcal/mole of fuel
(ACTUAL/STOICHIOMETRIC) HEAT OF REACTION:	0.987	
(ACTUAL/MAXIMUM) HEAT OF REACTION:	0.987	

DATA REDUCTION PROGRAM OUTPUT

RUN DATE:	07-07-88	EXPERIMENT NUMBER:	64
RUN TIME:	20:40	INTEGRATER RUN NUMBER:	366
INTERFACE HEIGHT:	5.0 cm	LAB PRESSURE:	735.7 ± 0.5 torr
BURNER DIAMETER:	19.0 cm	DRY-BULB TEMPERATURE:	23.0 ± 0.2 °C
FIRE SIZE:	40.8 ± 1.63 kW	WET-BULB TEMPERATURE:	16.9 ± 0.2 °C

SUPPLY FLOWRATES :

NATURAL GAS FUEL:	0.8067 ± 0.0323	g/sec
AIR ENTRAINED BY PLUME:	9.2380 ± 0.3759	g/sec
AIR ADDED TO UPPER LAYER:	27.9313 ± 1.7798	g/sec
TOTAL:	37.9760 ± 2.1880	g/sec

I = 27.1933 ± 0.6591 moles Air/mole Fuel
I_s = 9.7786 ± 0.1378 moles Air/mole Fuel

FUEL INLET REYNOLDS NUMBER: 493.4
FUEL INLET RICHARDSON NUMBER: 0.9403

FUEL COMPOSITION : (mole fractions)

METHANE	0.9444 ± 0.0100
ETHANE	0.0260 ± 0.0050
PROPANE	0.0074 ± 0.0020
NITROGEN	0.0154 ± 0.0020
CARBON DIOXIDE	0.0070 ± 0.0020

AIR COMPOSITION : (mole fractions)

OXYGEN	0.2062 ± 0.0010
NITROGEN	0.7688 ± 0.0020
WATER VAPOR	0.0155 ± 0.0004
CARBON DIOXIDE	0.0003 ± 0.0001
ARGON	0.0092 ± 0.0006

FUEL VISCOSITY:	109.57 μPoise
FUEL MOLECULAR WEIGHT:	17.06 g/mole
FUEL LOWER HEATING VALUE:	50.73 MJ/kg

PRODUCT LAYER ANALYSIS :

	mole fractions	mass fractions	mass fraction of plume equivalent source
HYDROGEN	0.0000 ± 0.00000	0.0000	0.0000
OXYGEN	0.1292 ± 0.00450	0.1458	-.0861
NITROGEN	0.7414 ± 0.01220	0.7326	0.6899
METHANE	0.0000 ± 0.00000	0.0000	0.0000
CARBON MONOXIDE	0.0000 ± 0.00000	0.0000	0.0000
CARBON DIOXIDE	0.0348 ± 0.00080	0.0540	0.2030
WATER VAPOR	0.0856 ± 0.01590	0.0544	0.1786
SOOT (C_8H)	0.0002 ± 0.00120	0.0008	0.0030
ACETYLENE	0.0000 ± 0.00000	0.0000	0.0000
ETHYLENE	0.0000 ± 0.00000	0.0000	0.0000
ETHANE	0.0000 ± 0.00000	0.0000	0.0000
ARGON	0.0088 ± 0.00070	0.0124	0.0117

UPPER LAYER EQUIVALENCE RATIO:	0.360 ± 0.0101
PLUME EQUIVALENCE RATIO AT INTERFACE HEIGHT:	1.447 ± 0.0851
STOICHIOMETRIC FUEL/AIR MASS RATIO:	0.0604
SAMPLE TEMPERATURE:	297.2 °C
HOOD TEMPERATURE:	152.8 °C

HEAT OF FORMATION PER MOLE OF FUEL:	-17.412	kcal/mole
HEAT OF FORMATION PER MOLE OF AIR:	-0.926	kcal/mole
HEAT OF FORMATION PER MOLE OF PRODUCTS:	-8.220	kcal/mole
HEAT OF FORMATION PER MOLE OF STOICHIOMETRIC PRODUCTS :	-20.455	kcal/mole
ACTUAL HEAT OF REACTION:	-189.384	kcal/mole of fuel
HEAT OF STOICHIOMETRIC REACTION:	-194.437	kcal/mole of fuel
(ACTUAL/STOICHIOMETRIC) HEAT OF REACTION:	0.974	
(ACTUAL/MAXIMUM) HEAT OF REACTION:	0.974	

Appendix C

Detailed Chemical Kinetics Modeling Programs

The reaction mechanism for methane combustion used for the investigation reported in Chapter 5 is included here. Although the programming limits allowed for a larger size (200 reaction steps with 50 species), a reaction set of 90 steps with 24 species was used. The reaction mechanism is compiled using the DINTERP program (Kee, et al. 1980) to create a binary "link" file. This link file (incorporating the thermodynamic data) is read along with a keyword input file (samples are enclosed) into the Plug Flow Reactor (PFR) program. The results of the computations are written into two files: PCON and PROP. These contain the species concentration profiles and the rate of progress (reaction rate) profiles as a function of time. Using CHEMCONC and CHEMRATE, these output files can be arranged into plottable data files.

Additionally, the concentration profiles for the minor components and radical species from the temperature sensitivity analysis presented in Chapter 5 are also included. Since the absolute tolerance was set to 1.0E-10, species with peak concentrations smaller than this are not reported.

********** METHANE REACTION MECHANISM **********

ELEMENTS
H O C N

SPECIES
H O OH HO2
CH3 CH3O CH2 CHO
C2H5 C2H3 C2H2O C2HO
N2 CO CO2 H2 O2 H2O H2O2
CH2O C2H6 CH4
C2H4 C2H2

REACTIONS	A	n	Ea
CH4=CH3+H	1.10E33	-5.9	105150.
CH4+H=CH3+H2	5.50E07	1.97	11207.
CH4+O2=CH3+HO2	7.94E13	0.	55887.
CH4+HO2=CH3+H2O2	2.00E13	0.	18000.
CH4+O=CH3+OH	1.20E07	2.1	7624.
CH4+OH=CH3+H2O	1.60E06	2.1	2462.
C2H6=CH3+CH3	2.00E32	-5.	92225.
CH3+CH3=C2H5+H	7.80E11	0.	13039.
CH3+CH3=C2H4+H2	1.00E16	0.	31792.
CH3+O2=CH3O+O	1.50E13	0.	28681.
CH3+O2=CH2O+OH	5.34E13	0.	34574.
CH3+O=CH2O+H	1.26E14	0.	2000.
CH3+OH=CH3O+H	4.52E14	0.	15500.
CH3+OH=CH2O+H2	4.00E12	0.	0.
CH3+HO2=CH3O+OH	2.00E13	0.	0.
CH3+CH2O=CH4+CHO	1.00E10	0.5	6000.
CH3O+O2=CH2O+HO2	1.00E13	0.	7170.
CH3O+M=CH2O+H+M	2.00E14	0.	19870.
CH2O+M=CHO+H+M	5.00E16	0.	76480.
CH2O+H=CHO+H2	2.50E13	0.	4000.
CH2O+O=CHO+OH	1.70E06	2.32	6200.
CH2O+OH=CHO+H2O	6.90E04	2.65	-8000.
CH2O+HO2=CHO+H2O2	1.00E12	0.	7888.
C2H6+H=C2H5+H2	5.40E02	3.5	5210.
C2H6+CH3=C2H5+CH4	0.55E00	4.0	8294.
C2H6+O=C2H5+OH	3.00E07	2.0	5115.
C2H6+OH=C2H5+H2O	6.30E06	2.0	645.
C2H5=C2H4+H	7.00E25	-4.1	42984.
C2H5+H=C2H4+H2	1.90E12	0.	0.
C2H5+O2=C2H4+HO2	2.00E12	0.	5000.
C2H4+M=C2H3+H+M	3.10E17	0.	98160.
C2H4+M=C2H2+H2+M	3.00E17	0.	79800.
C2H4+H=C2H3+H2	7.00E14	0.	14500.
C2H4+CH3=C2H3+CH4	3.97E11	0.	7988.
C2H4+O=CH3+CHO	1.60E09	1.2	741.
C2H4+OH=C2H3+H2O	3.50E13	0.	3012.
C2H4+OH=CH3+CH2O	1.30E12	0.	-765.
C2H3=C2H2+H	9.30E22	-3.7	37255.
C2H3+H=C2H2+H2	1.00E13	0.	0.

C2H3+O2=C2H2+HO2	1.60E13	0.	10400.
C2H3+O2=CH2O+CHO	4.00E12	0	0.
C2H3+O=C2H2O+H	3.00E13	0.	0.
C2H3+CH3=C2H2+CH4	1.00E12	0.	0.
C2H2+O=CH2+CO	4.10E08	1.5	1697.
C2H2+O=C2HO+H	4.00E14	0.	10660.
C2H2+OH=C2H2O+H	3.00E12	0.	1100.
C2H2O+H=CH3+CO	2.00E13	0.	0.
C2H2O+H=C2HO+H2	3.00E13	0.	1434.
C2H2O+M=CH2+CO+M	2.30E15	0.	57600.
C2H2O+O=CHO+CHO	2.00E13	0.	2300.
C2H2O+O=CH2O+CO	2.00E13	0.	0.
C2H2O+OH=CH2O+CHO	1.00E13	0.	0.
C2H2O+OH=C2HO+H2O	1.00E13	0.	2630.
C2HO+H=CH2+CO	1.50E14	0.	0.
C2HO+O-CO+CO+H	1.00E14	0.	0.
C2HO+O2-CO+CO+OH	1.46E12	0.	2500.
CH2+CH3-C2H4+H	4.00E13	0.	0.
CH2+CH2-C2H2+H+H	1.00E14	0.	0.
CH2+O2=CO2+H+H	1.30E13	0.	0.
CH2+O2=CH2O+O	5.00E13	0.	9000.
CH2+O2=CHO+OH	1.00E14	0.	3700.
CH2+O=CO+H+H	8.00E13	0.	0.
CH2+C2H2O=C2H4+CO	1.00E12	0.	0.
CH2+C2HO=C2H3+CO	3.00E13	0.	0.
CHO+M=CO+H+M	7.10E14	0.	16802.
CHO+H=CO+H2	2.00E14	0.	0.
CHO+OH=CO+H2O	5.00E13	0.	0.
CHO+O=CO+OH	3.00E13	0.	0.
CHO+O2=CO+HO2	3.00E12	0.	0.
CHO+CHO=CH2O+CO	2.00E13	0.	0.
CO+O2=CO2+O	5.00E13	0.	63169.
CO+OH=CO2+H	4.40E06	1.5	-740.
CO+O+M=CO2+M	5.30E13	0.	-4538.
CO+HO2=CO2+OH	1.50E14	0.	23573.
H+O2=O+OH	1.20E17	-0.91	16504.
O+H2=H+OH	1.50E07	2.0	7547.
H2+OH=H2O+H	1.00E08	1.6	3296.
O+H2O=OH+OH	1.50E10	1.14	17244.
H+H+M=H2+M	6.40E17	-1.0	0.
O+O+M=O2+M	1.00E17	-1.0	0.
O+H+M=OH+M	3.00E19	-1.0	0.
H+OH+M=H2O+M	1.41E23	-2.0	0.
H+O2+M=HO2+M	7.00E17	-0.8	0.
H+HO2=H2+O2	2.50E13	0.	693.
H+HO2=OH+OH	1.50E14	0.	1003.
OH+HO2=H2O+O2	2.00E13	0.	0.
O+HO2=O2+OH	2.00E13	0.	0.
O+OH+M=HO2+M	1.00E17	0.	0.
HO2+HO2=H2O2+O2	2.00E12	0.	0.
H+H2O2=H2O+OH	1.00E13	0.	3583.
H2O2+M=OH+OH+M	1.20E17	0.	45379.

********** SAMPLE INPUT FILES **********

```
CASE 1
ISOT                    (ISOTHERMAL CONDITIONS SELECTED)
PRES 1.0                (REACTOR PRESSURE, ATM)
TEMP 1034               (REACTOR TEMPERATURE, K)
REAC H2    .0102        (INPUT REACTANTS)
REAC O2    .0250        (SPECIFIED IN MOLE FRACTIONS)
REAC N2    .6628
REAC CH4   .0523
REAC CO    .0146
REAC CO2   .0694
REAC H2O   .1633
REAC C2H2  .0016
REAC C2H6  .0008
TEND 2.0E+01            (TIME TO END INTEGRATIONS, SEC)
TINC 1.0E-05            (INCREMENT OF TIME STEP, SEC)
PINT 1.0E+04            (PRINT INTERVAL)
RTOL 1.0E-06            (RELATIVE TOLERANCE)
ATOL 1.0E-10            (ABSOLUTE TOLERANCE)
END
```

```
CASE 2
ISOT
PRES 1.0
TEMP 546
REAC H2    .0102
REAC O2    .0250
REAC N2    .6628
REAC CH4   .0523
REAC CO    .0146
REAC CO2   .0694
REAC H2O   .1633
REAC C2H2  .0016
REAC C2H6  .0008
TEND 2.0E+01
TINC 1.0E-05
PINT 1.0E+04
RTOL 1.0E-06
ATOL 1.0E-10
END
```

```
CASE 3
ISOT
PRES 1.0
TEMP 600
REAC H2    .0102
REAC O2    .0250
REAC N2    .6628
REAC CH4   .0523
REAC CO    .0146
REAC CO2   .0694
REAC H2O   .1633
REAC C2H2  .0016
REAC C2H6  .0008
TEND 2.0E+01
TINC 1.0E-05
PINT 1.0E+04
RTOL 1.0E-06
ATOL 1.0E-10
END
```

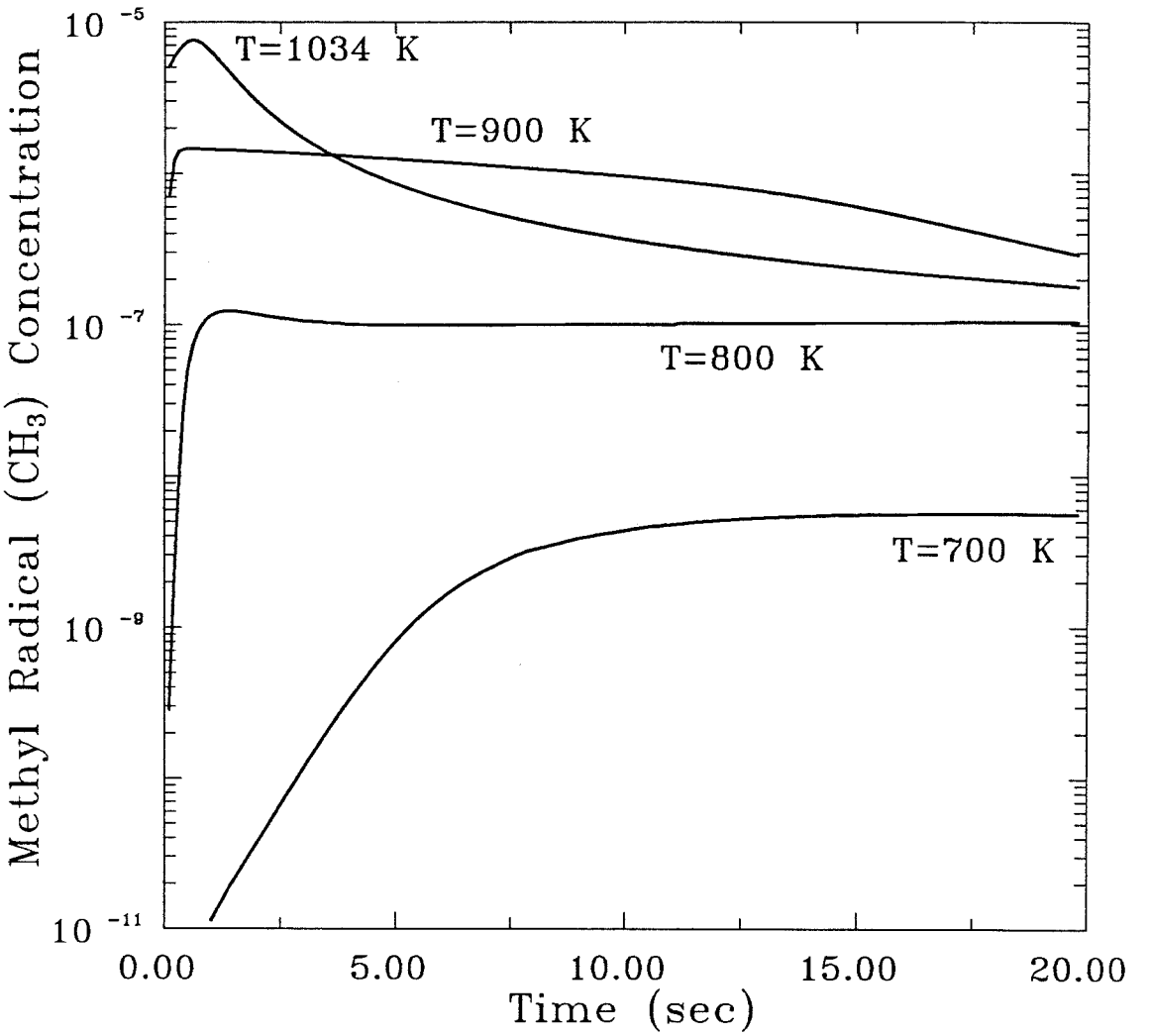

Figure C.1: Methyl radical concentration for a fuel-rich mixture introduced into an isothermal plug flow reactor

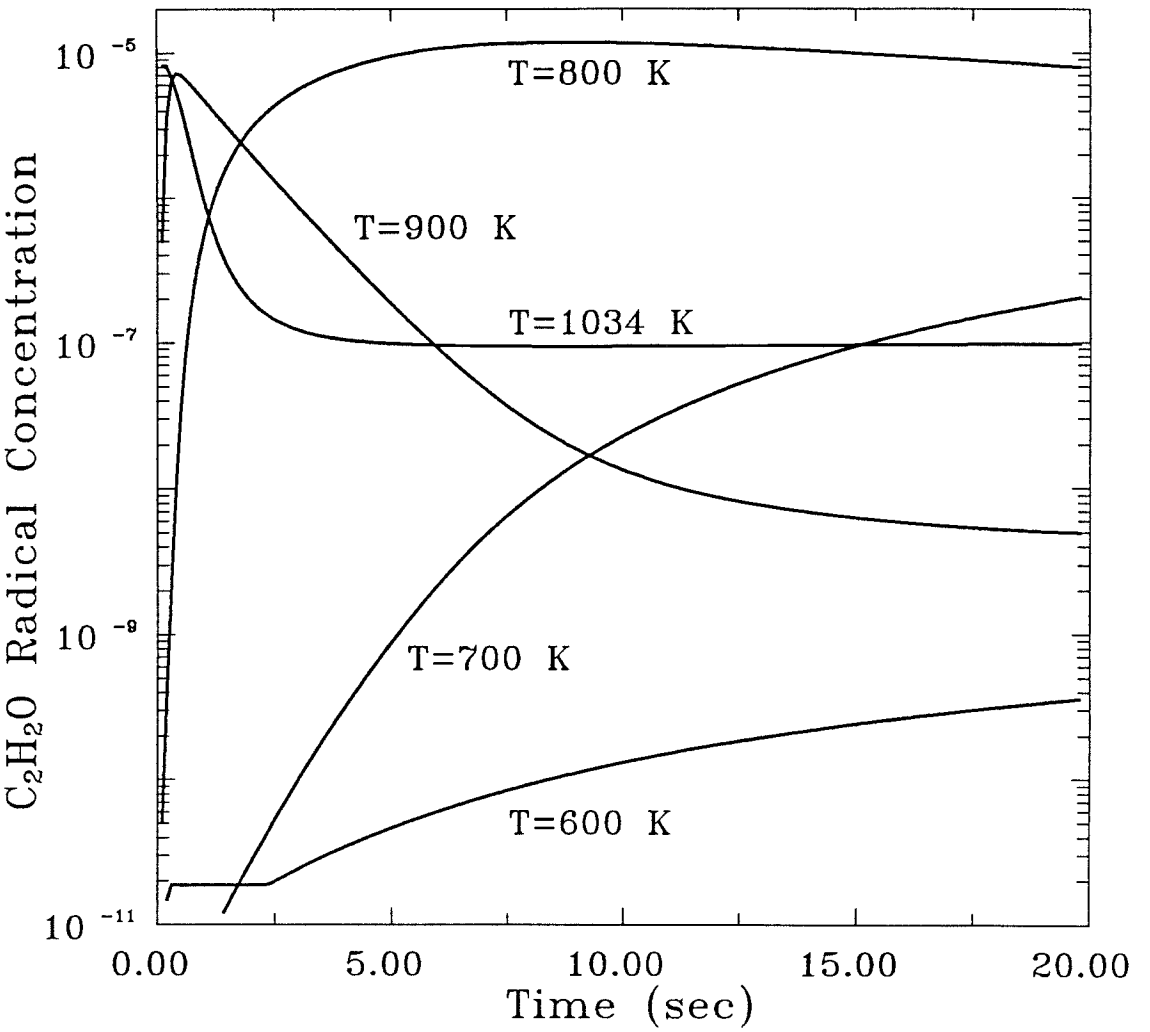

Figure C.2: C_2H_2O concentration for a fuel-rich mixture introduced into an isothermal plug flow reactor

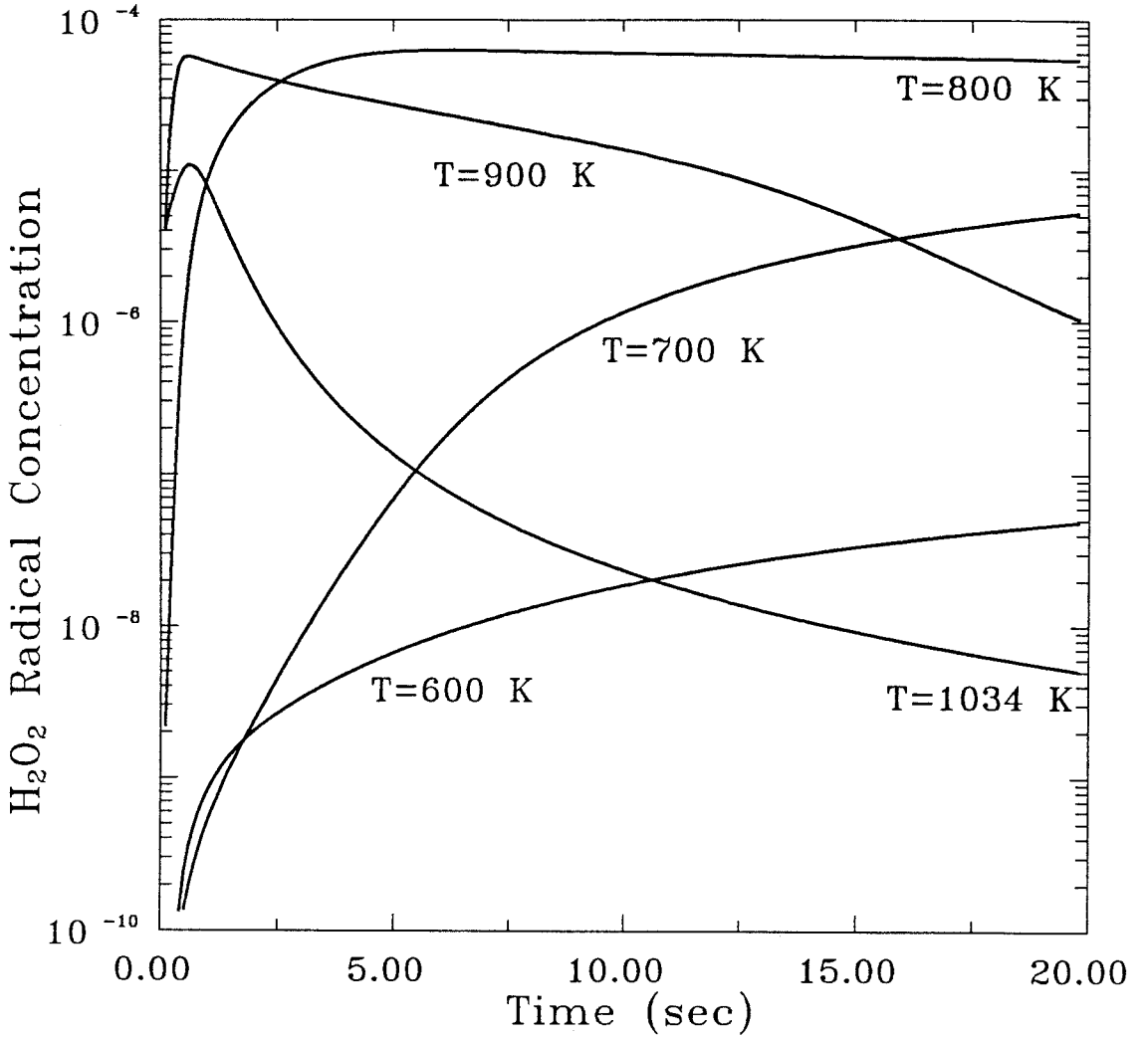

Figure C.3: H_2O_2 concentration for a fuel-rich mixture introduced into an isothermal plug flow reactor

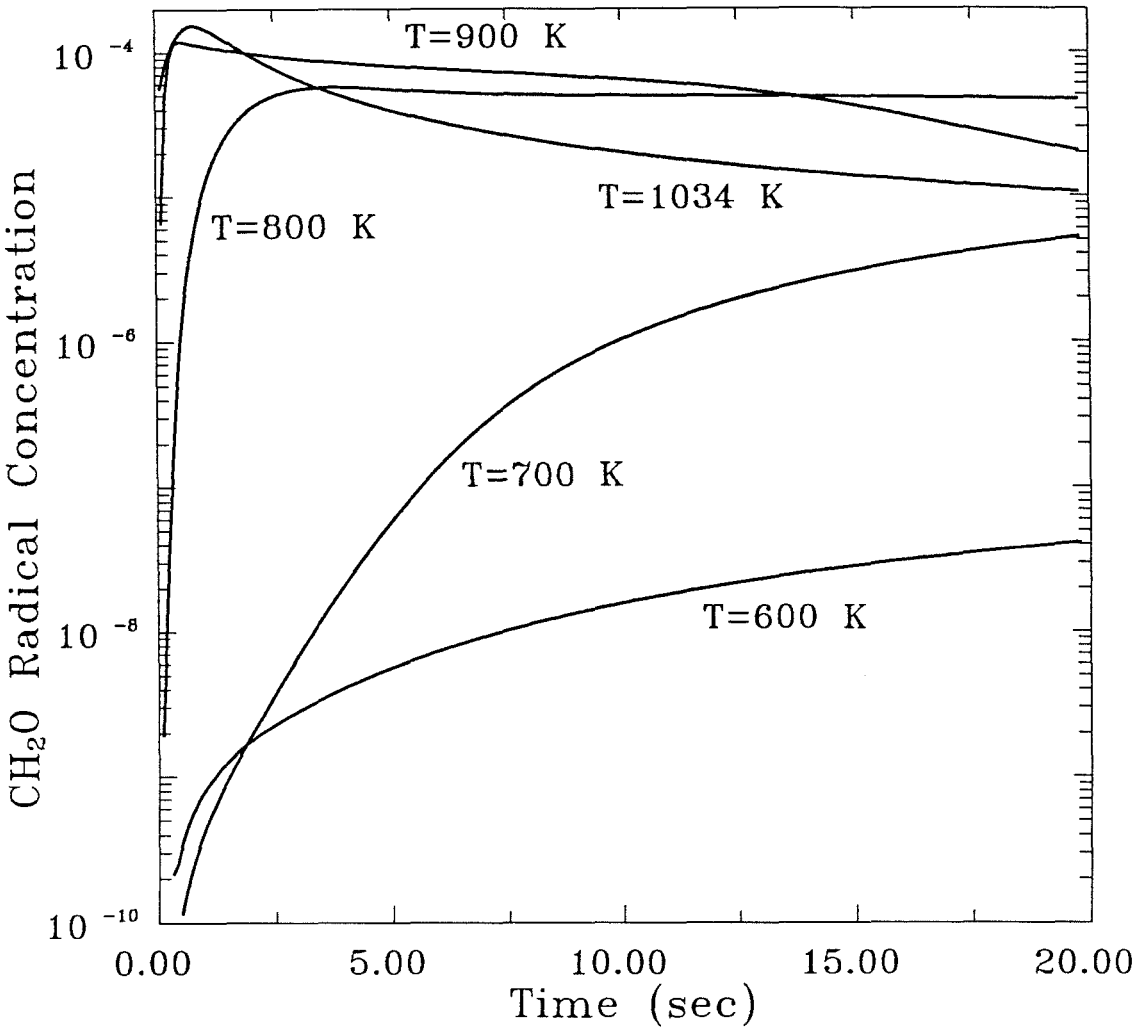

Figure C.4: CH_2O concentration for a fuel-rich mixture introduced into an isothermal plug flow reactor

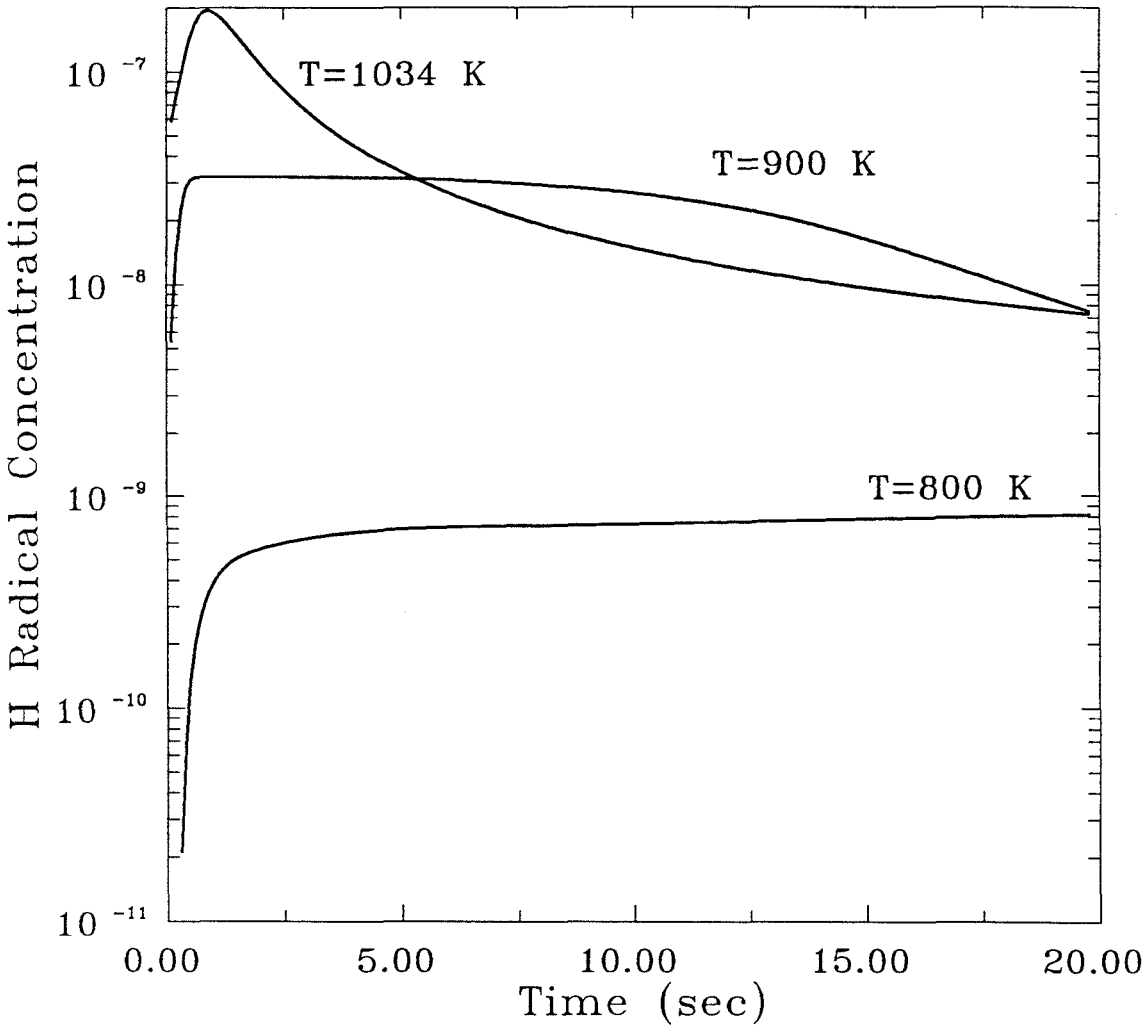

Figure C.5: H radical concentration for a fuel-rich mixture introduced into an isothermal plug flow reactor

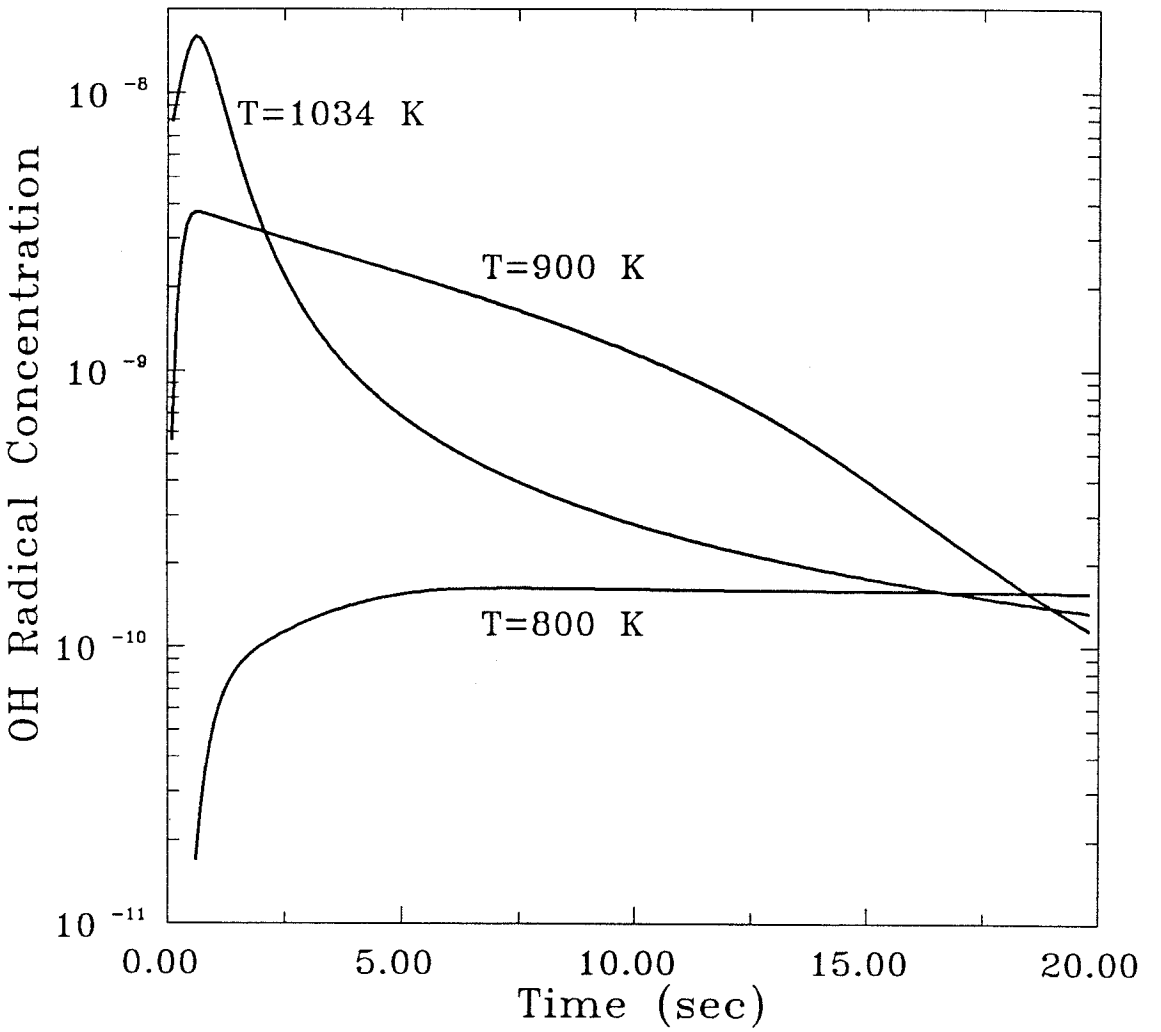

Figure C.6: OH radical concentration for a fuel-rich mixture introduced into an isothermal plug flow reactor

APPENDIX D

Tabulated Data from Experiments with Alternate Fuels

Chrom. Run No.	1004	1005	1006	1007	1008
Date	11-06-89	11-06-89	11-06-89	11-06-89	11-06-89
Time	12:05	12:27	12:49	13:11	13:35
Fuel Type	E	E	E	E	E
Configuration	1	1	1	1	1
Z_i (cm)	-30.0	-30.0	-30.0	-30.0	-30.0
D (cm)	19.0	19.0	19.0	19.0	19.0
$\dot{m}_{fuel}$ (g/sec)	0.259	0.286	0.358	0.446	0.604
$\dot{Q}$ (kW)	12.217	13.502	16.874	21.985	28.495
$\dot{m}_{added}$ (g/sec)	19.139	19.798	22.269	21.225	21.343
$\dot{m}_{ent}$ (g/sec)	N/A	N/A	N/A	N/A	N/A
I $(moles)$	71.531	66.950	60.259	44.082	34.200
φ_p	N/A	N/A	N/A	N/A	N/A
φ_ℓ	0.2026	0.2165	0.2405	0.3288	0.4238
Products (mole fr.)					
H_2	.0000	.0000	.0000	.0000	.0000
O_2	.1791	.1790	.1699	.1523	.1317
N_2	.7716	.7728	.7691	.7654	.7603
CH_4	.0000	.0000	.0000	.0000	.0000
CO	.0000	.0000	.0000	.0000	.0000
CO_2	.0283	.0302	.0334	.0453	.0579
H_2O	.0118	.0088	.0185	.0278	.0410
$C_8H(s)$	.0000	.0000	.0000	.0000	.0000
C_2H_2	.0000	.0000	.0000	.0000	.0000
C_2H_4	.0000	.0000	.0000	.0000	.0000
C_2H_6	.0000	.0000	.0000	.0000	.0000
Ar	.0092	.0092	.0092	.0091	.0091
T_{sample} $(°C)$	107.2	116.1	136.7	165.6	200.6
T_{hood} $(°C)$	72.2	76.1	84.4	98.9	121.1

Chrom. Run No.	1012	1021	1074	1075	1076
Date	11-06-89	11-16-89	12-19-89	12-19-89	12-19-89
Time	15:12	21:47	15:01	15:17	15:40
Fuel Type	E	E	E	E	E
Configuration	1	1	2	2	2
Z_i (cm)	-30.0	-30.0	10.0	10.0	10.0
D (cm)	19.0	19.0	19.0	19.0	19.0
$\dot{m}_{fuel}$ (g/sec)	0.302	0.287	1.167	1.174	1.161
$\dot{Q}$ (kW)	14.253	13.544	55.054	55.345	54.766
$\dot{m}_{added}$ (g/sec)	10.007	8.282	0.000	0.000	13.925
$\dot{m}_{ent}$ (g/sec)	N/A	N/A	12.913	14.086	14.086
I $(moles)$	32.059	27.921	10.710	11.621	23.354
φ_p	N/A	N/A	1.3506	1.2447	1.2447
φ_ℓ	0.4521	0.5148	1.3506	1.2447	0.6194
Products (mole fr.)					
H_2	.0000	.0000	.0211	.0132	.0000
O_2	.1108	.1060	.0127	.0163	.0865
N_2	.7488	.7506	.6896	.6993	.7408
CH_4	.0000	.0000	.0000	.0000	.0000
CO	.0000	.0000	.0252	.0195	.0000
CO_2	.0608	.0613	.1034	.1037	.0738
H_2O	.0706	.0721	.1218	.1250	.0910
$C_8H(s)$	.0000	.0010	.0004	.0006	.0011
C_2H_2	.0000	.0000	.0029	.0020	.0000
C_2H_4	.0000	.0000	.0147	.0120	.0000
C_2H_6	.0000	.0000	.0000	.0000	.0000
Ar	.0089	.0090	.0082	.0083	.0068
T_{sample} $(°C)$	135.6	133.9	243.9	255.6	295.6
T_{hood} $(°C)$	113.3	100.6	175.6	183.3	186.7

Chrom. Run No.	1190	1191	1192	1193	1194
Date	03-07-90	03-08-90	03-08-90	03-08-90	03-08-90
Time	23:52	00:15	00:39	01:05	01:31
Fuel Type	E	E	E	E	E
Configuration	2	2	2	2	2
Z_i (cm)	5.0	5.0	5.0	5.0	5.0
D (cm)	19.0	19.0	19.0	19.0	19.0
$\dot{m}_{fuel}$ (g/sec)	0.652	0.862	0.862	0.862	0.871
$\dot{Q}$ (kW)	30.760	40.648	40.654	40.654	41.083
$\dot{m}_{added}$ (g/sec)	0.000	0.000	1.925	3.061	5.334
$\dot{m}_{ent}$ (g/sec)	11.435	11.728	11.728	11.728	11.728
I $(moles)$	17.0155	13.207	15.367	16.643	18.995
φ_p	0.8481	1.0926	1.0926	1.0926	1.0926
φ_ℓ	0.8481	1.0926	0.9390	0.8670	0.7597
Products (mole fr.)					
H_2	.0000	.0000	.0000	.0000	.0000
O_2	.0435	.0202	.0400	.0470	.0581
N_2	.7299	.7151	.7236	.7275	.7347
CH_4	.0000	.0000	.0000	.0000	.0000
CO	.0088	.0182	.0145	.0125	.0079
CO_2	.0971	.1038	.0945	.0917	.0890
H_2O	.1095	.1252	.1124	.1083	.1000
$C_8H(s)$	.0000	.0000	.0000	.0000	.0000
C_2H_2	.0005	.0023	.0013	.0011	.0000
C_2H_4	.0020	.0067	.0051	.0034	.0016
C_2H_6	.0000	.0000	.0000	.0000	.0000
Ar	.0087	.0085	.0086	.0086	.0087
T_{sample} $(°C)$	257.8	278.9	286.7	291.7	300.0
T_{hood} $(°C)$	143.9	157.2	161.1	161.7	162.8

Chrom. Run No.	1214	1215	1216	1217	1218
Date	04-12-90	04-12-90	04-12-90	04-12-90	04-12-90
Time	00:36	01:08	01:41	02:13	02:45
Fuel Type	E	E	E	E	E
Configuration	2	2	2	2	2
Z_i (cm)	1.0	1.0	1.0	1.0	1.0
D (cm)	19.0	19.0	19.0	19.0	19.0
$\dot{m}_{fuel}$ (g/sec)	0.711	0.711	0.711	0.711	0.711
$\dot{Q}$ (kW)	33.522	33.526	33.526	33.531	33.531
$\dot{m}_{added}$ (g/sec)	0.000	2.058	3.916	5.131	6.922
$\dot{m}_{ent}$ (g/sec)	7.261	7.261	7.261	7.261	7.261
I $(moles)$	9.890	12.691	15.222	16.873	19.312
φ_p	1.4647	1.4647	1.4647	1.4647	1.4647
φ_ℓ	1.4647	1.1414	0.9516	0.8585	0.7501
Products (mole fr.)					
H_2	.0033	.0000	.0000	.0000	.0000
O_2	.0099	.0315	.0461	.0488	.0596
N_2	.6948	.7111	.7207	.7241	.7319
CH_4	.0003	.0002	.0000	.0000	.0000
CO	.0247	.0209	.0143	.0129	.0081
CO_2	.1060	.0953	.0902	.0886	.0868
H_2O	.1270	.1180	.1109	.1120	.1031
$C_8H(s)$	.0000	.0000	.0000	.0000	.0000
C_2H_2	.0058	.0036	.0043	.0009	.0000
C_2H_4	.0198	.0109	.0050	.0041	.0018
C_2H_6	.0000	.0000	.0000	.0000	.0000
Ar	.0083	.0085	.0086	.0086	.0087
T_{sample} $(°C)$	222.2	237.8	251.7	268.3	275.0
T_{hood} $(°C)$	123.9	135.6	143.3	149.4	151.7

Chrom. Run No.	1219	1220	1087	1088	1133
Date	04-12-90	04-12-90	01-04-90	01-04-90	01-21-90
Time	03:17	03:48	15:33	16:05	23:59
Fuel Type	E	E	P	P	P
Configuration	2	2	1	1	2
Z_i (cm)	1.0	1.0	-30.0	-30.0	5.0
D (cm)	19.0	19.0	19.0	19.0	19.0
$\dot{m}_{fuel}$ (g/sec)	0.711	0.707	0.474	0.632	1.062
$\dot{Q}$ (kW)	33.536	33.356	21.683	28.915	48.602
$\dot{m}_{added}$ (g/sec)	6.975	11.196	27.873	23.005	0.000
$\dot{m}_{ent}$ (g/sec)	7.261	7.261	N/A	N/A	10.034
I $(moles)$	19.382	25.265	85.481	52.906	13.728
φ_p	1.4647	1.4647	N/A	N/A	1.5737
φ_ℓ	0.7474	0.5734	0.2527	0.4083	1.5737
Products (mole fr.)					
H_2	.0000	.0000	.0000	.0000	.0069
O_2	.0628	.0856	.0933	.1178	.0233
N_2	.7326	.7426	.8169	.7569	.6941
CH_4	.0000	.0000	.0000	.0000	.0053
CO	.0090	.0007	.0000	.0000	.0179
CO_2	.0850	.0757	.0372	.0556	.0950
H_2O	.0998	.0865	.0429	.0608	.1234
$C_8H(s)$	.0000	.0000	.0000	.0000	.0018
C_2H_2	.0000	.0000	.0000	.0000	.0045
C_2H_4	.0021	.0000	.0000	.0000	.0042
C_2H_6	.0000	.0000	.0000	.0000	.0000
Ar	.0087	.0088	.0097	.0090	.0083
C_3H_6			.0000	.0000	.0152
T_{sample} $(°C)$	281.1	279.4	179.4	210.0	213.3
T_{hood} $(°C)$	161.7	151.1	87.8	108.9	142.2

Chrom. Run No.	1134	1135	1136	1137	1147
Date	01-22-90	01-22-90	01-22-90	01-22-90	01-28-90
Time	00:35	01:08	01:43	02:16	23:10
Fuel Type	P	P	P	P	P
Configuration	2	2	2	2	2
Z_i (cm)	5.0	5.0	5.0	5.0	5.0
D (cm)	19.0	19.0	19.0	19.0	19.0
$\dot{m}_{fuel}$ (g/sec)	1.274	1.287	1.287	1.287	1.273
$\dot{Q}$ (kW)	58.302	58.934	58.926	58.926	58.285
$\dot{m}_{added}$ (g/sec)	0.000	9.135	19.316	31.972	0.000
$\dot{m}_{ent}$ (g/sec)	10.202	10.202	10.202	10.202	9.174
I $(moles)$	11.636	23.003	33.311	47.593	10.467
φ_p	1.8566	1.8566	1.8566	1.8566	2.0601
φ_ℓ	1.8566	0.9391	0.6485	0.4539	2.0601
Products (mole fr.)					
H_2	.0088	.0000	.0000	.0000	.0110
O_2	.0136	.0705	.0860	.1184	.0107
N_2	.6813	.7257	.7412	.7519	.6740
CH_4	.0076	.0028	.0004	.0000	.0076
CO	.0226	.0130	.0048	.0010	.0224
CO_2	.0971	.0740	.0708	.0528	.0951
H_2O	.1270	.0931	.0851	.0660	.1312
$C_8H(s)$	.0018	.0002	.0006	.0009	.0031
C_2H_2	.0056	.0027	.0004	.0000	.0060
C_2H_4	.0056	.0025	.0004	.0000	.0057
C_2H_6	.0000	.0000	.0000	.0000	.0000
Ar	.0082	.0087	.0089	.0090	.0080
C_3H_6	.0208	.0069	.0012	.0000	.0250
T_{sample} $(°C)$	229.4	255.0	307.2	314.4	232.2
T_{hood} $(°C)$	145.6	160.0	177.8	155.6	132.2

Chrom. Run No.	1148	1149	1150	1151	1152
Date	01-28-90	01-29-90	01-29-90	01-29-90	01-29-90
Time	23:44	00:16	01:10	01:42	02:14
Fuel Type	P	P	P	P	P
Configuration	2	2	2	2	2
Z_i (cm)	5.0	5.0	1.0	1.0	1.0
D (cm)	19.0	19.0	19.0	19.0	19.0
$\dot{m}_{fuel}$ (g/sec)	1.280	1.280	0.800	1.019	1.019
$\dot{Q}$ (kW)	58.592	58.592	36.614	46.631	46.631
$\dot{m}_{added}$ (g/sec)	1.980	4.497	0.000	0.000	1.462
$\dot{m}_{ent}$ (g/sec)	9.174	9.174	7.437	7.693	7.693
I $(moles)$	12.659	15.516	13.507	10.970	13.055
φ_p	2.0601	2.0601	1.5964	1.9655	1.9655
φ_ℓ	1.7034	1.3897	1.5964	1.9655	1.6516
Products (mole fr.)					
H_2	.0108	.0045	.0078	.0122	.0049
O_2	.0293	.0459	.0243	.0200	.0413
N_2	.6878	.7035	.6939	.6791	.6944
CH_4	.0063	.0051	.0055	.0065	.0059
CO	.0185	.0166	.0172	.0199	.0181
CO_2	.0863	.0795	.0935	.0926	.1134
H_2O	.1230	.1137	.1232	.1229	.1134
$C_8H(s)$	.0037	.0027	.0025	.0028	.0023
C_2H_2	.0045	.0039	.0044	.0050	.0046
C_2H_4	.0047	.0038	.0044	.0051	.0044
C_2H_6	.0000	.0000	.0000	.0000	.0000
Ar	.0082	.0084	.0083	.0081	.0083
C_3H_6	.0169	.0122	.0150	.0258	.0212
T_{sample} $(°C)$	248.9	258.3	215.0	223.9	226.1
T_{hood} $(°C)$	144.4	151.1	110.0	111.7	112.8

Chrom. Run No.	1153	1154	1155	1156	1157
Date	01-29-90	01-29-90	01-29-90	01-29-90	01-29-90
Time	02:46	03:19	03:51	04:23	04:55
Fuel Type	P	P	P	P	P
Configuration	2	2	2	2	2
Z_i (cm)	1.0	1.0	1.0	1.0	1.0
D (cm)	19.0	19.0	19.0	19.0	19.0
$\dot{m}_{fuel}$ (g/sec)	1.018	1.024	1.024	1.024	1.024
$\dot{Q}$ (kW)	46.618	46.870	46.864	46.864	46.864
$\dot{m}_{added}$ (g/sec)	2.946	4.857	7.266	9.900	15.469
$\dot{m}_{ent}$ (g/sec)	7.693	7.693	7.693	7.693	7.693
I $(moles)$	15.1753	17.805	21.226	24.963	32.866
φ_p	1.9655	1.9655	1.9655	1.9655	1.9655
φ_ℓ	1.4209	1.2110	1.0158	0.8638	0.6561
Products (mole fr.)					
H_2	.0065	.0000	.0000	.0000	.0000
O_2	.0624	.0725	.0803	.0867	.0946
N_2	.7033	.7149	.7241	.7313	.7410
CH_4	.0048	.0043	.0029	.0014	.0003
CO	.0157	.0138	.0108	.0077	.0067
CO_2	.0698	.0654	.0640	.0622	.0612
H_2O	.1012	.0979	.0931	.0909	.0835
$C_8H(s)$	.0026	.0022	.0021	.0024	.0017
C_2H_2	.0042	.0037	.0023	.0014	.0002
C_2H_4	.0039	.0035	.0026	.0018	.0008
C_2H_6	.0000	.0000	.0000	.0000	.0000
Ar	.0084	.0085	.0087	.0087	.0089
C_3H_6	.0171	.0133	.0092	.0055	.0013
T_{sample} $(°C)$	225.6	227.8	238.3	243.9	288.3
T_{hood} $(°C)$	110.0	110.6	119.4	131.7	149.4

Fuel Type: E=Ethylene, P=Propylene

Configuration: 1=Uniform vitiated layer, 2=Two layer experiment